Федеральное государственное автономное образовательное учреждение

высшего образования «Уральский федеральный университет имени первого Президента России Б.Н. Ельцина»

Уральский энергетический институт
Кафедра «Атомные станции и возобновляемые источники энергии»

На правах рукописи

Сипана Правинкумар

РАЗРАБОТКА И ЭКСПЕРИМЕНТАЛЬНОЕ ИССЛЕДОВАНИЕ СПОСОБОВ ПОВЫШЕНИЯ ЭФФЕКТИВНОСТИ ФОТОЭЛЕКТРИЧЕСКИХ ЭЛЕКТРОСТАНЦИЙ, РАБОТАЮЩИХ В УСЛОВИЯХ ВЫСОКИХ ТЕМПЕРАТУР ОКРУЖАЮЩЕЙ СРЕДЫ (НА ПРИМЕРЕ РЕСПУБЛИКИ ИНДИЯ)

2.4.5. Энергетические системы и комплексы

ДИССЕРТАЦИЯ
на соискание ученой степени
кандидата технических наук

Научный руководитель:
Доктор технических наук, доцент,
Велькин Владимир Иванович

Екатеринбург – 2023

Federal State Autonomous Educational Institution Higher Education «Ural Federal University named after the first President of Russia B.N. Yeltsin»

Ural Power Engineering Institute
Department of «Nuclear Power Plants and Renewable Energy Sources»

As a manuscript

Seepana PraveenKumar

DEVELOPMENT AND EXPERIMENTAL INVESTIGATION FOR THE IMPROVEMENT EFFICIENCY OF SOLAR PHOTOVOLTAIC POWER PLANTS IN HIGH AMBIENT TEMPERATURES (OBSERVATION OF THE REPUBLIC OF INDIA)

2.4.5. Energy Systems and Complexes

DISSERTATION
Degree of Candidate of Technical Sciences

Scientific Supervisor:
Doctor of Technical Sciences, Associate Professor,
Velkin Vladimir Ivanovich

Yekaterinburg-2023

ACKNOWLEDGMENT

First and the foremost I offer my sincerest gratitude to my supervisor, **Prof. Vladimir Ivanovich Velkin**, Associate Professor, Department of Nuclear and Renewable Energy, Ural Power Engineering Institute of Ural Federal University, Ekaterinburg, Russia who has supported me throughout my thesis with their patience, knowledge, valuable advice, uninterrupted active supervision and constant encouragement. I attribute the level of my Doctoral's degree to their encouragement and effort without them this thesis, too, would not have been completed or written.

I am thankful to **Prof. Sergey Evgenvich Shcheklein**, (HOD) and **Prof. Oleg Lendovich Tashlikov** (Secretary) Department of Nuclear and Renewable Energy, Ural Power Engineering Institute of Ural Federal University, Ekaterinburg, Russia

I would like to thank all the staff members of Department of Nuclear and Renewable Energy who have been very patient and co-operative with me.

I am thankful to my senior graduates **Dr. Ephraim Bonah Agyekum, Dr. Abhinav Kumar, Dr. Naseer T. Alwan, and Dr. Mohammed Karem** Post-doctoral fellows, Department of Nuclear and Renewable Energy, Ural Power Engineering Institute of Ural Federal University, Ekaterinburg, Russia who continuously motivated, clearing concepts and encouraged me to do this research work.

I would also like to extend my gratitude to my colleagues Mr. Mohammed Abdulkhaleq Qasim, Mr. Motaz, Mr. Parviz, Mr. Boris friends who always encouraged and supported me in this thesis work.

I would like to thank **Ural Federal University** for giving me opportunity to use their resources and work in such a challenging environment. I am grateful to the individuals whom contributed their valuable time towards my thesis.

Last but not the least, I express my sincere gratitude to my parents, brothers, and sisters who have always supported me throughout all my studies at university and encouraged me with their best wishes.

Seepana Praveenkumar

Table of Contents

1 INTRODUCTION TO INDIA’S ENERGY GENERATION 1

1.1 Overview of India 1

1.2 Current State of India’s Energy India 2

1.3 India’s strategy reduction in GHG emissions 4

1.4 India's existing energy policies 4

1.4.1 Electricity law, 2003 [10] 4

1.4.2 National electricity policy law, 2005 4

1.5 Status of India’s Renewable Energy of sources 5

1.5.1 Tariff policy, 2006 5

1.5.2 Solar power potential in India. 5

1.5.3 Wind potential in India 5

1.5.4 Hydroelectrical potential in India 6

1.5.5 Wave Potential for India 6

1.5.6 Biomass Potential for India 7

2 EXPERIMENTAL INVESTIGATION INCORPORATED WITH DIFFERENT COOLING MECHANISMS FOR THE IMPROVEMENT EFFICIENCY OF THE SOLAR PV MODULE 8

2.1 Thermodynamic Calculations 10

2.1.1 Energy Efficiency Balance 10

2.1.2 Exergy Efficiency Balance 11

2.1.3 Entropy generation 11

2.2 Economic Analysis 12

2.3 Uncertainty analysis 13

3 TECHNO-ECONOMIC FEASIBILITY OF SOLAR PV PLANTS IN INDIA 14

3.1 Comparative analysis for solar tracking mechanism of solar PV plants in five unique climatic conditions in Southern India 14

3.1.1 Operation of solar tracking mechanism 14

3.1.2 Solar resources data in South India 14

3.1.3 Weather performance of the selected sites 18

3.1.4 Results and discussions 22

3.1.5 Economic results of a PV plant for three mechanisms 29

3.1.6 Sensitivity analysis for the proposed mechanism 30

3.1.7 Enviro-economic analysis 33

3.1.8 Comparative analysis of the present study 34

3.2 Techno-enviro-economic assessment of a 100 MW solar tower power plant (STPP) using dry-cooled and wet-cooled condenser model a case study in Republic of India. 36

3.2.1 Materials and Methodology 36

3.2.2 Selection of parameters for the analysis 37

3.2.3 Weather characteristic of the present study 40

3.2.4 Results and discussions 41

3.2.5 Comparative analysis in the present study 52

3.3 Techno-economic feasibility of standalone of hybrid System for the hydrogen production and electric vehicles in five unique climatic conditions in India 54

3.3.1 Description of HOMER software as hybrid model 55

3.3.2 Hybrid model system description for the present study 55

3.3.3 Solar PV module 56

3.3.4 Battery storage 57

3.3.5 Fuel Cell 57

3.3.6 Hydrogen Storage Tanks 58

3.3.7 Electrolyzer 58

3.3.8 Power Converter 58

3.3.9 Selection of potential Sites 59

3.3.10 Solar intensity of selected sites 59

3.3.11 Economic analysis for hybrid system 60

3.3.12 Levelized cost of energy 60
3.3.13 Net Present cost......60
3.3.14 Load Profile 61
3.3.15 Results and Discussion 62
3.3.16 Electricity generation......63
3.3.17 Hydrogen Production......67
3.3.18 Economic analysis 67
3.3.19 Environmental Impact and gasoline fuel replacement assessment 72
3.4 Limitations in the present study 73
3.5 Conclusions for chapter 2......74
4 EXPERIMENTAL INVESTIGATION OF ENHANCEMENT OF SOLAR PV COOLING ACTIVE COOLING......76
4.1 Experimental study on the performance and enhancement of a solar PV panel integrated with CPU heat pipes- an active cooling approach 76
4.1.1 Material and Methodology......76
4.1.2 Working principle of fanless heat pipe CPU sink......76
4.1.3 Construction of experimental setup 77
4.1.4 Experimental Setup......78
4.1.5 Weather characteristics of a PV panel 79
4.1.6 Temperature profile of a fanless heat pipe......80
4.1.7 Electrical Performance of a PV panel......82
4.1.8 Electrical Efficiency......83
4.1.9 Exergy analysis 85
4.1.10 Entropy analysis......85
4.1.11 Cost analysis 86
4.2 The experimental investigation incorporated with thermoelectric fans on the efficiency of a PV module 87
4.2.1 Materials and Methodology 87

4.2.2 Working principle of thermoelectric cooling..87

4.2.3 Construction of experimental test rig...89

4.2.4 Experimental setup of proposed mechanism 90

4.2.5 Weather characteristics of the experimental period..91

4.2.6 Temperature profile of a PV panel..92

4.2.7 Electrical performance on the PV module..93

4.2.8 Electrical Efficiency..94

4.2.9 Exergy efficiency...95

4.2.10 Economic analysis 95

4.2.11 Comparison of current results with published works 96

4.3 Photovoltaic (PV) solar panels integrated with u-shaped grid copper pipe, TEGs and aluminium oxide (Al_2O_3) nanofluid: An experimental investigation 98

4.3.1 Construction of experimental setup 98

4.3.2 Preparation of Al_2O_3 nanoparticle 100

4.3.3 Experimental Setup...101

4.3.4 Weather characteristics on the day of the experiment 102

4.3.5 Temperature distribution of PV panel..103

4.3.6 Electrical efficiency 104

4.3.7 Electrical performance of the PV panels 105

4.3.8 The effect of temperature gradient on TEGs 107

4.3.9 The effect of efficiency on TEGs..108

4.3.10 Economic analysis 110

4.4 Conclusions of chapter 4 112

5 EXPERIMENTAL INVESTIGATION FOR THE IMPROVEMENT EFFICIENCY OF SOLAR PV PANELS USING PASSIVE COOLING MECHANSIMS 114

5.1 The influence of discontinuous aluminium heat sinks for a thermal management solar PV to enhance output performance...114

5.1.1 Material and Methods 114

5.1.2 Aluminium Characteristics 114

5.1.3 Mathematical Modelling for Solar Cell 114

5.1.4 Experimental Test Rig 115

5.1.5 Performance Weather Characteristics..117

5.1.6 Thermal management...117

5.1.7 Power Characteristics of PV Panels..119

5.1.8 Efficiencies of a PV panel..121

5.1.9 Entropy Analysis..122

5.1.10 Cost analysis 124

5.2 Solar PV modules coupled with low-cost aluminum reflectors and integrated with PCM using natural air convection: An experimental investigation 125

5.2.1 Construction of experimental setup 125

5.2.2 Experimental setup...127

5.2.3 Weather characteristics 128

5.2.4 Temperature variations 129

5.2.5 Electrical efficiency and improvement 130

5.2.6 Electrical Performance of PV configurations 131

5.2.7 Exergy efficiency 132

5.2.8 Entropy generation...133

5.2.9 Economic analysis 133

5.3 Conclusions from the experimental study 135

List of Figures

Figure 1 Leading countries generation of REs in the world by 2021 [3] 1

Figure 2 Fastest economic develop countries in the world [4] 2

Figure 3 Energy Mix in India, 2021 [5]...2

Figure 4 Bhadla Solar Power Project, Rajasthan [6] 3

Figure 5 Muppandal wind Farm, Tamil Nadu [7]...3

Figure 6 Tehri Hydro Complex, Uttarakhand [8] 3

Figure 7 Vizhinjam wave energy, Kerala [9]..4

Figure 8 Installed Solar Capacity 31st March 2022 6

Figure 9 Installed Wind Capacity 31st March 2020 6

Figure 10 Classification of Biomass energy in India [17] 7

Figure 11 Selected potential sites in south Indian states...17

Figure 12 Module Characteristics at reference conditions 17

Figure 13 Efficiency curve of Inverter...18

Figure 14 Wind speed data for south-Indian states...20

Figure 15 GHI data for south-Indian states..22

Figure 16 Monthly output grid to PV system for FT mechanism in south -Indian states.......25

Figure 17 Monthly output grid to PV system for SAT mechanism in south -Indian states.....27

Figure 18 Monthly output grid to PV system for DAT mechanism south -Indian states 29

Figure 19 LCOE corresponding to project life time period..31

Figure 20 Effect of LCOE corresponding to the project life time period...............................32

Figure 21 Effect of LCOE corresponding to sales tax rate 33

Figure 22 Selected potential for STPP model using QGIS 37

Figure 23 Flow chart of the simulation process in the SAM program (modified from [96] with license number: 5407500931944)..38

Figure 24 The configuration of STPP technology (obtained from SAM) 38

Figure 25 Monthly DNI for the selected sites India 41

Figure 26 Total electricity output to grid dry-cooled STPP plant for six potential sites.........44

Figure 27 Effect of SM and TES on the LCOE (dry-cooled model) in different cities of India 45

Figure 28 Total electricity output to grid wet-cooled STPP plant for six potential sites.........47

Figure 29 Effect of SM and TES on the LCOE (wet-cooled model) for potential sites in India 49

Figure 30 Effect of sales tax rate on LCOE: dry cooled (left); wet cooled (right) at 6 h TES for SM of 2 50
Figure 31 Effect of Up-Front fee on LCOE: dry cooled (left); wet cooled (right) at 6 h TES for SM of 2 50
Figure 32 Effect of solar multiple on NCC: dry cooled (left); wet cooled (right) at 6 h TES for SM of 2 51
Figure 33 The schematic representation used for the hybrid system 56
Figure 34 Graphical presentation of selected potential sites 59
Figure 35 Monthly dependence selected sites (a) solar radiation and (b) clearness index 60
Figure 36 Hydrogen Load 62
Figure 37 Electric load 62
Figure 38 Monthly electricity production (a) Ludhiana (b) Indore (c) Mumbai (d) Kolkata (e) Chennai 64
Figure 39 Performance of the FC at the selected locations 66
Figure 40 SOC of the battery system at various sites (a) Chennai, (b) Indore (c) Kolkata (d) Ludhiana (e) Mumbai 68
Figure 41 Level of hydrogen tank at the selected locations 69
Figure 42 Monthly hydrogen production for the selected locations 70
Figure 43 Net present cost at five selected locations 71
Figure 44 Working operation of Heat Pipe [147] 77
Figure 45 CPU heat sink 78
Figure 46 Construction of cooled PV panel incorporated with CPU heat sink 78
Figure 47 Experimental test rig 79
Figure 48 Time dependence of solar radiation, and ambient temperature 79
Figure 49 Time dependence of relative humidity, and wind speed 80
Figure 50 Timed dependence of a temperature profile 81
Figure 51 Thermal image: a) cooled PV panel, b) Un-modified PV panel 81
Figure 52 Temperature dependence of a) Voltage b) Current 82
Figure 53 Variation of power for cooled and Un-cooled PV panel 83
Figure 54 Variation of electrical efficiency of a PV panel 83
Figure 55 variation of exergy analysis for proposed mechanism 85
Figure 56 Variation of entropy generation for proposed mechanism 86
Figure 57 Left: Cooling mechanism using (TEC), Right: Flow of air [157] 88
Figure 58 Working principle of TEC [158] 88

Figure 59 Cooled PV panel with thermoelectric coolers 89
Figure 60 Parts of the TEC (a) fan for big TEC (b) TEC (c) heat sink (d) fan for small TEC 89
Figure 61 The experimental test rig: a) Front view of test rig ;b) rear view of the test rig, and; c) schematic diagram of test rig 91
Figure 62 Weather performance of a PV panel (a) Solar radiation & humidity, and (b) ambient temperature & wind speed. 92
Figure 63 Time dependence (a) temperature profile (b) change in temperature 93
Figure 64 Time dependence of thermal imager (a) cooled PV panel (b) un-cooled PV panel 93
Figure 65 Time dependences: a) Output power for the cooled and un-cooled PV modules, and b) improvement in power. 94
Figure 66 Time dependence (a) Electrical Efficiency (b) Improvement for both PV modules 94
Figure 67 Time dependence exergy efficiency of a PV module 95
Figure 68 Construction of experimental setup at each stage 100
Figure 69 Preparation of Al_2O_3: a) Magnetic stirrer, b) Volumetric flask, and C) Ultrasonic Cleaner 100
Figure 70 Experimental Test rig: 1) Al_2O_3 nanofluid storage tank, 2) Water storage tank, 3) Water pump 4) DT-1207 Battery, 5) PV/TEG/nanofluid panel, 6) PVT Panel, 7) Reference PV panel 8) Water storage tank lay on ground, 9) Solar Pyranometer, 10) 2K-digital logger, 11) Digital Anemometer, 12) Clamp meter, 13) Thermometer 101
Figure 71 Schematic diagram: 1) Nanofluid storage tank, 2) Water pump, 3) PV/TEG/nanofluid PV panel, 4) Humidity Sign, 5) Water storage tank, 6) PVT panel, 7) Reference PV panel 8) Solar radiation, 9) Water storage tank lay on ground 102
Figure 72 The schematic of rear side of PV panel (a) With u-shaped grid copper pipe (left) (b) PV/TEG/ u-shaped grid copper pipe (right) 102
Figure 73 Time dependence: a) solar radiation & wind speed, and b) relative humidity & ambient temperature 103
Figure 74 Time dependence a) Temperature profile b) reduction in temperature with respect to the referenced PV panel 104
Figure 75 Time dependence a) electrical efficiency, and b) improvement in electrical efficiency with respect to the referenced PV panel 105
Figure 76 Time dependence a) voltage, and b) current 106
Figure 77 Time dependence a) with water pump, and b) without water pump 107
Figure 78 Time dependence temperature gradient of TEGs 107

Figure 79 Time dependence TEG efficiency 108
Figure 80 (a) vertical, and (b Horizontal direction of heat sink..116
Figure 81 Images for the PV panels (a) modified heat sink, (b) Reference...........................116
Figure 82 (a) Modified PV panel (b) Reference PV panel 117
Figure 83 Weather Characteristics (a) solar radiation & Ambient temperature, and 118
Figure 84 Temperature characteristics of both PV panels 118
Figure 85 Temperature distribution: a) Thermal images, b) cooled PV panel, c) referenced PV Panel...119
Figure 86 Current and Voltage for the PV panels...120
Figure 87 Variation of power on both the panels 121
Figure 88 Efficiency variation and improvement in the PV panel 122
Figure 89 Exergy efficiency assessment on the PV panel 122
Figure 90 Entropy generation for cooled and un-cooled PV panel 123
Figure 91 Construction of experimental test rig: a) preparation of PCM/ZnO mixture, b) PCM filled in aluminium container, c) aluminium reflectors coupled to PV panels, d) K-type thermocouples attached to PV modules, e) aluminium heat sinks fixed to back surface of PV module, and f) aluminium container with PCM fixed to back side of PV aluminium 126
Figure 92 Experimental test rig...127
Figure 93 Schematic diagram a) Front surfaces reference and modified PV panels, b) back surface of modified PV panel 128
Figure 94 Time dependence: a) Solar heat flux and relative humidity; b) Ambient temperature & wind speed 128
Figure 95 Time dependence: a) Temperature profile, b) Temperature reduction..................129
Figure 96 Time dependence: a) Electrical efficiency b) Improvement in electrical efficiency 130
Figure 97 Time dependence electrical performance 131

List of Tables

Table 1 Uncertainty achieved from the experiment [25,26,65,66] 13
Table 2 Selected location in southern Indian states. 15
Table 3 Technical parameters for the present study 15
Table 4 Financial Parameters for the study 18
Table 5 Economic analysis of PV mechanism 29
Table 6 Environmental analysis due to solar PV technology 34
Table 7 Performance parameters with other literatures 34
Table 8 Selection of Potential sites 37
Table 9 Technical parameters for the present study 39
Table 10 Financial parameters for the present study 39
Table 11 Technical and economic results for STPP dry-cooled plant 44
Table 12 Technical and economic analysis of STPP (Wet-cooled) model 48
Table 13 Reduction of carbon emission use of CSP technology 51
Table 14 CSP technology with other published works, for comparison 52
Table 15. Selected potential sites 59
Table 16 Component sizing and life cycle cost 61
Table 17 System architecture of optimum systems for each location 63
Table 18 Electricity production summary for the PV and FC at various cities 65
Table 19 Excess electricity, unmet electric load, and capacity shortage in various cities 65
Table 20 Performance of the battery system 66
Table 21 Comparison with other studies 71
Table 22 Emissions avoided as a result of the use of PV power plant 73
Table 23 Comparison work with other literature 84
Table 24 Parameters used for LCOE calculations 86
Table 25 Estimated LCE calculations 86
Table 26 Description of the big and small TEC 90
Table 27 Economic analysis for the present study 96
Table 28 Results from previous studies for comparison 97
Table 29 Characteristics of a PV panel 98
Table 30 Technical characteristics of TEGs 99
Table 31 Characteristics of IMM-Water-Pump 99
Table 32 Al_2O_3 Nano particle characteristics 101
Table 33 Comparison with other studies 109

Table 34 Parameters used for LCOE calculations 110
Table 35 LCOE calculations 111
Table 36 Comparison study with other literatures 123
Table 37 Economic parameters used to calculate LCOE 125
Table 38. Characteristics of the PV panel 127
Table 39 Comparison with other literature works 131
Table 40 Cost estimation of PV panels 133
Table 41 Economic analysis calculations 134

General description of work

The development of renewable energy in the world has become sustainable, and 10-20% of annual electricity generation is from renewable energy sources (REs) in developed and developing countries. The geographical location of countries such as India is near equatorial territories, which makes it possible to effectively use the most affordable renewable source, especially solar energy. However, in addition to the undeniable advantages of solar photovoltaic (PV) technologies has one significant drawback: at temperatures above 25 °C, the ambient temperature increases by 1 °C, and the efficiency of the PV panels drop by 0.5%. Thus, when heating the surface of the solar PV panels to 70 °C, the production efficiency decreases by 20-25%.

Hence, the present study is dedicated to developing the experimental study of ways to increase the efficiency of photovoltaic and thermodynamic solar power plants operating at high ambient temperatures.

India is the seventh-largest country and the most populous in the world, and it will be ahead of China in terms of population in 2022. India ranks third in the world regarding the installed capacity of all generating stations (450 GW). India is the seventh-largest country and the most populous in the world, and it will be ahead of China in terms of population in 2022. India ranks third country in renewable energy generation (about 38%). Although, India, in the field of solar energy generation, still needs to catch up to developed countries located in more northern latitudes (USA and China). The Government of India 2003 adopted the Electricity Law, which determines that by 2070 the use of renewable energy in India should be about 100%. Therefore, an increase in the share of production due to solar energy is of scientific interest. Therefore, in solar energy, they are alternate ways to develop and maintain and reduce the temperature of solar photovoltaic, which signifies the present study.

The degree of elaboration of the research topic: Research on the use of renewable energy sources for power supply to rural and isolated settlements and the development of power plants based on renewable energy sources were carried out by well-known Russian scientists were engaged in research on the use of renewable energy for energy supply and the development of power plants based on solar energy: Alekseev V.A., Alekseenko S.V., Alferov Zh.I., Amerkhanov R.A., Bezrukikh P.P., Butuzov V.A., Elistratov V.V., Kirpichnikova I.M., Strebkov D.S., Kharchenko V.V., Sheryazov S.K., Shcheklein S.E. and many others. Among the foreign scientists are Aoife Foley (Queen's University Belfast, UK), Soteris A. Kalogirus (Cyprus University of Technology, Cyprus), Tara Chandra Kandpal (India Institute of

Technology, Delhi, India), Ranga Pitchumani (Virginia Polytechnic Institute and State University, USA), Henrik Lund (Aalborg University, Denmark) and Christ N. Markides (Imperial College, London). However, none of the scientists have considered the influence of the Indian monsoon on the degree of insolation. Therefore, the present study, has focused on considering the influence of the monsoon in summer.

The purpose of the study:

Development and experimental study of ways to increase the efficiency of photovoltaic power plants operating at high ambient temperatures (on the example of the Republic of India)

To achieve this goal, the following tasks were set:

1. Study of the solar energy in the Republic of India, taking into account the influence of the monsoon in summer.

2. Calculation of the potential of solar stations using the sun tracking mechanism for the Southern regional states of India assessment of techno-economic analysis of these systems based on the application programs System Advisor Model (SAM), National Renewable Energy Laboratory, USA.

3. Development and experimental analysis of active and passive methods of reducing the temperature of solar photovoltaic modules to increase their efficiency in countries with hot climates, including in the southern territories of Russia.

The object of research: solar energy enhancement of PV panel efficiency of the Republic of India.

Research Subject: The subject of the study is ways to increase the efficiency of solar photovoltaic panels in areas of hot climate such as India.

Scientific novelty of the dissertation research:

1. The calculation of the solar energy potential for the territory of the Republic of India has been performed, considering the influence of the monsoon.

2. Designs of five experimental stands have been developed for studies of increasing the efficiency of solar PV panels with different (**active and passive**) cooling methods.

3. The results of an experimental study of increasing the performance of the solar PV panels with the use of a heat pipe for cooling the structure, allowing to increase the efficiency of the solar PV panels up to 3 %

4. The results of the application of the thermoelectric cooling method to increase the efficiency of the solar PV panels using a thermoelectric generator (TEG), which allows to increase the efficiency of the solar PV panels by 5%, are presented.

5. The results of an experimental study of an active method for increasing the efficiency of solar PV panels with the use of a heat exchange coil, nanoparticles from Al_2O_3 powder and TEG cooling, allowing to increase the efficiency of solar PV panels by 8.5%, are obtained.

6. The results of cooling the solar PV panels with a passive method using aluminium fins, which allows to increase efficiency by 4%, are presented.

7. The results of the application of a passive method of cooling the solar PV panels using aluminium reflectors and paraffin wax, which allows to increase the efficiency of the solar PV panels by 14%, are presented.

The main provisions of the dissertation submitted for defense:

1. The results of calculating the solar potential in the Republic of India, considering the influence of the monsoon.

2. Calculated results of using the sun tracking mechanism for the Southern regional states of India and a technical and economic analysis of these systems based on the System Advisor Model (SAM) application programs of the National Renewable Energy Laboratory, USA.

3. Results of development and experimental analysis of various active and passive methods of reducing the temperature of solar photovoltaic modules and increasing the efficiency of Solar PV panels for countries with hot climates.

The validity and reliability of the research results:

1. The scientific results obtained in the work are based on the classical provisions of the theory of renewable energy sources;
2. Satisfactory correspondence of the results of calculations obtained during experiments on full-scale samples during the days of peak solar intensity in the Urals with previously known experimental and theoretical data of other researchers;
3. The good agreement with the theory and laws in the field of thermodynamics, hydrodynamics, solar energy and other RES, performed using applications for calculating RES, such as PVsyst, System Advisor Model (SAM), Quantum Geographic Information System (QGIS), HOMER, RETScreen, as well as the results obtained by other authors and scientists.

Personal contribution: The author personally participated in:

1. Proposed a map of the territorial zoning of the Republic of India with the definition of the most effective zones for the placement of solar stations, taking into account the monsoon period.

2. Developed and installed five experimental stands, conducted a series of studies to improve the efficiency of various active and passive methods to increase the efficiency of solar power lines.
3. Theoretically and experimentally proved the effectiveness of the developed active and passive methods of increasing the efficiency of the solar PV panels at high ambient temperatures.
4. Performed processing and analysis of the data obtained, generalization and publication of research results and recommendations on the use of solar PV panels in the conditions of equatorial countries.

Approbation of Work: The research results were presented and discussed at the following international conferences, and at scientific conferences:

1. International Conference "Energy, Ecology, Climate 2020, July 6—July 16, 2020 (WCAEE-ICEEC-2020, Moscow);
2. XVII International Conference "Renewable and Small Energy - 2020. Energy efficiency. Autonomous power supply systems for stationary and mobile consumers (NRU Moscow Power Engineering Institute (MPEI), Moscow, Russia, April 23-24, 2020);
3. International Conference on the Latest Trends in Energy and Engineering (ICRTESE 2021) at the Rajiv Gandhi Institute of Petroleum Technology, Jais, Amethi;
4. International Conference on Materials for New Technologies-2021 (ICMET-21), Lovely Professional University, Phagwara, Punjab, India, February 18-19, 2022;
5. International Conference on Smart and Intelligent Systems – ICSIS 2023, Amrita Vishwa Vidyapeetham, Chennai, India, March 16-18, 2022;
6. XIX International Conference "Renewable and Small Energy – 2022". Energy saving. Autonomous power supply systems for stationary and mobile objects, Moscow Power Engineering Institute (MEI), Moscow, Russia, October 20-21, 2022.

Publications: A total of 22 articles were published on the international databases related Scopus and Web of Science that is related on the topic of the dissertation. Further, 3 papers are published in the Russian VAK Journals recommended by the Higher Attestation Commission.

The structure and scope of the thesis: The dissertation consists of an introduction, 5 chapters, a conclusion, a **218** bibliography. The total dissertation also consists of **175** pages, **97** figures, and **41** tables.

1 INTRODUCTION TO INDIA'S ENERGY GENERATION

With the increase in the population around the work simultaneously, there is an increase in the energy generation mix. However, in the late 18th-century, energy was generated using primary sources such as coal, diesel, and petrol [1]. These excess primary energy sources increased the Greenhouse Gases and depletion of the ozone layer. Therefore, most researchers around the globe have focused on Renewable Energy sources (REs) as an alternative energy source [2]. The REs sources are clean, reliable, and productive; using REs sources can decrease the global warming effect. Moreover, these REs that accepted around the world. According to the world statical reports presented in the Fig.1 shows leading Renewable energy sources in the world as of 2021 reports [3]. The figure shows that China is the top country with a 1012 GW share, followed by USA, Brazil, and India. On the hand, Russia stands in position with 56 GW worldwide. The present research is more focused on developing countries like India, which held the fourth position worldwide with 147 GW.

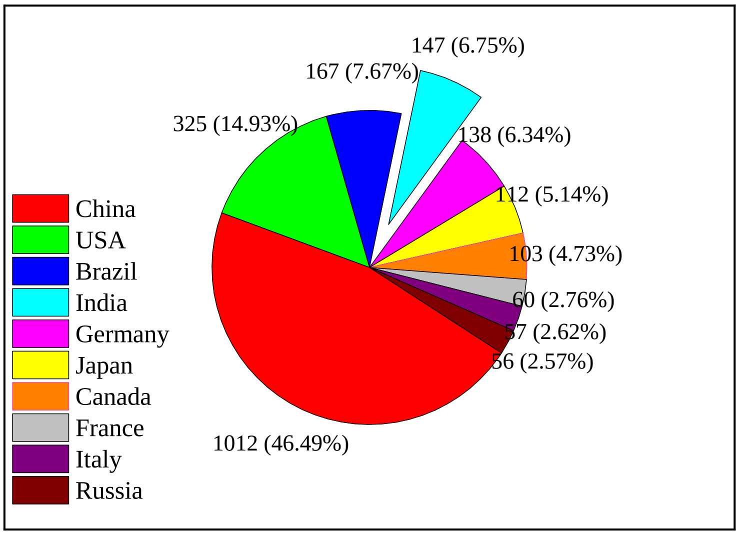

Figure 1 Leading countries generation of REs in the world by 2021 [3]

1.1 Overview of India

India is the seventh-largest country in the world. According to the census rate 2021, more than 1.5+ billion people are in India, and it is also the second-largest populated country in the world, next to China. Moreover, India has 28 states and eight union territories. Therefore, a large amount of energy is required for the country. However, according to the sources, India is ranked top of the world's fastest-developing, with an average increase of 7.2 % GDP countries shown in Fig.2. [4].

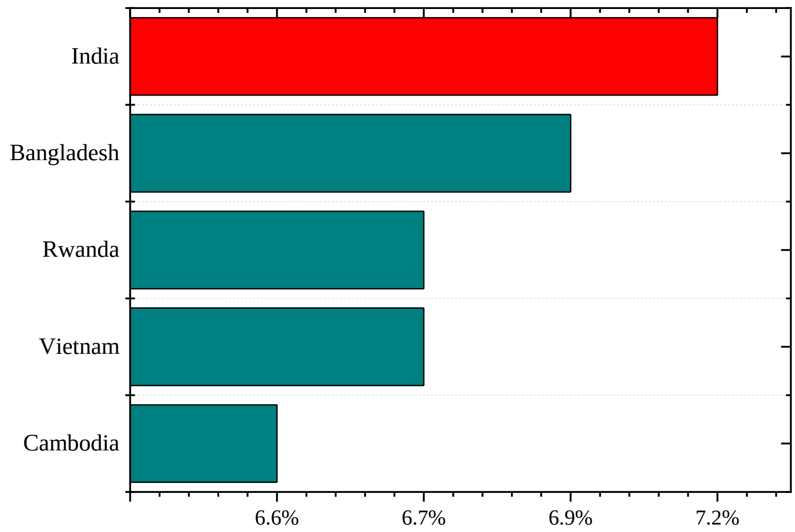

Figure 2 Fastest economic develop countries in the world [4]

1.2 Current State of India's Energy India

The reports of the Ministry of New Renewable Energy (MNRE) of India 2021. The country installed a total of grid of 400 GW for power generation through different energy mixes, as shown in Fig.3 [5]. Moreover, coal has an over 50% share in energy generation, followed by REs sources such as wind and solar projects sharing 27.5%. Furthermore 11.7 % shared by small and large hydro-power plants in the country.

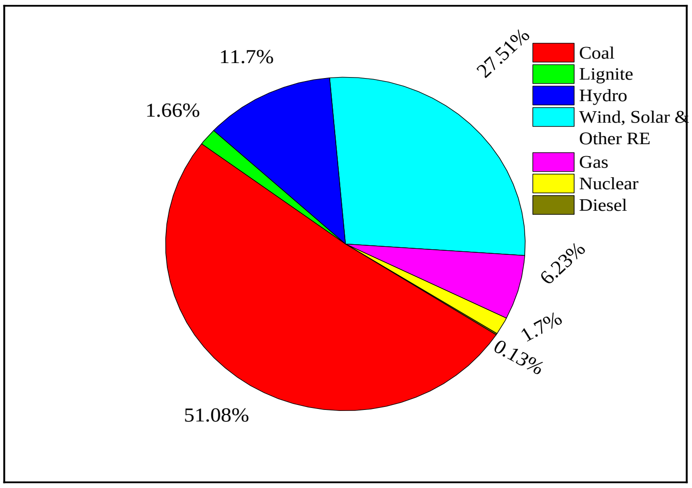

Figure 3 Energy Mix in India, 2021 [5]

India has more than five largest wind farms and over 40 solar large-scale projects in various states installed capacity of above 1MW. The total energy generated by these REs at the end of March 2021 is around 40.2 GW. However, the Bhandla Solar project is recorded as the world's largest solar park as of 2021, with a total installed capacity of 2.245 GW, as shown in Fig.4 [6]. Moreover, the Muppandal wind power plant, Tamil Nadu, is the largest wind farm installed capacity of 1.5 GW in the nation as shown is Fig.5 [7]. In addition, India has around

197 small and large-scale hydropower plants. The Tehri hydropower complex, Uttarakhand, is the largest hydropower plant in the country, with an installed capacity of 2.4 GW, as shown in Fig.6 [8]. Furthermore, India has a 150 kW Pilot wave energy plant at Vizhinjam, Kerala. The Vizhinjam world's first wave plant that was operating oscillating water column technology since 1991, as shown in Fig.7 [9].

Figure 4 Bhadla Solar Power Project, Rajasthan [6]

Figure 5 Muppandal wind Farm, Tamil Nadu [7]

Figure 6 Tehri Hydro Complex, Uttarakhand [8]

Figure 7 Vizhinjam wave energy, Kerala [9]

1.3 India’s strategy reduction in GHG emissions

India is one of the top countries producing carbon gas emissions, which causes depletion of the ozone layer. India has a history of contributing GHG gases since the 19th century. Therefore, India adopted new strategies to decrease GHG gases, such as reducing the lower by 1 billion tonnes of carbon by the year 2030 and generating energy by 50% by REs. However, the commission to achieve zero carbon intensity is planned by 2070.

1.4 India's existing energy policies

India, like developing countries, should work on policies for the RE mix. These energy policies can help increase the development of countries' economies. Therefore, the government of India set has energy policies are

1.4.1 Electricity law, 2003 [10]

The electricity act 2003 was introduced as the first imposed by the government of India. Earlier to this law government of India is guided by several laws such as the electricity act, 1910; the supply act, 1948; electricity commission regulatory law,1998. However, in early 1947 India was ruled by the British crown. Moreover, the 1910 act is not a part of the Indian government act. After colonization in 1947, the Indian government found considerable difficulties implementing these electricity laws. Therefore, the Indian government 2003 strictly enforced the electricity law 2003. The law is consolidated for the development of Industries, transmission, distribution, generation, etc.;

1.4.2 National electricity policy law, 2005

The government adopted the national electricity policy law in 2005. The policy aims to achieve the following objectives to supply electricity to all the households, per capita electricity should be increased, the Minimum lifeline consumption of electricity should be increased from 1 unit per head to 10 units per head by 2012, and the viability of electricity sector and protection of consumers’ interests.

1.5 Status of India’s Renewable Energy of sources

Electricity generation using Renewable energy is recommended and considered one of the best options because it is clean, reliable, economical, and soundless. Therefore, RE sources such as solar, wind, hydro, and wave play a crucial role in the development of the energy sector. However, as discussed earlier, in section 1.3, the power ministry has targeted developing India's energy sector to reduce GHG gases by 2070 and increase the generation of electricity using REs. In the present section, current existing REs in India.

1.5.1 Tariff policy, 2006

The power ministry 2006 proposed for the first time a tariff policy. The tariff policy included a renewable energy electricity generation mix. The significant aim of this policy is to purchase some percentage of energy and generate electricity for the households. Moreover, the rate for energy purchase that is applicable to the tariffs will be fixed by State electricity regulatory commission from the starting session of the budget (i.e., April 1, 2006) [11].

1.5.2 Solar power potential in India.

India is a densely populated country next to China, with high solar radiation. For the generation of electricity, immense energy is required. Therefore, the government of India launched a national program under the scheme of late prime minister Jawaharlal Nehru in 2009 and announced the construction of 20 GW of solar power plants by 2022. In 2014 the existing government gradually increased the capacity from 20 GW to 100 GW in solar power potential strength. Accordingly, information from Solargis India's global horizontal irradiance is 5.4 to 6.2 kWh/m2. Indeed, the top-most part of India is near Mount Everest, so in winter, there is a consequence in climatic conditions. Fig.8 shows the total installed capacity of the solar power plant in India by March 2022 was 174 GW. Figure 8 observes the construction of power plants in India has increased in the last five years.

1.5.3 Wind potential in India

India can generate electricity through its wind speed; as of now, India has installed over 40.53 GW. According to the reports, wind speed capacity can be southern, western, and eastern directions of India. The power costs in India have been rapidly decreasing since 2017[12]. Moreover, the government of India commissioned a plan to develop 5 GW by 2022 and 30 GW by 2030 offshore wind to dedicate to the nation. Nevertheless, the ministry of new renewable energy will be the nodal point of contact with state governments developing offshore wind in India. For that, India required potential sites to locate offshore wind sites[13]. Therefore, the average wind speed lasting from 5m/s greater than 6.7m/s is the target for India's wind plants. Fig.9, the development of wind capacity in India

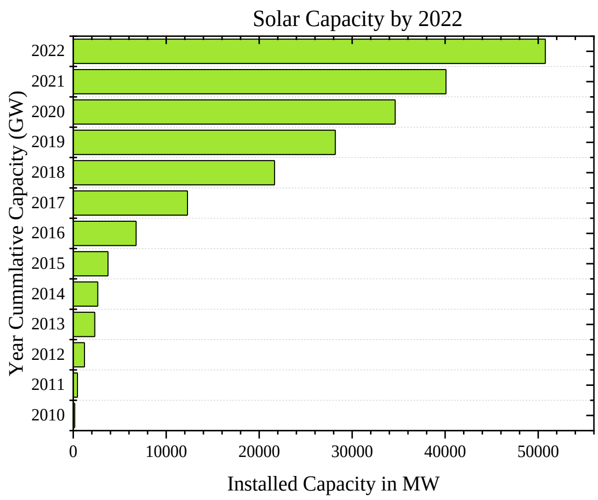

Figure 8 Installed Solar Capacity 31st March 2022

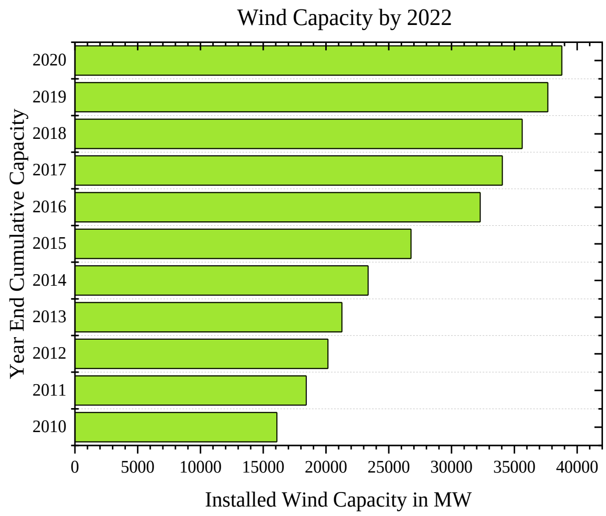

.

Figure 9 Installed Wind Capacity 31st March 2020

1.5.4 Hydroelectrical potential in India

Globally, India ranked 5th largest Hydropower by capacity. As to the reports, India has installed large-scale hydropower plants 46 GW and other small hydroelectric power plants with a total capacity of 4.683 GW Moreover, the hydroelectric potential identified by the government of India is estimated at a large scale of 148.83GW, a small scale of 6.78 GW (i.e., capacity is less than 25 MW), and 56 potential sites with pumped storage are actively working with the ability of 94 GW. The central government of India has planned to develop large-scale river basins for the Godavari, Madurai, Vamsadhara, Mahanadi, and Narmada, but it doesn't work because of the opposition of tribal people residing in the country [14].

1.5.5 Wave Potential for India

India has the potential to meet the generation of electricity by 54 GW (i.e., tidal and wave) by ocean energy. However, the estimation assumption is based on theoretical but does not necessarily constitute a practically exploitable potential. In fact, for 40 years, India started efforts to assess and harness tidal power, yet it has not achieved a breakthrough. According to Prof. Prasad Kumar Bhaskaran, India has a high potential to extract tidal energy from the east and west coast of the country. Still, the significant disadvantage is a lack of technology. However, India has potential in the southern states; the high waves are active in monsoon seasons [15]. Moreover, it is the potential to develop on the Kerala coast. There are other reasons from the ministry of new and renewable energy for not pursuing tidal energy as a high investment cost. However, many efforts were made by the government to extract tidal power from the sea coast. For instance, in 2007 and 2011, India developed two significant projects in Gujarat and the West Bengal coast with 50 MW and 3.75MW, respectively. The selected projects dropped because access budget, and the government added a statement for every MW. The amount spent on the project was INR 63.50 Crores in Durgaduani, West Bengal, while for the Gulf of Kutch in Gujarat, the total money spent for every megawatt was INR 15 Crores.

1.5.6 Biomass Potential for India

Biomass is also an alternative form of energy generation in India, accounting for 14% of energy generation consumption in India. According to Ghosh et al. [16] the current biomass availability of more than 5 million metric tons per year. The anticipation of biomass for each year is 150 million metric tons per year, almost equal to 1.8 GW. However, India currently uses its biomass for electricity generation is 32%. Figure 10 shows the classification of biomass potential in India.

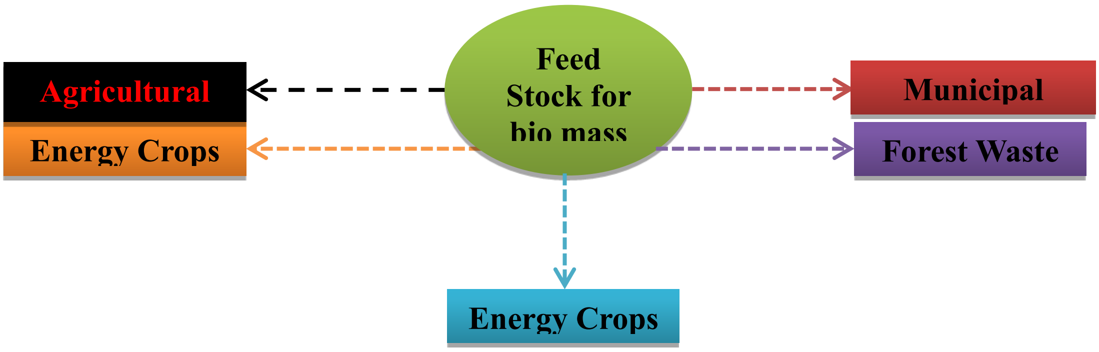

Figure 10 Classification of Biomass energy in India [17]

2 EXPERIMENTAL INVESTIGATION INCORPORATED WITH DIFFERENT COOLING MECHANISMS FOR THE IMPROVEMENT EFFICIENCY OF THE SOLAR PV MODULE

Electricity exhibited from solar PV is one of the best technologies and is a vital RE sources based on availability. The continuous advancements in solar energy that has widely accepted by experiments. However, a temperature rise will affect the output arrangement with such enhancements to PV panels. Improving in the temperature of each 1 ˚C in the ambient temperature drops the output performance of a PV panel. Therefore, researchers embraced recent technologies to remove heat dissipation from the solar PV panels viz passive and active cooling methods. In simple words, the passive cooling (i.e., fins, PCM) method does not require external forces to cool down the PV panels. In discrepancy, the active cooling meets an external force (i.e., fans, water, ultrasonic) to cool the PV model.

In recent years, experimenters proposed several technologies to minimize the temperature of PV modules and control heat dissipation from solar PV panels, including passive and active cooling. Preet et al. [18] performed an experimental investigation using water-based PV/T-PCM and water-based with a double absorber plate at different mass flow rates. Their study reveals that PV/T-PCM showed more effective results than the conventional and PV/T systems. Abdallah et al. [19] investigated four cooling methods: perforated rib sink, PCM, ducted fins forced convection, and galvanized ducted with forced convection. The study showed that the PV panel incorporated with ducted fins forced convection has a relatively low temperature of about 39 ˚C. Nisar et al. [20] performed an experimental investigation on floating solar PV panels. The outcome of their study is that if the water is fully covered, then the reduction is 28% in evaporation, while the water is partially covered, then the reduction in evaporation is 17%, respectively. B et al. [21] approached plant cooling, greenhouse cooling, PCM, and coir pitch for a 50 W PV panel. The critical finding from work in the maximum power output found in coir pitch and the maximum temperature reduction found in plant cooling + greenhouse. Raina et al. [22] used integrated rectangular fins in the PV module in hotter and colder climatic conditions in New Delhi, India, and Bergen, Norway. Preliminary results showed that the average temperature reduction for more desirable hot climatic conditions is 10 ˚C, and for the colder climatic, temperature reduction remains unchanged. Kabeel et al. [23] investigated the performance of PCM and finned plate solar air heaters. They concluded that the improvement in the daily efficiency is 10.8-13.6% by integrating PCM with solar air heater. Browne et al. [24] employed PV/T with PCM for the examination of the thermal performance of a PV module. The performance results show that the temperature reduction for the modified system with PV/T-PCM is 6 ˚C. Furthermore, Agyekum et al. [25–27] performed three experiments by employing Aluminum with a cotton wick, PCM, and an ultrasonic humidifier. Their study shows that the average reduction in temperature and improvement in electrical efficiency is from 12-24 °C and 5-12%, respectively. Al-Waeli et al. [28] proposed a new thermal enhancement method, i.e., water filled with PCM and nano-particles. The authors found an improvement in PV efficiency from 8 to 13%.

On the other hand, Zubeer et al. [29] performed an experimental investigation on a CPV system and the concentrated PV with a water cooling system that flows on the front surface of the PV panels. Their study showed that the improvement in the temperature reduction, electrical efficiency, and energy payback time is 48.5%, 17.7%, and 3.23 yr. Lebbi et al. [30] designed a new hybrid PV/T Bi fluid system to improve electrical performance. The hybrid system cooled the forced air circulation at the rear side of a PV panel and self-cooled the front side with water. Their study found that temperature reduction and improvement in electrical efficiency are 15 ˚C and 5.7%, respectively. Murali et al. [31] examined the enhancement by developing a solar tunnel dryer using mobile shrimps. The observed results from their study found that the average temperature reduction was 20 ˚C, and electrical efficiency improved to 12%. Navakrishnan et al. [32] implemented thermal energy storage with two heat transfer fluids to enhance the PV module. Their study results show that the temperature drop is 7.5 °C, and the improvement in electrical efficiency is 15%. Gad et al. [33] also employed different PCMs for summer and winter to improve the thermal performance of a PV panel. Their study results showed that PCM SP31 gel with 3 cm thickness had a better performance in summer, while the PCM SP15 gel with 2.5 cm had a better performance in winter. Moreover, the average reduction in temperature in summer is 20.6 ˚C, and an improvement in efficiency is 11.5%. In contrast, the temperature reduction was found at 14.1 ˚C for the winter, and the efficiency improvement was 7.2%. Bevilacqua [34] et al. proposed a thermal model proposed a thermal model including spray cooling to improve the thermal performance of a PV module. They observed the average increase in electrical power was 7.8 %. Eliminshawy et al.[35] performed an experimental investigation with an integration buried heat exchanger on the rear side of a PV model. The experimental results revealed that the temperature reduction in a cooled PV panel is about 15 °C, and the maximum thermal efficiency of the cooled PV panel is 45%. The literature review covered by supra, shows that much work has been completed globally to improve a PV module's thermal efficiency. Therefore, the present study also aimed to improve the efficiency of a PV module by incorporating CPU heat sinks, thermoelectric cooling, PVT/TEG/nanofluids as a active cooling approach, and irregular brush-shaped aluminium fins and low-cost aluminium reflectors/PCM/ZnO nano-particles are examined experimentally as a passive cooling approach. The experimental investigations are examined under actual weather conditions in a Ural Federal University, Yekaterinburg City, Russian Federation.

2.1 Thermodynamic Calculations

As we know, energy, exergy, and entropy generation calculations evolved with the thermodynamics analysis. Therefore, in the present, a detailed thermodynamic analysis was presented.

2.1.1 Energy Efficiency Balance

Energy efficiency is also well known as the first law of thermodynamics, and it is quantitative measurement. Energy efficiency illustrated as the ratio of energy output (P_{out}) from the PV panel to the energy input (P_{in}). The energy efficiency of a PV panel expressed in **Eq. (1-6)**. [36–38]

$$\eta = \frac{P_{out}}{P_{in}} = \frac{V_{oc} I_{oc} FF}{A I_s} = \frac{\dot{E}_{x_{sun}}}{A I_s} \tag{1}$$

Where, Power output (P_{out}), and Power input (P_{in}), V_{oc} is open circuit voltage, I_{oc} is shor-circuit current, FF is the filling factor

$$P_{out} = V_m I_m = \dot{E}_{x_{ele}} \tag{2}$$

Here V_m, I_m subjected to Voltage (V), and Current (A) obtained from the experiment, recorded by the clamp meter [39]

$$P_{in} = A I_s \tag{3}$$

Also, I_s, is the solar radiation recorded solar power meter (W/m^2), and A is the area of a PV panel (m^2).

The net effect of a result as shown in Eq. 4 because the impact of short circuit impact increase slightly, as decrease in in the open circuit and filling factor [40,41]

$$\eta_c = \eta_{Tref}[1 - \beta\left(T_c - T_{ref}\right) + \gamma log_{10} I(t) \tag{4}$$

The solar efficient can be taken as zero, now Eq.4 will be modified to Eq. (5) [42–44]

$$\eta_c = \eta_{Tref}[1 \beta_{ref}\left(T_c - T_{ref}\right) \tag{5}$$

Where, η_{Tref} is standard reference temperature taken 15%, β_{ref} is the temperature coefficient taken as 0.004/K[45].

The improvement of efficiency of a cooled PV panel can be estimated by **Eq. (6)** [46].

$$\eta_{improvement} = \left(\frac{\eta_{cooled,PV}}{\eta_{ref,PV}} - 1\right) \times 100\% \tag{6}$$

2.1.2 Exergy Efficiency Balance

In thermodynamics, the exergy is the qualitative measurement of work. Hence, exergy is defined as the maximum function that a substance can perform, which is potential can be converted into work. In other terms is defined as the ratio of the total output of exergy to the total input in exergy. The exergy balance of the present study is shown in **Eq. (7).** [47,48]

$$\psi_{System} = \frac{Ex_{out}}{Ex_{in}} \tag{7}$$

The exergy output by the PV module is given by **Eq. (8)**. [48–51]

$$Ex_{out} = V_m I_m - \left(1 - \frac{T_a}{T_{cell}}\right) hA(T_{cell} - T_a) \tag{8}$$

Where T_a is the ambient temperature during the day of the experiment (K), T_{cell} cell temperature at the time of the experiment (K), h_c is the convective heat transfer, A is the total surface of the PV Panel (m^2).

The convective heat transfer of a PV module is estimated in (W/m^2.K) **Eq. (9).** [52,53]

$$h_c = 5.7 + 3.8v \tag{9}$$

Where, v is the wind speed during the experimental day (m/s)

The exergy input of a PV module is given by **Eq. (10).** [39]

$$Ex_{in} = \left(1 - \frac{T_a}{T_s}\right) AI_s = \dot{E}_{x_{sun}} \tag{10}$$

Here, T_s is the surface temperature that assumed to be 5762 K

The exergy efficiency of the PV can be obtained from **Eq. (11).**

$$\psi_{System} = \frac{V_m I_m - \left(1 - \frac{T_a}{T_{cell}}\right) h_c A(T_{cell} - T_a)}{\left(1 - \frac{T_a}{T_s}\right) AI_s} \tag{11}$$

2.1.3 Entropy generation

Entropy is the third law of thermodynamics, a quantitative measure in thermodynamics. The calculation of entropy generation suggests the total amount of irreversibility available in the system. The entropy generation of a PV module is given in **Eq. (12).** [54,55]

$$\dot{S_{gen}} = \frac{\dot{E}_{x_{lost}}}{T_{amb}} \tag{12}$$

Where, $\dot{E}_{x_{lost}}$ is the lost exergy in the system (W/K), expressed in the **Eq. (13).** [56,57].

$$\dot{E}_{x_{lost}} = \dot{E}_{x_{sun}} - \dot{E}_{x_{ele}} - \dot{E}_{x_{th}} \tag{13}$$

Where, thermal exergy is calculated using **Eq. (14).** [58]

$$\dot{E}_{x_{th}} = \left(1 - \frac{T_a}{T_{cell}}\right) hA(T_{cell} - T_{amb}) \tag{14}$$

Finally, the entropy generation is computed by using **Eq. (15).**

$$\dot{S}_{gen}(\frac{W}{K}) = \frac{\left(1 - \frac{T_a}{T_s}\right) I_s A - V_{mp} I_{m_p} - \left(1 - \frac{T_a}{T_s}\right) hA(T_{cell} - T_a)}{T_{amb}} \tag{15}$$

2.2 Economic Analysis

Economic analysis (LCE) is one of the significant parameters in Renewable energy sources. The crucial role of LCE analysis entails the cost and energy products. The objective of LCE in the present study is to determine whether the project may move further or if modifications are needed. The following parameters that are used in calculation of economic analysis **Eq. (16-18)** [59–61]

$$K_{O\&M} = \frac{1 + r_n}{1 + i_{eff}} \tag{16}$$

Where, r_n is the nominal discount rate (%), i_{eff} is the effective discount rate (%).

$$CRF = \frac{i_{eff} \times (1 + i_{eff})^n}{\left((1 + i_{eff})^n\right) - 1} \tag{17}$$

Here, CRF is capital recovery factory (%), n is life time of a PV Pant

$$CELF = \left(K_{O\&M} \times \frac{1 - K_{O\&M}^n}{1 - K_{O\&M}}\right) CRF \tag{18}$$

Where, $CELF$ is Constant escalation levelization factor

Furthermore, Levelized cost of operation & management $LC_{O\&M}$ given by **Eq. (19).**

$$LC_{O\&M} = C_{O\&M} \times CELF \tag{19}$$

Here, $C_{O\&M}$ is the cost of operation and management annually

Moreover, investment cost of a PV project is presented in **Eq. (44).**

$$LC_{inv} = CRF \times C_{inv} \tag{20}$$

Where, C_{inv} is the initial investment of a PV Project

Finally, the levelized cost of energy of a system ($LCOE_{Sys}$) calculated by **Eq. (45).**

$$LCOE_{Sys} = \frac{LC_{inv} + LC_{O\&M} + LC_{fuel}}{E_{annaual}} \tag{21}$$

2.3 Uncertainty analysis

The role of uncertainty error analysis is to measure the error in the experiment. Nevertheless, the experimental uncertainty may occur because of environmental conditions, handling of equipment, and operating conditions. A few specific types of equipment were used to calculate uncertainty analysis in the present investigation. The total uncertainty achieved from the present research is shown in the list below **Table 1**. For instance, the accuracy of a specific device in B_z the **Eq.22**. will help achieve the total uncertainty is A_z in the experiment. However, information about accuracy will be available from the manufacturers [62–64].

$$A_z = \frac{B_z}{\sqrt{3}} \tag{22}$$

The total uncertainty $P(X)$ can be achieved is presented in **Eq. (23).**

$$\begin{aligned} P(X) = Square\ root\ of\ [&(Uncertainity\ of\ Pyranometer)^2 \\ + &(Uncertainilty\ of\ \text{thermocouple})^2 \\ + &(\text{Uncertainity of clamp meter})^2 \\ + &(\text{Uncertainity thermometer})^2 \\ + &(Uncertainity\ of\ digital\ anemometer^2)\ ] \end{aligned} \tag{23}$$

Table 1 Uncertainty achieved from the experiment [25,26,65,66]

Measuring Device	Units	Range	Accuracy (%)	Uncertainty (%)
Thermometer	˚C	-30 to 70	±2	1.15
Clamp Meter		-	±3%	1.732
Wind velocity	m/s	0-30	±3	1.732
TM-207 Pyranometer	W/m^2	0-2000	±5	2.886
K type Thermocouple	˚C	–270 to 1260	±0.75	0.433

The total uncertainty achieved from the experiment by using measurement devices such as thermometer, clamp meter, digital anemometer, pyranometer and thermo couple is 3.23%.

3 TECHNO-ECONOMIC FEASIBILITY OF SOLAR PV PLANTS IN INDIA

In this section, a techno-economic assessment of solar PV plants accessed for eleven locations in republic India is studies. Simultaneously, the results of feasible locations for the installation of solar PV plants are discussed.

3.1 Comparative analysis for solar tracking mechanism of solar PV plants in five unique climatic conditions in Southern India

In this section, a techno-economic assessment of a solar tracking mechanism of a PV plant for five south-Indian states which have a unique weather condition are discussed and presented.

3.1.1 Operation of solar tracking mechanism

In the present study, we considered three solar tracking mechanism that are prominently known as fixed tracking mechanism (FT), single axis tracking mechanism (SAT), and dual-axis tracking (DAT) mechanism [67] [68]. The FT mechanism is fixed to its position and it can't change its position with respect to sun [69]. Therefore, to increase the efficiency and achieve maximum energy from the sun to solar PV plants, several researchers are focused on the tracking mechanism and found that solar tracking mechanism is can be alternate option for the fixed tracking mechanism[70]. There are two type different type of mechanism Viz., SAT, and DAT [71]. The SAT mechanism can alter its position in a single direction either horizontal or vertical. While for the DAT mechanism can change it position on all the direction according to the movement of sun [72].

3.1.2 Solar resources data in South India

India has different zones i.e., north, south, east and west sections. In the present study, we conducted a techno-economic assessment for the large-scale solar PV plants only for south-Indian states where there is a high potential solar radiation. The south-Indian states selected for the assessment are namely Andhra Pradesh, Tamilnadu, Kerala, Karnataka, and Telangana. Hence, from each state one potential location is selected for the techno-economic assessment i.e., Vishakhapatnam (VSKP), Madurai (MDU), Thiruvananthapuram (TVC), Bangalore (SBC), and Hyderabad (HYD) for Andhra Pradesh, Tamilnadu, Kerala, Karnataka, and Telangana, respectively. Further, all the selected locations have a unique climatic weather condition. The selected potential sites have a certain limitation such that the site is must be economically developed, available transportation facilities from all the possible ways. The geographical coordinates, technical parameters, and financial parameters for the present study, for the selected sites are presented in **Table.2, Table.3, and Table.4**. Similarly, selected potential sites are presented in **Fig.11.**

Table 2 Selected location in southern Indian states.

Region	Location	Lat (^{0} N)	Long (^{0} E)	DNI (kWh/m^2/day)	GHI (kWh/m^2/day)
Andhra Pradesh	VSKP	17.68	83.21	4.6	5.4
Telangana	HYD	17.38	78.48	4.8	5.7
Tamil Nadu	MDU	9.92	78.11	5.0	5.9
Kerala	TVC	8.48	76.95	4.5	5.5
Karnataka	SBC	12.97	77.54	5.5	5.8

Table 3 Technical parameters for the present study

Description	Characteristics	Value	Reference
System Design	Modules pers string in subarray	12	[73]
	Strings in parallel subarray	53744	[73]
	Modules in subarray	64,488	[73]
	Strings in V_{oc} at reference condition	772.8 V	Calculated by SAM
	Strings in V_{mp} at reference condition	656.4 V	Calculated by SAM
Inverter	**Model: Yaskawa Soleectria Solar: SGI 750 XTMM**	-	
	Total Number of Inverters	22	[73]
	DC to AC ratio	1.21	Calculated by software
	Name Plate DC capacity	20 MW_{dc}	Calculated by software
	Total Inverter capacity	17 MW_{dc}	Calculated by software
	Maximum DC Power	0.78 MW_{dc}	Calculated by software
	Power used during operation	3.71 kW_{dc}	Calculated by software
	Maximum DC voltage	820 V_{dc}	Calculated by software

	Maximum AC current	1263.77 A_{dc}	Calculated by software
	Minimum MPPT DC Voltage	545 V_{dc}	Calculated by software
	Maximum MPPT DC Voltage	820 V_{dc}	Calculated by software
Module Characteristics			
Manufacturer	SunPower SPR-E19-310-COM		
Physical Characteristics	Material: Mono-c-Si		[74]
	Module Length	1.631 m	Calculated by software
	Module Width	1 m	Calculated by software
Lifetime and Degradation	Total Irradiance	1000 W/m^2	Calculated by software
	Cell Temperature	25 ^{0}C	Calculated by software
	Maximum Power	310.149 W_{dc}	Calculated by software
	Maximum Power Voltage	54.7 V_{dc}	Calculated by software
	Maximum Power Current	5.7 A_{dc}	Calculated by software
	Open Circuit Voltage	64.4 V_{dc}	Calculated by software
	Short Circuit Current	6.0 A_{dc}	Calculated by software
	Annual DC degradation rate	0.5 % /year	[75][73][76]

Fig. 12. depicts that module characteristics for solar PV panel obtained from the SAM model. Although the solar model is manufactured by the company American energy sage with the Department of Energy, America. Since such type of the material for the development of model of technology is Mono-c-si, and the cost for the production of such solar technology is

around 0.40 $/Wdc. Simultaneously, **Fig.13.** depicts efficiency curve parameter of a solar PV panel that is obtained from the SAM model program shows the inverter efficiency curve selected for the present study. Hence, the Yaskawa Solectria Solar company is also designed by the U.S. company and the cost of those inverter is also achieved from the SAM program is 0.06 $/Wdc.

Figure 11 Selected potential sites in south Indian states

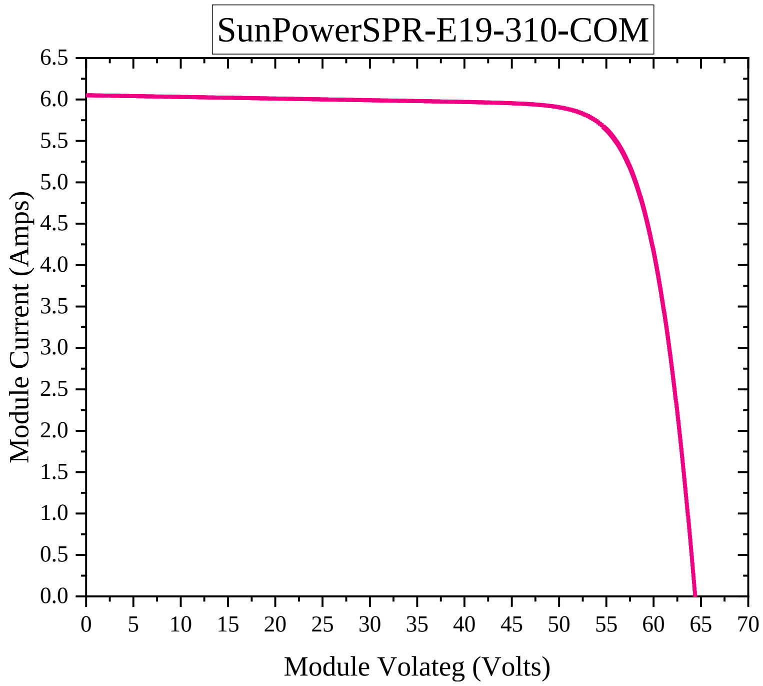

Figure 12 Module Characteristics at reference conditions

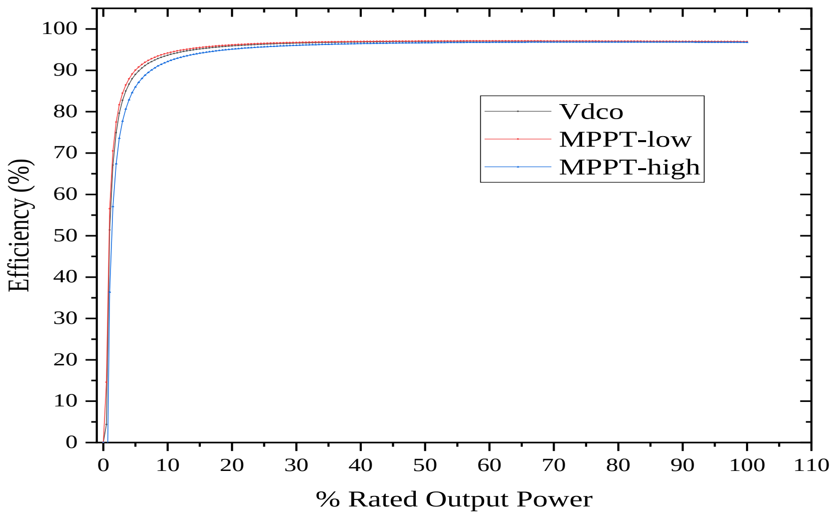

Figure 13 Efficiency curve of Inverter

Table 4 Financial Parameters for the study

Description	Financial Parameter	Value	Reference
Analysis parameter	Analysis period	25 Years	[77,78]
	Inflation rate	2.9 % / Year	[79,80]
	Real discount rate	10 % / Year	[81–83]
	Nominal discount rate	13.19 % / Year	Calculated by SAM
Project tax	Federal income tax rate	25 % / Year	[84]
	State income tax rate	6.5 % / Year	[85]
	Sales tax	5 % of total direct	[86]
	Internal rate of return	11%	Information from the experts

3.1.3 Weather performance of the selected sites

The weather performance for south Indian states is presented in this section. The wind speed profile for all the of all the selected sates is depicted in **Fig.14**. From the findings it was found that the average annual wind speed for the selected VSKP, MDU, TVC, SBC, and HYD are 4.72 m/s, 2.81 m/s, 3.53 m/s, 3.44 m/s, and 3.20 m/s, respectively. It was also observed that the average wind speed is recorded highest for the VSKP site, and low for MDU site, this is because of VSKP site is located to the coastal areas of Andhra for Andhra Pradesh. While, MDU location is central area of Tamil Nadu state. Furthermore, weather characteristic global horizontal irradiance (GHI) is depicted in **Fig.15.** From the observation it can be stated that GHI for all the locations is high from March to May because of solar radiation is high during this period. Simultaneously, there is a drop in GHI from June to November due to rainy and winter seasons that covers clouds and causes effect to the solar radiation. Finally, it can be concluded that the GHI is starts is increasing slowly from December to February due to increase in solar radiation in the solar PV plant.

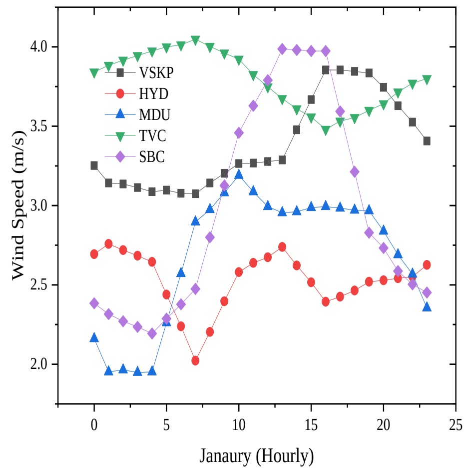

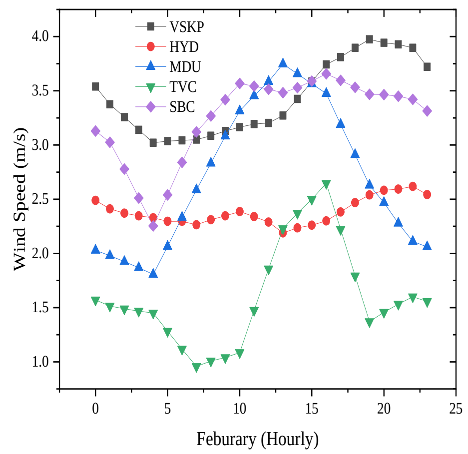

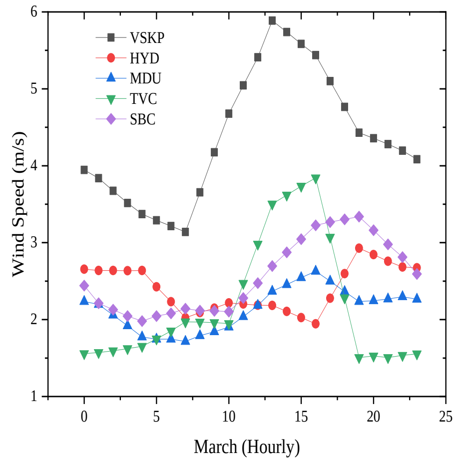

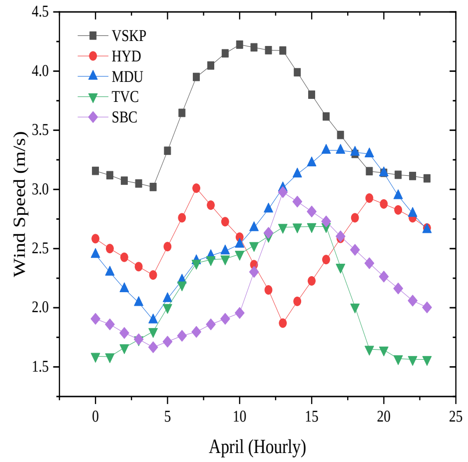

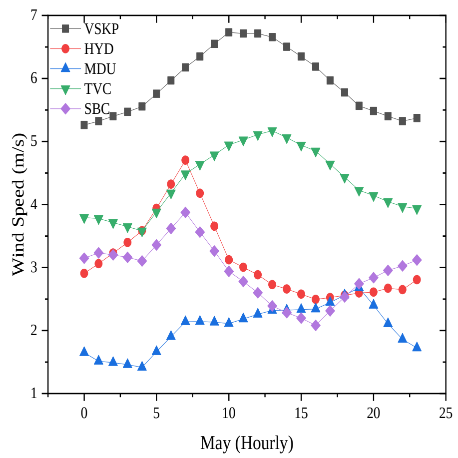

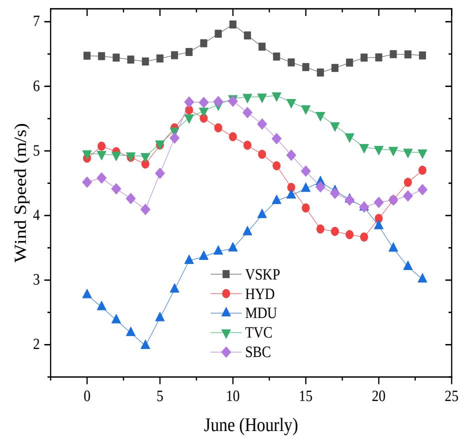

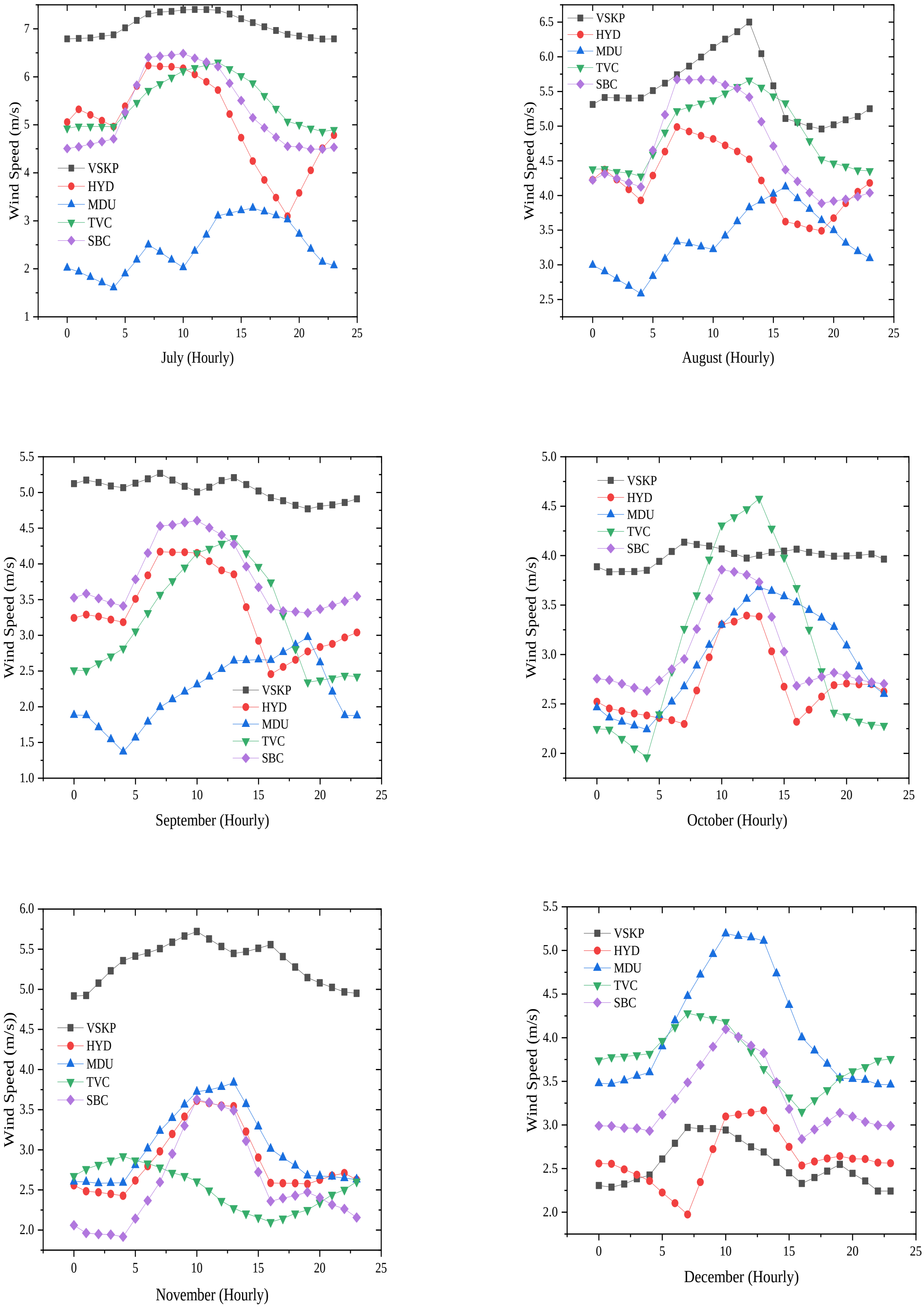

Figure 14 Wind speed data for south-Indian states

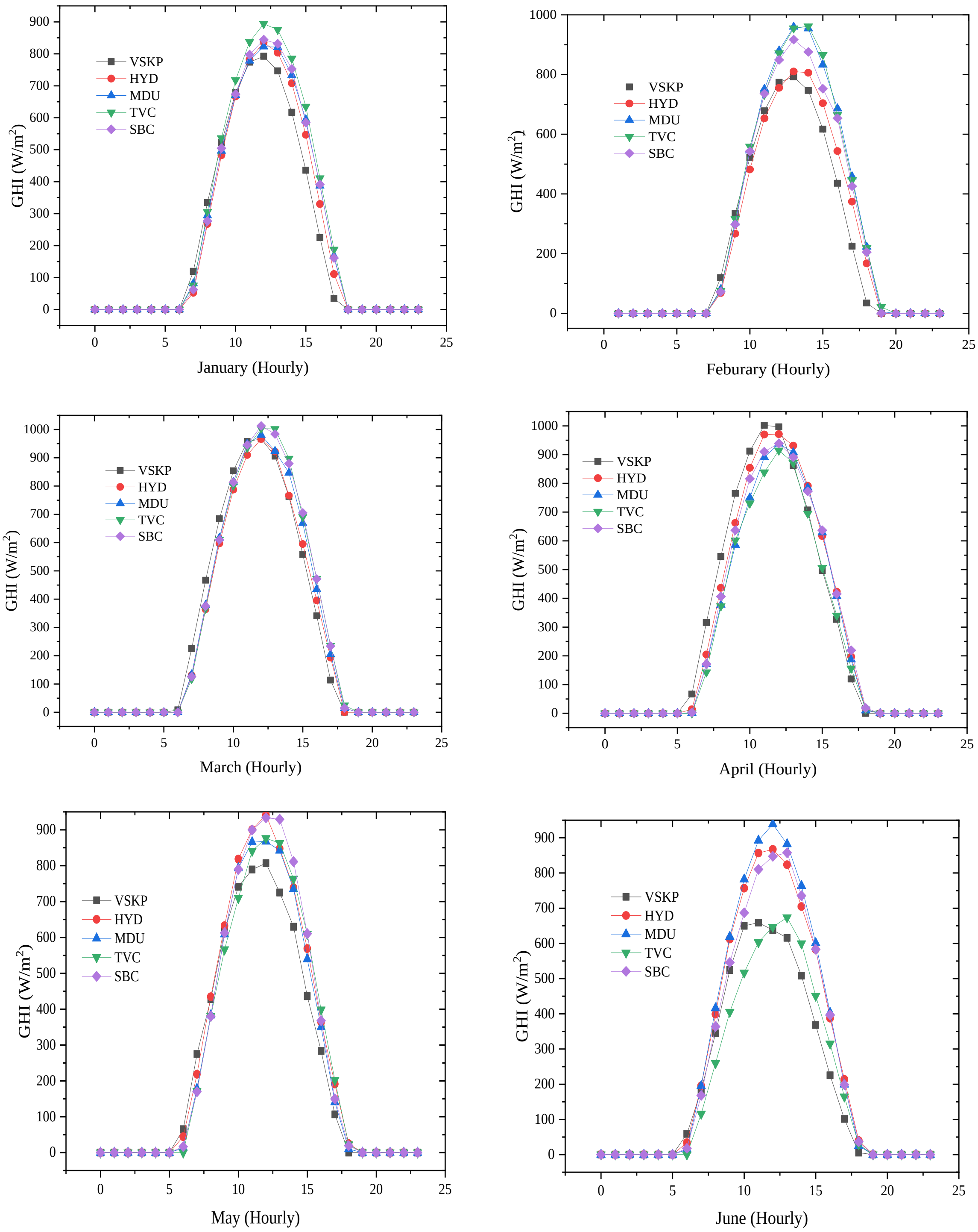
GHI (W/m^2)
VSKP
HYD
MDU
TVC
SBC
January (Hourly)
Feburary (Hourly)
March (Hourly)
April (Hourly)
May (Hourly)
June (Hourly)

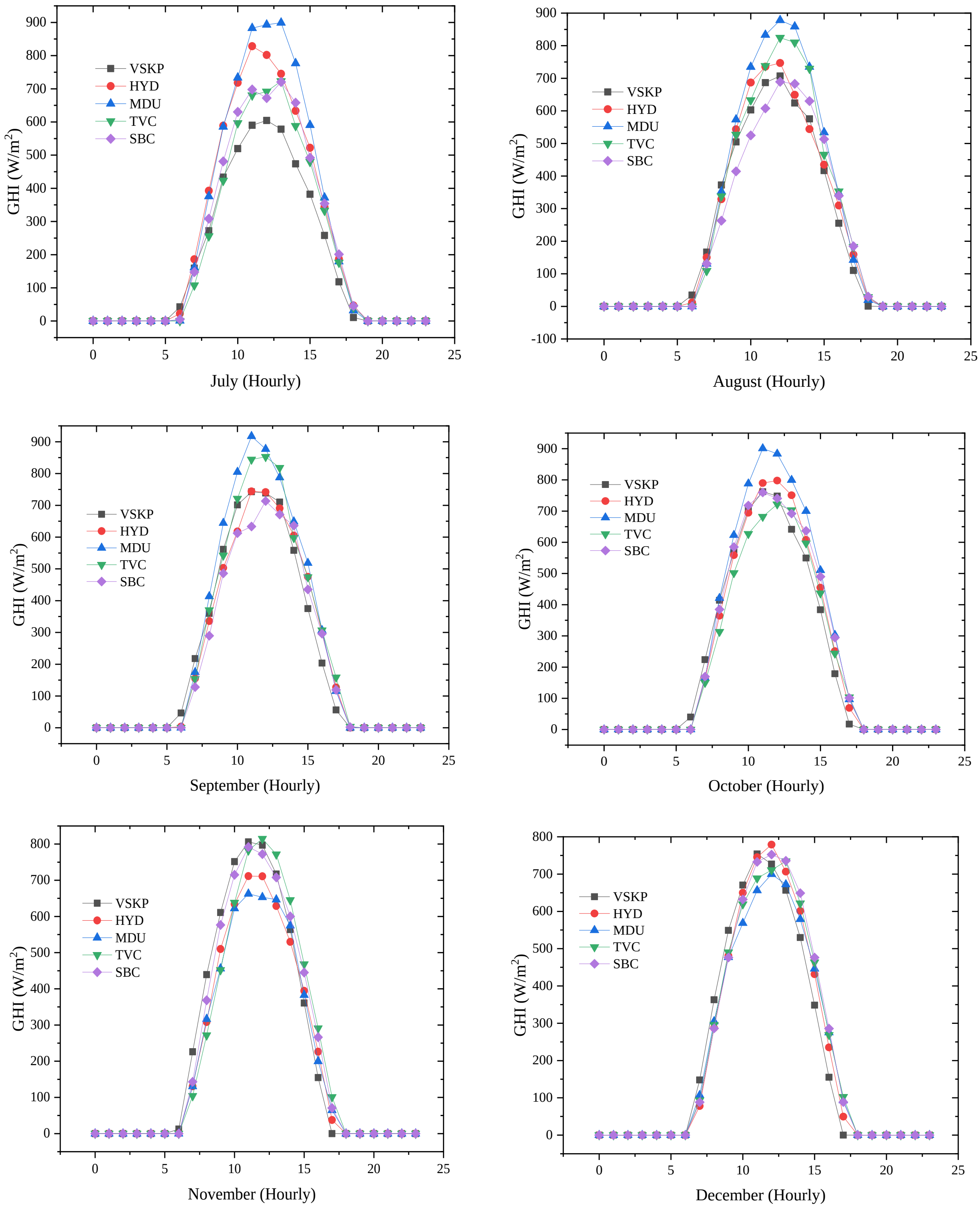

Figure 15 GHI data for south-Indian states

3.1.4 Results and discussions

In this section, the obtained results for a 20 MW solar PV plants for south Indian states are presented. The techno-economic assessment for a solar PV panel is conducted using SAM program. The technical and financial parameters are taken from the available literatures, and a few parameters are calculated by the SAM program.

3.1.4.1 Technical results of proposed three mechanisms

In this study, we designed a 20 MW solar PV plant for the assessment for three proposed mechanisms at different regions in south Indian states. Hence, this section will discuss the obtained results for the simulation. The technical results from the study that HYD and MDU sites recorded highest annual energy for three mechanisms. Since, the significant drawback of solar PV panels is that because of availability of good solar radiation the sun actively works during the day light and goes offline during the sunset and cloudy seasons, such type of significant draw back may cause effect on the capacity factor. The electricity export from grid to the system for three mechanisms are shown in **Fig.16., Fig.17.,** and **Fig.18.** From the findings it is revealed that because of low solar radiation from sun the performance of a PV panel decreases from April to August. Hence, the electricity export to grid from the PV system is also decreases. While, from September again, the solar radiation starts increasing rapidly. Simultaneously, the electricity output from grid to the system starts increasing again. Although, the same trend follows for the SAT, and DAT mechanism with higher annual energy output from the system. The annual energy generated from the PV system during the first year of the project for FT mechanism is for VSKP, HYD, MDU, TVC, and SBC for the selected potential sites in south Indian states of India are recorded as 33.1 GWh, 33.6 GWh, 33.8 GWh, 31.9 GWh, and 33.5 GWh, with a CF of 19 %, 19.2 %, 20 %, 18.2 %, 19.1 %, respectively which is depicted in the **Fig.16**. While the annual energy for recorded for the SAT system, which is depicted in **Fig.17.** in the SAT system the obtained maximum annual energy generated from the grid to the system for the selected locations potential sites in south-Indian states are followed by 38.9 GWh, 40.4 GWh, 41.9 GWh, 40.2 GWh, and 41.3 GWh at also the capacity factor for the selected potential sites in the SAT system are 22.2 %, 23.0 %, 24 %, 23 %, and 24 %, respectively. Finally, in the case of the DAT system as depicted in **Fig.18.** the solar annual energy generated from the solar PV power in the selected sites are recorded around of 44.9 GWh, 45.6 GWh, and 46.2 GWh, 44.9 GWh, and 44.2 GWh, for the VSKP, HYD, MDU, TVC, and SBC, respectively were recorded in the first year of the project. Similarly, the recorded CF for the selected sites DAT mechanism was 25.3 %, 25.8 % 26.4 %, and 25.1 VSKP, HYD, MDU, TVC, and SBC respectively. Therefore, from the data it is clear that DAT system generated more annual energy for the first year of annual year of the project while compared to that of SAT, and FT mechanism, respectively. This is due to DAT can alter its position on all the directions from south to north, and east to west. Further, the results suggests that HYD site is generated more annual energy from the present analysis.

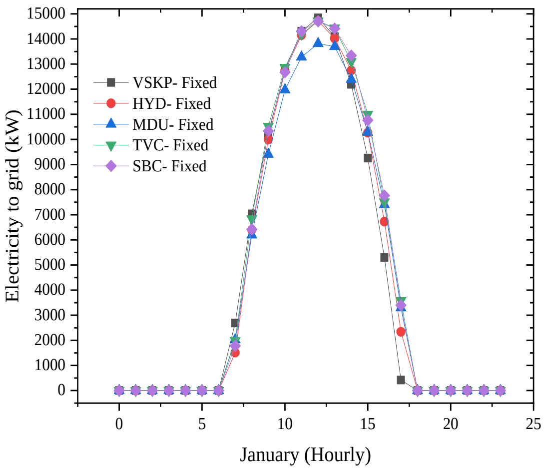
VSKP- Fixed
HYD- Fixed
MDU- Fixed
TVC- Fixed
SBC- Fixed
Electricity to grid (kW)
January (Hourly)

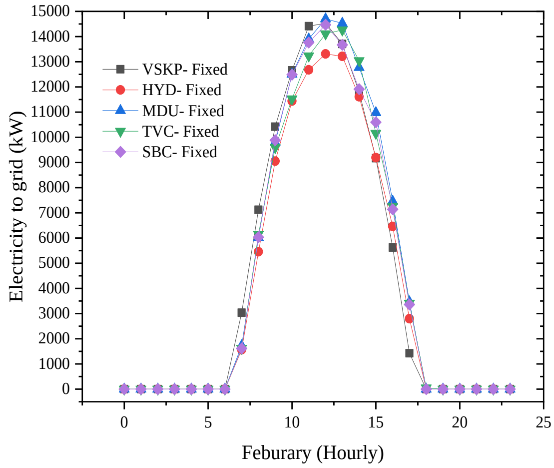
VSKP- Fixed
HYD- Fixed
MDU- Fixed
TVC- Fixed
SBC- Fixed
Electricity to grid (kW)
Feburary (Hourly)

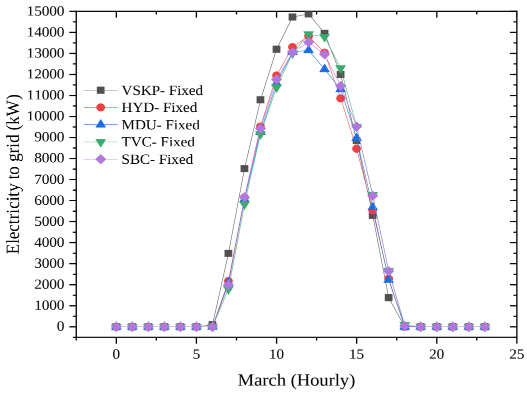
VSKP- Fixed
HYD- Fixed
MDU- Fixed
TVC- Fixed
SBC- Fixed
Electricity to grid (kW)
March (Hourly)

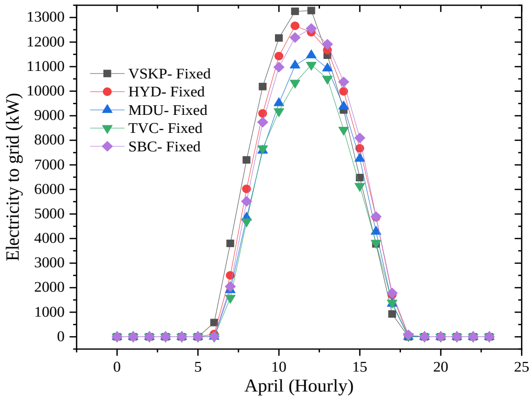
VSKP- Fixed
HYD- Fixed
MDU- Fixed
TVC- Fixed
SBC- Fixed
Electricity to grid (kW)
April (Hourly)

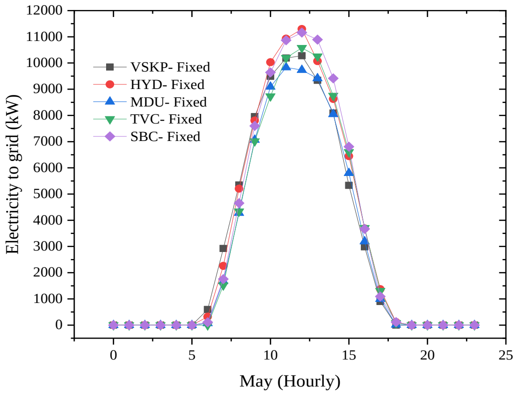
VSKP- Fixed
HYD- Fixed
MDU- Fixed
TVC- Fixed
SBC- Fixed
Electricity to grid (kW)
May (Hourly)

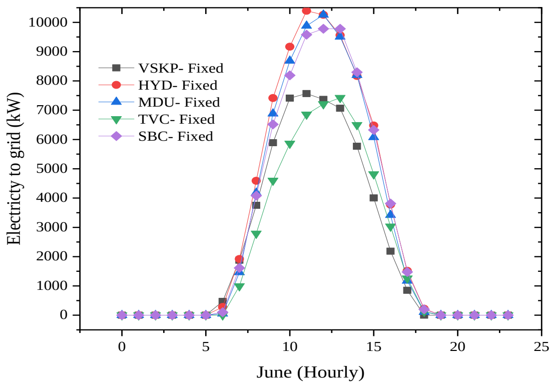
VSKP- Fixed
HYD- Fixed
MDU- Fixed
TVC- Fixed
SBC- Fixed
Electricity to grid (kW)
June (Hourly)

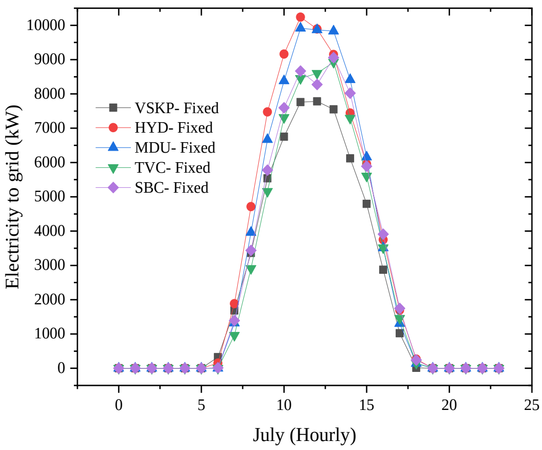
VSKP- Fixed
HYD- Fixed
MDU- Fixed
TVC- Fixed
SBC- Fixed
Electricity to grid (kW)
July (Hourly)

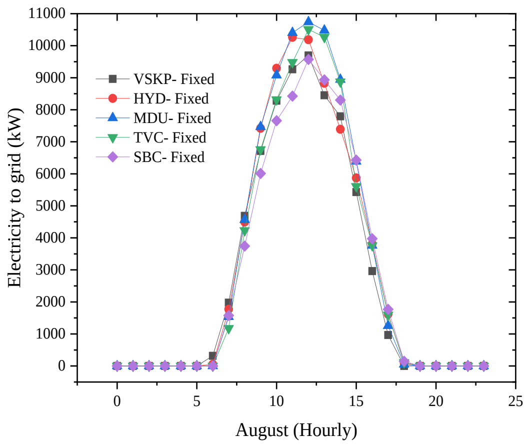
VSKP- Fixed
HYD- Fixed
MDU- Fixed
TVC- Fixed
SBC- Fixed
Electricity to grid (kW)
August (Hourly)

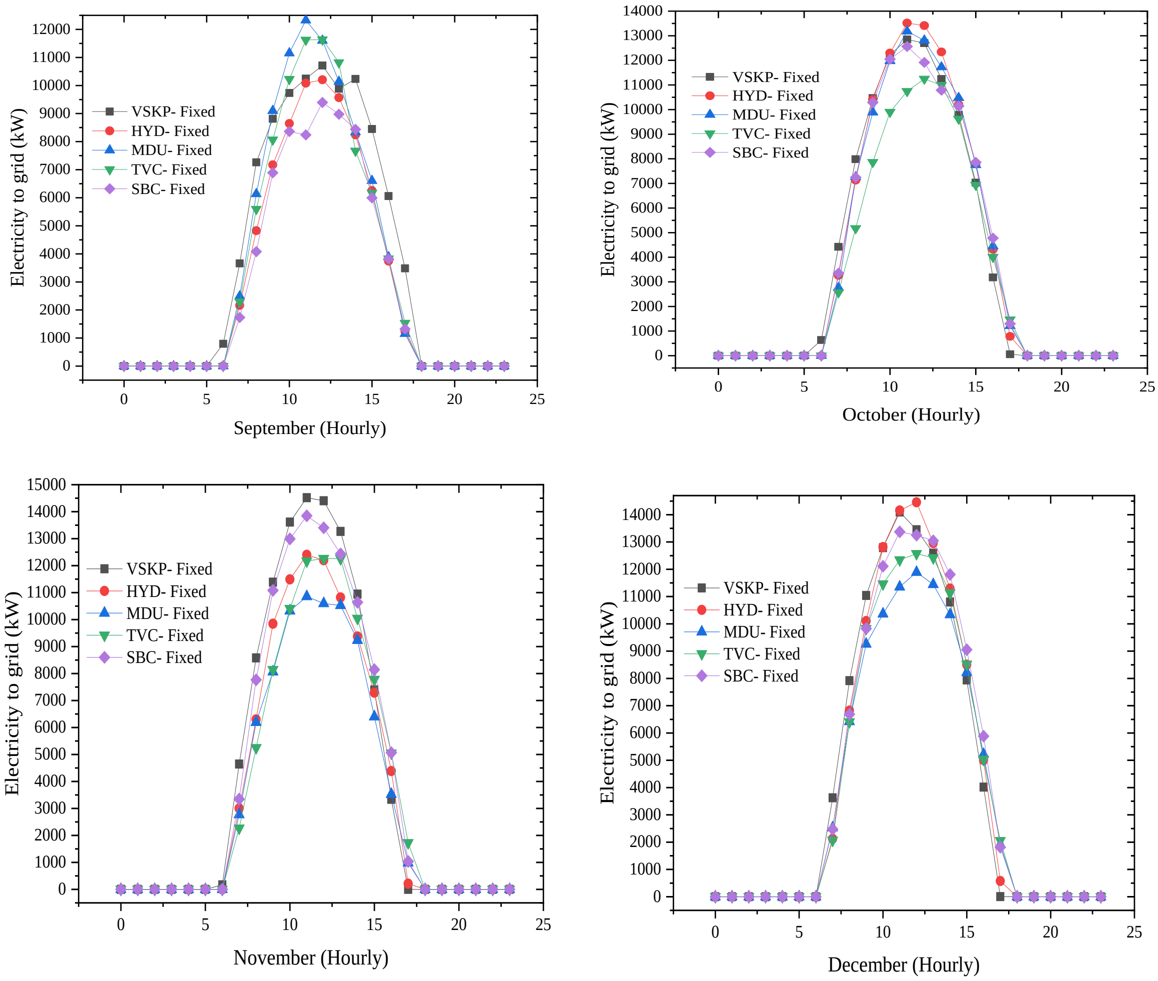

Figure 16 Monthly output grid to PV system for FT mechanism in south -Indian states

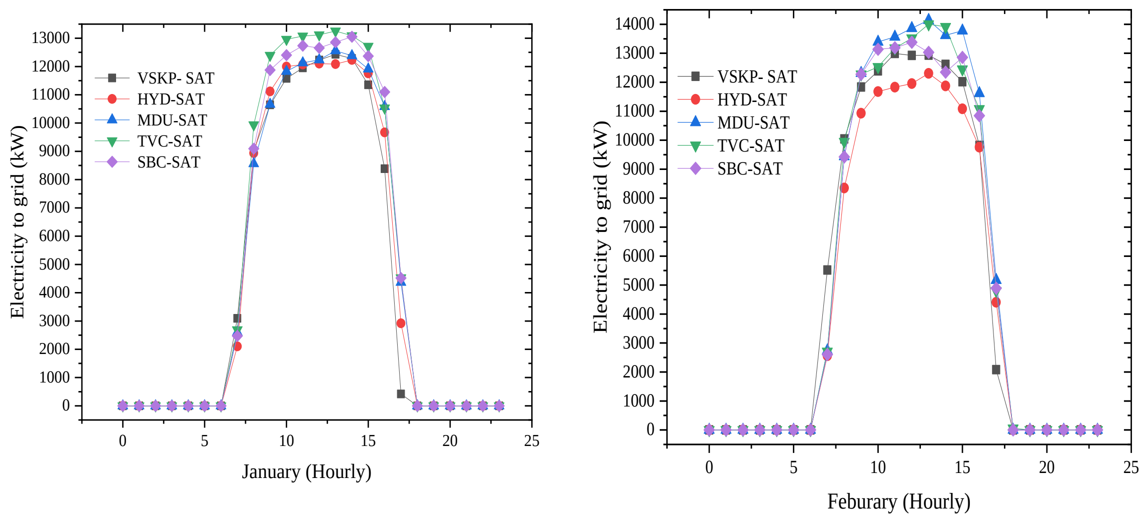

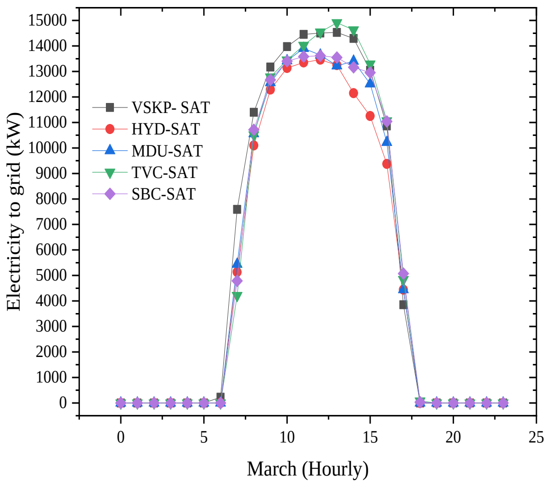
VSKP- SAT
HYD-SAT
MDU-SAT
TVC-SAT
SBC-SAT
Electricity to grid (kW)
March (Hourly)

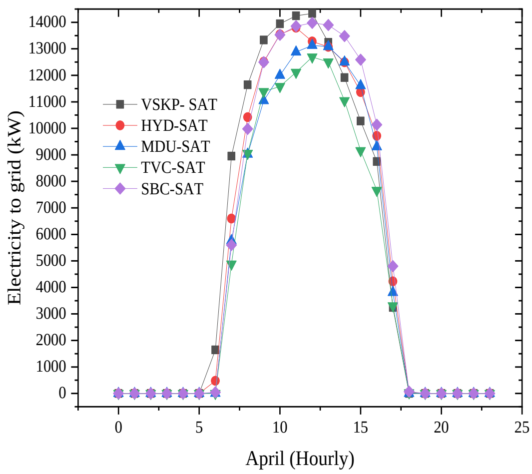
VSKP- SAT
HYD-SAT
MDU-SAT
TVC-SAT
SBC-SAT
Electricity to grid (kW)
April (Hourly)

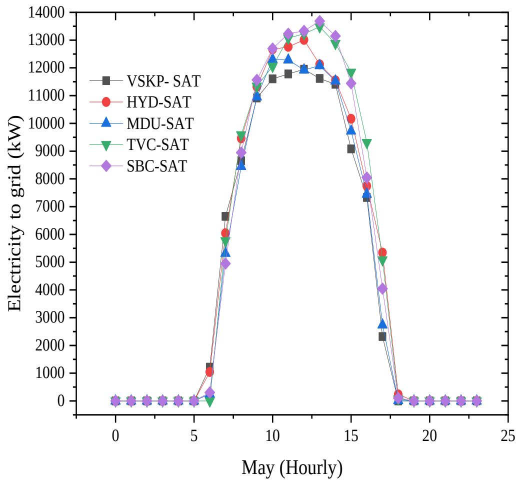
VSKP- SAT
HYD-SAT
MDU-SAT
TVC-SAT
SBC-SAT
Electricity to grid (kW)
May (Hourly)

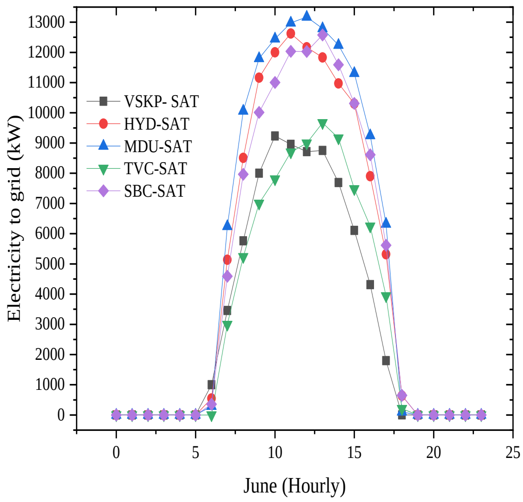
VSKP- SAT
HYD-SAT
MDU-SAT
TVC-SAT
SBC-SAT
Electricity to grid (kW)
June (Hourly)

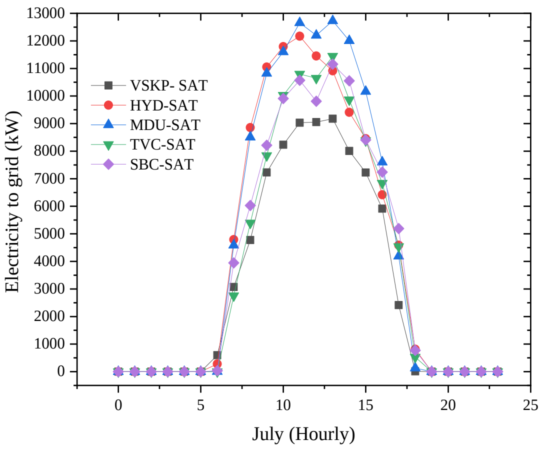
VSKP- SAT
HYD-SAT
MDU-SAT
TVC-SAT
SBC-SAT
Electricity to grid (kW)
July (Hourly)

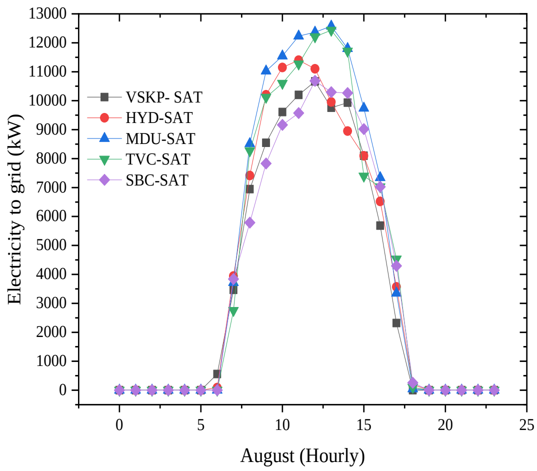
VSKP- SAT
HYD-SAT
MDU-SAT
TVC-SAT
SBC-SAT
Electricity to grid (kW)
August (Hourly)

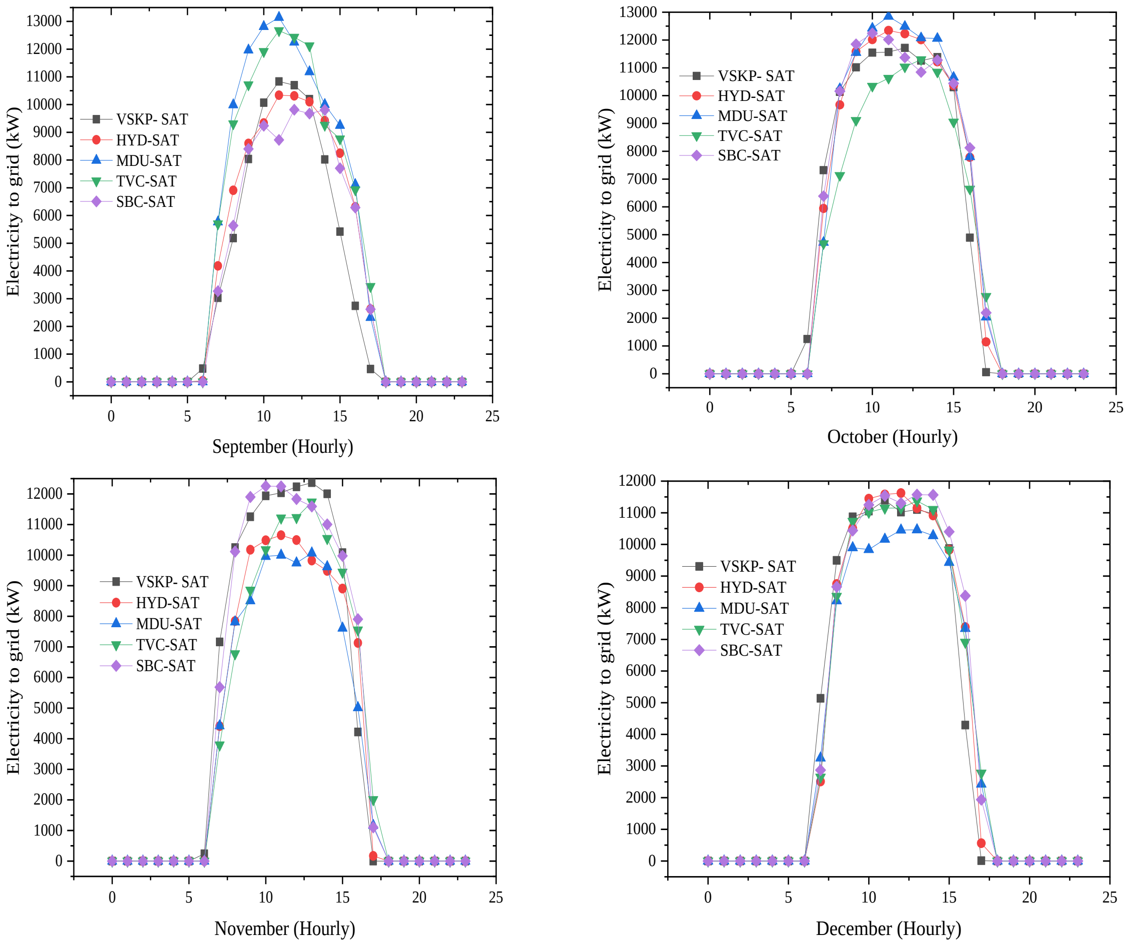

Figure 17 Monthly output grid to PV system for SAT mechanism in south -Indian states

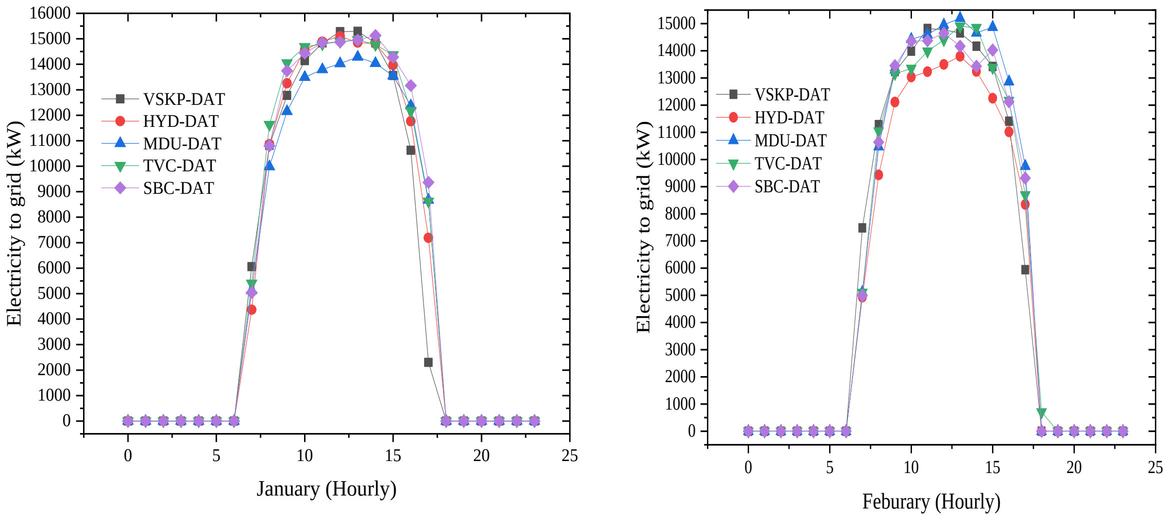

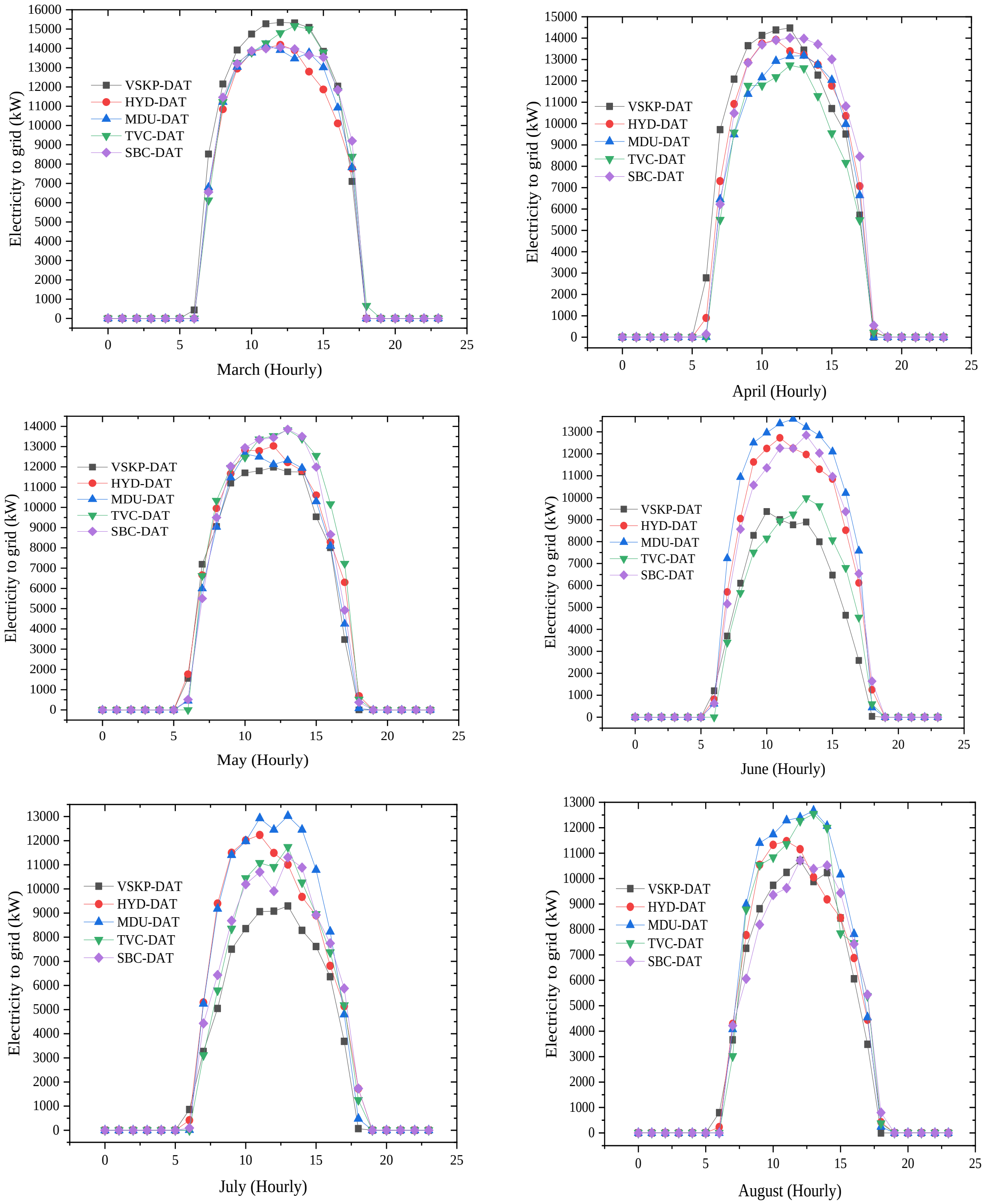
Electricity to grid (kW)
March (Hourly)
April (Hourly)
May (Hourly)
June (Hourly)
July (Hourly)
August (Hourly)
VSKP-DAT
HYD-DAT
MDU-DAT
TVC-DAT
SBC-DAT

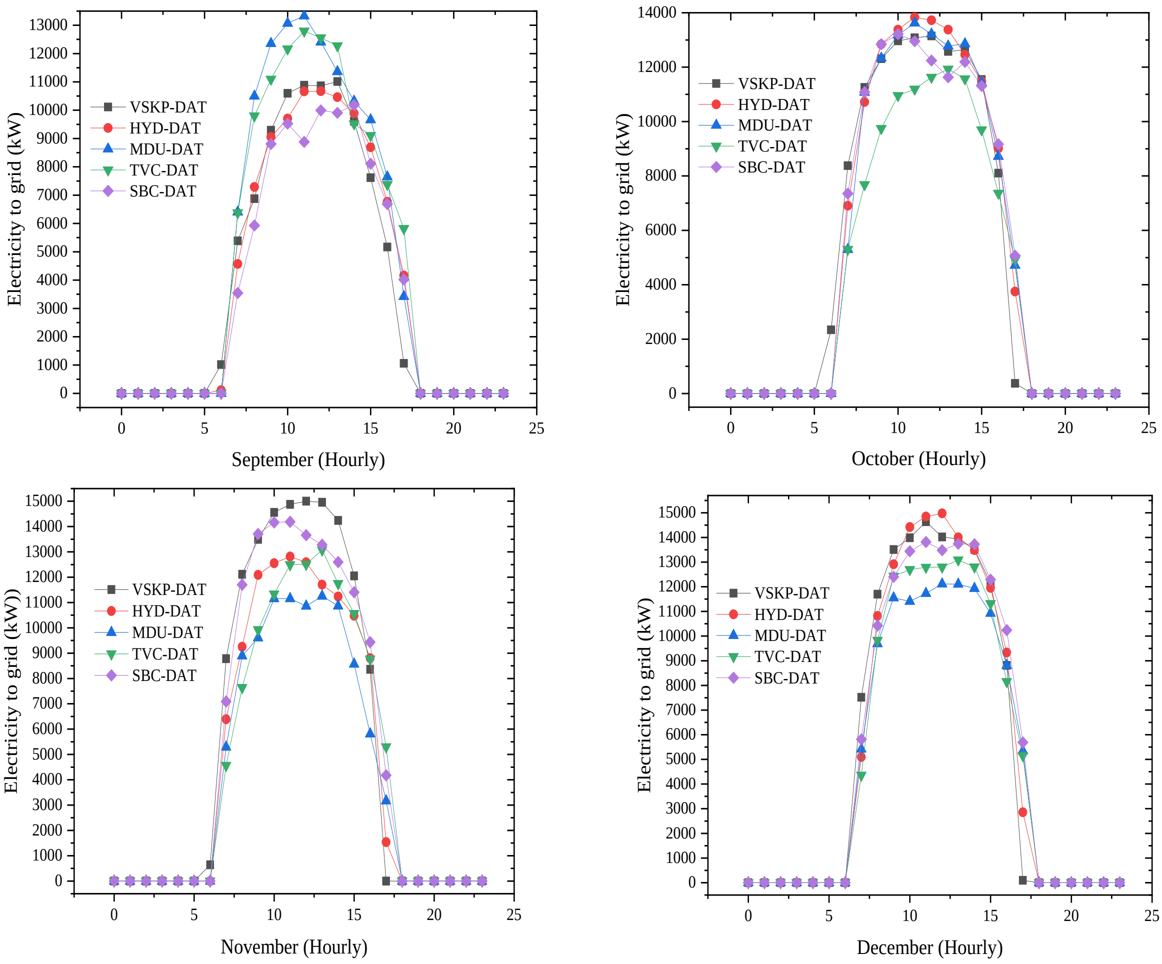

Figure 18 Monthly output grid to PV system for DAT mechanism south -Indian states

3.1.5 Economic results of a PV plant for three mechanisms

The present section, signifies the detailed economic analysis of the solar PV plants for the proposed mechanisms. The obtained economic analysis of a solar PV plants in five south-Indian stated are presented in **Table.5.**

Table 5 Economic analysis of PV mechanism

Type of Mechanism	**Cities**	**Metrics**					
		LCOE (nominal), ¢/kWh	**LCOE (real), ¢/kWh**	**Net present value, M$**	**Net capital cost, M$**	**Equity, M$**	**Size of debt, M$/**
FT	VSKP	5.01	4.22	1.800	22.65	6.80	15.85
	HYD	4.95	4.17	1.687	22.65	6.80	15.85
	MDU	5.04	4.25	1.861	22.65	6.80	15.85
	TVC	5.14	4.34	2.062	22.65	6.80	15.85
	SBC	4.95	4.19	1.684	22.65	6.80	15.85
SAT	VSKP	4.44	3.75	0.495	22.65	6.80	15.85
	HYD	4.33	3.56	0.182	22.65	6.80	15.85

	MDU	4.22	3.60	0.159	22.65	6.80	15.85
	TVC	4.35	3.67	0.227	22.65	6.80	15.85
	SBC	4.26	3.53	0.287	22.65	6.80	15.85
DAT	VSKP	4.08	3.06	0.626	22.65	6.80	15.85
	HYD	4.00	3.42	0.906	22.65	6.80	15.85
	MDU	3.97	3.34	1.046	22.65	6.80	15.85
	TVC	4.08	3.44	0.646	22.65	6.80	15.85
	SBC	4.00	3.42	1.054	22.65	6.80	15.85

From the recorded results, for the proposed mechanism for south-Indian countries the LCOE (real) calculated and presented in this section. From the findings it is observed that the LCOE for the three mechanisms are for all the five selected plants ranges from 3 to 5 ¢/kWh. Similarly, from the results it was also observed that of HYD, and SBC sites are recorded low LCOE for all the three mechanisms. Moreover, it was also observed that NPV for the three mechanisms showed a positive impact, and it signifies the PV system for selected locations of all the three mechanisms are viable.

3.1.6 Sensitivity analysis for the proposed mechanism

In this section, the sensitivity analysis results are presented and discussed for the proposed mechanism for south-Indian states in India. The essence of sensitivity analysis will provide an additional information to the investors and decision makers, that either selected potential location is either feasible for installing solar PV plants. Although, it acts as a predication of the selected project may be for the more reliable. Finally, sensitivity analysis, allows the decision-makers (i.e., government body or private investors) for the additional improvements in the project in the future as well. Hence, this segment a sensitivity analysis for a 20 MW solar PV plants for the five south-Indian states for proposed mechanism is presented and discussed. In this study, the sensitivity analysis three significant sensitivity analysis is conducted by varying analysis period, sales rate, annual interest rate.

First sensitivity analysis for designed 20 MW solar PV plant is introduced by varying LCOE with analysis period. Results from the findings recorded that the LCOE of five selected states decreases with increases in the analysis period of all the three mechanisms. Moreover, it was observed from the findings the LCOE of TVC is highest during the first year of the project. Simultaneously, LCOE is low for the SBC, and HYD for all the three solar tracking mechanism. Furthermore, the DAT mechanism is recorded the lowest LCOE in analysis period for all the selected sites. Hence, it is evident that DAT mechanism is feasible for the installation of a 20 MW solar PV project in all the five states in India. The analysis is presented in **Fig.19.**

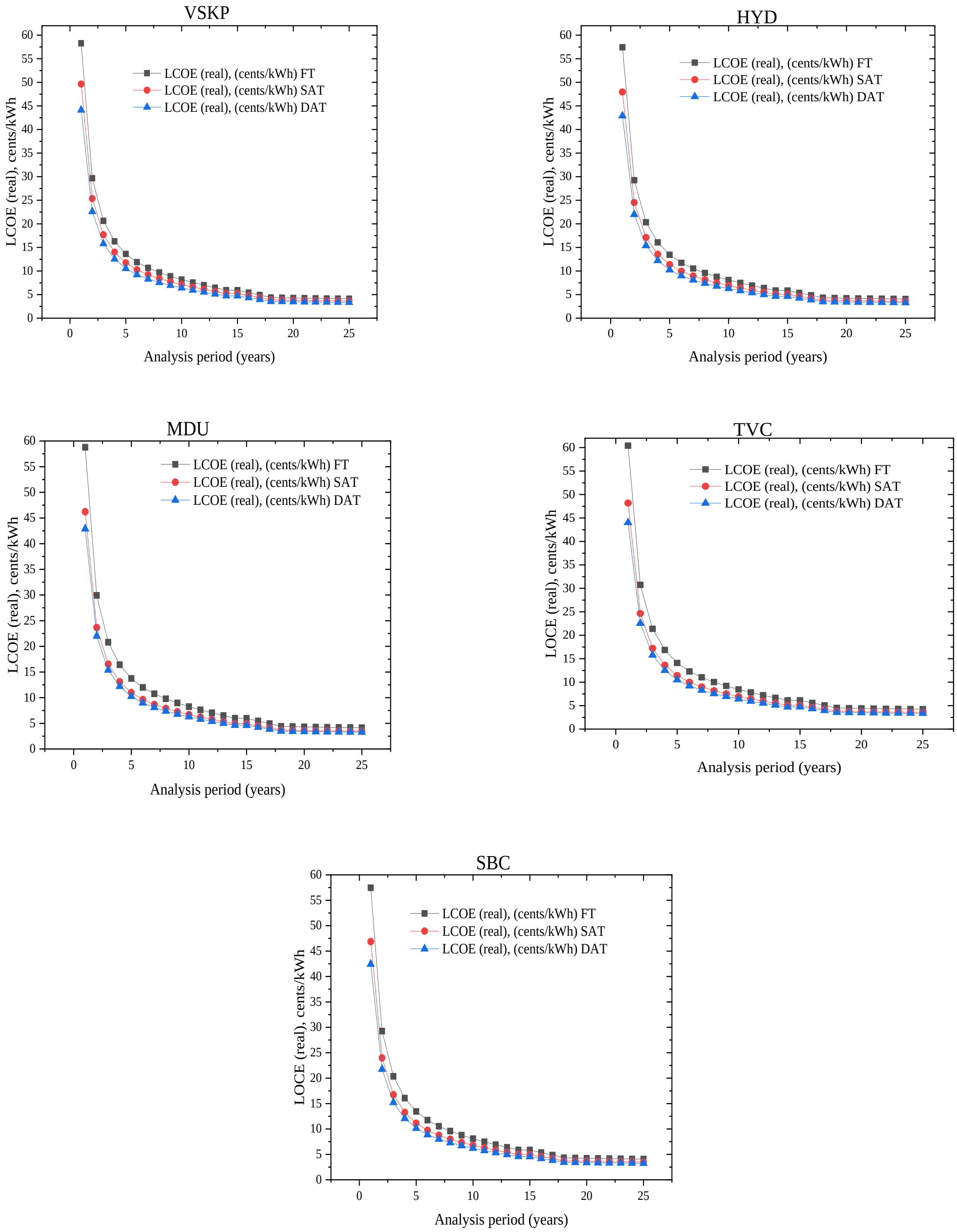

Figure 19 LCOE corresponding to project life time period

In the second sensitivity analysis we conducted analysis between project time period with net present value is depicted in **Fig.20**. It was observed from the simulation data for a 20 MW solar PV project, for south Indian states. The behavior of NPV for a FT, and SAT mechanism is negative for the entire project period. While, for the DAT tracking mechanism we achieved a positive value only after 17 years. Hence, from the observations it concludes that NPV has positive impact only on DAT mechanism.

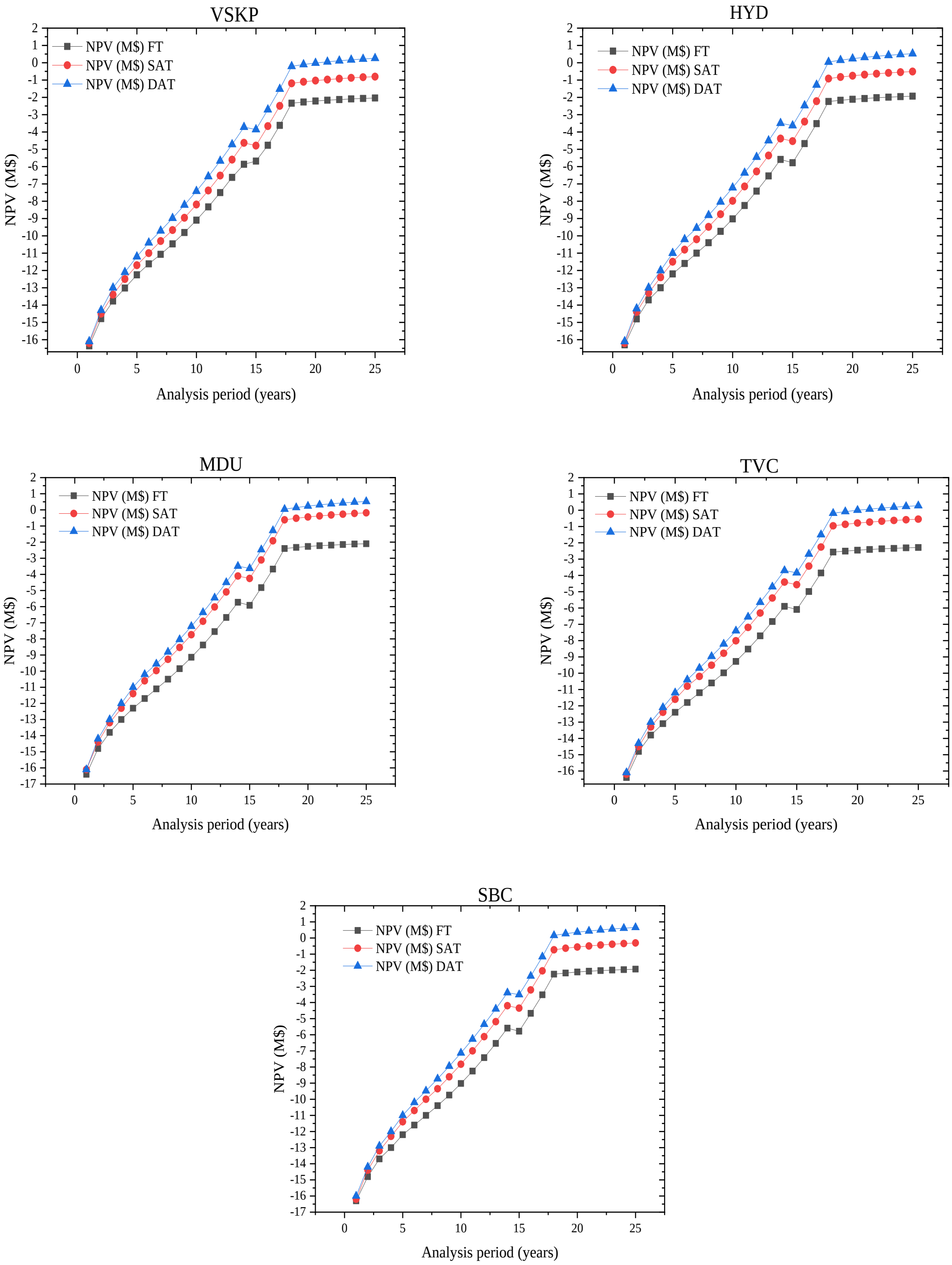

Figure 20 Effect of LCOE corresponding to the project life time period

In the final sensitivity analysis, the behavior of LCOE with sales tax rate is presented for a solar PV plant in south-Indian countries are presented in this section. The recorded data is shown in **Fig.21**. From the observation it is clear evident that increase in the sales tax rate, the LCOE of a solar PV project is also increases gradually. Although, it was observed that increase in sales tax rate the LCOE of FT mechanism is high compared to SAT, and DAT mechanisms.

Furthermore, from the findings it is revealed that LCOE is low for DAT mechanism in all the selected locations.

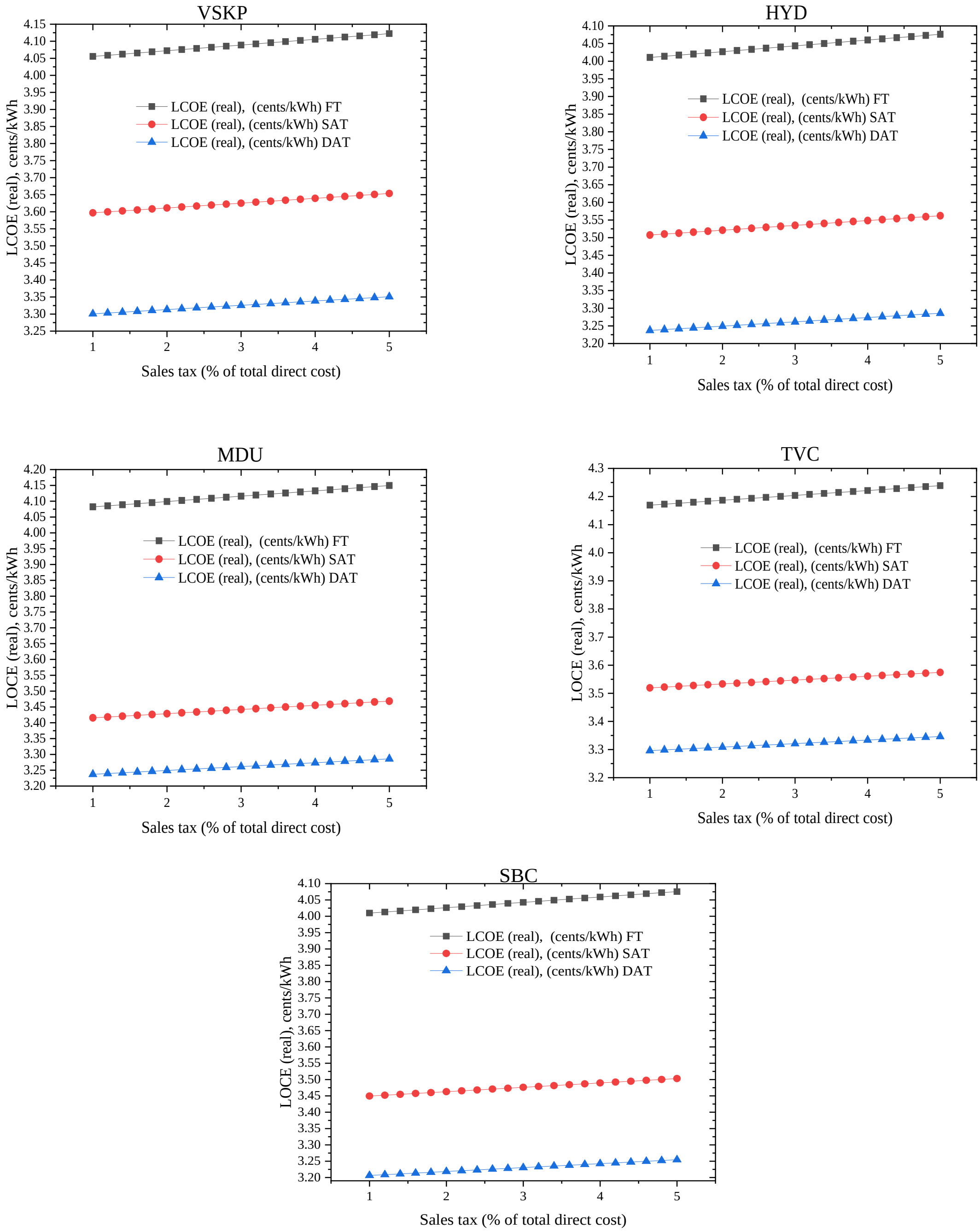

Figure 21 Effect of LCOE corresponding to sales tax rate

3.1.7 Enviro-economic analysis

The effect of environment analysis of the present study accessed for south-Indian countries are presented in this section. The mitigation factor for the present study, is presented in **Eq. (24)**

$$Mit_{CO_2} = E_g \times F_e \tag{24}$$

Here, Mit_{CO_2}, E_g, and F_e signifies the mitigation factor, electricity generated by PV plant and emission factor, respectively. The emission factor for the present study is taken as 0.8274 $kgCO_2/kWh$. **Table 6** shows the environmental analysis caused for three mechanisms.

Table 6 Environmental analysis due to solar PV technology

Site	FT		SAT		DAT	
	Annual Energy (kWh)	Carbon footprint, (metric tons of CO_2e)	Annual Energy (kWh)	Carbon footprint, (metric tons of CO_2e)	Annual Energy (kWh)	Carbon footprint, (metric tons of CO_2e)
VSKP	33,075,000	27,366,255	38,969,000	32,242,950.6	44,287,000	36,643,063.8
HYD	33,577,000	27,781,609.8	41,372,000	34,231,192.8	45,573,000	37,707,100.2
MDU	33,786,000	27,954,536.4	41,919,000	34,683,780.6	46,195,000	38,221,743
TVC	31,879,000	26,376,684.6	40,176,000	33,241,622.4	44,385,000	36,724,149
SBC	33,549,000	27,758,442.6	41,334,000	34,199,751.6	45,160,000	37,365,384

3.1.8 Comparative analysis of the present study

To compare with other studies, a detailed survey has been conducted and listed in **Table 7**. The list will provide a review from location, software/program used, and key findings from their study.

Table 7 Performance parameters with other literatures

Reference	Location, Country	Developed System	Software	Key Findings
[73]	Wa, Sunyani, Nsawam, Ghana	A 20 MW solar PV with and without DC battery solar tracking mechanism	SAM	1.Annual energy generated 36 GWh for SAT, and 43 GWh for DAT Mechanism. 2.CF range is between 16 to 18% for both mechanism 3.LCOE is minimized from 5-6 ¢ /kWh for both mechanism
[87]	NUST lake Islamabad, Pakistan	A 100kW FPV designed	SAM	1.4.5 MW of Power generated 2.LCOE of a system 5.6 ¢ /kWh

[88]	Quetta, Pakistan	A 2.5 MW for SAT, DAT mechanism	PV_{Syst} Software	1.4.44 GWh annual generation. of electricity 2.CF is 20.3% 3.LCOE of 0.026 $/kWh DAT generated 34.3% higher annual electricity
[89]	Riyadh, Saudi Arabia	Solar PV powered with EESS	SAM	1.331 GWh annual energy generated. 2.CF is 26.7 %. 3.LCOE is minimized 5.44 ¢ /kWh.
[90]	Bangladesh	1.4 MW mini grid system	MATLAB/Simulink, Homer	1.228 tons of carbon dioxide can be saved per year for 2500 house holds 2.Cost of energy is 18.3 US cents
[91]	Sweden	sizing and rule-based operation of grid-connected PV battery system	SAM	1.Three different operations proposed NPV increases with batter capacity
[92]	Doha, Qatar	Long term solar PV	SAM	1.200 MW is already in operative since 2020 2.Satellite generated data recorded from 2003-2013. 3.Solar PV and CSP coupled with DC system
[93]	Sweden	design of a grid-connected PV system	MATLAB	1.Reduction in battery life cost more than 9% time Overestimate of batter capacity is 243 kWh
[94]	Dubai, UAE	Comparison study off/on PV grid system for 4.08 kW	RETscreen	1.CF ranges between 3-5 % 2.NPV increase more than 41% 3.Less initial investment
[95]	Northwest, China	$5kW_p$ with and Without battery system	SAM	1.0.49 MWh highest annual electricity for Urumqi 0.56 MWh lowest annual electricity for Yinchaun

Present study	VSKP, HYD, MDU, TVC, HYD, South India	20 MW solar PV system is selected for techno-economic assessment analysis for three mechanisms	SAM	1.DAT mechanism better results for the selected 2. locations HYD location is feasible to install PV system

3.2 Techno-enviro-economic assessment of a 100 MW solar tower power plant (STPP) using dry-cooled and wet-cooled condenser model a case study in Republic of India.

Solar tower power plant (STPP) is a part of REs that are potential to produce electricity in the world. However, STPP plants is a classified by Concentrated solar power (CSP) plant. The general importance of CSP plant is able to convert sun energy to electrical energy. CSP plants technology plays a viable and promising role in the development of renewable energy (RE) technology. Meanwhile, CSP technology is a young and modern technology compared to other RE technologies. From the researcher's point of view CSP can be developed to generate electricity and also it can easily be enlarged all around the world. CSP technologies use mirrors to focus the sun's light energy and generate it to heat. Another, additional potential advantage of using CSP plants is the presence of an inherent thermal storage that is able to generate power during absence of sunset or during cloudy hours and CSP technology is also helpful to collect solar energy from the sun and convert it to heat, and vice versa.

3.2.1 Materials and Methodology

The selection of potential sites and modelling was done using system advisor model (SAM) that was supplied by the National Renewable Energy Laboratory (NREL), funded by the department of Energy (DoE), Unites State of America (USA). SAM program was used by the researchers for the assessment of potential sites for the country. However, the packet SAM program consists typically four types namely solar Parabolic trough collector (PTC), Solar tower power plant (STPP), linear Fresnel for the generation of electricity. In the present investigation a STPP is used to access the performance of techno-economic-enviro access for the performance of six potential sites in India. The selected potential sites for India cartesian co-ordinates of the present study are shown in **Table.8**. A graphical representation of selected sites is shown in **Fig.22.** Finally, the simulation flow chart used for the presented techno-enviro-economic assessment in SAM is presented in **Fig.23.**

Table 8 Selection of Potential sites

State	Selected cite	Station Code	Latitude (˚N)	Longitude (˚E)
Madhya Pradesh	Bhopal	BPL	23.25	77.40
Uttar Pradesh	Jhansi	VGLB	25.53	78.65
Punjab	Jalandhar	JUC	31.29	75.56
Andhra Pradesh	Srikakulam	CHE	18.32	83.91
West Bengal	West Medinipur	MDN	22.42	87.32
Tamil Nadu	Erode	ED	10.90	78.37

Figure 22 Selected potential for STPP model using QGIS

3.2.2 Selection of parameters for the analysis

In the present study, a 100 MW STPP is selected to access the performance for six potential locations in India. The plants such as STPP generates its electricity from the direct available of solar energy through the focused on the solar radiation which is mirror is directly mounted to the tower heat exchanger of a plant. The collector field is also made up of an array of mirrors which is prominently known as heliostat filed of the plant. The configuration STPP is shown in **Fig.24.** Moreover, the technical and financial parameters are presented in **Table.9,** and **Table. 10.** In the present study, technical parameters and financial parameters are taken according to India or taken from other studies.

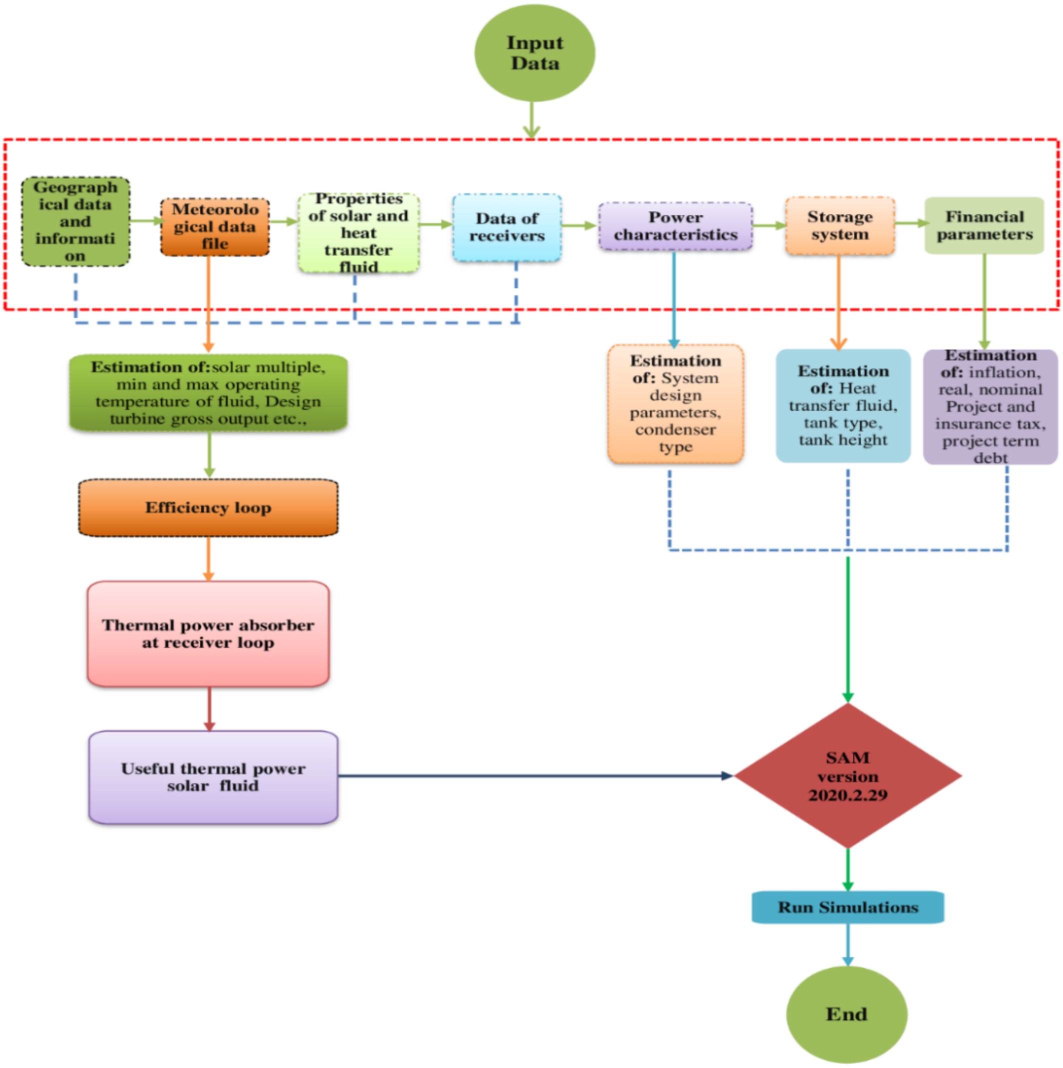

Figure 23 Flow chart of the simulation process in the SAM program (modified from [96] with license number: 5407500931944)

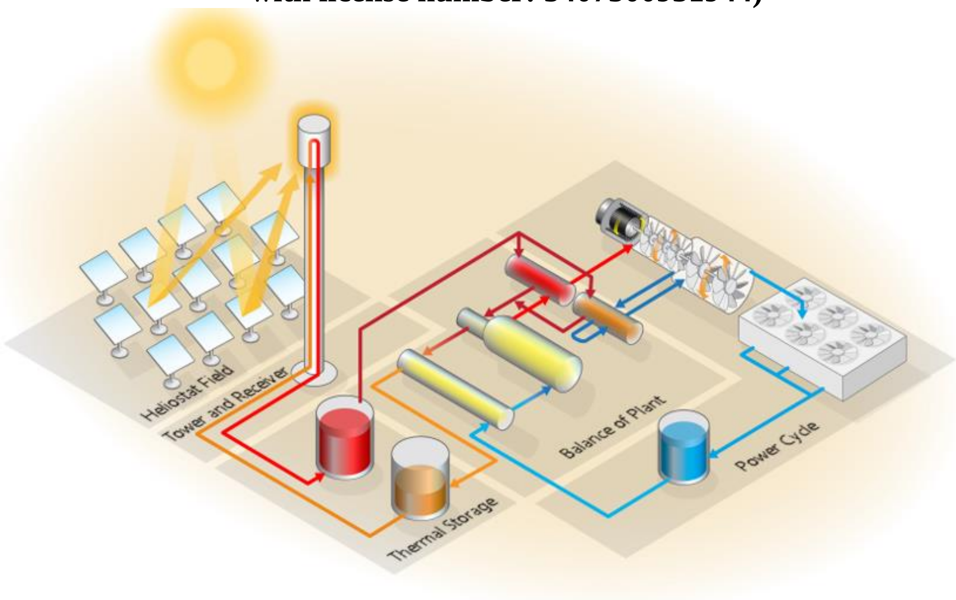

Figure 24 The configuration of STPP technology (obtained from SAM)

Table 9 Technical parameters for the present study

Location and Resources	**Bhopal, Jhansi, Jalandhar, Srikakulam, West Medinpur, and Erode**
System Design	Plant Capacity: 100 MW; Heat transfer Hot & Cold temperature: 574^{0} C and 290 ^{0} C; TES: 2 to 12 Hours
Heliostat field	Number of Heliostats: 8790; Heliostat Height &Width: 12.2m; Minimum & Max Heliostat distance to tower heigh ratio:9.5m and 0.75m; Water usage per wash 0.70 L/m^2
Tower and Receiver	Solar type: 2.40; Receiver thermal power: 670 MWt; Material type: Stainless steel AISI316; Heat transfer fluid: Salt (60% $NaNO_3$, 40% KNO_3)
Power Cycle	Boiler operating pressure: 100 Bar; Type of Condenser: Dry-cooled and wet-cooled
Thermal Storage	Type of storage: Two tank; Height of tank:12m; Tank fluid minimum height:1m; storage tank volume:17000 m^3

Table 10 Financial parameters for the present study

Financial Parameters	**Value**	**Ref**
Real discount rate (Per Year)	10%	[97]
Nominal discount rate (Per year)	12.42%	Calculated value
Project tax and insurance rates		
Annual Insurance rate	0.5%	
Sales tax (of total direct cost)	18 %	Taken from India
Federal Income tax rate (Year)	25%	Taken from India
Project term debt		
Debt Percent	70%	
Tenor (Years)	18	
Annual interest rate	6.5%	
Moratorium (Years)	5	
Up-front fee	2.75 %	

3.2.3 Weather characteristic of the present study

Fig.25. shows the monthly average directly normal Irradiance (DNI) for the selected potential sites in India. It can be seen that for the most of sites the peak energy generates from the plant i.e., dry season occurs from the month October to May; hence the beam irradiance is also very high at selected sites on those seasons. It was also observed that for the other months such from June, July and August there is relatively low irradiance because of the effect of rainy season or monsoon season. Furthermore, the locations such as Jalandhar, and Erode experiences a relatively low irradiance from the month of November to February; this is because the Jalandhar site experiences extremely cold weather conditions that exists in the northern side of India, whereas the Erode site experiences heavy rainfall during the period from November to February.

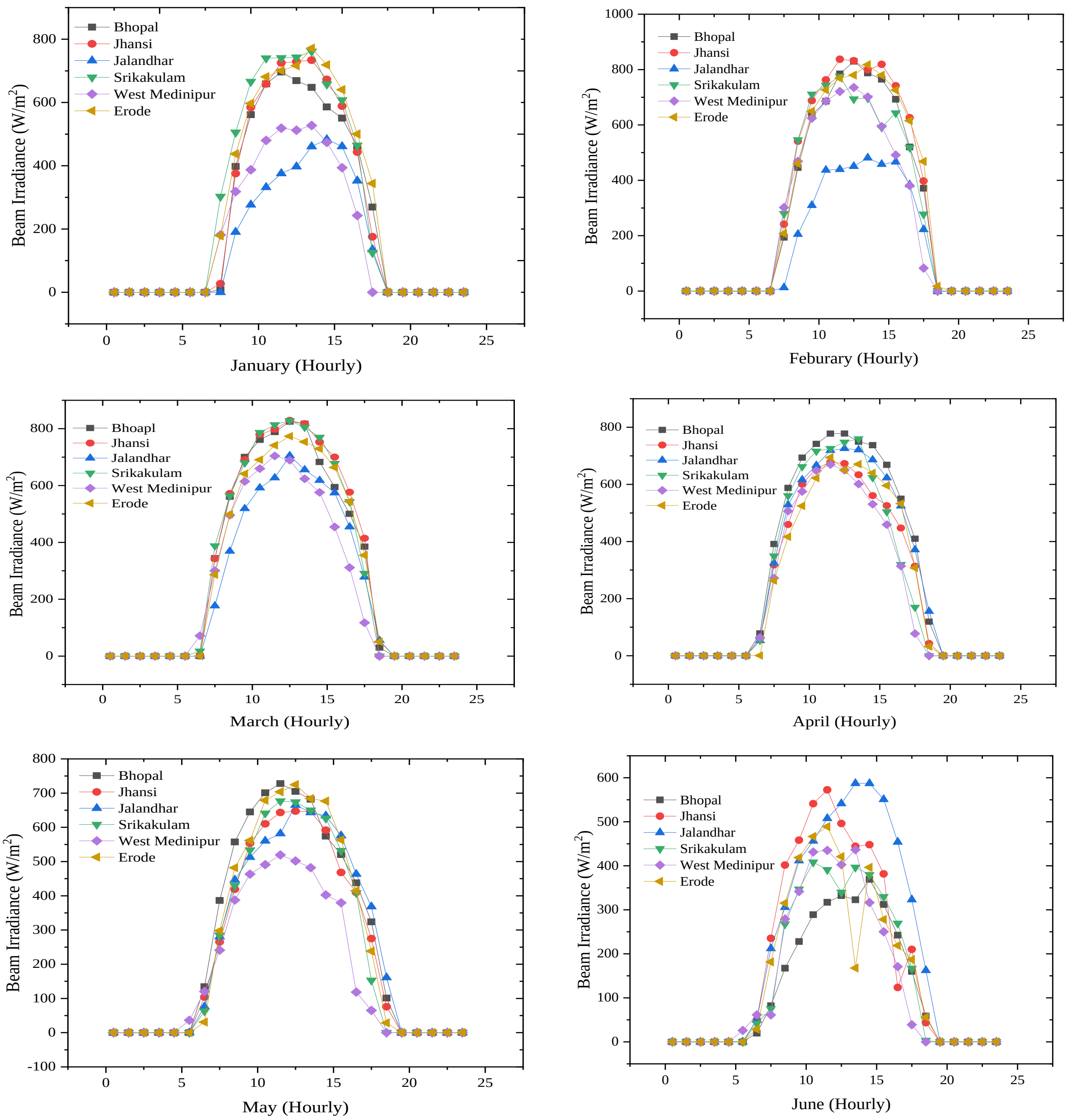

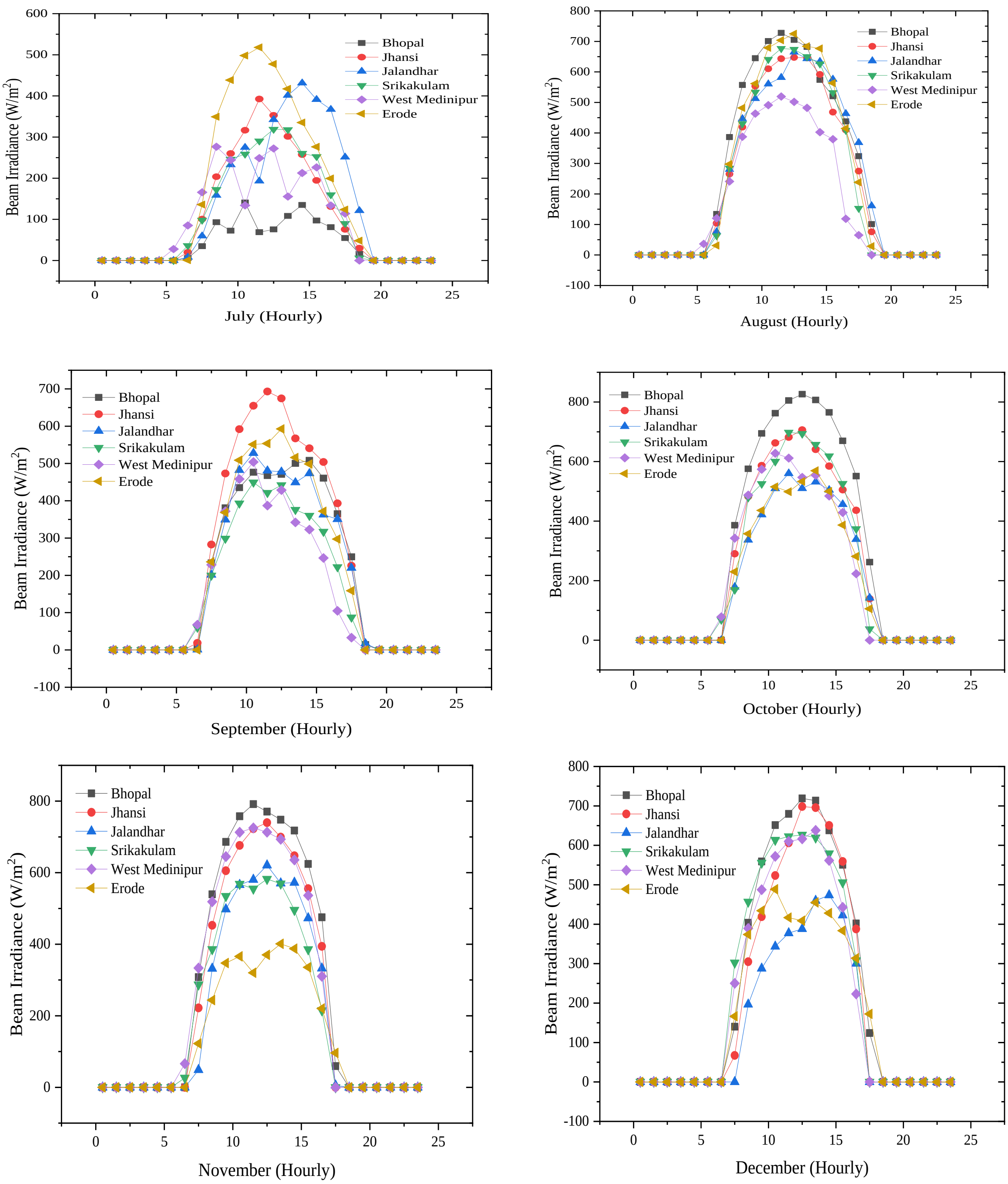

Figure 25 Monthly DNI for the selected sites India

3.2.4 Results and discussions

The present section offers the results and discussion obtained from the SAM program for a 100 MW STPP for the six different climatic zones in India. However, the present section if further, divided into two section two discuss the results of different cooling models. Finally, the sections offer sensitivity analysis for both wet and dry cooled models.

3.2.4.1 Electricity generation for dry-cooled STPP plant in six potential sites

The hourly electricity output grid system for a dry-cooled STPP plant for six potential sites in India is presented in **Fig.26.** The findings result from the present study, shows that from September to February the sites experience maximum solar radiation, except but Erode city this is due to Erode experiences heavy rainfall during this period. However, the recorded electricity export to the grid from the selected STPP plant for the six potential sites achieved about 100 MW during the dry-season for all the selected sites. The total electric power output to the grid in the March to August months of the year is reduced, which are also the sunny months of the year, the decrease in the electricity output is due to the effect of less solar radiation within that period.

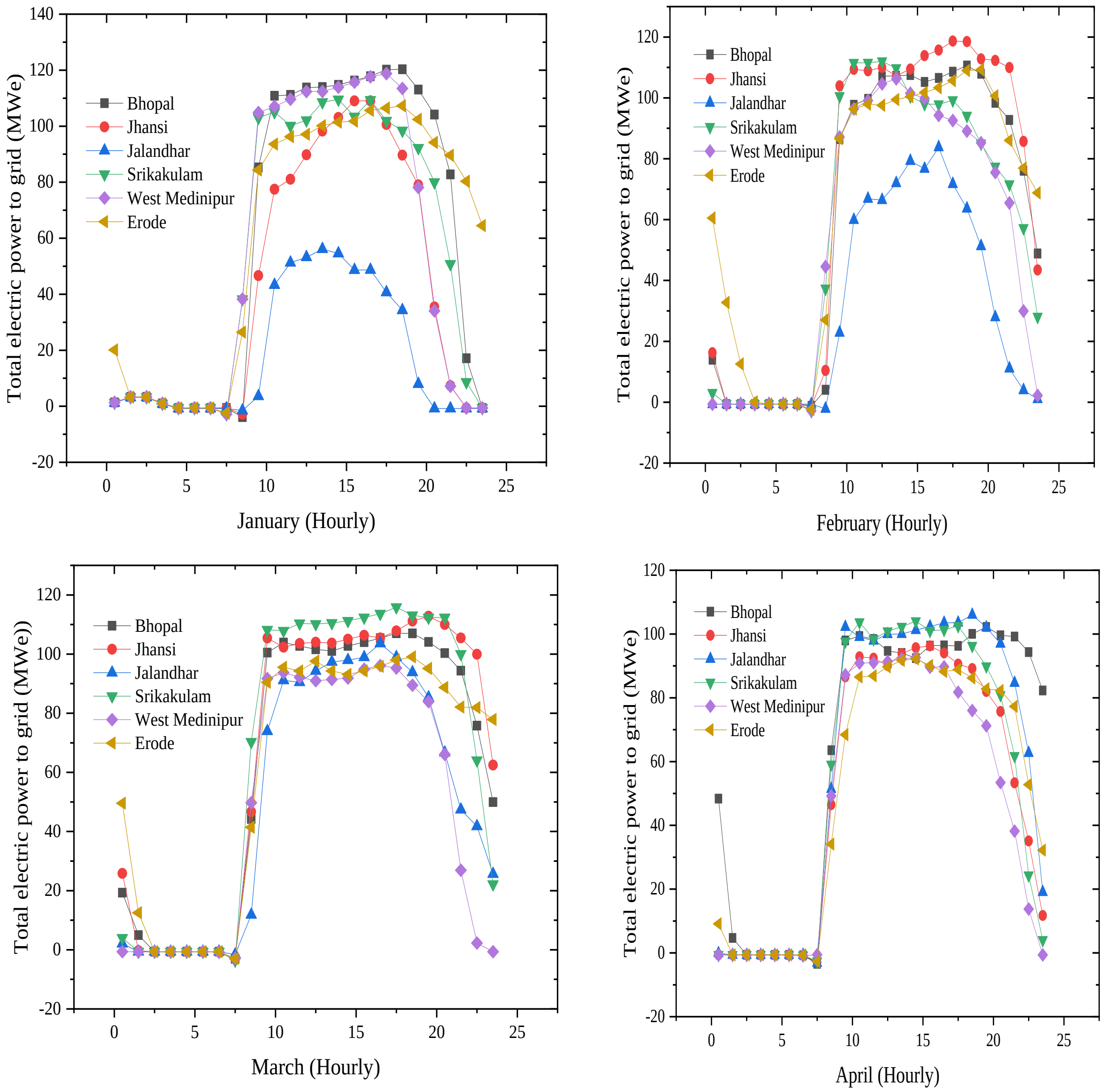

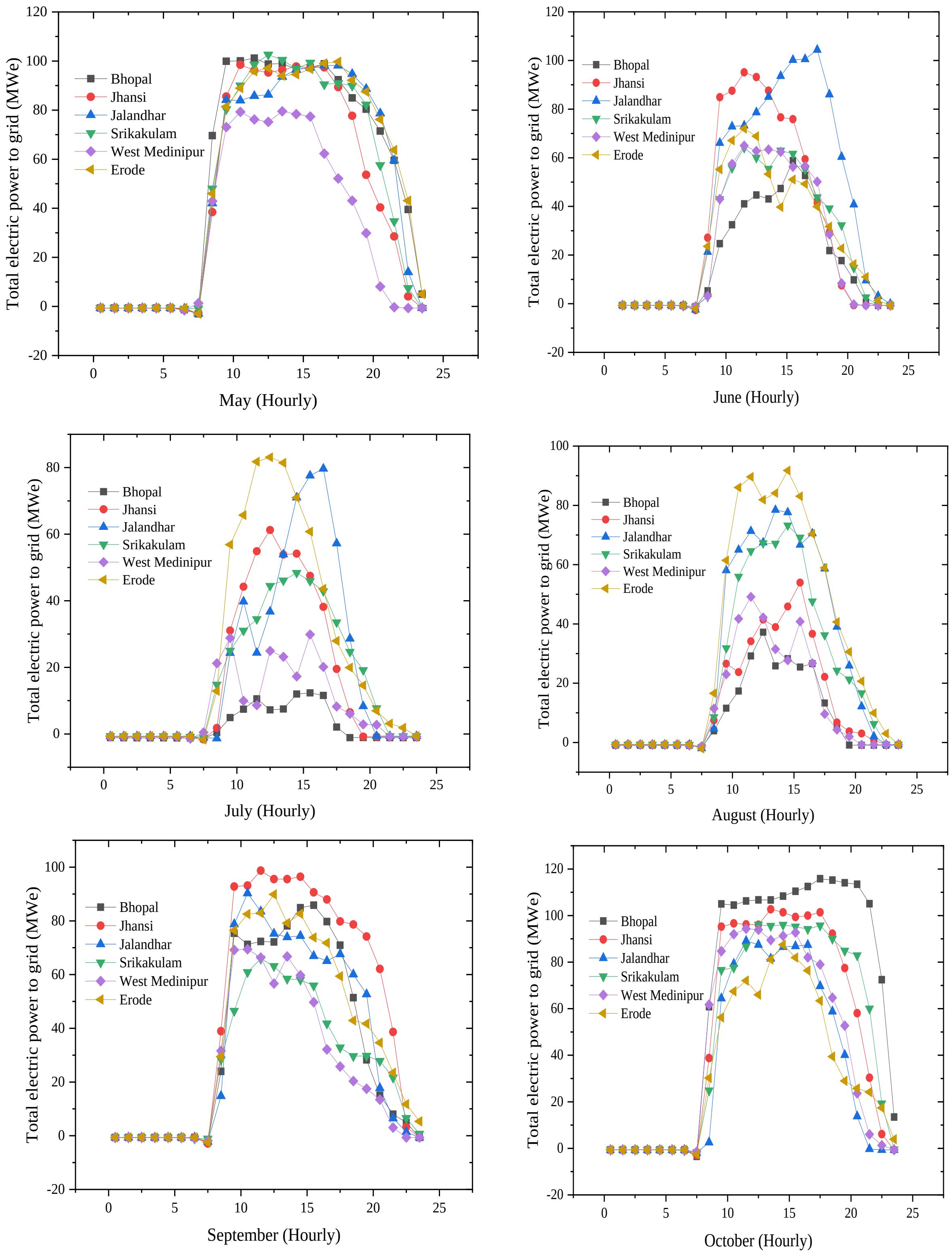
Total electric power to grid (MWe)
Bhopal
Jhansi
Jalandhar
Srikakulam
West Medinipur
Erode
May (Hourly)
June (Hourly)
July (Hourly)
August (Hourly)
September (Hourly)
October (Hourly)

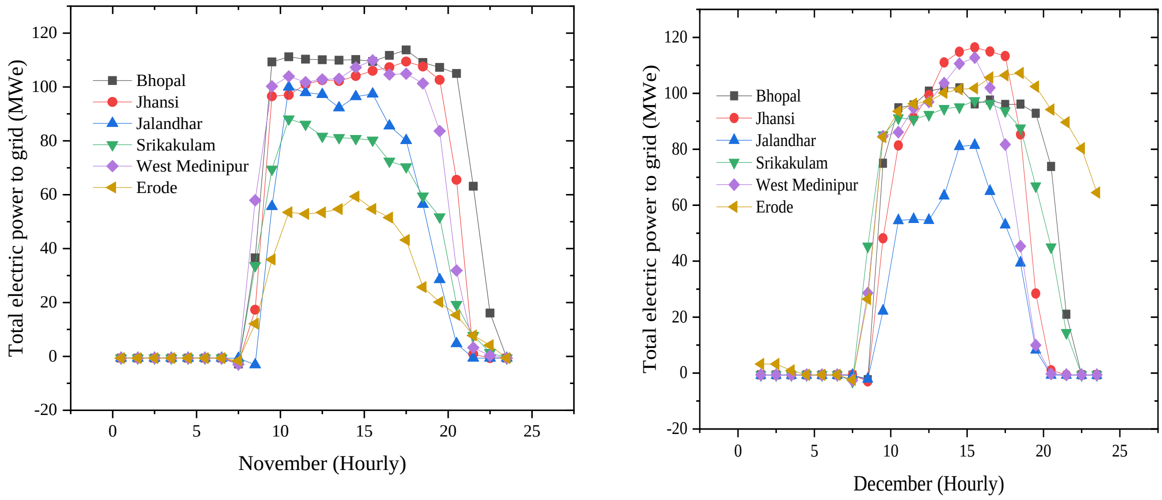

Figure 26 Total electricity output to grid dry-cooled STPP plant for six potential sites

From the findings it was observed that the during the first year of project recorded about 376.269 GWh, 364.845 GWh, 300.678 GWh, 353.159 GWh, 301.156 GWh, and 349.090 GWh, for the Bhopal, Jhansi, Jalandhar, Srikakulam, West Medinipur and Erode a total electricity generated of respectively. Meanwhile the capacity factor of Bhopal, Jhansi, Jalandhar, Srikakulam, West Medinipur and Erode during the first year of project is 41.5%, 40.2%, 33.2%, 39%, 33.2%, and 38.5%, respectively. Further, it was observed that sites Bhopal and Jhansi as well as Srikakulam and Erode, which has a nominal capacity factor difference. **Table.11**. highlights the performance of dry cooled STPP plant for the selected sites for the first year of project.

Table 11 Technical and economic results for STPP dry-cooled plant

Site	Annual energy (GWh)	Capacity factor (%)	Levelized Cost of Electricity (LCOE) (real), cents per kWh	Net Present Value (NPV), USD
Bhopal	376.269	41.5	13.22	15,312,089
Jhansi	364.845	41.5	13.62	15,311,053
Jalandhar	300.678	40.2	16.40	15,307,957
Srikakulam	353.159	33.2	14.065	15,310,368
West Medinipur	301.156	39	16.37	15,307,712
Erode	349.090	33.2	14.21	15,310,214

3.2.4.2 Economic analysis of the dry-cooled system for the selected sites in India

The results of economic analysis achieved for the study is summarized in **Table 11**. The results summarize that all the six selected sites are feasible to install CSP plants due to the recorded sites has positive NPV which indicates that a project at that site will break even at a faster rate than the other sites. The financial optimization of 100 MW of STPP plant is presented in the **Fig.27.** From the data of each potential site, LCOE is optimized by varying the SM from 1 to 5, with an increment 0.2. The results indicate that the value of LCOE decreases as the SM in-creases for the given TES capacity. The decreasing trend is followed until a minimum LCOE value is achieved, after which the trend starts to increase again. The SM at which the minimum LCOE is obtained can be said to be the optimal SM for that TES. shows the economic comparison of the six sites in this study. The LCOE under the optimization configuration in the Bhopal, Jhansi, Jalandhar, Srikakulam, West Medinipur, and Erode sites can be minimized to 12.01 cents/kWh, 12.25 cents/kWh, 13.87 cents/kWh, and 12.51, 13.74, 13.11 cents /kWh for SM within the region of 1.4–1. 8.

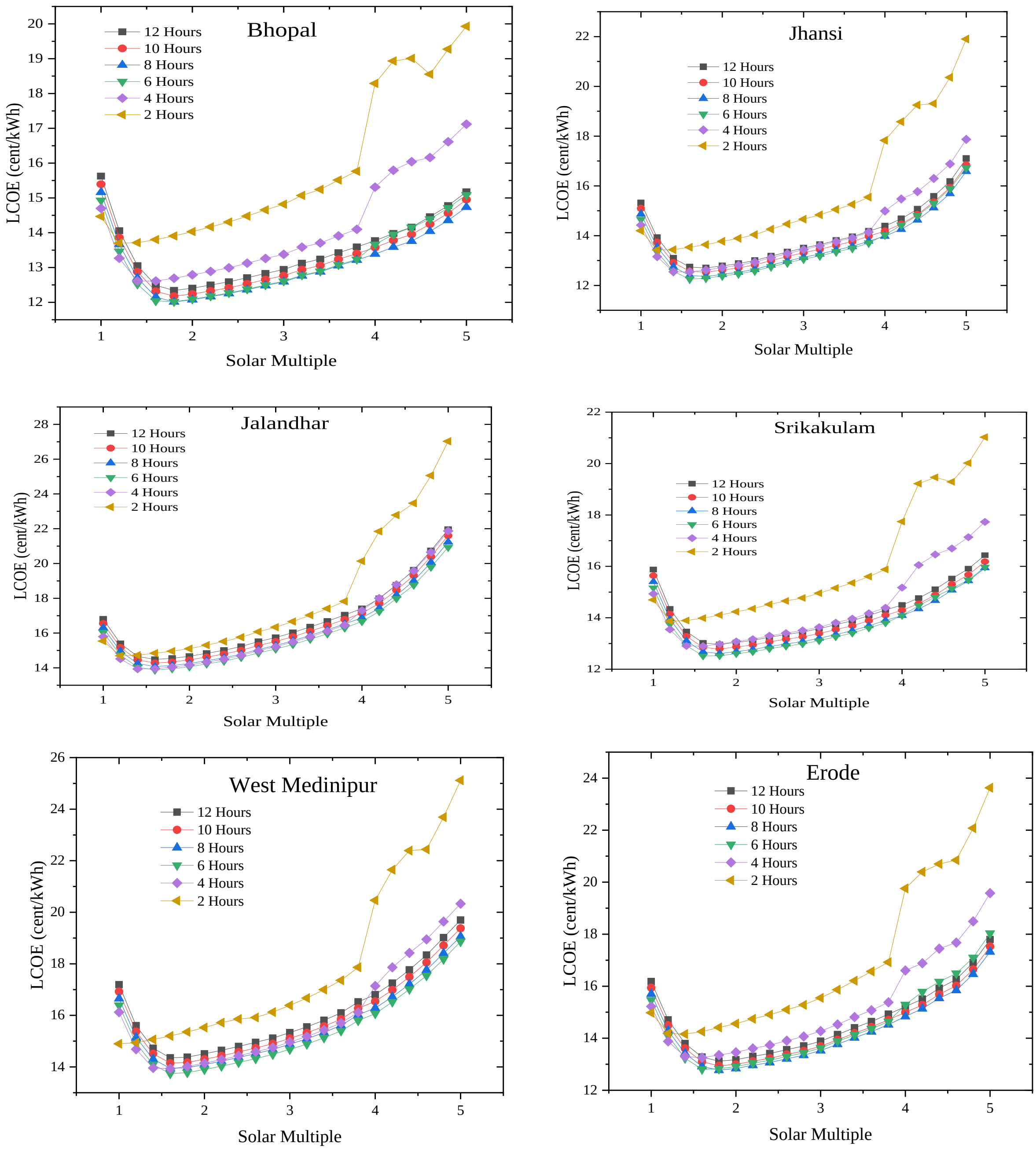

Figure 27 Effect of SM and TES on the LCOE (dry-cooled model) in different cities of India

3.2.4.3 Electric generated for STPP (Wet-Cooled) model for the selected potential sites in India

Fig.28. depicts the total electric power output for the wet-cooled STPP model at the six potential sites. It was observed that, the behavior of electricity output performance of the wet-cooled STPP model is not much significantly different from the electricity generation output of the dry-cooled model presented so far. Although, the significant drawback of using the wet-cooled STPP model is that it consumes more water compared to that of the dry-cooled STPP model. In comparison the annual output electricity generated by the wet-cooled STPP is higher than the dry-cooled STPP model.

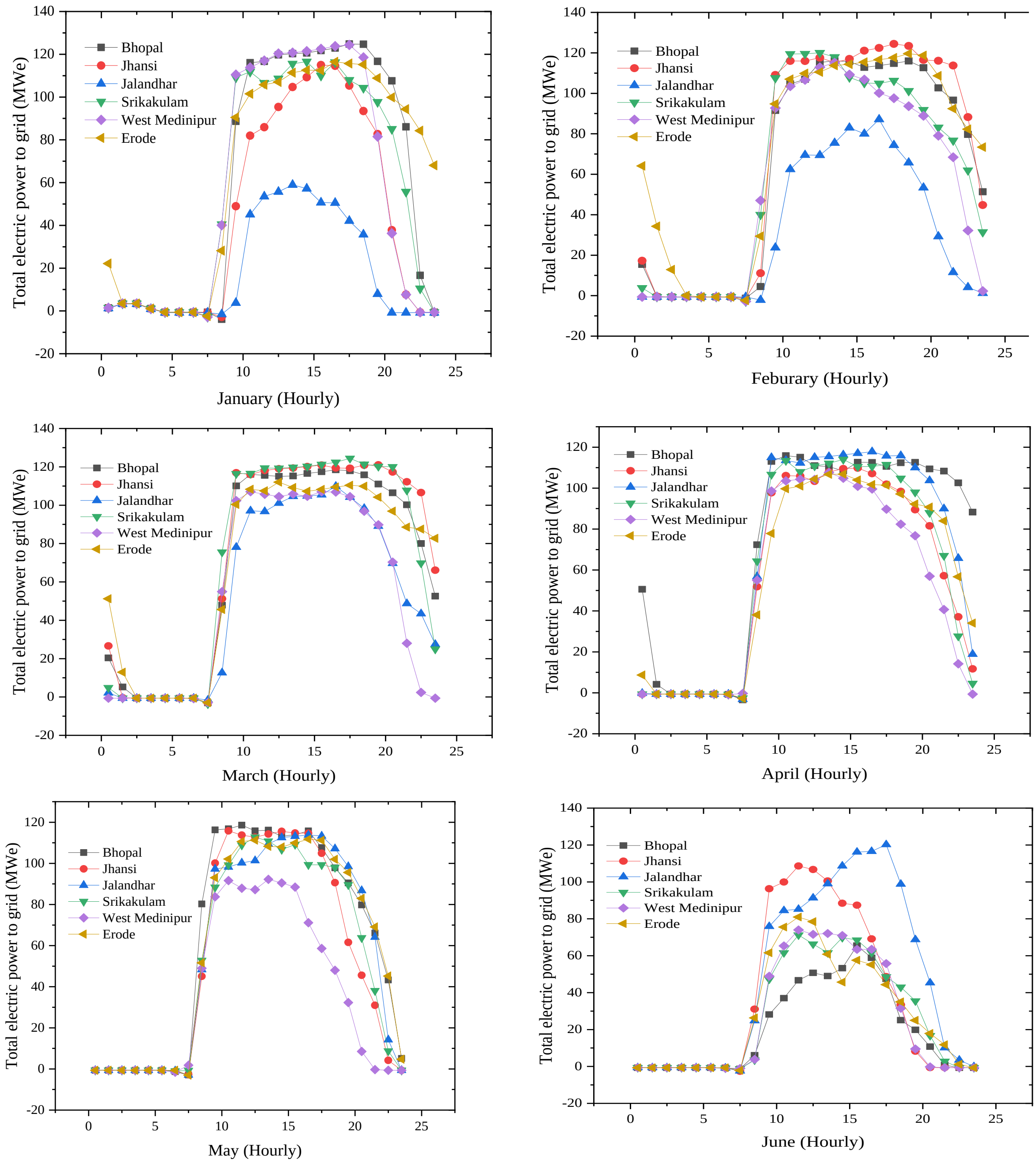

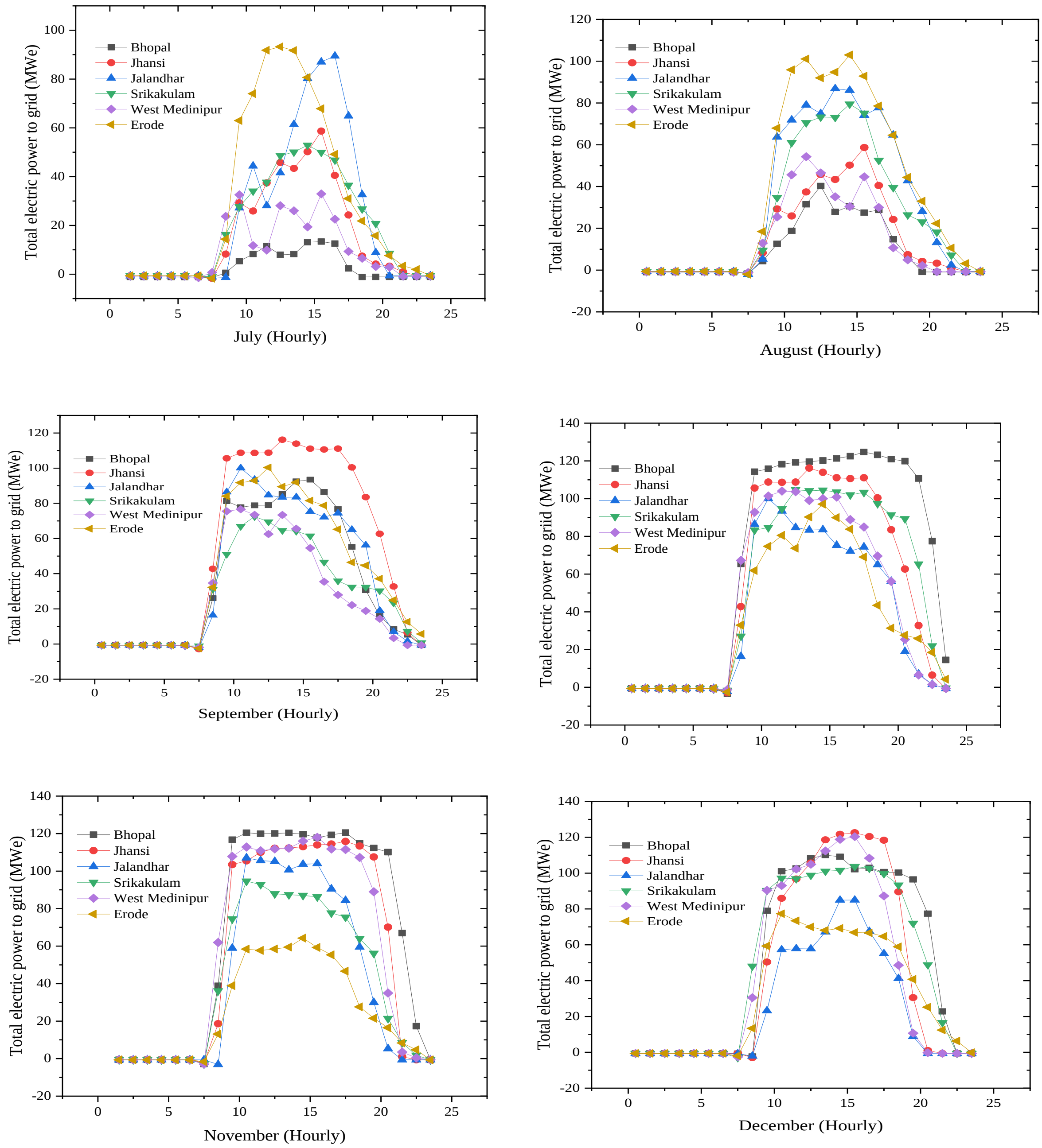

Figure 28 Total electricity output to grid wet-cooled STPP plant for six potential sites

3.2.4.4 Economic analysis for STPP (Wet-cooled) model for six potential sites

The economic analysis results of STPP wet-cooled model are shown in **Table.12**. The results of all the sites shows a positive NPV which means all the selected potential sites are viable to install in the locations. Moreover, the results from the **Fig.29.** presented that the optimized solar multiple falls between the range of 1 to 1.8. Further, it can be observed that the for the development of the wet-cooled model within the stimulated range of the achieved SM values leading to help the cut down on the cost. This significant reason is due to the increase of each SM increases the development of the capital cost for the entire plant. Meanwhile, the

LCOE outcome of wet-cooled STPP plant is lower than the dry-cooled STPP plant. From the obtained results it can be seen that results, the SM for the selected site system located at the Erode, Bhopal, and Srikakulam sites at 8 h TES is 1.8, while the Jalandhar and West Medinipur sites optimized at 6 h TES have an optimal SM of 1.6. The Jhansi site had an optimized TES of 6 h, with an SM of 1 at an LCOE of 11.53 USD cents/kWh.

Table 12 Technical and economic analysis of STPP (Wet-cooled) model

Site	Annual energy (GWh)	Capacity factor (%)	Levelized Cost of Electricity (LCOE) (real), cents per kWh	Net Present Value (NPV), USD
Bhopal	410.740	45.3	11.88	19,464,646
Jhansi	401.175	44.2	12.21	25,342,286
Jalandhar	330.133	36.4	14.09	19,734,204
Srikakulam	382.817	42.2	12.55	16,915,063
West Medinipur	329.713	36.4	13.89	15,083,772
Erode	387.021	42.7	12.52	15,477,209

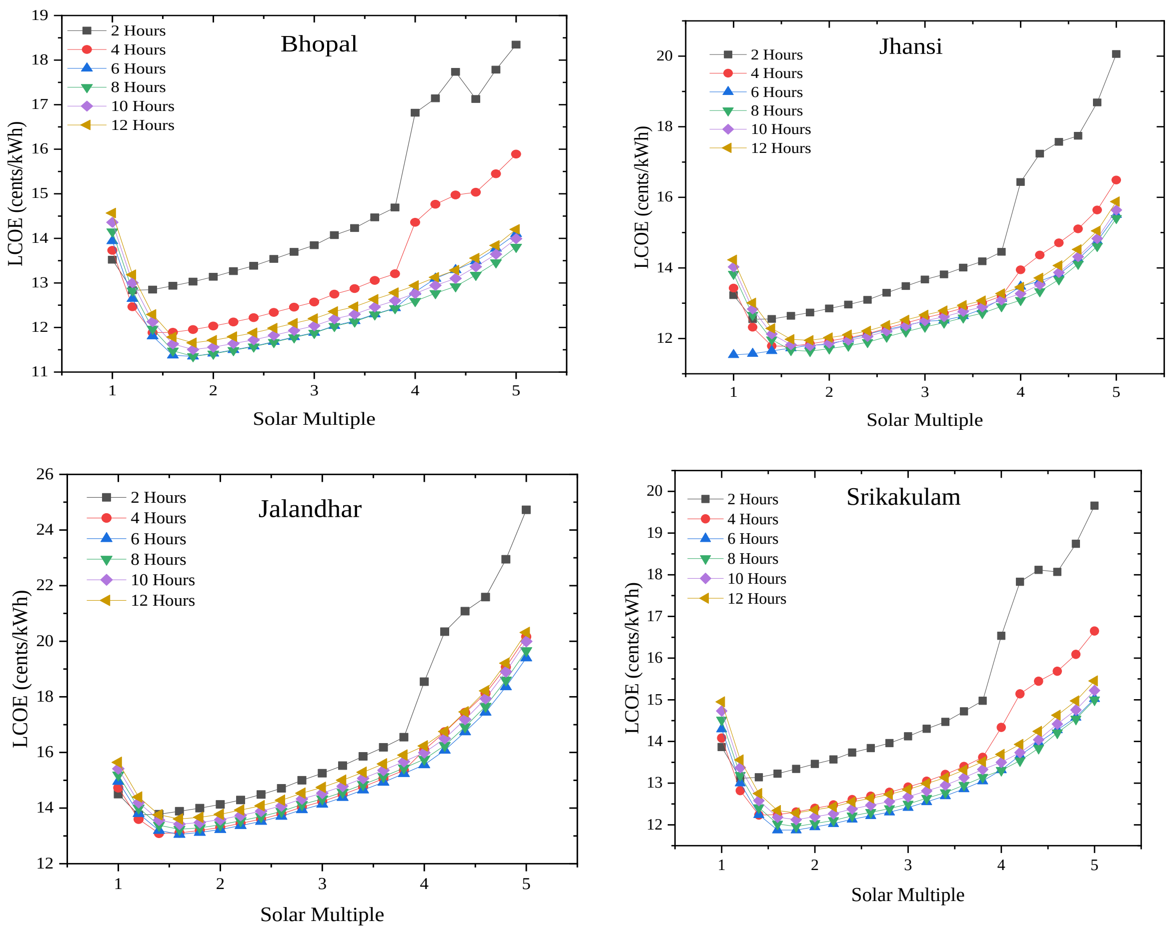

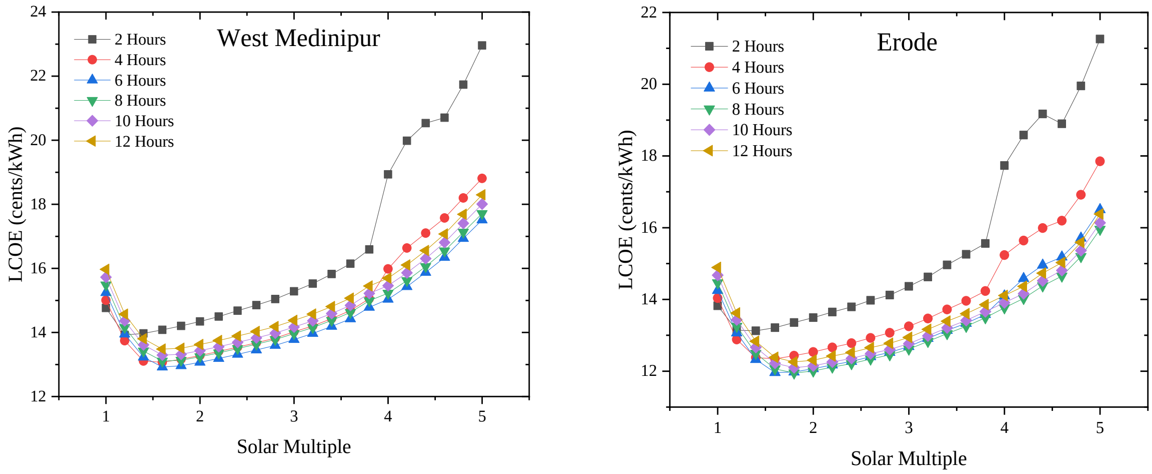

Figure 29 Effect of SM and TES on the LCOE (wet-cooled model) for potential sites in India

3.2.4.5 Sensitivity analysis

Sensitivity analysis plays a significant role in the development of projects such type of plants. Moreover, sensitivity analysis also provides the effect of parameters or factors on the technical and economic performance of the study. In the present computational study, the effect of LCOE on the sales tax rate, up-front fee, and solar multiple were considered for the sensitivity analysis. The first sensitivity analysis is conducted on sales tax rate on the economic feasibility with sales tax rate ranges from 1-5%. Similarly, the second sensitivity analysis is conducted on the up-front fee with the range of 1-5%. Finally, the third sensitivity analysis is conducted on the solar multiple (SM) with the range of 1-5.

Fig.30. shows that varying sales tax rate for dry and wet-cooled STPP plants showed a significant impact on the LCOE for the selected locations. The results clearly indicated with increase in sales tax rate the LCOE is also increases. It is also observed that LCOE of Jalandhar site relatively high compared to all other five potential sites for both dry and wet-cooled models, this is due to relative effective low solar radiation on that site. Moreover, the LCOE of Bhopal site is lowest LCOE with increase in the sales tax rate for both condenser models. In the case of Srikakulam and Erode, follows the same trend as economic analysis with a nominal difference. The impact of sales tax on LCOE was observed to be more impactful on the dry cooled plant than that of the wet cooled module.

Fig.31. represent the up-front fee on the energy cost from the STPP plant for the selected potential sites. The impact of up-front fee is positive for all the selected potential sites. It can be clearly observed from the graphs the up-front fee is relatively affect less than that of dry-cooled condenser model for the selected potential sites. From the findings it also observed that

the LCOE higher for the Jalandhar site as expectedly with an increase in the up-front fee for both models. Moreover, Bhopal site is recorder lower LCOE for the selected potential site.

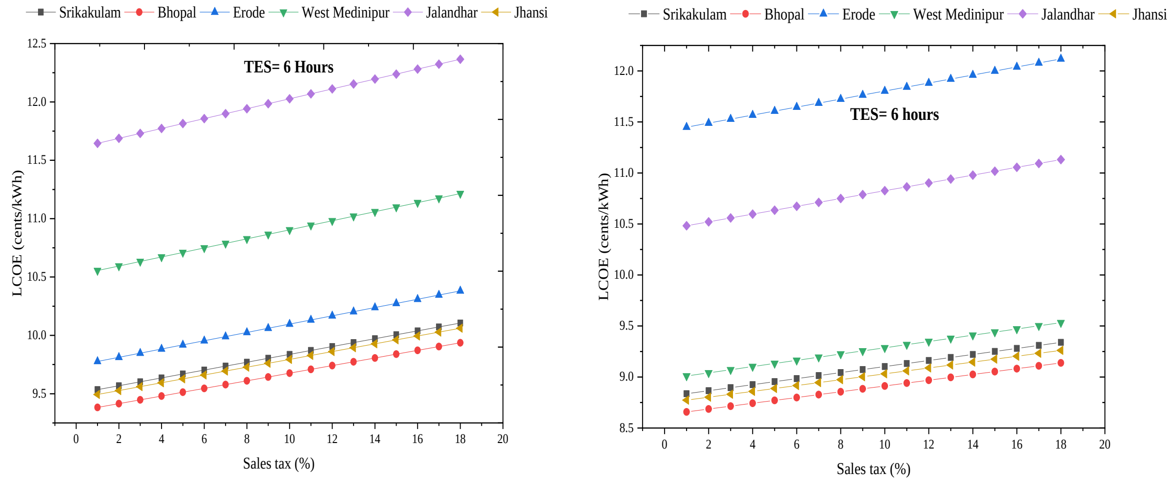

Figure 30 Effect of sales tax rate on LCOE: dry cooled (left); wet cooled (right) at 6 h TES for SM of 2

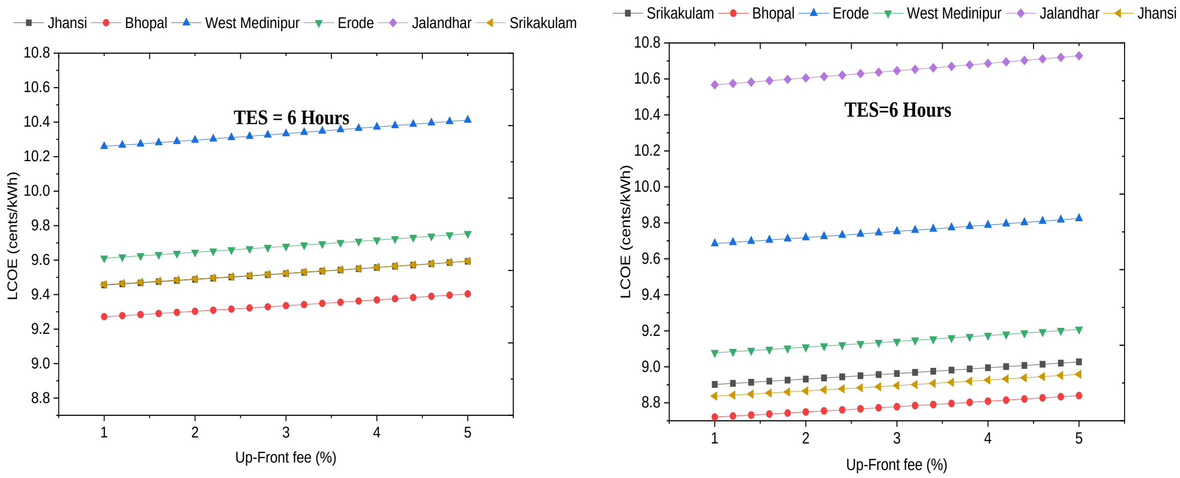

Figure 31 Effect of Up-Front fee on LCOE: dry cooled (left); wet cooled (right) at 6 h TES for SM of 2

The last sensitivity analysis in the present investigation is conducted by varying solar multiple with net capital cost (NCC) of six STPP plants. It can be seen from the **Fig.32.** that the SM has significant effect on the NCC on the STPP plant for six potential sites. It can be observed that NCC for the dry-cooled condenser is optimized between the solar multiple range of 1 to 2, and decreases after reaching maximum an optimum SM. the maximum NCC for wet-cooled model is 7.32521 ($/W), 7.32519 ($/W), 7.32399 ($/W), 7.3247 ($/W), 7.95507 ($/W), 7.3243 ($/W) for the various STPP sites, respectively. On the other hand, the maximum NCC achieved for the dry-cooled model for the Bhopal, Jhansi, Jalandhar, Srikakulam, West Medinipur, and Erode sites are 6.83789 ($/W), 6.83777 ($/W), 6.83772 ($/W), 6.8377($/W), 6.83754 ($/W), 6.83636 ($/W) at the SM range of 2.

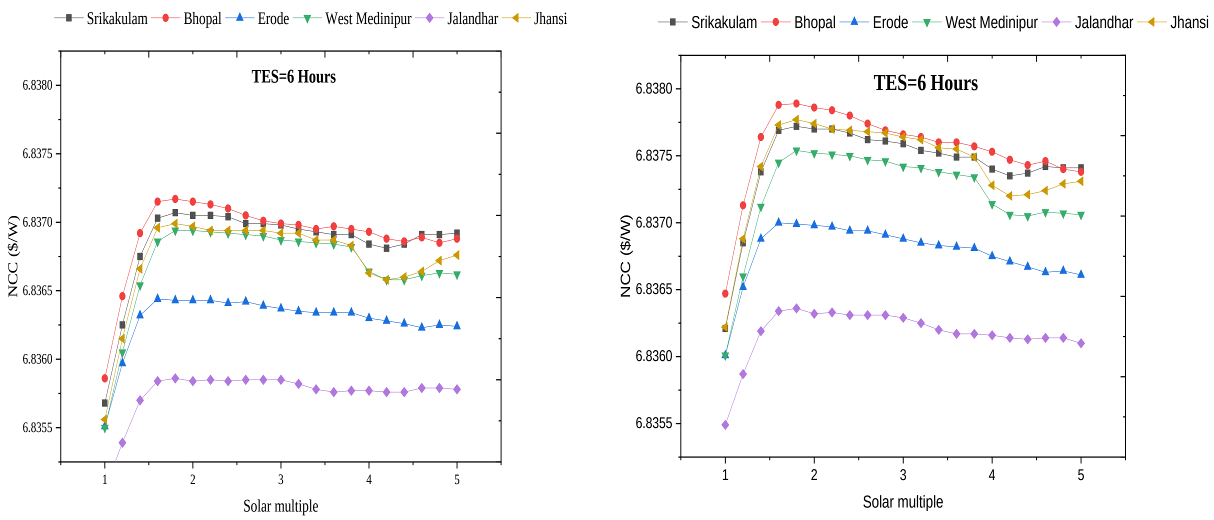

Figure 32 Effect of solar multiple on NCC: dry cooled (left); wet cooled (right) at 6 h TES for SM of 2

3.2.4.6 Environmental impact assessment for the selected potential sites

The outcome of the environmental assessment for the selected various STPP plants sites are presented in **Table.13**. It was on noted that Bhopal site is recorded the highest reduction in carbon gas emissions about 31132.5 for dry-cooled condenser model and 33984.63 metric tons for wet-cooled condenser model, this is due to the electricity generated in both condenser model for Bhopal site is higher while compared to other sites. However, if government of India is planned to implement to such sites in the country, then India can reduce overall of about 169,219.62 metric tons of CO_2e per year for dry-cooled STPP plant. On the other hand, it the wet cooled condenser model was deployed in the selected site then India can reduce about 185,469.9 metric tons of CO_2e for the selected locations. Further, findings observed that the wet-cooled model can reduce up to 9.6 % of carbon emission while compared to the dry-cooled condenser.

Table 13 Reduction of carbon emission use of CSP technology

Selected potential site	**Dry-cooled**		**Wet-cooled**	
	Generated Annual Energy (kWh)	Carbon footprint generated, metric tons of CO_2e	Generated Annual Energy (kWh)	Carbon footprint generated, metric tons of CO_2e
Bhopal	376269000	31132.50	410740000	33984.63
Jhansi	364845000	30187.28	401175000	33193.22
Jalandhar	300678000	24878.10	330133000	27315.20
Srikakulam	353159000	29220.38	382817000	31674.28
West Medinipur	301156000	24917.65	329713000	27280.45
Erode	349090000	28883.71	387021000	32022.12

3.2.5 Comparative analysis in the present study

The present study, is also compared with other published studies the results of the proposed of dry-cooled and Wet-cooled STPP models' system are compared with already published literatures from the various studies available till date by considering CSP parameters such as base on the available technologies, parameters, configurations and also due to economic criterion, i.e., Simulation software, TES, and LCOE. The results as presented in the current work fall within the range of values obtained in other studies, as demonstrated in **Table.14.**

Table 14 CSP technology with other published works, for comparison

Ref	Location, Country	CSP Technology	TES, Hours	LCOE
[98]	Quetta, Pishin, Gotki, Nawabshah, Rahim Yar Khan, Bahawalpur, Pakistan	Parabolic Trough Collector (PTC)	15	Quetta, 15.3 USD cents/kWh; Pishin, 14.7 USD cents/kWh; Gotki, 26.9 USD cents/kWh; Nawabshah, 23.9 USD cents/kWh; Rahim Yar Khan, 27.9 USD cents/kWh; Bahawalpur, 29.2 USD cents/kWh
[99]	Navrongo and Tamale, Ghana	STPP, and PTC	12	13.67 an14.73 USD cents/kWh for STPP; 28.83 and 25.83 USD cents/kWh for PTC
[100]	Jamshoro, Pakistan	parabolic solar dish/Stirling system (PSDS)	-	0.13 USD/kWh
[101]	Dodoma site, Sulunga site Tanzania	PTC, STPP	4	13.0–14.4 USD cents/kWh for PTC, 11.6–12.5 USD cents/kWh for STPP

[97]	Ethiopia	Central receiver system (CRS), linear Fresnel reflector (LFR)	12	9.44 USD cents/kWh for CRS, 10.35 USD cents/kWh for LFR
[102]	Algiers, Algeria	STP	-	0.235 USD/kWh
[103]	Maan, Jordan	PSDS	-	0.115 USD/kWh
[104]	Tianjin, China	PSDS	-	0.2535 USD/kWh
[105]	Oujda, Morocco	PTC	-	0.25 EUR/kWh
[106]	Sokoto, Nigeria	STP, LFR PTC	-	17.71 USD cents/kWh for STPP, 26.33 USD cents/kWh for LFR, 18.04 USD cents/kWh for PTC
[107]	Ahmedabad, Barmer, New Delhi, India	PTC	-	16–21 USD/kWh
[108]	China	LFR STP, PTC	6 –15	0.14 USD/kWh for LFR, 0.17 USD/kWh for PTC, 0.15 USD/kWh for
[109]	Bangladesh	STPP, PTC	-	13–14 BDT/kWh for STPP 15–17 BDT/kWh for PTC
[110]	Bangladesh	PTC	-	9.86 USD cents/kWh
[111]	Larnaca, Cyprus	PTC	4	18.14–19.26 USD cents/kWh
[112]	Sevilla, Spain	STPP	3	21.77 USD cents/kWh
[113]	Neom, Saudi Arabia	STPP	16	7.84 USD cents/kWh

Present Study	Bhopal, Jhansi, Jalandhar, Srikakulam, West Medinipur and Erode	STPP Dry Cooled	12	Bhopal, 13.22 cents/kWh; Jhansi, 13.62 cents/kWh; Jalandhar, 16.40 cents/kWh; Srikakulam, 14.065 cents/kWh; West Medinipur, 16.37 cents/kWh; and Erode city, 14.21 cents/kWh
Present Study	Bhopal, Jhansi, Jalandhar, Srikakulam, West Medinipur and Erode	STPP Wet Cooled	12	Bhopal, 12.40 cents/kWh; Jhansi, 12.90 cents/kWh; Jalandhar, 13.44 cents/kWh; Srikakulam and West Medinipur, 12.75 cents/kWh; Erode, 12.96 cents/kWh

3.3 Techno-economic feasibility of standalone of hybrid System for the hydrogen production and electric vehicles in five unique climatic conditions in India

In the present study, a techno-economic assessment conducted for the production of hydrogen (H_2) in five metropolitan cities. However, H_2 production plays a major role in the sustainable development in the world. A lot of researchers around the world has done to achieve the H_2 production from solar PV hybrid system. For instance, Agyekum et al. [114] obtained a techno-economic assessment for the production of H_2 for agricultural facilities. Their study concludes that the total H_2 from the system is 8816kg/year at cost of 4.5 $/kg. Song et al. [115] designed a hybrid energy system using surplus photovoltaic power in northeast China. Their study concludes that the H_2energy is produced about 700 kg/day and the cost of system is 0.0615$/kWh. Rad et al. [116] also conducted a techno-enviro-economic analysis in rural areas of Iran for H_2 production. The results from their study concludes that LCOE is minimized from 0.096-0.233$/kWh for on grid and off-grid system. Gu et al. [117] also conducted a techno-economic analysis on green methanol plant, for the production of H_2 energy. Their study significant achieve is to decrease the carbon dioxide emission in China. Wang et al. [118] performed a techno-economic solar/wind/bioethanol H_2 production via membrane reactor. Their study concluded that energy efficiency, H_2 cost, and CO_2 reduction rate is reduced to

62.48%, 4.16$/kg, and 835.55 ton/year. Naseer et al. [119] performed a techno-economic analysis for Egyptian climatic condition for production of hydrogen in five unique cities. The results concluded that the overall efficiency and LCEO for system for the five cities are 7.69-9.37% and 4.54-7.48$/kg, respectively. Therefore, from the literature survey a huge work has done for production of hydrogen for different climatic. However, India is one of the densest countries in the world with huge companies. India is one of the countries that generates 3% of gross domestic product in the transportation sector. Since, India is looking climatic mitigations and strategies, it has the opportunity to improve such strategies and actions to best align with the larger goals of minimizing its GHG emissions from its energy systems. From the reports India stands one 15 out of 20 countries effecting the population with concentrations of particulate matter 2.5 [120]. Hence, it is an urgent need to find alternative ways of meeting the country's energy needs for the road transport and electricity sectors. Electrical charging vehicles is one of the possible alternative methods to reduce GHG. Similarly, in this present study, a techno-economic assessment for the production of hydrogen load represents a refueling station for 20 hydrogen fuel cell vehicles with a tank capacity of 5 kg for each location. Although, the present study, is unlike other studies on India, considered five different locations at a time for the techno-enviro-economic analysis which gives a wider coverage area to help policy and decision makers during the planning period for the analysis. In contrast, the literature covered so for, of such studies on India, this study also assessed additionally the avoided carbon dioxide emissions (CO_2) emissions from the generated electricity utilizing from the PV power plant and also the gasoline fuel replacement. Moreover, such studies are important since the focus is also to help find alternative ways of meeting the country's energy demand without polluting the environment. It is therefore expected to provide information on the potential greenhouse gas (GHG) emissions that could be prevented should the proposed configurations at the various locations be implemented.

3.3.1 Description of HOMER software as hybrid model

The HOMER is an optimization tool developed by NREL in U.S. Moreover, the software evaluates the technical and financial aspect of off-grid or on-grid system hybrid system. HOMER software is allowing to combine two or more renewable energy system for the generation of electricity. To that attempt in the present study, we also studied a combination of hybrid PV system to produce electricity and hydrogen production from the PV system.

3.3.2 Hybrid model system description for the present study

In the present study, the hybrid model used for the generation of electricity, hydrogen production and electric vehicles are consisting of solar PV plants electrolyzer, FC, battery, a system converter, and hydrogen tank. The flow chart is shown in **Fig.33.** Similarly, the mathematical models that are evaluated for the calculation of each component is presented in further sections.

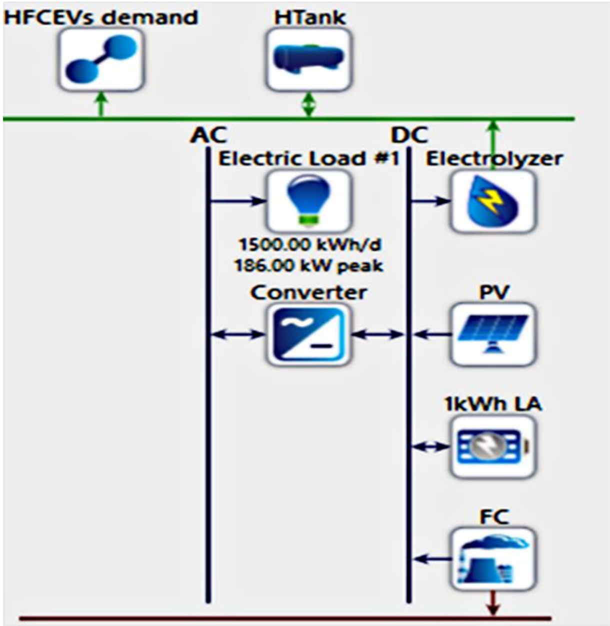

Figure 33 The schematic representation used for the hybrid system

3.3.3 Solar PV module

A solar PV module is consisting of several PV cells that uses sunlight energy to electrical energy. A generic flat plate PV module was selected for the analysis, and it has a temperature coefficient of -0.5 and an efficiency of 13%. The total electricity generated power by a PV array is calculated using **Eq. (25)** [121]

$$P_{PV} = V_{PV} I_{PV} Z_{PV} \tag{25}$$

Where, V_{PV}, I_{PV}, and Z_{PV} are voltage, current and number of PV modules

Moreover, for optimum voltage and current can be further calculated is presented in **Eq. (26-31)**[121]

$$V_{PV} = V_{mp}\left[1 + 0.0539\log\left(\frac{I_T}{I_{st}}\right)\right] + \beta_0 \Delta T \tag{26}$$

Here, $\Delta T = T_{cell} - T_{st}$

$$T_{cell} = T_A + 0.02 I_T$$

Here, V_{mp} , I_T, I_{st}, β_0, ΔT, T_A, and T_{st} are maximum voltage, total solar radiation on PV panel, total solar radiation consideration 1000 W/m^2, voltage temperature coefficient, temperature difference, ambient temperature from the atmosphere, and standard temperature at 25 ^{0}C

Moreover,

$$i_{PV} = i_{SC}\left(1 - c_1\left[exp\left(\frac{V_{PV} - \Delta V}{C_2 V_{oc}}\right) - 1\right]\right) + \Delta i \tag{27}$$

$$c_1 = \left(1 - \frac{i_{mp}}{i_{SC}}\right)\exp\left(\frac{-V_{mp}}{C_2 V_{oc}}\right) \tag{28}$$

$$c_2 = \frac{V_{mp}/V_{OC^{-1}}}{\ln\left(1 - i_{mp/i_{SC}}\right)} \tag{29}$$

$$\Delta V = V_{PV} - V_{mp} \tag{30}$$

$$\Delta i = \alpha_0\left(\frac{I_T}{I_{st}}\right)\Delta T + \left(\frac{I_T}{I_{st}} - 1\right)i_{SC} \tag{31}$$

Here, i_{SC}, V_{oc}, i_{mp}, and α_0 are the short-circuit current, open-circuit current, maximum power, and the temperature coefficient, respectively.

3.3.4 Battery storage

A battery storage is an electrochemical device that stores energy and release electricity on demand. For example, the energy produced by solar PV plants are can be stored in batteries and can be used as alternative source of electricity in the absence of sunlight. The state of charge of battery storage is estimated using **Eq. (32)** [122]

$$SOC(t) = SOC(t-1) \times \int_{t-1}^{t} \frac{P_b(t) \times \eta_{bat}}{V_{bus}} \tag{32}$$

Here, V_{bus}, η_{bat}, $P_b(t)$ are voltage bus, battery efficiency, and batteries load power (kW), respectively can be estimated in **Eq. (33)** [123]

$$P_b(t) = \frac{k \times Q_1(t) \times \exp(-k) + Q(t) \times k \times c \times (1 - \exp(-k\Delta t))}{1 - \exp(-k\Delta t) + c \times (k\Delta t - 1 + \exp(-k\Delta t)} \tag{33}$$

Herer, the available energy at the beginning of the operating interval and above the min SOC is denoted by $Q_1(t)$, the constant energy storage rate is represented by k, the storage capacity ratio is also denoted by c, Q(t) represent the total energy at the start of the passage of time, and Δt is the time interval.

3.3.5 Fuel Cell

The working principle of fuel cell is same as battery. The significant benefit of fuel cell it does not require any additional external charge such as battery. However, a fuel cell uses chemical energy for the generation of electricity, and it has two electrodes, an anode and cathode. Hence, the generated by fuel cell is given in **Eq. (34-35)** [124]

$$P_{FC} = N * V_{FC} * I_{FC} \tag{34}$$

Here, N, V_{FC}, and I_{FC} are number of cells in the stack, output voltage of fuel cell, and current of fuel cell, respectively.

Moreover, output voltage of fuel cell can be estimated as

$$V_{FC} = E - V_{act} - V_{con} - V_{\Omega} \tag{35}$$

In which, E, V_{act}, V_{con}, and V_{Ω} signifies fuel cell internal storage, activation voltage, concentration voltage, and ohmic voltage

3.3.6 Hydrogen Storage Tanks

The hydrogen can be stored in two storages either compressed or cryogenic fluids. The storage hydrogen gas will be to generate electricity or further used for refueling cells.

3.3.7 Electrolyzer

The working principle of electrolyzer is to separate the hydrogen and water by using electrolyzer process. However, the separated hydrogen is stored in the hydrogen tank for the fuel generation for power generation. The power generation of electrolyzer is expressed as **Eq. (36)** [123]

$$P_{EZ} = \frac{\dot{m}_{H_2}\, HHV_{H_2}}{\eta_{H_2}} \tag{36}$$

Here, $\dot{m}_{H_2}$, HHV_{H_2}, η_{H_2}, and P_{EZ} are the mass flow rate hydrogen generated to the electrolyzer (kg/s), is the heating value of hydrogen fuel, is the total efficiency of the electrolyzer, and the DC power of the electrolyzer.

The rate of the obtained hydrogen can be calculated using **Eq. (37)** [125]

$$R_{hydrogen} = \frac{I_{ele} \times \eta_F \times N_c}{2F} \tag{37}$$

Where the total number of cells in series in the electrolyzer is represented by N_c, the current of the electrolyzer is represented by I_{ele}, F is the Faraday's coefficient and η_F represent the Faraday efficiency which can be estimated using **Eq. (38)** [125]

$$\eta_F = 96 \times exp\left(\frac{0.09}{I_{ele}} - \frac{75.5}{I_{ele}^2}\right) \tag{38}$$

3.3.8 Power Converter

A power converter is used in any hybrid system that converts AC to DC and DC to AC. Simultaneously, power from solar PV panel to fuel cells is DC supply. A DC/AC conversion is important during the use of household equipment, whiles the AC/DC conversion is needed to help store a current in batteries. The inverter's output power P_{out} depending on the input power P_{in} as well as its efficiency η_{inv} can be estimated using **Eq. (39)** [126]

$$P_{out} = P_{in} \times \eta_{inv} \tag{39}$$

3.3.9 Selection of potential Sites

In the present study, we selected five potential metropolitan cities which are economical feasible from all parts of India (North, East, West, South and central cities which have unique weather characteristics. However, selected location are Ludhiana, Indore, Mumbai, Chennai, and Kolkata are presented in **Fig.34.** Similarly, the selected locations coordinates are presented in **Table.15.**

Figure 34 Graphical presentation of selected potential sites

Table 15. Selected potential sites

City	Latitude (^{0} N)	Longitude (^{0} E)
Ludhiana	30.901	75.857
Indore	22.719	75.857
Mumbai	19.076	72.877
Chennai	13.082	80.270
Kolkata	22.572	88.363

3.3.10 Solar intensity of selected sites

The solar radiation and clear index of selected sites is presented in **Fig.35.** available from the National Aeronautics and Space Administration (NASA) surface meteorology and solar energy database. The monthly average solar radiation of for Ludhiana is 5.58 kWh/m^2/day, for Indore is 5.80 kWh/m^2/day, for Mumbai is 6.05 kWh/m^2/day, for Chennai is 5.95 kWh/m^2/day, and for Kolkata is 5.19 kWh/m^2/day, respectively in **Fig.35a**. On the other hand, the clearance index of the selected five sites is presented in **Fig.35b**. The findings revealed that the average clearance index for the Ludhiana is 0.612, for the Indore is 0.570, for the Mumbai is 0.630, for the Chennai is 0.537, and for the Kolkata is 0.516, respectively.

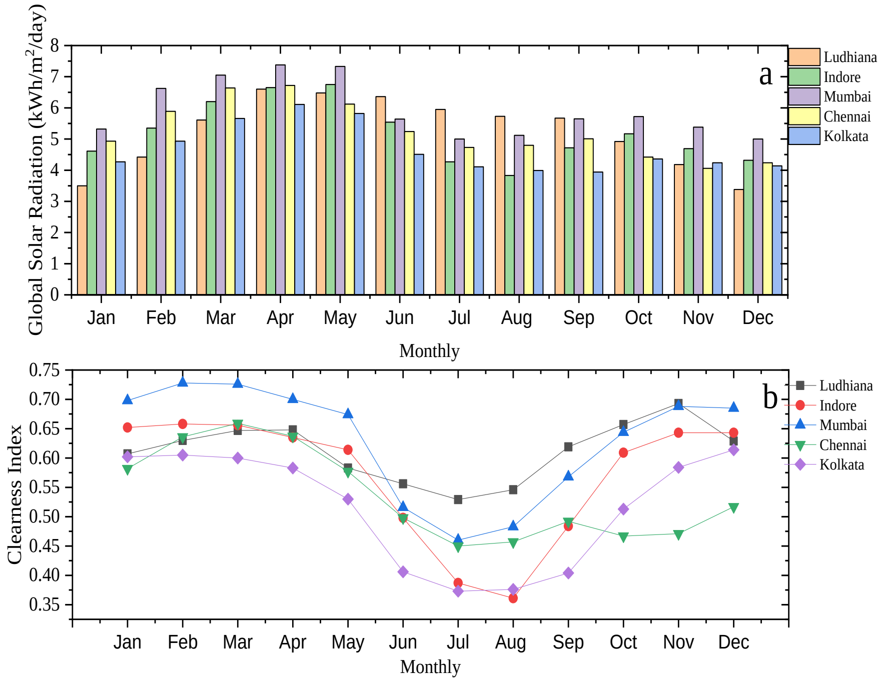

Figure 35 Monthly dependence selected sites (a) solar radiation and (b) clearness index

3.3.11 Economic analysis for hybrid system

In the present section, an economic analysis is discussed either the selected project is economically feasible or alter the methods of the project. The economic analysis used in the present hybrid system are LCOE and NPC.

3.3.12 Levelized cost of energy

The levelized cost of energy is widely accepted analysis among the renewable energy sector. It is defined as the ratio of the average cost per kWh of valuable electrical energy produced by the system. The LCOE is presented in the following **Eq. (40)** [127]

$$LCOE = \frac{NPC\ (\$)}{\sum_{h=1}^{h=8760} P_{load}(h)(kWh)} \times CRF \tag{40}$$

3.3.13 Net Present cost

The net present cost (NPC) is defined as the system's life cycle cost, the present value for the various installations, as well as the cost of operations in the entire lifespan of the project. In the present study, 25 used years for the analysis. Moreover, the total NPC is the HOMER's significant economic output parameter because all the selected systems based on the NPC. The remaining other economic outputs are calculated by finding the NPC. Therefore, the NPC of the present study is calculated by using **Eq. (41)** [127]

$$C_{NPC} = \frac{C_{annual,total}}{CRF\ (i, R_{project})} \tag{42}$$

Here, $C_{annual,total}$, CRF, i, $R_{project}$ signifies the total annual cost, capital recover factor, real interest rate, and project lifetime of the study

The CRF is a ratio that is employed to estimate the present value of an annuity and can be mathematically estimated using **Eq. (43)**

$$CRF_{(i,N)} = \frac{i(1+i)^N}{((1+i)^N - 1)} \tag{43}$$

The cost of various components is presented in **Table.16.** In this study a nominal discount rate and inflation rate are taken as 8%, and 2%.

Table 16 Component sizing and life cycle cost

Component	Initial cost	Replacement	O & M	Size Simulated	Ref
PV	$350/kW	$350/kW	$10/kWyr	1000, 2000, 3000, 3500 kW	[128]
Electrolyzer	$100/kW	$100/kW	$8/kWyr	1000, 1500, 2500, 3000, 3500 kW	[128]
Battery	$300/unit	$300/unit	$10/unit/year	500, 1000, 1500, 2000, 3000 strings	[129]
Fuel Cell	$450/kW	$400/kW	$0.15/kW/op.hr	100, 150, 200, 250 kW	[130]
Hydrogen tank	$1.5/kg	$0.5/kg	$0.6/kg/yr	1000, 2000, 3000, 4000 kg	[130]
Converter	$300/kW	$300/kW	$0/kW/yr	HOMER automatic optimization.	-

3.3.14 Load Profile

Fig.36. depicts the hydrogen load for 20 refueling stations for the 20 hydrogen fuel cell vehicles with a tank capacity of 5 kg. Thus, a daily hydrogen load of 100 kg has been estimated for the study. The refueling is assumed to be take place from evening 20:00 till morning 8:00. Hence, a 100 kg/day is equally distributed for the 12 h. The electric load will require electricity of 1500 kWh/d, and the peak demand is also 186 kW. On the other hand, the electric load represents the demand of the neighboring communities where these hydrogen production refueling station will be constructed. This is a synthetic electricity load profile obtained from the HOMER software for the purposes of the analysis as depicted in **Fig.37.**

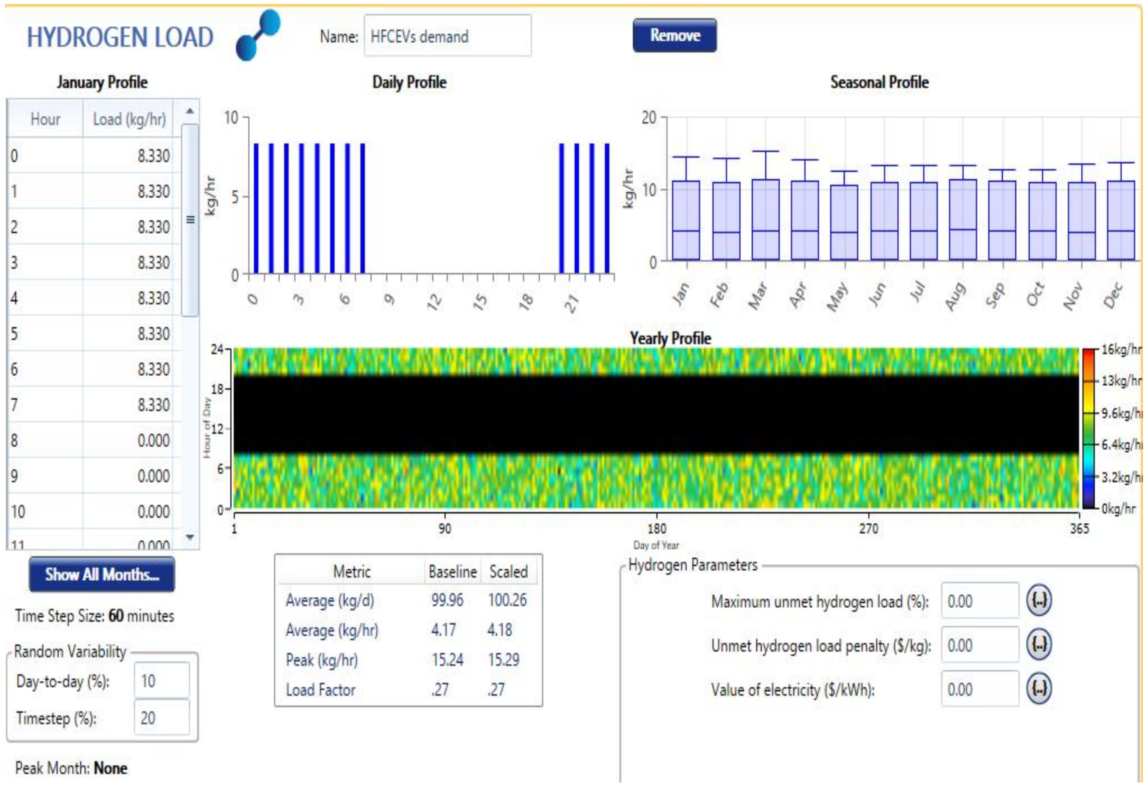

Figure 36 Hydrogen Load

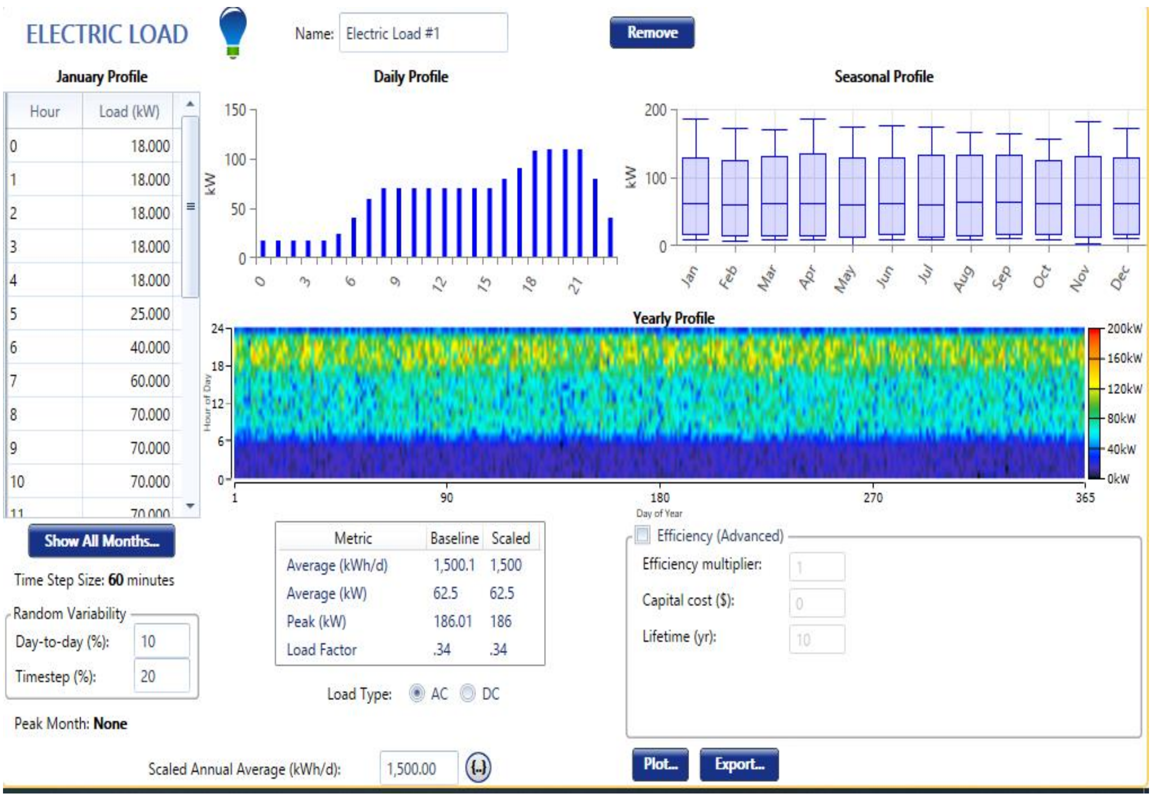

Figure 37 Electric load

3.3.15 Results and Discussion

This section presents the outcome results of HOMER simulation and optimized configuration for the selected locations. The section further divided into technical, economical, and environmental aspects. Operational characteristics such as excess electricity, annual energy production, unmet load, hydrogen production, capacity shortage, etc., were assessed for each of the simulated systems at the various locations in the country.

3.3.16 Electricity generation

The load following (LF) control strategy was used for the simulation. The LF configuration is one of the best strategies with high RE sources. The system architecture for each location is presented in **Table.17.** The results suggest that the configuration of the optimum system is dependent on the location since the weather characteristics at each location varies. For instance, whereas a 3000 kW PV module with an FC of 100 kW and a 4000 kg hydrogen tank will be able to meet the investigated load demand presented supra for Ludhiana, the same cannot be said of some other cities. The number of batteries and the converters, however, remained constant for all studied locations, whiles the other components vary in size.

Table 17 System architecture of optimum systems for each location

Location	PV (MW)	Fuel Cell (kW)	Battery (Strings)	Electrolyzer (MW)	Hydrogen Tank (kg)	Converter (kW)
Ludhiana	3	1	500	2.5	4000	172
Indore	3.5	1	500	1.5	3000	172
Mumbai	3	1	500	1.5	2000	172
Kolkata	3.5	1	500	2.5	4000	173
Chennai	3.5	1.5	500	1.5	4000	172

The monthly electricity generation of five selected sites is presented in **Fig.38.** The electricity generated from the PV power plant for Ludhiana, Indore, Mumbai, Kolkata, and Chennai are 95.9 % to 96.6, respectively. On the other hand, the fuel cell produced achieved is 3.4 % to 4.14 % for the selected five locations. Since the electricity production of each month is affected by the solar radiation in each month. The findings also revealed, that the highest electricity from the month of February and April, due to rich availability of solar radiation. Electricity generation from the PV module is, however, affected by the poor weather conditions in the months of June through to August due to the monsoon or rainy season within that period. The outcome of the simulation with respect to electricity production suggests that a PV only system in terms of electricity generation may suffer from production shortfalls during the monsoon period. It is therefore imperative to develop a hybrid system consisting of other energy sources to support the PV system during that period of the year. Since the idea is to help cut down on GHG emissions, it will be appropriate to integrate a wind power system rather than a conventional power plant such as a diesel generator.

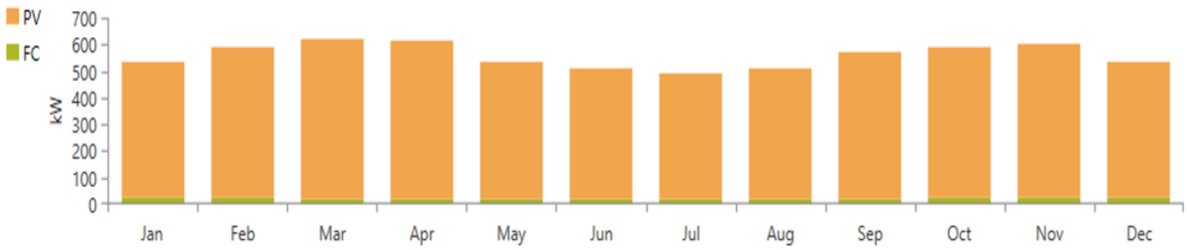

(a)

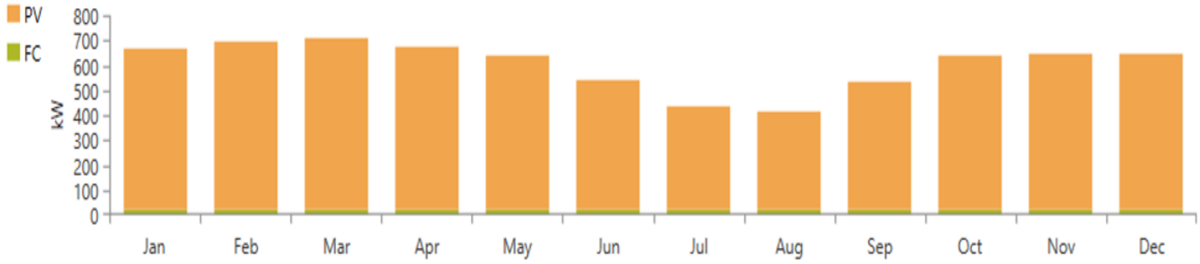

(b)

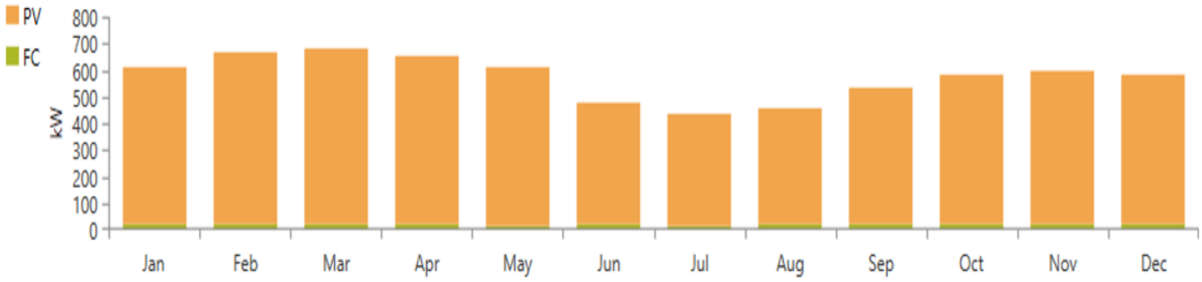

(c)

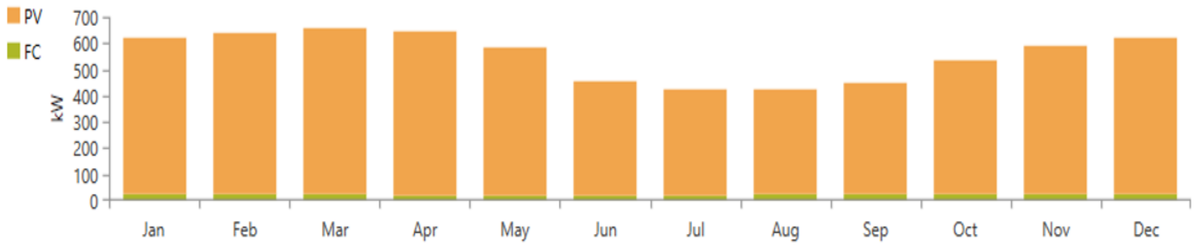

(d)

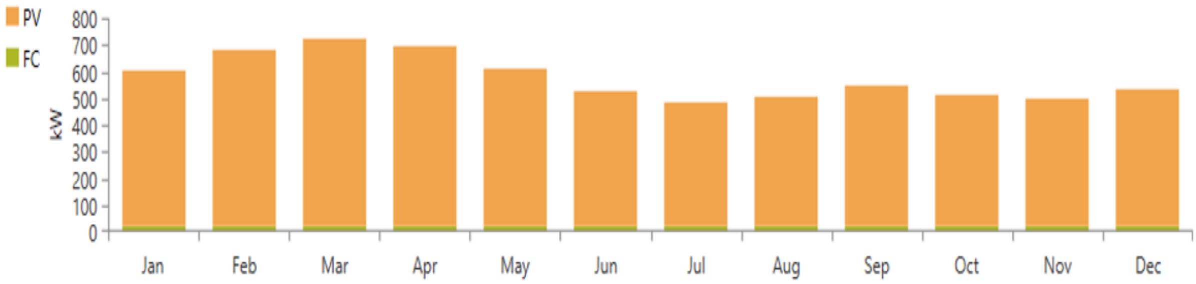

(e)

Figure 38 Monthly electricity production (a) Ludhiana (b) Indore (c) Mumbai (d) Kolkata (e) Chennai

The details of electricity generation from the various configuration at selected potential locations in presented **Table.18.** It was observed from the findings, the highest electricity generated of a PV plant is Indore city due to availability of relatively high solar radiation in that city compared to the remaining cities.

Table 18 Electricity production summary for the PV and FC at various cities

City	Production Summary	
	Flat Plate PV (GWh/yr)	**Fuel cell (GWh/yr)**
Ludhiana	4.70	0.184
Indore	5.09	0.180
Mumbai	4.85	0.172
Kolkata	4.84	0.195
Chennai	4.63	0.200

The results of electricity access, unmet electric load, and capacity energy storage are presented in **Table.19.** From the table it was observed that excess electricity generation from the plant is achieved by Indore city. A 100% renewable fraction was recorded at all cities since the electricity generation was solely generated from the PV module and hydrogen FC. However, the maximum renewable penetration for Ludhiana, Indore, Mumbai, Kolkata, Chennai is 8.269%, 8.355%, 8.375%, 5.835%, 7.468% and, respectively. The least renewable penetration was recorded at Kolkata since that enclave recorded the least solar radiation among the studied cities. Similarly, the unmet electric load for Ludhiana, Indore, Mumbai, Kolkata, and Chennai are 60.3 kWh/yr, 64.3 kWh/yr, 66.3 kWh/yr, 60.4 kWh/yr, and 64.3 kWh/yr, respectively. In addition, the findings of capacity of shortage of five selected locations are 5.5kWh/yr to 540kWh/yr, respectively, for the selected locations.

Table 19 Excess electricity, unmet electric load, and capacity shortage in various cities

City	Excess Electricity (GWh/yr)	Unmet Electric Load (kWh/yr)	Capacity Shortage (kWh/yr)
Ludhiana	0.65	60.3	537
Indore	1.10	64.3	540
Mumbai	0.97	66.3	543
Chennai	0.78	64.3	535
Kolkata	0.43	60.4	538

The performance of fuel cell capacity factor, fuel consumption and hours of operation of the selected hybrid system is depicted in **Fig.39.** The mean electrical efficiency of a FC cell for all the selected location are 14.3%. It can be seen from the results that the highest period of operation of the FC occurred at Kolkata, with the highest capacity of 22.9%, and the least hours of operation of the FC however occurred at Chennai where the least CF was also recorded.

On the other hand, the battery system of various configurations at the five potential locations are presented in **Table.20.** It was observed that the annual throughout for the Ludhiana, Indore, Mumbai, Chennai and Kolkata are 81,360 kWh/yr, 81,264 kWh/yr, 82,783 kWh/yr, 73,991 kWh/yr, and 80,337 kWh/yr, respectively. It is evident from the finding the

Chennai experienced lowest annual throughout, while the Mumbai experienced highest. The battery wear cost can be explained as the cost of cycling the energy through the battery bank. In this HOMER simulation, if the properties of the storage system show that the storage life is limited by throughput, HOMER assumes that the storage bank needs a replacement in a situation whereby its entire throughput is equal to its lifetime throughput. The storage wear cost is calculated using. **Eq. (20)**. The performance of battery for all five selected location is depicted in **Fig.40.**

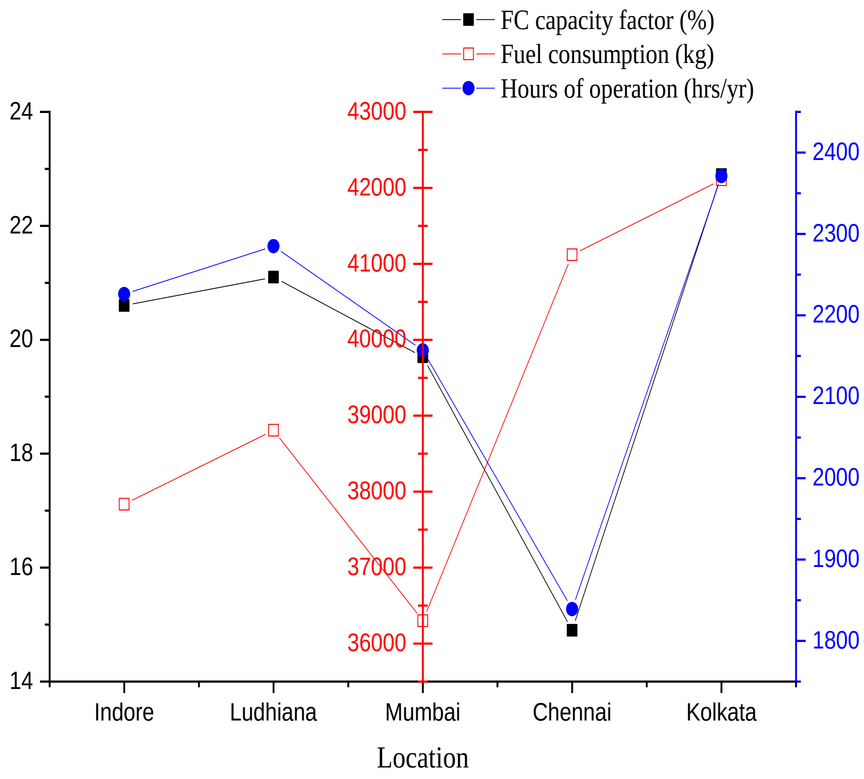

Figure 39 Performance of the FC at the selected locations

$$C_{bw} = \frac{C_{rep,batt}}{N_{batt} \times Q_{lifetime} \times \sqrt{n_n}} \tag{20}$$

Here, $C_{rep,batt}$, N_{batt}, $Q_{lifetime}$, n_n signifies the storage bank's replacement cost is denoted ($), number of storage tanks, single storage tank (kWh), is the efficiency (lifetime). The storage wear cost for the storage system at all sites remained the same at a cost of 0.419 $/kWh.

Table 20 Performance of the battery system

Location	Energy In (kWh/yr)	Energy Out (kWh/yr)	Storage Depletion (kWh/yr)	Annual throughput (kWh/yr)
Ludhiana	90,849	72,771	102	81,360

Indore	91,270	73,103	97.8	81,264
Mumbai	92,445	74,043	97.7	82,783
Chennai	82,641	66,180	74.9	73,991
Kolkata	89,710	71,855	97.5	80,337

3.3.17 Hydrogen Production

The performance level of the hydrogen tank for the whole year and day are depicted in **Fig. 41.** Since, the effect of relatively lower solar insulation that achieved at the beginning of the year affected the level of the hydrogen tank for the selected five locations at the beginning of the year. Although, the production of hydrogen at all sites, however, began to increase from the February month of the year and hits peak between April and June but decreased to considerably between August and October at Indore and Kolkata due to the effect of monsoon season. The production is, however, stable in Ludhiana and Mumbai all through the year except in January due to winter season. From the findings it is revealed that, the highest hydrogen production occurred at Kolkata with 82,054 kg/year, followed by Chennai with 79,030 kg/year. Ludhiana, Indore, and Mumbai followed with 78,524 kg/year, 76,935 kg/year and 74,510 kg/year, respectively. Further, the production of hydrogen consumption by the FC at Kolkata location is found to be the highest among all sites. It is recorded as a consumption of 42,107 kg/year representing 53.5% of the hydrogen produced, Chennai followed with 41,118 kg/year (52.9%), Ludhiana, Indore, and Mumbai with 38,809 kg/year (51.5%), 37,835 kg/year (50.8%) and 36,301 kg/year (49.8%), in that order. The monthly hydrogen production at the various locations is presented in **Fig. 42**. The monthly production of hydrogen followed the same trend as that of the electricity production. It can be observed from the study that the seasons had a significant effect on the monthly output.

3.3.18 Economic analysis

The economic analysis performance of all the selected five locations is presented and discussed. The generated LCOE for Ludhiana, Indore, Chennai, Mumbai and Kolkata are 0.45$/kWh, 0.44$/kWh, 0.46$/kWh, 0.41$/kWh, and 0.48$/kWh, respectively. The recorded LCOE is lowest for Mumbai, and while highest for Kolkata. The LCOE value is significantly depended on the electrical generation of the hybrid system. It is important to note that the capacity of the used PV module significantly played an important role in the various LCOE recorded at the various locations in the study.

Moreover, the least operation cost (OC), which is the annualized value for all costs and revenues other than the initial capital costs, was recorded at Mumbai Indore, Chennai, Ludhiana, and Kolkata also followed with $111,075, $117,351, $122,750, $l24,405 and $130,357, respectively.

The net present cost (NPC) is defined as the present value of the total project cost that is experienced by the facility over the entire lifetime of the project, subtracted the present value of all the revenue that accrued over the project's lifetime, for the various locations are presented in **Fig. 43.** In the present study, the cost includes such as for the replacement cost, capital cost, operating and maintenance (O&M) cost, since in the present study there is no fuel cost, hence it can be assumed to be zero (0), whereas the salvage value also forms part of the revenues been taken into consideration. Hence, the total NPC is calculated as presented under the method section, and it includes the addition of all the total discounted cash flows for every year in the lifetime of the project. The PV system for all the configurations at the various sites contributed the highest cost to the entire NPC for each location, whiles the hydrogen tank incurred the least cost.

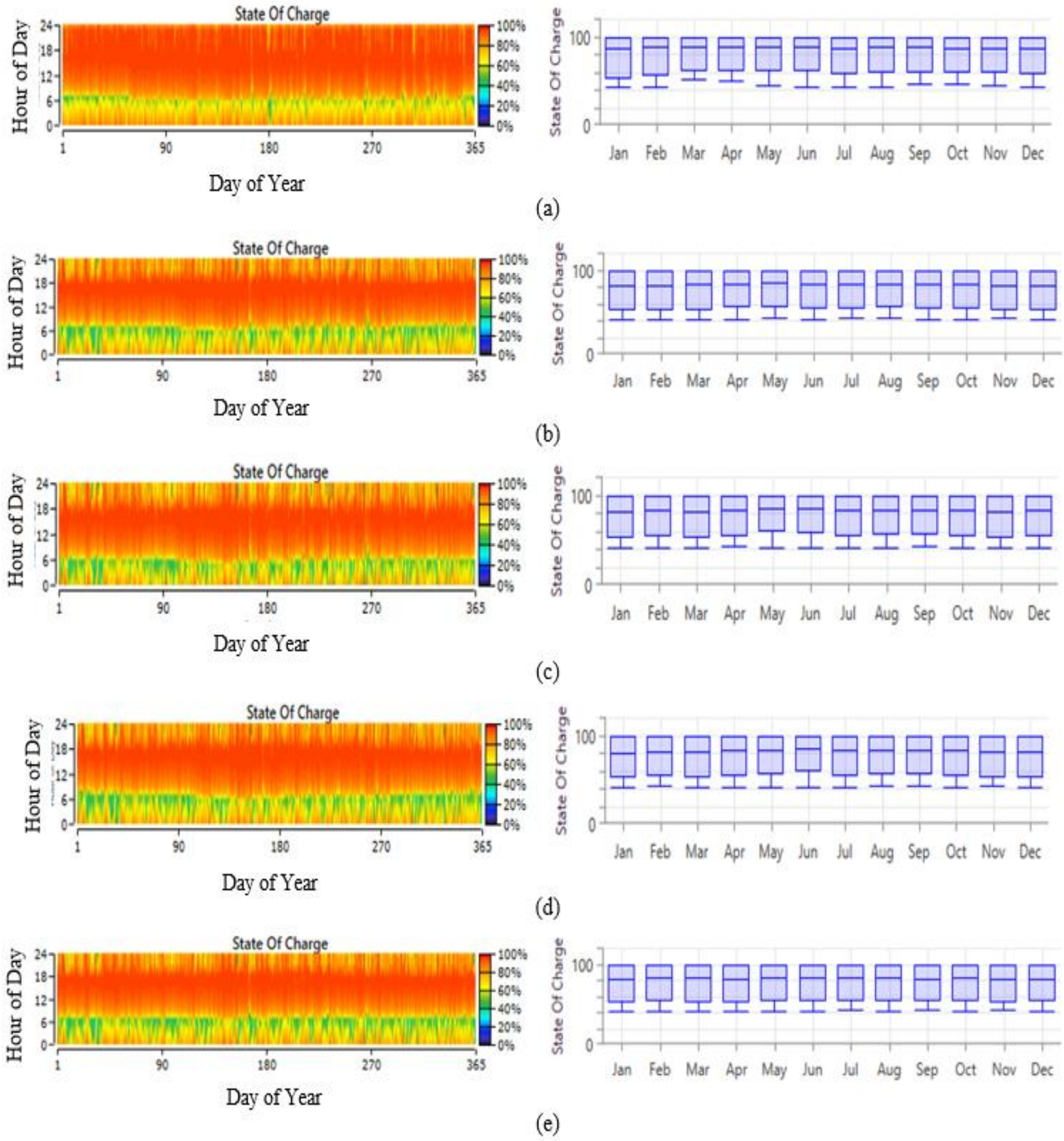

Figure 40 SOC of the battery system at various sites (a) Chennai, (b) Indore (c) Kolkata (d) Ludhiana (e) Mumbai

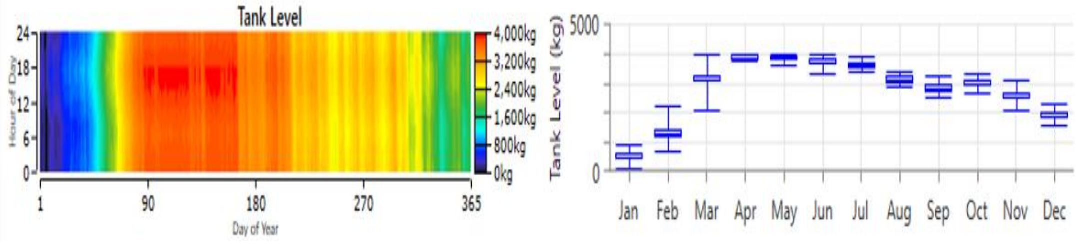

Day of Year

(a) Chennai

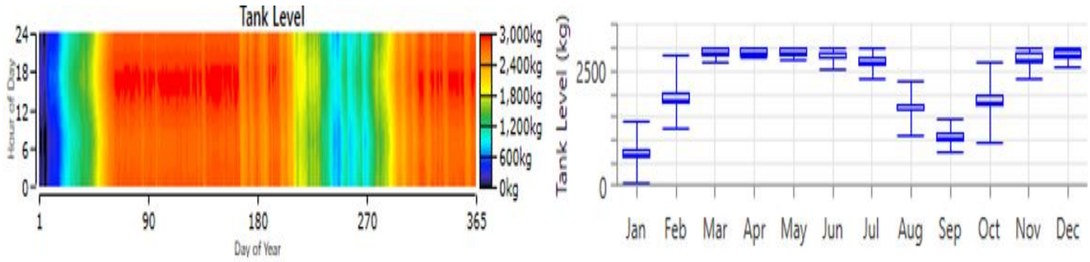

Day of Year

(b) Indore

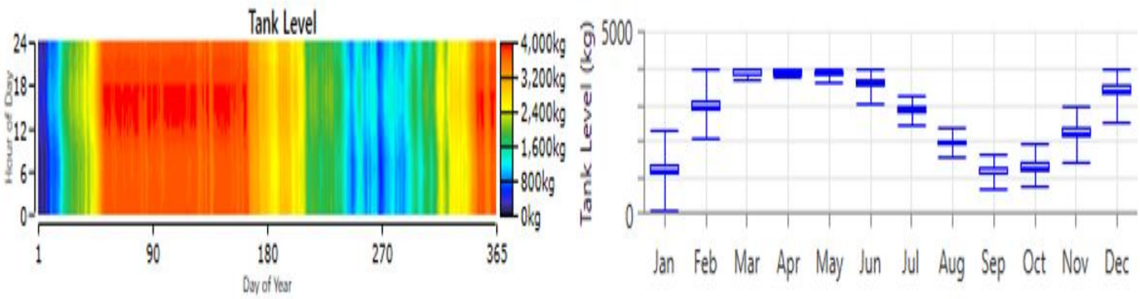

Day of Year

(C) Kolkata

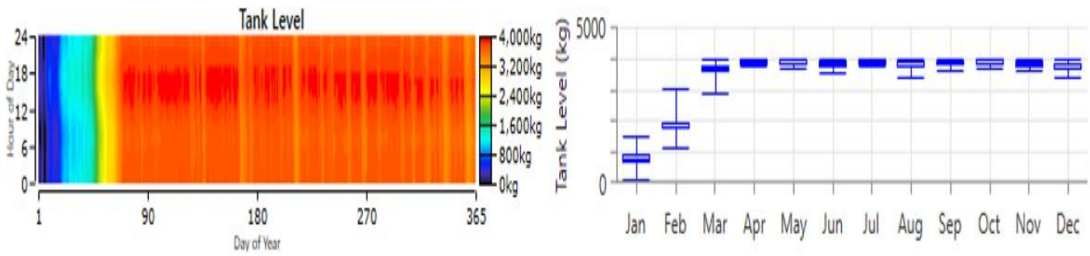

Day of Year

(c) Ludhiana

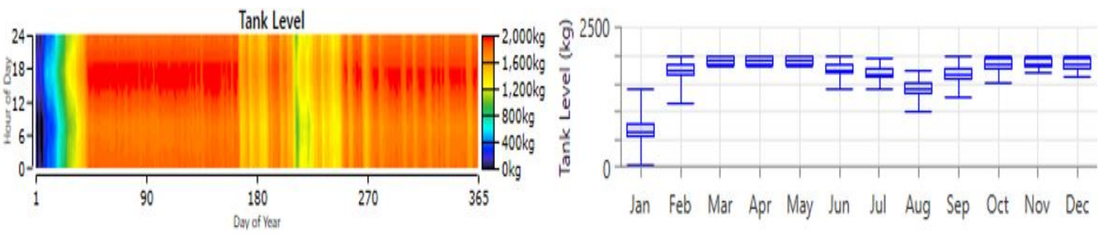

(e) Mumbai

Figure 41 Level of hydrogen tank at the selected locations

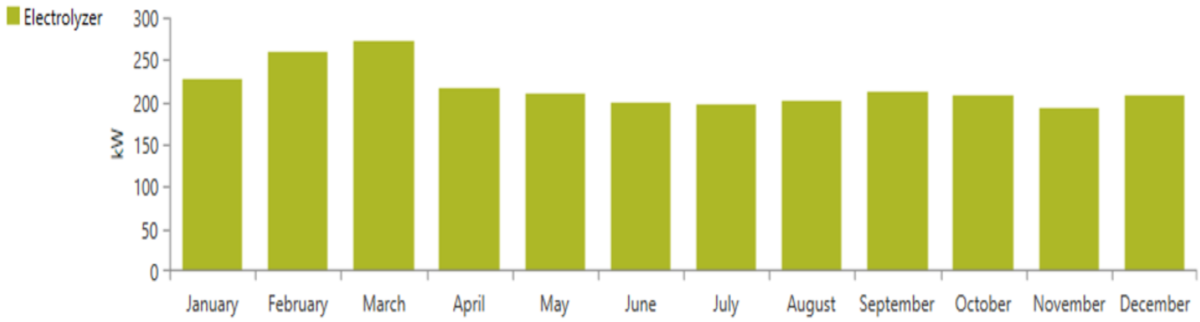

(a) Chennai

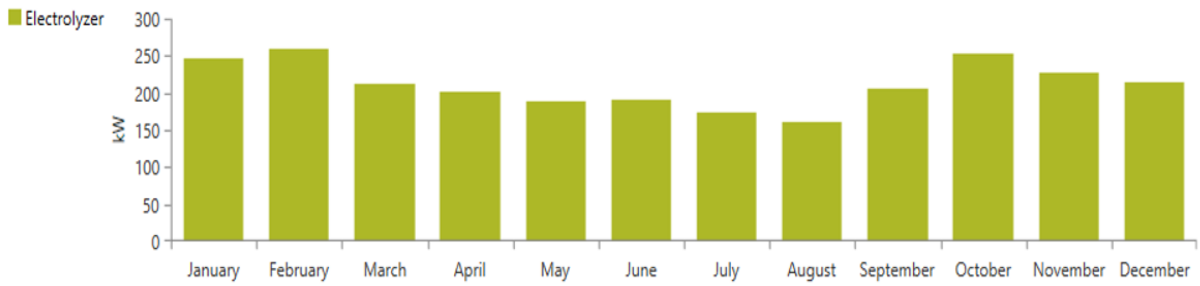

(b) Indore

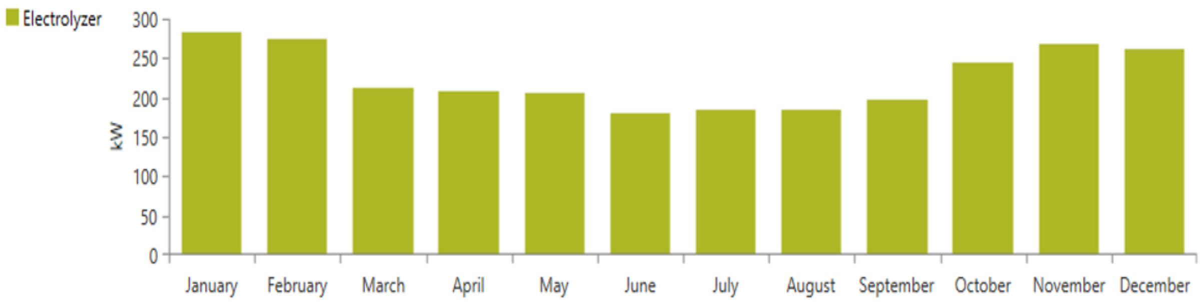

(c) Kolkata

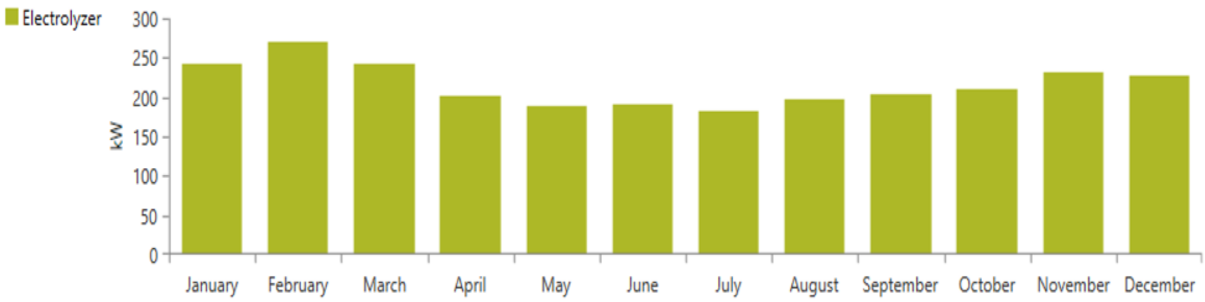

(d) Ludhiana

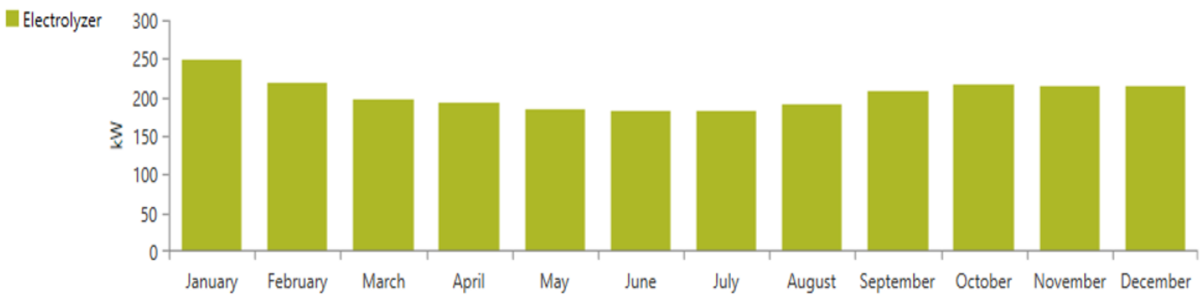

(e) Mumbai

Figure 42 Monthly hydrogen production for the selected locations

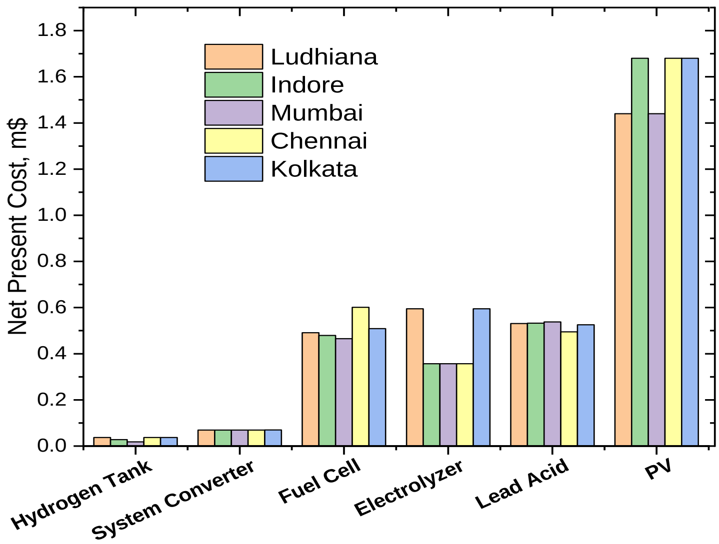

Figure 43 Net present cost at five selected locations

The levelized cost of hydrogen (LCOH) is defined as the ratio between annualized cost and the annual electricity cost to the annual hydrogen generated. Moreover, it is an effective indicator used to evaluate the hydrogen production process. The LCOH can be expressed in the **Eq. (44)**

$$LCOH = \frac{C_{annualized} - (V_{ele} \times E_l)}{M_{hydrogen}} \quad (44)$$

Here, $C_{annualized}$, V_{ele}, E_l, $M_{hydrogen}$ signifies annualized cost, on grid configuration, cost of electricity to the grid $/kWh, and the total hydrogen gained at the electrolyzer output in kg.

From the findings, it can be seen that the LCOH of selected locations Ludhiana, Indore, Mumbai, Chennai, and Kolkata are 3.11 $/kg, 3.16 $/kg, 3.00 $/kg, 3.11 $/kg, and 3.17 $/kg. Simultaneously the cost of LCOH is in India is compared with other literatures are cheap and economically viable in **Table 21.**

Table 21 Comparison with other studies

Reference	**Locations, Country**	**Configuration**	**LCOE, $/kWh**	**LCOH $/kg**
[131]	Dhahran City, Kingdom of Saudi Arabia	PV, Wind turbine, batteries, electrolyzer, hydrogen tank	0.593	36.32
[132]	Qatar	PV, Wind turbine, batteries, electrolyzer, hydrogen tank	11.495	2.092

[133]	Abbas City, Iran	PV, Wind turbine, converter, electrolyzer, hydrogen tank	1.55	0.547
[134]	Doha Intl Airport, Qatar	Wind, Solar, Hydrogen	11.45	2.092
[121]	Abha Area, Saudi Arabia	PV/Wind/FC/Hydrogen	1.208	43.1
[135]	Tocantins, Brazil	PV/Battery/Hydrogen	1.351	0.41 $/kg
[136]	North-East, India	photovoltaic/hydrogen	0.509-0.689	16.1-18.5
[137]	Izmir-Cesme, Turkey	Wind/PV/Hydrogen	0.146-0.152	7.526-7.866
[138]	Jeju Island, Korea	REs/Hydrogen	0.03	4.2-9.54
[123]	Khuzestan province, Iran	Solar/wind/hydrokinetic	0.1155	4.59
[139]	Bostegan, Iran	Wind/Solar/Diesel/Battery	1.343	5.53
[140]	Squamish, Canada; Brisbane and Adelaide, Australia; Los Angeles and Golden, USA	PV/Wind/Battery/Hydrogen	0.50-1.52	17.2-38.4
[141]	Badakhshan, Afghanistan	Wind/Hydrogen	0.0529-0.1135	3.887-10.823
[142]	South Africa	Wind/Hydrogen	0.098-0.14	6.34-8.97
[143]	Al-Kharj, Saudi Arabia	Wind/Electrolyzer/Hydrogen	0.6208	9.34
[144]	Sarwark, East Malyasia.	PV/Battery/Fuel Cells	0.323	99.9
Present Study	Ludhiana, Indore, Mumbai, Chennai, Kolkata, India	PV/Hydrogen/Fuel Cell/ Electrolyzer	0.41 – 0.48	3.00 – 3.22

3.3.19 Environmental Impact and gasoline fuel replacement assessment

The avoided carbon dioxide emissions of the PV module for electricity generation can be estimated using **Eq. (45). Table 22** depicts the environmental values in the present study.

$$Mit_{CO_2} = E_g \times F_e \tag{45}$$

Here, the Mit_{CO_2}, E_g, and F_e are mitigation of carbon dioxide, annual energy produced, and emission factor taken 0.8274 kgCO_2/kWh for India in the present study **Eq. (46).**

Moreover, the quantity of gasoline is estimated using equation [145]

$$M_{GFuel} = \frac{M_{H2} \times LHV_{H2}}{LHV} \tag{46}$$

Here, M_{GFuel}, M_{H2}, LHV_{H_2}, LHV_{GFuel} signifies gasoline fuel, annually produced hydrogen, the lower heating value of the gasoline fuel and the hydrogen that is values 44 MJ/kg and 120 MJ/kg, respectively. Also, the possible CO_2 emissions that could be avoided when gasoline fuel is replaced with hydrogen can be calculated using **Eq. (47).**

$$A_{CO_2} = M_{GFuel} \times SE_{CO_2} \tag{47}$$

Table 22 Emissions avoided as a result of the use of PV power plant

Location	Total electricity, (kWh/ year)	Carbon footprint, (metric tons of CO_2e)	Replacement for gasoline fuel, (kg)	CO_2 reduction per annum (kg/yr)
Kolkata	4,839,464	4004.17	223,783.64	514,702.37
Chennai	5,037,903	4168.36	215,536.36	495,733.63
Ludhiana	4,890,424	4046.34	214,156.36	492,559.63
Mumbai	5,030,800	4162.48	203,209.09	467,380.91
Indore	5,272,806	4362.72	209,822.73	482,592.28

3.4 Limitations in the present study

India is one of the largest and dense countries among the world. However, the territory of India is divided into four regions i.e., North, East, West, and South. The present techno-economic assessment is focused only on the few regions of India. For instance, techno-assessment of solar tracking mechanism of solar PV technology is focused only on south-Indian states of India. On the other hand, a similar techno-economic assessment of solar tower power plant based on two different condensers (dry-cooled, and wet-cooled) has been addressed. However, the present studies have not considered land cost of plant, this is due to the land cost can be varied from location to location and region-to-region, which may impact the calculations of LCOE and NPV values. Therefore, in futures studies the affection of soiling losses, annual degradation and probability figures should be considered, which will act as reference material for the future studies.

3.5 Conclusions for chapter 2

The present chapter assessed the performance of solar tracking mechanism in five different regions of south-India states. Similarly, a techno-assessment of STPP CSP plant with two different condensers in different regions of India. The following conclusion can be made from the present study are:

1) A techno-assessment of 20MW solar PV system has been studied for VSKP, HYD, MDU, TVC, and SBC different climatic conditions in a south-India state. This study includes three different mechanisms i.e., FT, SAT, and DAT have been considered.
2) The annual energy output ranges from 31 GWh to 33 GWh for FT mechanism, 38 GWh to 42 GWh for the SAT mechanism, and 44 GWh to 46 GWh for the DAT mechanism, respectively, for the first year of project at the selected sites. Similarly, the capacity factor (CF) ratio n of 18 % to 25 % which is feasible for the South Indian climatic countries from other the available studies.
3) The recorded LCOE for the FT mechanism from 4.5 ¢/kWh to 5 ¢/kWh, for SAT mechanism, the obtained LCOE ranges from 4.25 ¢/kWh to 4.5 ¢/kWh, and similarly, the obtained LCOE for DAT mechanism is ranged from 4.0 ¢/kWh to 4.25 ¢/kWh, respectively.
4) Finally, the results shows that the DAT mechanism is promising in all aspects. In addition, the simulation results suggests that HYD and SBC based locations generated similar energy output, LCOE and CF ratio. However, we conclude that HYD is the best feasible site to install the solar tracking mechanism due to the site is well equipped with infrastructure, transportation system. In addition, the Telangana state is craved out of the Andhra Pradesh state and formed new state government in 2014.
5) Results from the simulation of solar tower power plant (STPP) a 100 MW was simulated for two condenser models at BPL, VGLB, JUC, CHE, MDU, and ED is considered. The simulation results for the selected potential results revealed that STPP dry-cooled model BPL generated the maximum energy of 376 GWh and a capacity factor of 41.5%, which is followed by VGLB, JUC, CHE, MDU, and ED, which generated maximum energy of 364 GWh, 300 GWh, 353 GWh, 301 GWh, and 349 GWh and CF of 40.2%, 33.2%, 39%, 33.2%, and 38.5%, respectively.
6) Similarly, for the STPP wet-cooled model, the maximum energy generated for selected six potential sites was 410 GWh, 401 GWh, 330 GWh, 382 GWh, 329 GWh, and 387 GWh, with a capacity factor of 45.3%, 44.2%, 36.4%, 42.2%, 36.4%, and 42.7%, respectively.

7) The solar multiple (SM) for dry-cooled STPP model is ranged between 1.4 and 1.8 for the potential six sites. On the other hand, for the wet-cooled STPP model is ranged between SM ranged between 1 and 1.8.
8) The LCOEs for dry-cooled STPP model is ranged 13.22 ¢/kWh to 16.37 ¢/kWh for the selected sites. Similarly, the LCOE of wet-cooled STPP model is ranged from 11.88 ¢/kWh to 14.22 ¢/kWh.
9) From the CSP simulated the STPP wet-cooled model is the better technology to be constructed at the selected six sites due to it is recorded the highest annual energy generation and the LCOE, comparatively than dry-cooled model. Additionally the Bhopal site was identified to be the best site for the construction of both STPP technologies.
10) Finally, the techno-economic performance of a solar PV performance for the five potential sites in India i.e., Ludhiana, Indore, Mumbai, Chennai, and Kolkata. The hydrogen load consists of a refueling station for 20 hydrogen fuel cell vehicles with tank capacities of 5 kg of each location. From the present study, the following conclusions can be drawn:
11) The production of hydrogen for the selected sites Ludhiana, Indore, Mumbai, Chennai, and Kolkata are 78,524 kg/year, 76, 935 kg/year, 74,510 kg/year, 79,030 kg/year, and 82,054, respectively. From the results the Kolkata generated highest hydrogen from the hybrid system, and least for Mumbai.
12) The LCOH for the hydrogen for the selected sites Ludhiana, Indore, Mumbai, Chennai, and Kolkata 3.22 $/kg, 3.11 $/kg, 3.00 $/kg, 3.16 $/kg, 3.17 $/kg, respectively. Further, the LCOH is highest is recorded for Ludhiana and lowest for Mumbai, respectively.
13) The LCOE for the selected sites Ludhiana, Indore, Mumbai, Chennai, and Kolkata are 0.45 $/kWh, 0.44 $/kWh, 0.41 $/kWh, 0.46 $/kWh, and 0.48 $/kWh, respectively. The highest LCOE is generated for Kolkata site, due to lowest electricity generation from the plant, and lowest for Mumbai due to electricity is high.
14) In future studies, it is recommended the present is focused on electricity generation and hydrogen system for the five selected locations. Moreover, we recommended recommend a comparative analysis between on-grid and off-grid system to study the impact of technical parameters, economic and environmental analysis.
15) Finally, other resources such as biomass, wind, and hydro can be combined to generate the electricity and hydrogen production.

4 EXPERIMENTAL INVESTIGATION OF ENHANCEMENT OF SOLAR PV COOLING ACTIVE COOLING

4.1 Experimental study on the performance and enhancement of a solar PV panel integrated with CPU heat pipes- an active cooling approach

The present proposed a mechanism using a CPU fanless heat pipe sink as a cooling mechanism. The heat pipe combines metals such as aluminum and copper that will help in the natural ventilation and cooling of the PV panel. The proposed cooling mechanism will help without water under an ambient temperature of 25 °C (for instance, in cold climatic conditions). In contrast, in the case of hot-rigid climatic conditions, the proposed cooling mechanism will work with the help of water or other liquid substances.

4.1.1 Material and Methodology

We used two PV panels with identical characteristics to a 30W PV panel in the present experimental work. In the PV panel, we included an Al sheet on which proposed fanless heat pipe sinks were integrated vertically for the modified PV panel. In the proposed cooling mechanism, four fanless heat pipe sinks were used and mounted to the Aluminum sheet to increase the thermal conductivity between the PV panel, Al sheet, and fanless heat pipe HY-107 thermal grease was applied to the proposed mechanism. Moreover, to hold the CPU heat sinks firmly, a connecting rod is passed between them. A universal silicone gel is also employed to keep firmly between the Al sheet and PV panels.

4.1.2 Working principle of fanless heat pipe CPU sink

CPU heat sinks have a crucial role in the cooling process for the cooling mechanism because the advantages of using CPU sinks are that they are simple machining, simple structure, and cheaper cost. However, the heat flux at the CPU has dramatically increased; as a result, CPU-sized increased power is found in modern technologies [146]. Meanwhile, the size of heat sinks and fans and the level of noise increase with fan speed. As a result, the demand has significantly risen for better cooling [147]. Two-phase cooling systems, such as heat pipes and thermosyphon, have emerged as viable heat transfer devices as alternatives to traditional heat sinks, with effective thermal conductivity over 200 times that of copper. Simultaneously, heat pipes have a few drawbacks, such as pressure drop.

Therefore, to overcome such problems in the heat pipe, the highest capillary pressure must be greater than the sum of all the pressure drops inside the heat pipe. Therefore, the primary condition for heat pipe operation is as depicted in **Eq. (48).**

$$\Delta P_c \geq \Delta P_l + \Delta P_v + \Delta P_g \tag{48}$$

where ΔP_c presents the maximal capillary force within the wick structure of a heat pipe, and ΔP_l denotes the pressure drop required to return the liquid from the condenser section to the evaporation section. ΔP_v is the pressure drop required to transfer vapor state from the evaporation to the condenser section, and ΔP_g is the pressure drop induced by a difference in gravitational potential energy (that can be either negative, positive or zero depending on the heat pipe orientation and direction of fluid flow). However, with referring to the **Fig.44**. [148] to the operation of fanless heat pipe are as follows: the evaporation of working fluid is enabled by the heat added at the evaporator portion by conduction through the wall of the heat pipe; under the effect of the vapour pressure decrease caused by the evaporation of the working fluid, vapour travels from the evaporator section to the condenser section; In the condenser part, the vapour condenses, releasing its latent heat of evaporation; Under the influence of capillary force and liquid pressure drop, liquid returns from the condenser section to the evaporator section through the wick.

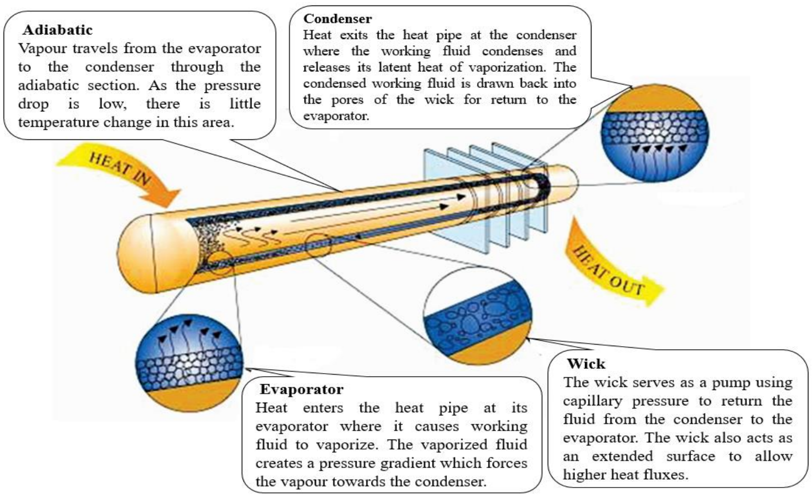

Figure 44 Working operation of Heat Pipe [147]

4.1.3 Construction of experimental setup

In the present work, an aluminum sheet of 60mm*30mm is used for building the setup. The aluminum sheet is placed on the rear side of the PV panel using universal silicone gel paste. Simultaneously, we employed a thermal grease paste HY-107 paste to increase the thermal conductivity between the PV panel and aluminum sheet. Four CPU fanless heat pipe sinks, as shown in **Fig.45.** were mounted vertically on the aluminum sheet, and a rectangular aluminum rod crossed between the two heat sinks to hold them firmly. The construction of the experimental test rig is shown in **Fig.46.** The modified PV panel (i.e., Cooled PV panel) is immersed under a rectangular basin containing 50 L of water. The rectangular basin size is the same as that of a PV panel. Moreover, seven K-Type thermocouples were placed at different locations for the PV panel to measure the temperature every 30 minutes.

Figure 45 CPU heat sink

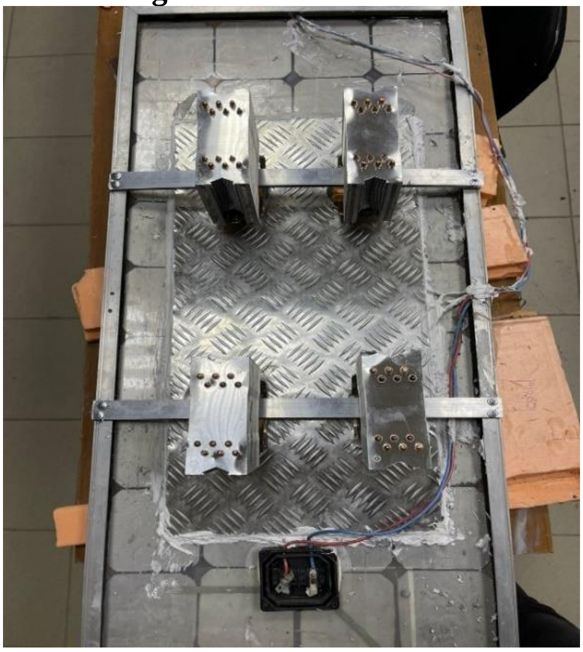

Figure 46 Construction of cooled PV panel incorporated with CPU heat sink

4.1.4 Experimental Setup

The experimental test rig PV panel integrated with a CPU heat sink **(left side)** and un-modified PV panel **(right side)** are shown in **Fig.47.** We employed a rectangular basin containing 50 L of water to the PV panel. Simultaneously, aluminum insulators covered the rear side of a modified PV panel to minimize the water loss from the evaporation. The temperatures of the water and PV panels were recorded during the experimental day using digital loggers. The clamp meter measures the voltage and ampere of a PV Panel. Moreover, we used a digital anemometer, TM-207 solar power meter, and GM 1362-EN-01 temperature thermometer to record wind speed, solar radiation, ambient, and relative humidity data.

Figure 47 Experimental test rig

4.1.5 Weather characteristics of a PV panel

This section shows the performance of the weather characteristics such as solar radiation, ambient temperature, relative humidity, and wind speed. The results from the findings are in Fig.15 the average solar radiation is 999.25 W/m^2, and the average ambient temperature is 27.38 ^{0}C. The findings of relative humidity and wind speed are demonstrated in **Fig.48.** The results show that the average relative humidity and wind speeds are 38.54% and 4.0-6.0 m/s, shown in **Fig.49**.

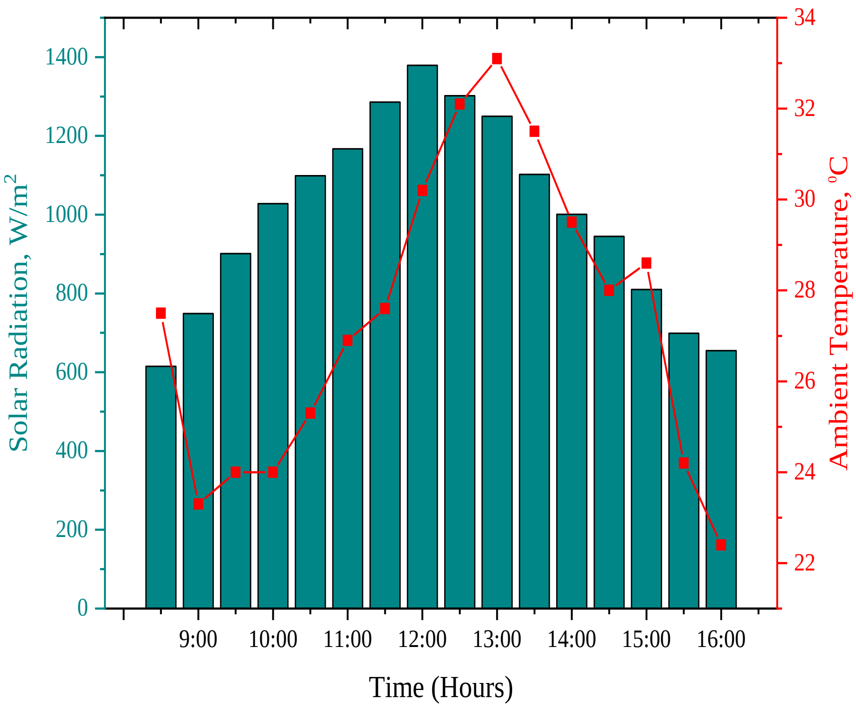

Figure 48 Time dependence of solar radiation, and ambient temperature

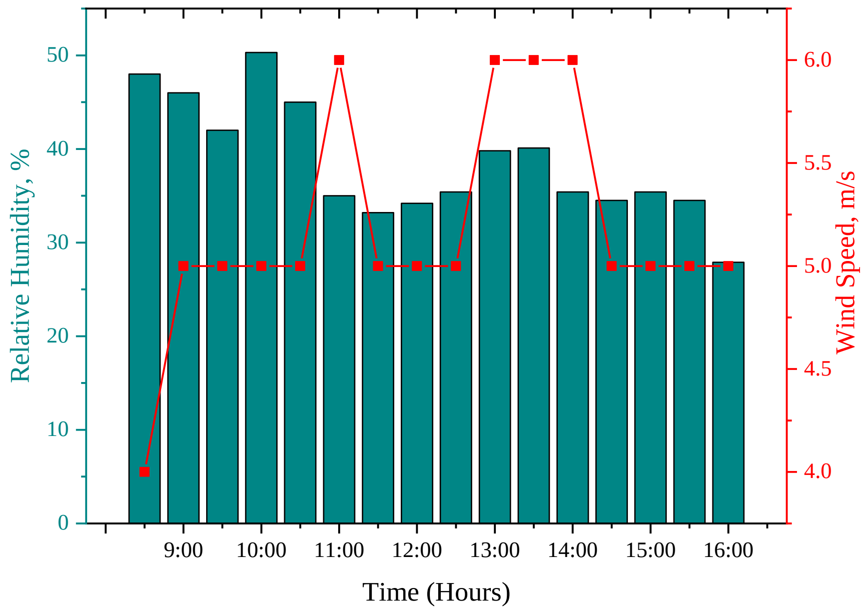

Figure 49 Time dependence of relative humidity, and wind speed

4.1.6 Temperature profile of a fanless heat pipe

The performance of a PV is a fundamental parameter identifying the performance of a PV system, and it also justifies that the selected mechanism is feasible for the cooling mechanism. Therefore, in the present study, a fanless heat pipe sink was employed at the rear end of a PV panel. In this study, we used seven K-type thermocouples were used for thermal management to measure the temperature of both modified and un-modified PV panels. The resolution of the thermocouple is 0.1 ˚C.

The temperature profile of the under-tested PV panel is depicted in **Fig.50**. The interpretation of the temperature difference between the PV panels is also superimposed in **Fig.50**. The behavior of the temperature profile can be seen; the average temperature for cooled and un-cooled recorded on the day of the experiment are 41.46 °C and 48.49 ˚C, respectively. The reduction in the average temperature of the PV panel is 6.72 ˚C. Moreover, the temperature of both PV panels that hit peaks for a cooled PV panel is 50.26 ˚C against 60.19 ˚C for Un-cooled PV at 13:30 hrs. The obtained thermal image profiles using Testo software are shown in **Fig. 51a,** for the modified PV panel and **Fig.51b,** for the un-modified PV panel. The thermal images for the present study, recorded around the 11: 30 am on the day of the experiment, and the findings reveal that the maximum temperature of a modified PV panel is 41.6 °C, against un-cooled PV panel is 35.7 °C. However, using a data logger, the temperature findings for a cooled PV panel is 45.3 °C for a modified PV panel, against 39.7 °C un-modified. The temperature difference happens because the thermocouples are in close contact with PV panels, while thermographic images are seized away from PV panels.

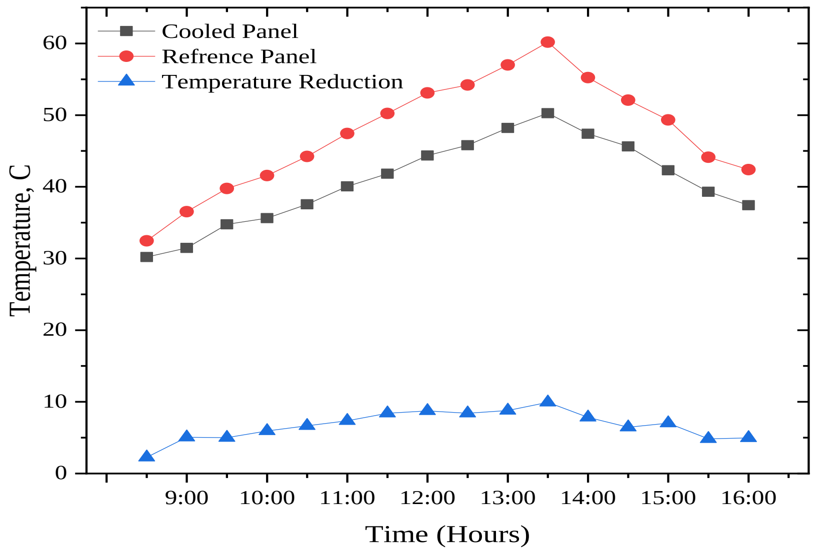

Figure 50 Timed dependence of a temperature profile

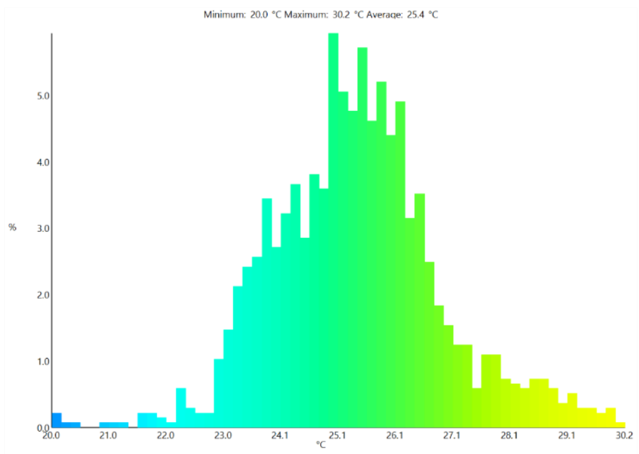

(a)

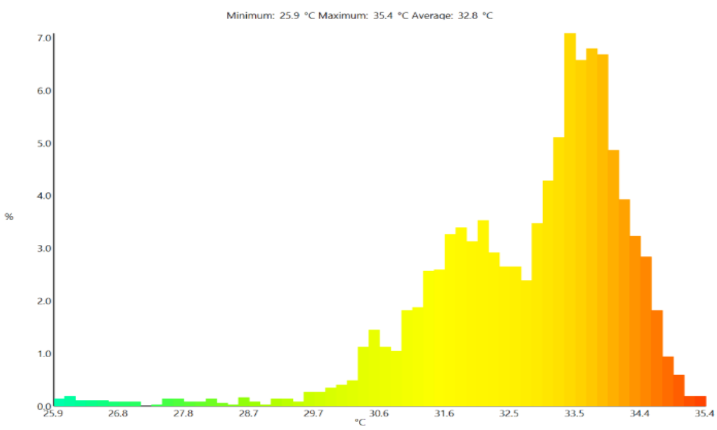

(b)

Figure 51 Thermal image: a) cooled PV panel, b) Un-modified PV panel

4.1.7 Electrical Performance of a PV panel

It has been recognized from the experimental study that the temperature increase negatively influences the performance of PV panels. The evolution of the voltage and current version for both PV panels is shown in **Fig.52**. It has been seen that the behavior of voltage and PV panels has a similar pattern of solar intensity, as shown in **Fig. 52.** as it slowly increases until it hits peak time at 12:30 hrs and starts to decrease on the second half-day of the experiment. A cooled PV module's average voltage and current are 18.36 V and 0.59 A. At the same time, the recorded average voltage and current for an un-cooled PV module are 17.01 V and 0.55 A.

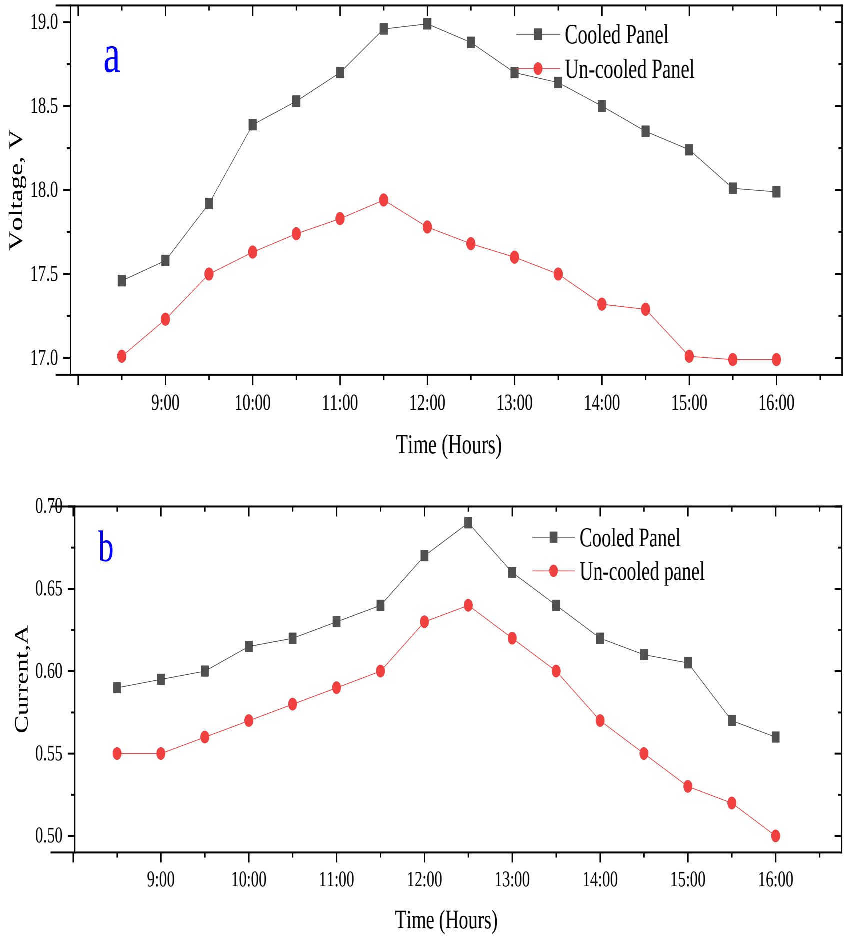

Figure 52 Temperature dependence of a) Voltage b) Current

Similarly, **Fig.53.** shows the output performance of a PV Panel. The solar PV panels' total power output increases until the experiment's midday and starts decreasing until the sunset. The results revealed that the average power of a modified PV panel is 11.39 W against a 9.73 W Uncooled PV panel. The maximum power hits for a modified and un-modified PV plant are 12:30 hrs.

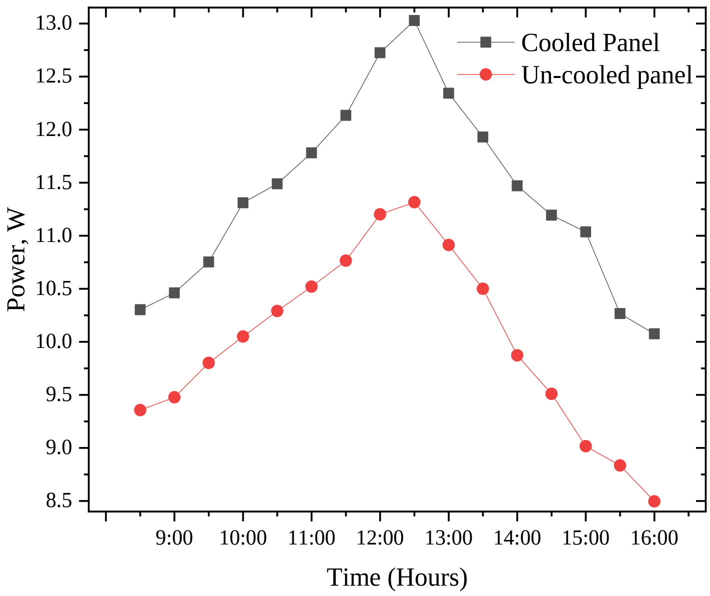

Figure 53 Variation of power for cooled and Un-cooled PV panel

4.1.8 Electrical Efficiency

The PV unit's electrical efficiency with integrated CPU fanless heat pipes for both PV modules is presented in **Fig.54**. It has been observed that the electrical efficiency of both PV modules decreases as the day passes the first half and hits a minimum at 13:30 hrs. The average electrical efficiency of a PV module from the data achieved for a cooled PV panel is 14.05%, against 12.76% for an un-cooled PV panel. Therefore, the electrical performance increases by 2.98 %. Therefore, the proposed work has a significant effect over the other published work listed below in **Table 23** either active or passive cooling mechanism.

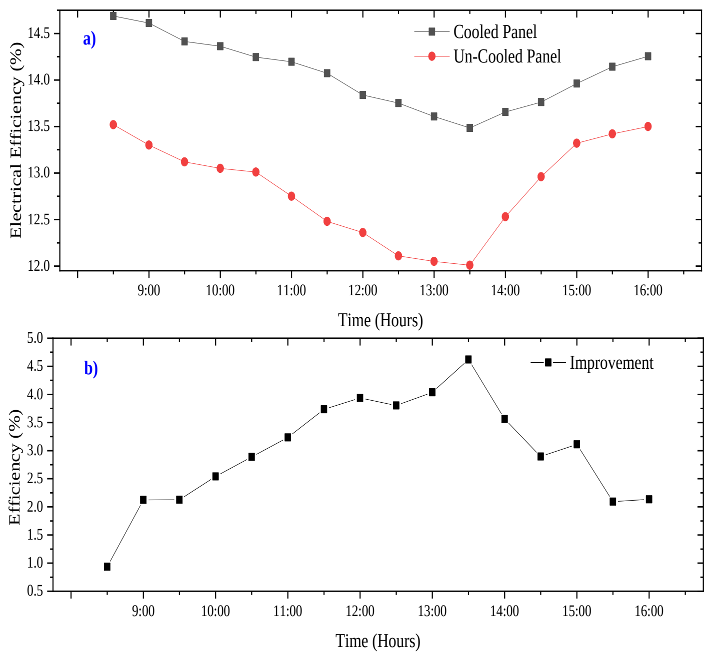

Figure 54 Variation of electrical efficiency of a PV panel

Table 23 Comparison work with other literature

Reference	Type of Cooling	Proposed Mechanism	Key Results
[65]	Active and Passive	Fins and Ultrasonic Humidifier	• The temperature of cooling is reduced by 14.61˚C. • Improvement in electrical efficiency by 6.8%. • A total 1.5L water consumed due to evaporation
[150]	Active and Passive Cooling	PCM and PVT/PCM	• A hybrid PVT/PCM was performed at 800W/m^2. • Electric efficiency is reduced for PV/T system is 6.98%, and for PV/T PCM system is 8.16%.
[151]	Passive Cooling	Water Pipe	• Maximum and minimum solar radiation achieved 1081W/m^2, and 461 W/m^2 • Difference in power output is 2.7 W • Average electrical efficiency is improvement is 8.6%.
[152]	Passive Cooling	Water	• Heating rate and the cooling rate is operated experimentally. • Average difference in temperature is 5 ˚C.
[153]	Active Cooling	Thermo-electric model	• The average RMSE is 1.75 ˚C. • The MAE is 1.14 ˚C • Experimental data is validated with MATLAB/Simulink
[154]	Active Cooling	Water Heat Exchanger	• Numerical results are compared with the experimental results • Reduction in average power output from the experiment is 4W. The average reduction in temperature is 16 ^{0}C

[155]	Active Cooling	PV/T Air Collector	• Electrical efficiency of a PV Panel is increased from 5.5 to 7.5 (approx.). • Thermal efficiency is increase from 46.5% to 49%
Present Study	Passive Cooling	Fanless CPU Heat Pipe sink with Water	• Average temperature is achieved 6.74 °C. • The power output is achieved 17%. • Energy, Exergy, and Entropy improved for cooled PV panel 10.1%, 81.55%, and 9.88%.

4.1.9 Exergy analysis

Fig.55 depicts the exergy efficiency for both PV modules throughout the experimental day. The finding shows that the behavior of exergy analysis follows the electrical efficiency trend of a PV panel shown in **Fig.55.** The exergy analysis starts to decrease as the solar radiation increases until 13:30 hr and follows the upward movement of the decrease in the solar radiation. The average exergy efficiency is 7.88% for the cooled PV module and 4.54% for the uncooled PV module.

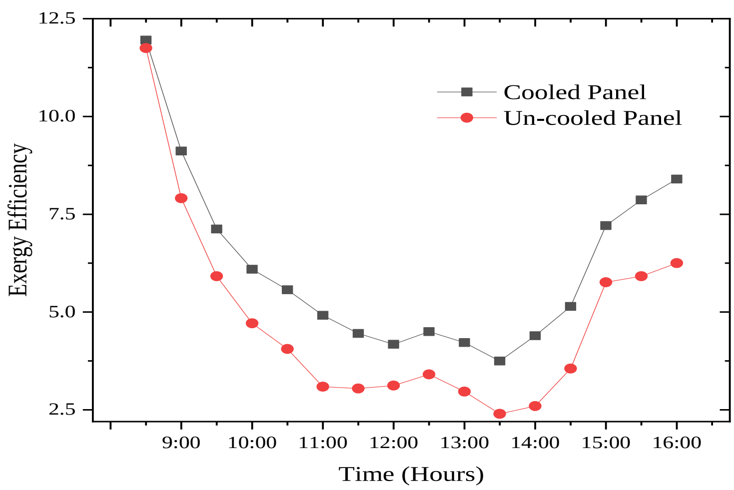

Figure 55 variation of exergy analysis for proposed mechanism

4.1.10 Entropy analysis

The evaluation of entropy generation of a PV panel with the proposed mechanism is displayed in **Fig.56.** As can be depicted, results from the electrical and exergy efficiency, the behavior of entropy generation behaviors in the opposite trend. As the day progresses, the entropy increases with the increase in solar radiation, hitting maximum at mid-noon of the day and decreasing on the experiment's second half-day for the proposed cooling mechanism.

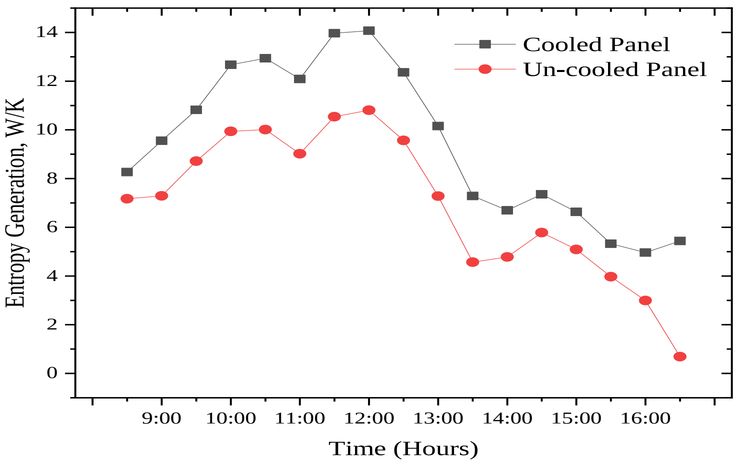

Figure 56 Variation of entropy generation for proposed mechanism

4.1.11 Cost analysis

The economic analysis of the present experimental study is estimated in **Table24**, and **Table 25**. In the present study, we used two PV panels with similar characteristics, aluminum sheet, CPU heat sinks, thermocouples, thermal glue, and silicone gel. The parameters employed in the present study are shown in **Table 24.** The economic analysis is calculated in two scenarios. The first scenario is for the poor climatic conditions where solar radiation is very nominal. On the hand, the second case is where the solar radiation is for 365 days. In addition, we believed that the panel output energy for 10 hours daily. The total power generated by the cooled PV panel is 11.39 W against the 9.73 W un-cooled PV panel. Moreover, **Table 25,** depicts the economic analysis calculations for the present study.

Table 24 Parameters used for LCOE calculations

Parameters	**Cooled PV ($)**	**Un-Cooled PV ($)**
PV Panel	50	50
Aluminum Sheet	8	0
Fanless heat Pipe sink	14.25*4=57	0
Thermal grease	1	1
Silicone Gel	2	2
Thermocouples	2	2
Total, ($)	**120**	**55**

Table 25 Estimated LCE calculations

Parameters	**Cooled PV**	**Un-Cooled PV**	**Reference**
Effective discount rate (i_{eff}), %	5	5	[61]
Nominal escalation rate (r_n), %	1	1	[61]
$K_{O\&M}$	0.96	0.96	Calculated

Capital recovery factor (CRF)	0.065	0.065	Calculated
Constant escalation levelized factor O&M, (CELF), %	0.9975	0.9975	Calculated
Annual operation and maintenance cost ($C_{O\&M}$), $	3.75	3.75	Calculated
Life time of the years (n), years	25	25	-
Total investment cost (C_{inv}), $	120	52	Calculated
Levelized cost of fuel (LC $_{f}uel$), $/kWh	0	0	-

4.1.11.1 Scenario 1: for 105 days

The assumption made for the economic assessment is that the total power generated by PV power plants remains the same throughout the period obtained from the present study for the cooled PV panel and un-cooled PV panel is 11.95 kWh, and 10.216 kWh, respectively. As shown in Tab 4. the cooled PV panel costs $ 120 and $ 55 for the un-cooled PV panel. The calculation of LCOE findings shows that for the scenario, i.e., for 105 days is 0.96 $/kWh, against for the un-cooled PV panel is 0.61$/kWh.

4.1.11.2 Scenario 2: for 365 days

In the second scenario, we considered 12 months (365 days) for the hot-rigid condition where the solar intensity is available for the entire year. The power generated for 365 days from the experiment for the cooled PV panel is 41.53 kWh, against 35.51 kWh for the un-cooled PV panel in a year. The proposed mechanism's estimated LCOE for the entire year is 0.277 $/kWh against un-modified is 0.206 $/kWh. The LCOE achieved for the cooling technology is slightly high because of the incorporation of additional materials such as a heat sink and aluminum sheet to the rear side of a PV panel.

4.2 The experimental investigation incorporated with thermoelectric fans on the efficiency of a PV module

In the present segment, to investigate the PV panel's performance using thermoelectric cooling by the principle of "Pieter cooler" to reduce the cost of a PV module investigated.

4.2.1 Materials and Methodology

The section describes the materials that are used to develop the experimental test ring. The experiment took into consideration into two PV panels, one is prominently well-known as cooled PV panel modified with integrated TEC. On the other hand, the PV panel without any changes i.e., un-cooled panel.

4.2.2 Working principle of thermoelectric cooling

The direct conversion of temperature difference into an electrical voltage and vice versa is known as the thermoelectric effect. Thermoelectric is prominently known as the "Peltier effect," which causes heat exchange and temperature difference. Thermoelectric coolers (TEC) are integrated at the back side of a PV panel by transmitting thermal transfer material with the cold part on the panel. Simultaneously, the heat sink using an excellent thermal transfer material, is mounted on the warm part of the TEC to disperse the warm air into the ambient. In the present study, the TEC for the present study is depicted in **Fig.57**, and finally, the working principle of a PV panel is illustrated in **Fig.58**. The working principle of the thermoelectric module is the Peltier effect which generates cooling. The significant focus is to create a heat flux between the P-N junction. The Peltier cooler enables one section of a module to the other section of a module in the direction of the current. A voltage is applied across the device to get one of the sides hot whiles the other becomes cold. In TECs, their performance depends on the ambient temperature, Peltier parameters, the design of the heat exchange as well as the Peltier module's geometry. When a voltage is applied between two dissimilar conductors, say A and B, there will be heat at the junction. The rate $\frac{dq}{dt}$ [156] of the heat generated can be expressed as indicated in **Eq. (49).**

$$\frac{dq}{dt} = (\pi_A - \pi_B)I \tag{49}$$

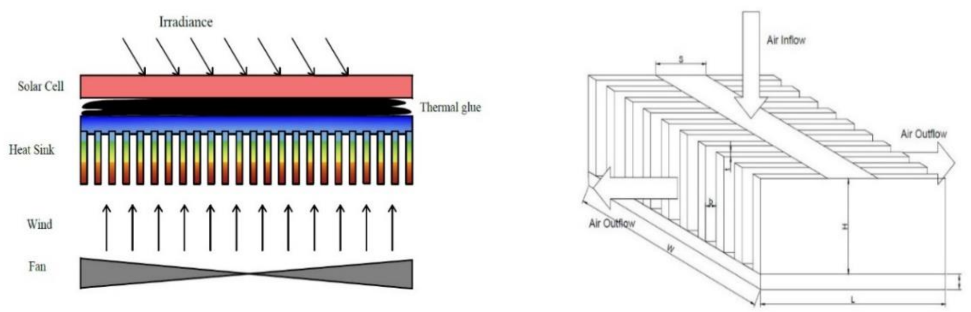

Figure 57 Left: Cooling mechanism using (TEC), Right: Flow of air [157]

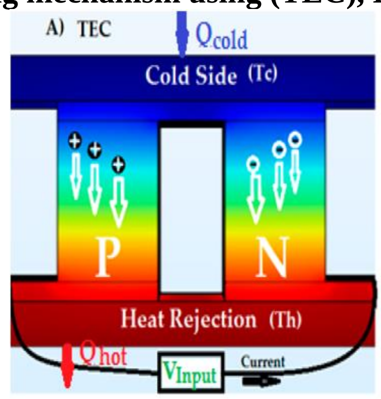

Figure 58 Working principle of TEC [158]

4.2.3 Construction of experimental test rig

The experimental test rig was built and studied at Ural Federal University, Russia. An aluminum sheet was included on which thermoelectric coolers were mounted on the rear end of a PV panel as shown in **Fig.60**. A total of 4 thermo electric coolers were imposed to construct for the testing. Finally, the various parts of the TEC used for the cooling are presented in **Fig. 61.** Furthermore, the parameters of the TEC are presented in **Table 26.**

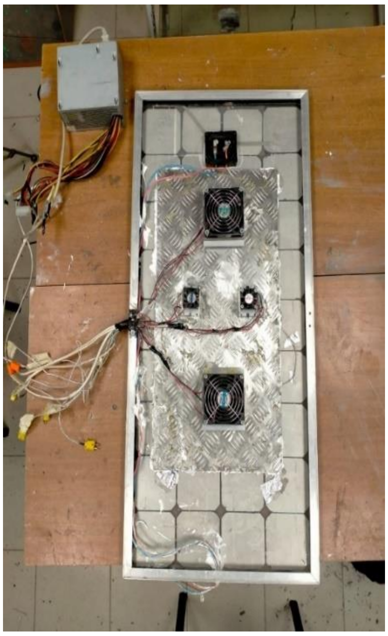

Figure 59 Cooled PV panel with thermoelectric coolers

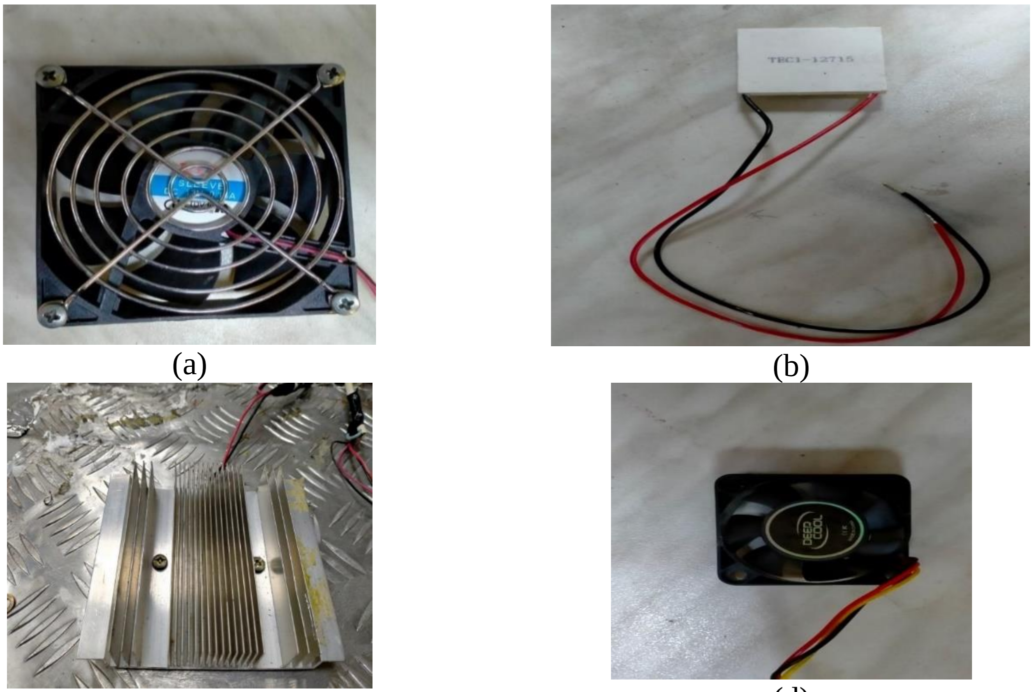

(a) (b)

(c) (d)

Figure 60 Parts of the TEC (a) fan for big TEC (b) TEC (c) heat sink (d) fan for small TEC

Table 26 Description of the big and small TEC

Bigger TEC		Smaller TEC	
Model	AV-F9025MS	Fan Dimension	40X40X10 mm
Name	DC12V BRUSHLESS FAN	Bearing Type	Hydro Bearing
Consuming Current	0.18 A	Consuming power	1.44 W
Consuming Power	2.16 W	Operating Voltage	10.8～13.2V DC
Consuming Current	0.18 A	Consuming Current	0.12 A
Operation Voltage	DC 6.8-12.8 V	Fan Speed	4500±10% RPM
Rated Voltage	12V DC	Power Input	0.48 W
weight	40g	Noise	24.3 dB(A)
Size	80x80x25mm	Maximum Air Flow	4.82 CFM
Acoustic Noise ***	27.82dB	Started Voltage	7V DC
Insulation Level	UL Class A	Rated Voltage	12V DC
DC Line Length	200mm	Net Weight	15.5 g
Life Expectance	50,000 hours at 25 degrees		
Rated Speed	3000 R.P.M.		
Connector	2pin-ph2.5		
Certificate	UL, CE		
Rotation Direction	Counter-clockwise		

4.2.4 Experimental setup of proposed mechanism

In the present study, a small aluminum sheet was employed at the rear end of the PV panel. For better contact between the aluminum sheet, and the back of the PV panel, thermal glue paste is used for thermal conductivity. Simultaneously, we employed a silicone gel is used to fix the PV panel. Finally, we hired four thermal electric coolers for the PV panel and settled on the aluminum sheet. However, to measure the temperature every 30 minutes, seven k-type thermocouples were installed at the back of the PV panel. The thermometer is deployed to measure the humidity and ambient temperature. The digital anemometer measures the wind speed. The installed test rig is shown in **Fig.61**.

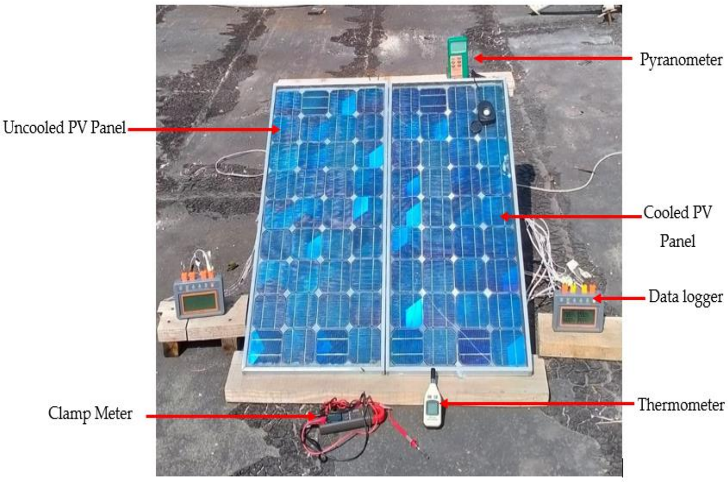

(a)

(b)

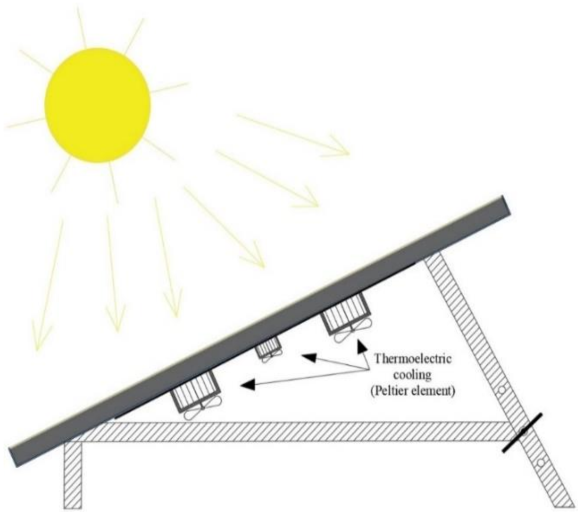

(c)

Figure 61 The experimental test rig: a) Front view of test rig ;b) rear view of the test rig, and; c) schematic diagram of test rig

4.2.5 Weather characteristics of the experimental period

The weather characteristics for the proposed cooling mechanism in the section are presented. Weather data existed recorded using a solar pyranometer, a thermometer, and a digital anemometer. From the findings, the solar radiation of the present study slowly increases and hits a maximum at 13:00 during the first half-day of the experiment and starts decreasing gradually in the second half-day. The highest solar radiation recorded at 13:00 is 1173 W/m^2, and the minimum at 17:00 is 414 W/m^2. The average humidity for the proposed work was recorded using the thermometer was 26.82%. Simultaneously, the present work's average temperature and wind speeds are 32.49 $^{\circ}$C and 5.2 m/s, respectively. Finally, the weather characteristic performance of both PV panels is shown in **Fig. 62**.

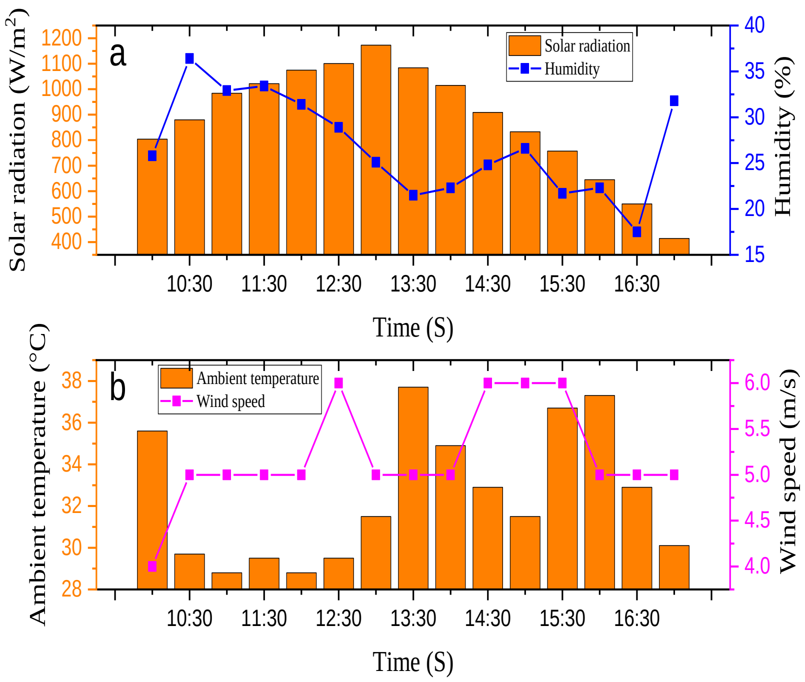

Figure 62 Weather performance of a PV panel (a) Solar radiation & humidity, and (b) ambient temperature & wind speed.

4.2.6 Temperature profile of a PV panel

We employed seven k-type thermal couples with a resolution of 0.1 °C for the proposed mechanism to record the temperature profile. The thermocouples were installed at different locations on the back side of a PV panel. The temperature profile for a PV panel is shown in **Fig 63a**. From the recorded results, the highest temperature recorded for a cooled PV panel is 40.05 ˚C at 13:30, while for the un-cooled PV panel is 56.09 ˚C at the same time. Moreover, the average temperature for the cooled PV panel is 33.37 ˚C, against 45.60 ˚C for the un-cooled PV panel for the entire experiment period. The average reduction in temperature is 12.23 ˚C which is effective for the thermoelectric cooler. The decrease in temperature profile for the period of the experiment depicted in **Fig 63b**. The Testo thermo imager is employed to record the temperature profile of a PV panel at the time of the experiment. The results are depicted in **Fig. 64.** From the findings of the thermal imager, the average temperature for a cooled PV panel temperature distribution is 33.85 ˚C, while for the un-cooled PV panel is 45.98 ˚C. The difference between the calculated results to thermal imager record is because of the thermocouples are in close contact to the PV panels, while thermal images is taken away from the PV panel.

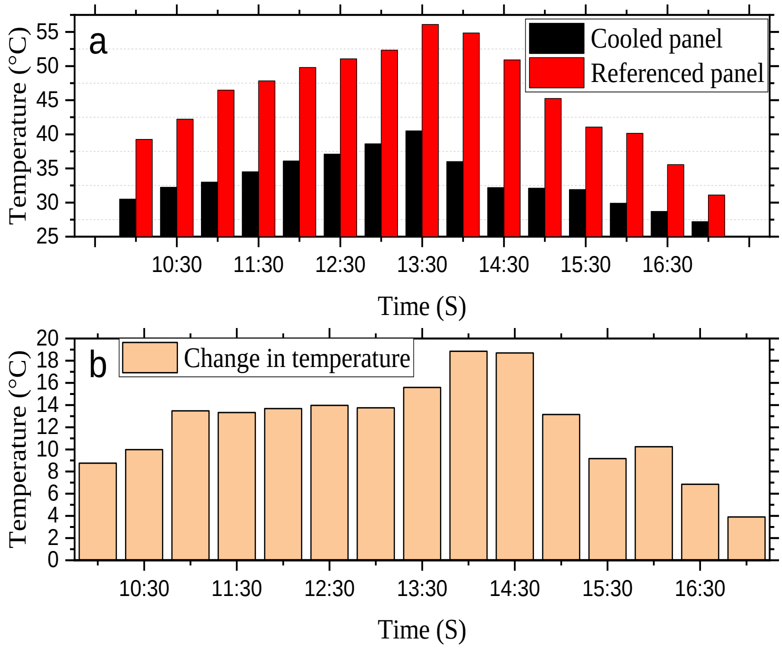

Figure 63 Time dependence (a) temperature profile (b) change in temperature

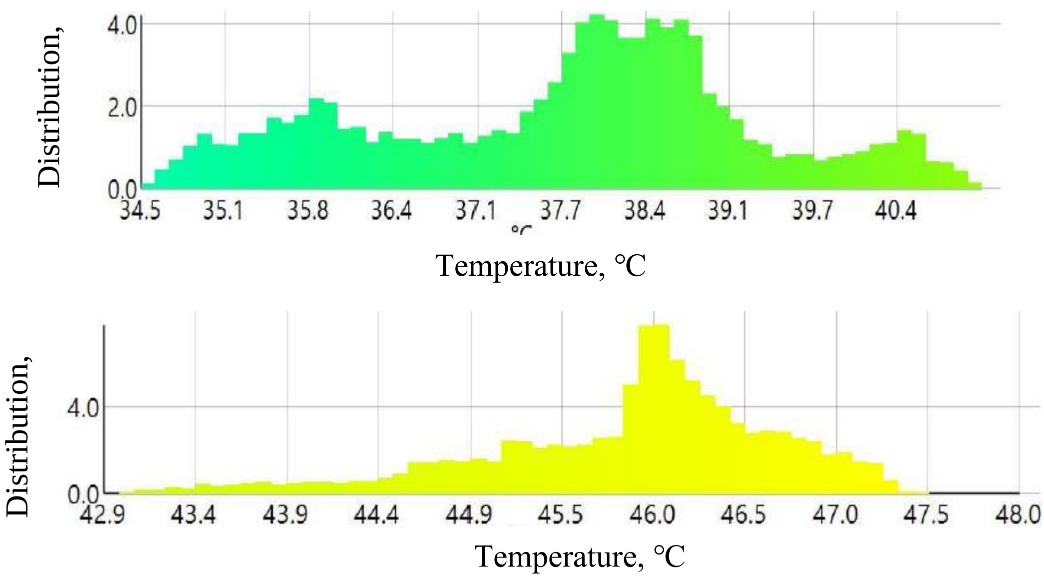

Figure 64 Time dependence of thermal imager (a) cooled PV panel (b) un-cooled PV panel

4.2.7 Electrical performance on the PV module

The electrical performance of the proposed mechanism is depicted in this segment. The average power output for a cooled PV panel is 6.31 W, while the uncooled PV panel is 5.22 W during the entire experiment period. This power increase in the cooled PV panel by 1.09 W, and an overall improvement is 20.88%. The findings revealed that the power of the cooled PV panel increases simultaneously, increases the temperature of a PV module, and hits maximum at 13:00. The thermoelectric cooler positively affected the output of the cooled PV module during the hot temperature period. It also introduced some stability in power production, which is very important for solar PV plants. On the other hand, the improvement of the power depicted in **Fig.65 (a, b).**

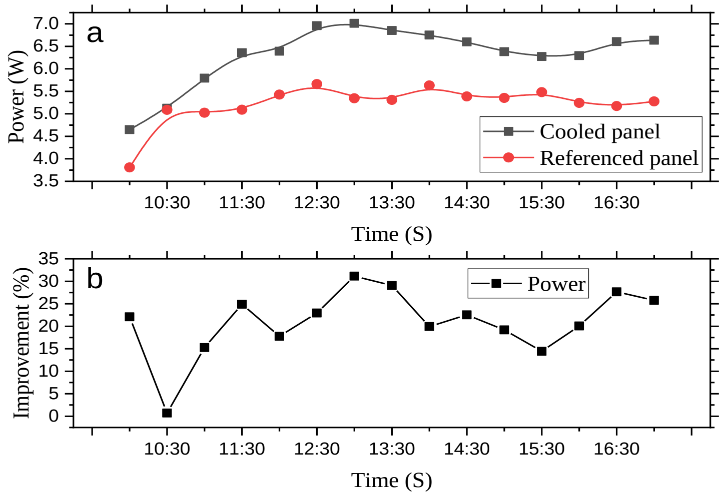

Figure 65 Time dependences: a) Output power for the cooled and un-cooled PV modules, and b) improvement in power.

4.2.8 Electrical Efficiency

The electrical efficiency of a PV module was evaluated and presented in this segment. The finds revealed that the average efficiency of a cooled PV panel is 13.8%, as against 14.5% for the un-cooled panel. The average improvement in the electrical efficiency is 0.7% for the proposed study. Similarly, from the calculations, the highest efficiency recorded for the cooled PV module is 14.8%, as against 14.6% for the un-cooled PV panel. Simultaneously, the lowest electrical efficiency for the cooled and un-cooled PV modules is recorded at 13:00 hrs, 13.1%, and 14.07%, respectively. The electrical efficiency and improvement of the proposed study is depicted in **Fig.66**.

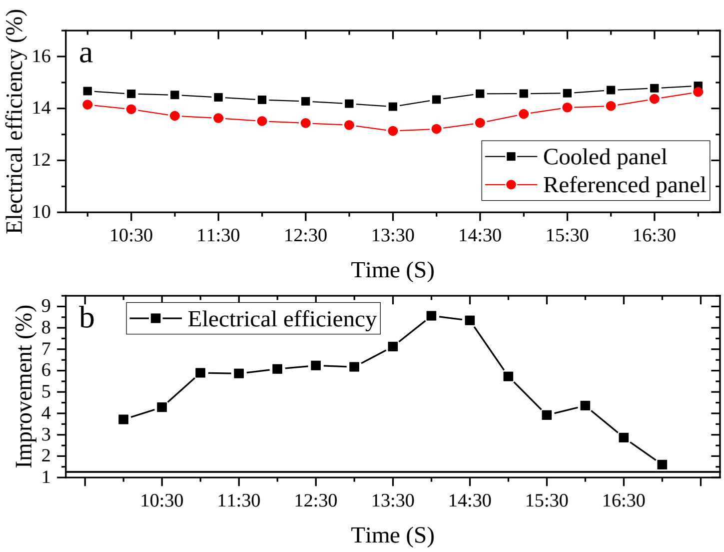

Figure 66 Time dependence (a) Electrical Efficiency (b) Improvement for both PV modules

4.2.9 Exergy efficiency

Exergy analysis is seen as a powerful tool to assess the thermodynamic and economic performance of a thermodynamic system. It provides an alternative platform for estimating and comparing a PV power plant. Such analysis produces important since it deals with the minimization of irreversibility or the delivery of maximum exergy. The results obtained for the estimation of the exergy efficiency for both panels are presented in **Fig. 68**. The average exergy efficiency for the cooled panel is 8.85% as against 7.17% for the referenced PV panel. Obviously, the exergy efficiency decreases with increasing incident solar radiation, the periods with high intensity of solar radiation i.e., during middays the exergy recorded the least exergy efficiencies.

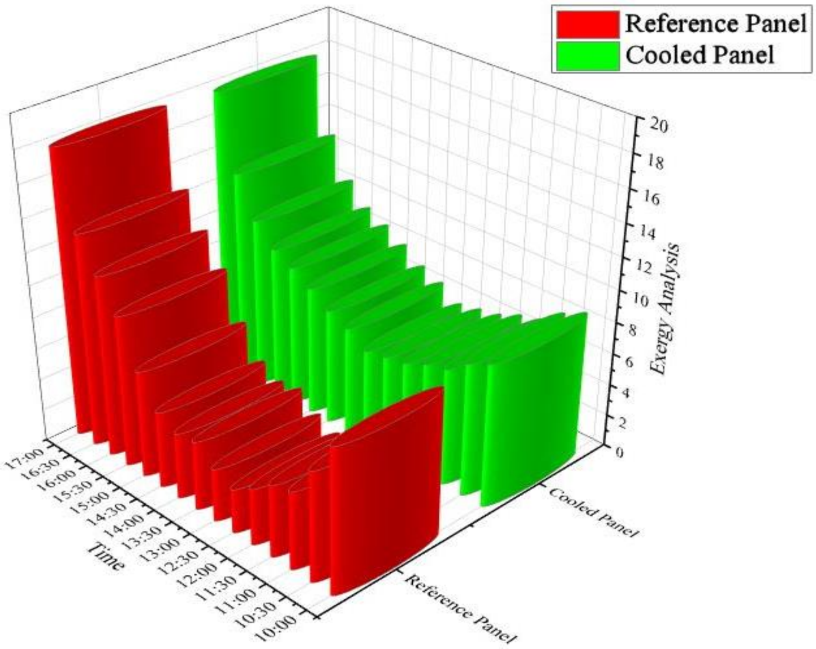

Figure 67 Time dependence exergy efficiency of a PV module

4.2.10 Economic analysis

For PV projects, cost estimation plays a significant role. The Levelized Cost of Energy (LCOE), the most applied method to evaluate the economic viability of power-generating projects, is used in this analysis. To ease obtaining a full year of electricity generation for both modules. Since two PV panels were used for the proposed cooling mechanism, 1) modified with a four thermoelectric cooler, the cost of two giant fans is $11, while the two smaller fans are $ 7.00, which equals $18.00. On the other hand, each PV panel costs $ 50.00. Thermal glue holds the contact between the fan and the aluminum plate to increase the thermal conductivity, costing $3.00. The aluminum that is mounted to the PV panel is $0.50. Hence, the total investment cost is $71.50 against $50.00 for the reference PV panel. We also assumed that the operation and maintenance costs for both PV panels are $3.50. Simultaneously, the nominal and escalation rate is taken from the other studies 1% and 5%, respectively [61]. **Table 27** economic analysis used in the present study.

Table 27 Economic analysis for the present study

Parameter	Cooled PV	Referenced PV	Reference
Nominal escalation rate (r_n), %	1.00	1.00	[61]
Effective discount rate (i_{eff}), %	5.00	5.00	[61]
$K_{O\&M}$, %	0.96	0.96	Calculated
Capital recover factor (CRF),	0.065	0.065	Calculated
Constant-escalation levelization factor O&M, (CELF)	1.10	1.10	Calculated
Annual operation and maintenance cost ($C_{O\&M}$), $	3.00	3.00	Calculated
Investment cost ($\boldsymbol{C_{inv}}$), $	71.5	50	Calculated
Life time of plant	30 yr	30 yr	Calculated

In the present study, for the total electricity generation from the PV power plant for the LCE calculations, two scenarios were assumed, i.e., for 120 days for cold regions such as Russia and a 365 days scenario for hot rid climatic conditions. For the LCE calculations, an assumption was made effective working period.

4.2.10.1 Scenario 1: 365 days

The obtained energy for the period of an year about 20.732 kWh and 17.155 kWh for the cooled and referenced module for a 365-day period, assuming a 9-hour operating period. Due to this effect, the cooled PV module recorded an LCOE of 0.410 $/kWh for the 365 days period. In contrast, the referenced PV module recorded LCOE of 0.414 $/kWh for the same period.

4.2.10.2 Scenario 2 for 120 days

In the second scenario, the electricity generated for the 120-day period for the cooled PV module is 6.816 kWh, as against 5.640 kWh for the referenced module. An amount of 1.247$/kWh was recorded by the cooled panel for the 120-day period whiles the referenced module recorded 1.265 $/kWh. The findings from the economic analysis study suggests that the cooled PV module still remained relatively cheaper in terms of cost of energy despite the higher investment cost. This is due to the fact that the cooled module generated more power than the referenced module due to the enhancement in the performance of the cooled module.

4.2.11 Comparison of current results with published works

For the better understanding comparing the current study to other published literature works makes significant achievement. Hence, the present study is compared with other studies and the results are presented in the **Table.28.**

Table 28 Results from previous studies for comparison

Reference	**Cooling Mechanism**	**T_{PV} without Cooling, ℃**	**T_{PV} with Cooling, ℃**	**Temperature Reduction, ℃**
[159]	Forced convection induced Fans	59.88	53.64	6.24
[160]	DC brushless fan	50.87	44.77	6.1
[161]	Fan Cooling	44	37	7
[162]	DC brushless Air-Cooling Mechanism	39.65	37.09	2.56
[163]	Forced air over the heat sink	42.2	23.9	18.3
[164]	Cooling system on maximum allowable temperature	45	30	15
[165]	Air cooling technique DC fan	71.5	55.8	15.7
[166]	Aluminum heat sink	62.3	52.1	12.2
[167]	Yellow petroleum jelly	60.3	55.7	4.3
[168]	PCM-RT35	53	42	11
[169]	Fin cooling	49.9	43.3	5.90
[170]	Microencapsulated phase change material	32.8	31.0	1.8
[171]	Thermosyhon Heat pipe	79.1	68.26	10.84
[172]	Heat sink Air cooled	85.3	72.8	12.5
[173]	Heat sink fins	85	77.6	7.4
[174]	Evaporative Cooling Principle	73	64	8
Current study	Thermoelectric cooling	45.60	33.37	12.23

4.3 Photovoltaic (PV) solar panels integrated with u-shaped grid copper pipe, TEGs and aluminium oxide (Al_2O_3) nanofluid: An experimental investigation

In the third active cooling method study, a 50 W of each solar PV plant is used to access the performance of a solar PV panel. A solar PV panel is used to examine the performance of a hybrid PV/TEG/Al_2O_3 nanofluid, and a U-shaped grid copper pipe incorporated at the back side of a PV panel. The system of three PV panels i.e., referenced PV panel (referenced PV module), PV panel with simple u-shaped grid copper pipe, and PV panel modified by incorporating U-shaped grid copper pipe. For the present study, purpose we modified our PV panel with simple u-shaped grid copper pipe, and PV panel modified by incorporating U-shaped grid copper pipe as PVT, and PVT/TEG/nanofluid. However, in the present experimental investigation we also prepared 1% volume concentration of Al_2O_3 that employed at the back side of PV panel by using u-shaped grid copper pipe and TEGs. Finally, a techno-enviro-economic analysis is presented and discussed in the present study.

4.3.1 Construction of experimental setup

To examine the impact of nanofluid/TEGs on PVT systems, three PV panels are considered for the experimental investigation two PV panels i.e., PV with simple grid evaporator, and PV modified by incorporated with u-shaped grid copper pipe/TEG/ Al_2O_3 nanofluid system. **Table 29** highlights the technical data of a 50 W Delta PV modules.

Table 29 Characteristics of a PV panel

Parameter	Value	Unit
Model	Monocrystalline	-
Weight	4.4	kg
Length × Breadth × Height	670×550×25	mm
Maximum power current	2.77	A
Maximum power voltage (U_{mp})	18.05	V
Open circuit voltage (U_{oc})	22.5	V
Short-circuit current (I_{sc})	3.1	A
Fill Factor	0.71	%
Maximum power	50	W
Cell efficiency (η_{ref})	19	%
Temperature coefficient (β_{ref})	0.041	K^{-1}
Temperature Range	-40 to 85	°C

The construction of present experimental setup for the modified PV panel is developed in several stages. In the first stage of the development, the front and back surface of PV panel is well cleaned, on that five K-type thermocouples were installed at different locations on the back side of a PV panel for the three selected PV panels. The significant use of K-type thermocouples was to record the temperature distribution of PV panel. At the second stage, an aluminium sheet size of (600 mm×400 mm) is placed with the help of silicone gel by covering the thermocouples. Moreover, eight identical TEGs (TEC-12706), manufactured by Hebei I.T. Shangai Co., Ltd., are attached on the top of aluminium sheet with the help of universal silicone gel. The significant usage of TEGs that are at the rear side of the PV module is to convert the temperature difference and heat flow into useful power. However, the TEGs characteristics are given in **Table 30**. At the third stage, a four more K-type thermocouples were used to record the temperature of the cold side of TEGs, as shown in **Fig. 68C**. Furthermore, to ger an effective heat transfers all the components we employed a thermal grease HY-107 between the aluminium sheet and the back side of the PV panel. At fourth stage, we attached u-shaped grid pipe for both modified PV panel i.e., PVT, and PVT/TEG/nanofluid. For the fifth stage, we drilled a 10mm diameter holed for both PVT and PVT/TEG/nanofluid systems. The two holes are drilled in such a way that one on the top of the PV panel for the entry of the fluid, and other on the bottom for the exits of the fluid. Moreover, at sixth stage a total of three storage tanks are installed i.e., one for PVT system, second for PVT/TEG/nanofluids system, and the last tank is placed at the ground level. Furthermore, the storage tanks were covered with aluminium insulators for both PVT and PVT/TEG/nanofluids at the entry point of the fluid for the cooling purpose. For the final stage, for the circulation of working fluid from the storage tank a 0.35W IMM-Water-Pump connected to both modified PV panels. The characteristics of an IMM-Water-Pump are given in **Table 31**.

Table 30 Technical characteristics of TEGs

Parameter	Value	Units
Dimension	40×40×3.9	mm
Temperature working environment	-55 to 88	°C
Maximum current	4.3-4.6	A
Maximum voltage	14.4-16.4	V
Resistance	1.98-2.30	Ohm
Maximum heat	50-57	W

Table 31 Characteristics of IMM-Water-Pump

Parameter	Value	Units
Number of revolutions	5550	RPM/min
Operating current	0.12	A
Operating voltage	3	V DC
Power	0.35	W
Debit	80	L/H

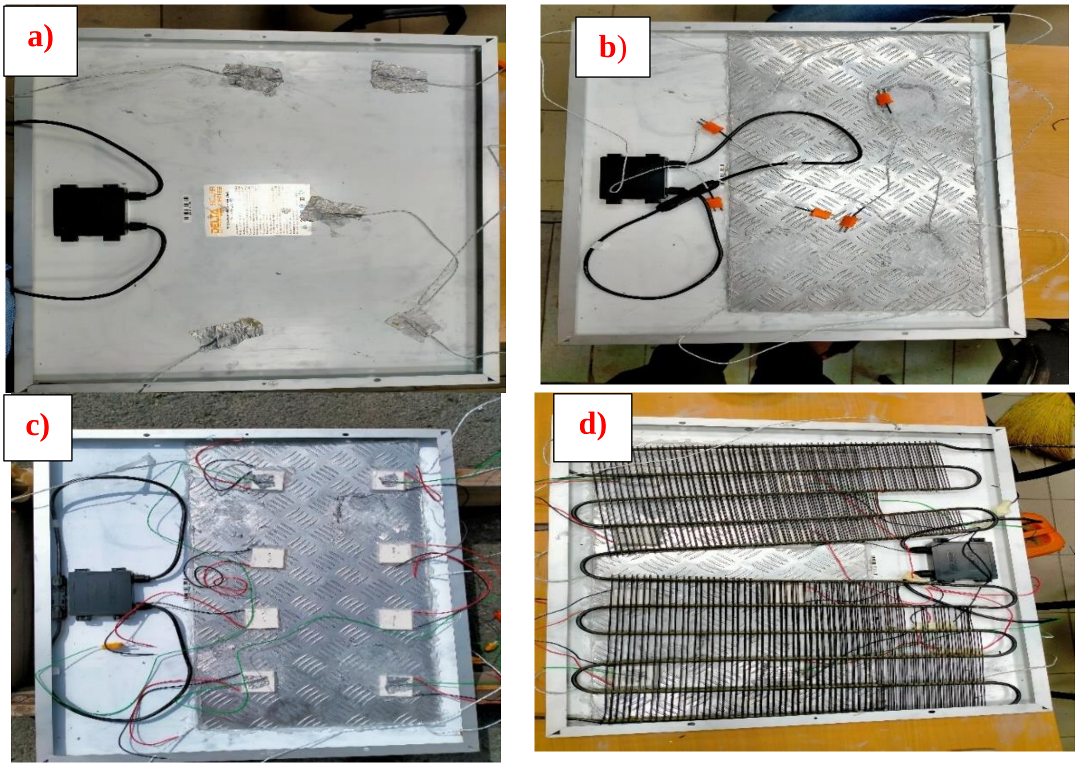

Figure 68 Construction of experimental setup at each stage

4.3.2 Preparation of Al_2O_3 nanoparticle

In this section the preparation of Al_2O_3 nanoparticle is depicted in **Fig.69.** The nanoparticles are purchased from the local Russian company i.e., Him-reactive, with a purity of 97%. The properties of Al_2O_3 nanoparticle is depicted in **Table 32**. Hence, in order to prepare 1% of Al_2O_3 nanoparticle a distilled water is used as a base fluid. The Al_2O_3 nano particle are immediately added and mounted on the magnetic stirrer and dispersed well as depicted in **Fig.69.** (left). To disperse particles into homogenously, the stirred nanofluid mixture is place on 150W ultra-sonicator at room temperature for an hour as shown in **Fig.69** (right).

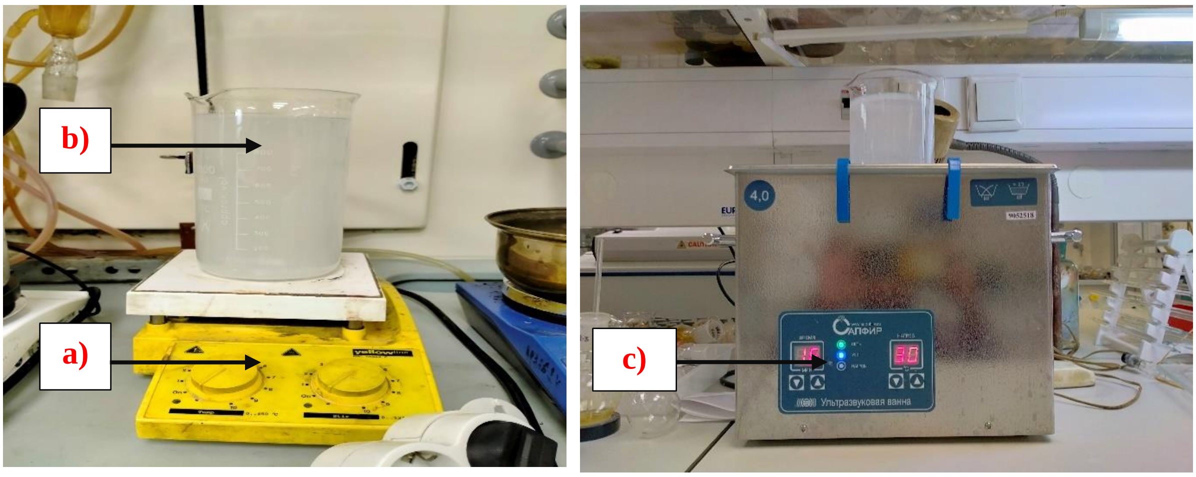

Figure 69 Preparation of Al_2O_3: a) Magnetic stirrer, b) Volumetric flask, and C) Ultrasonic Cleaner

Table 32 Al_2O_3 Nano particle characteristics

Shape	Mean diameter	Purity	Thermal conductivity	Density
Spherical	10-30 nm	97 %	37.5 (W/m. K)	3.95 g/cm^3

4.3.3 Experimental Setup

The experimental setup constructed and tested in the natural weather characteristics of Yekaterinburg City, Russian federation. However, before conducting the tests the PV panels were well-cleaned and mounted on the wooden stands. The test-rings of the present experimental investigations were installed around 07:30 morning and monitored the performance of three PV configurations, however, the actual test readings are taken from every 08:00 morning for every 30 minutes interval of time. The experimental setup of three PV configurations i.e. Reference PV panel (right), PV panel with simple u-shaped grid copper (middle), and PV panel modified with TEG's/u-shaped grid copper pipe are shown in **Fig.70.** The schematic of three PV configurations is shown in **Fig.71, and Fig. 72.**

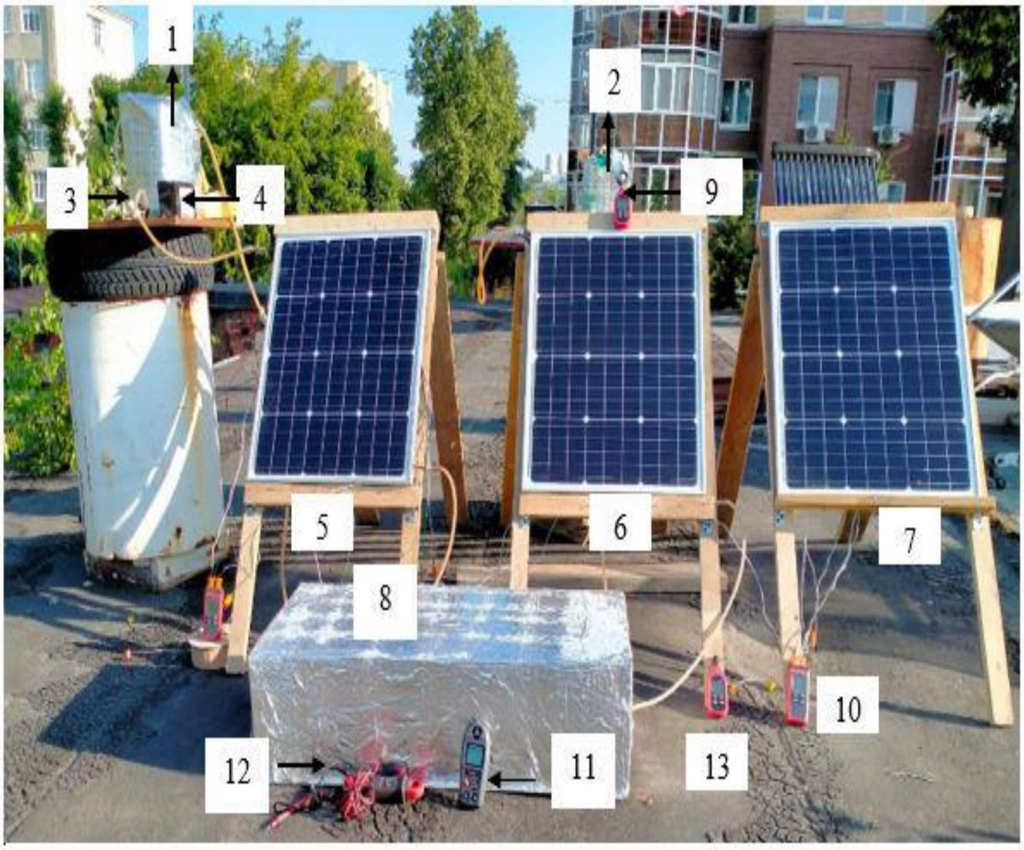

Figure 70 Experimental Test rig: 1) Al_2O_3 nanofluid storage tank, 2) Water storage tank, 3) Water pump 4) DT-1207 Battery, 5) PV/TEG/nanofluid panel, 6) PVT Panel, 7) Reference PV panel 8) Water storage tank lay on ground, 9) Solar Pyranometer, 10) 2K-digital logger, 11) Digital Anemometer, 12) Clamp meter, 13) Thermometer

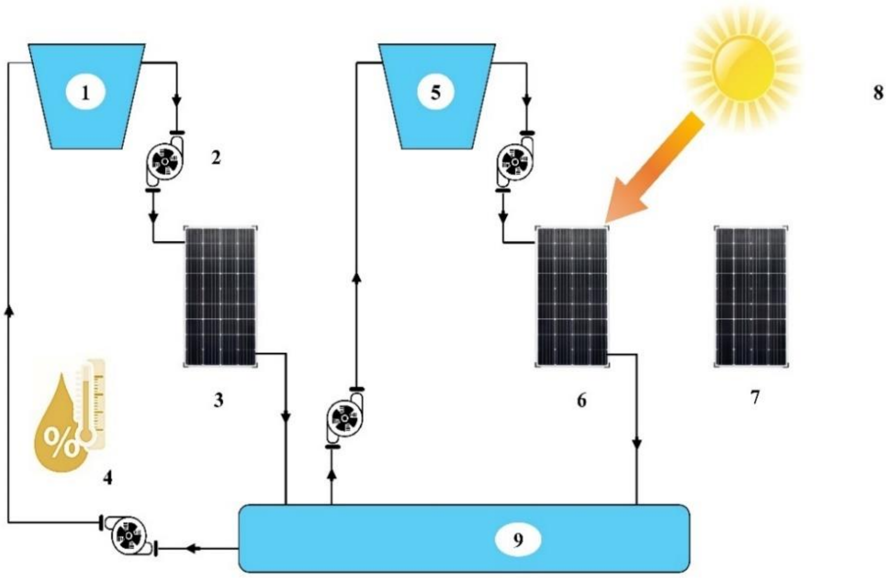

Figure 71 Schematic diagram: 1) Nanofluid storage tank, 2) Water pump, 3) PV/TEG/nanofluid PV panel, 4) Humidity Sign, 5) Water storage tank, 6) PVT panel, 7) Reference PV panel 8) Solar radiation, 9) Water storage tank lay on ground

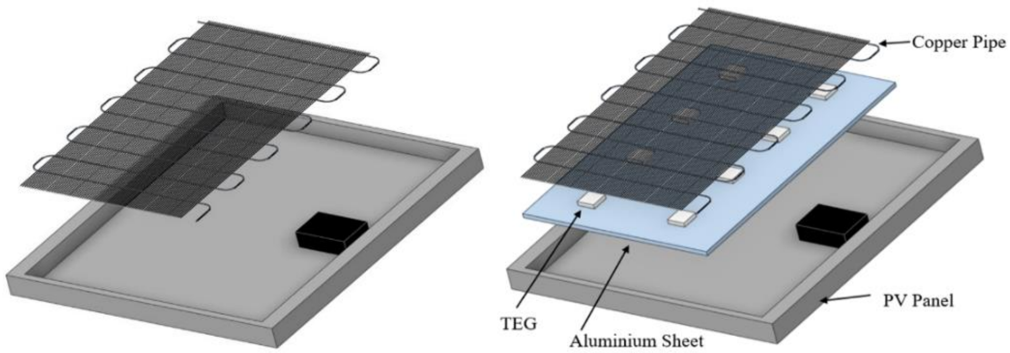

Figure 72 The schematic of rear side of PV panel (a) With u-shaped grid copper pipe (left) (b) PV/TEG/ u-shaped grid copper pipe (right)

4.3.4 Weather characteristics on the day of the experiment

The section is dedicated to the results and outcomes of the performance of three PV configuration for the three PV configurations i.e., refenced PV panel, PVT (PV with simple water), and PVT/TEG/nanofluid (PVT/TEG/nanofluids with u-shaped grid copper pipe) are presented and evaluated. Since the experimental test were conducted under real outdoor experiments in Russian Federation. The progression of solar radiation, wind speed, relative humidity, and ambient temperature profiles for the experimental study are presented in **Fig.74.**

From the results it was observed that the performance of the weather characteristics on the weather performance it is fact that the associated values of solar radiation and ambient temperature is directly related temperature. The increase in the solar radiation values also affects the ambient temperature as shown in **Fig.74a.** On the other hand, the values associated to the relative humidity and wind sped are indirectly proportional to each other i.e., an increase in one lead to a reduction in the other. The relationship between humidity and wind speed is expected, as higher relative humidity values are often recorded in the early mornings after sun set or at nigh-time whenever the atmospheric conditions are calm at the same time low wind speed likely to be recorded as shown in **Fig.74b.** Hence, the weather characteristics from the present study showed that the recorded solar irradiance values start from 378W/m^2, which reached a maximum at solar radiation of 1357 W/m^2 at mid-day of the, and immediately starts decrease on the second half day of the experiment. The average solar radiation during the experimental day is 917 W/m^2, and the average ambient temperature day is 38.4 °C as shown in **Fig.74a.** Similarly, the average relative humidity is 28.2 %, and the wind speed achieved for the experimental day is 4-6 m/s depicted in **Fig.7b.**

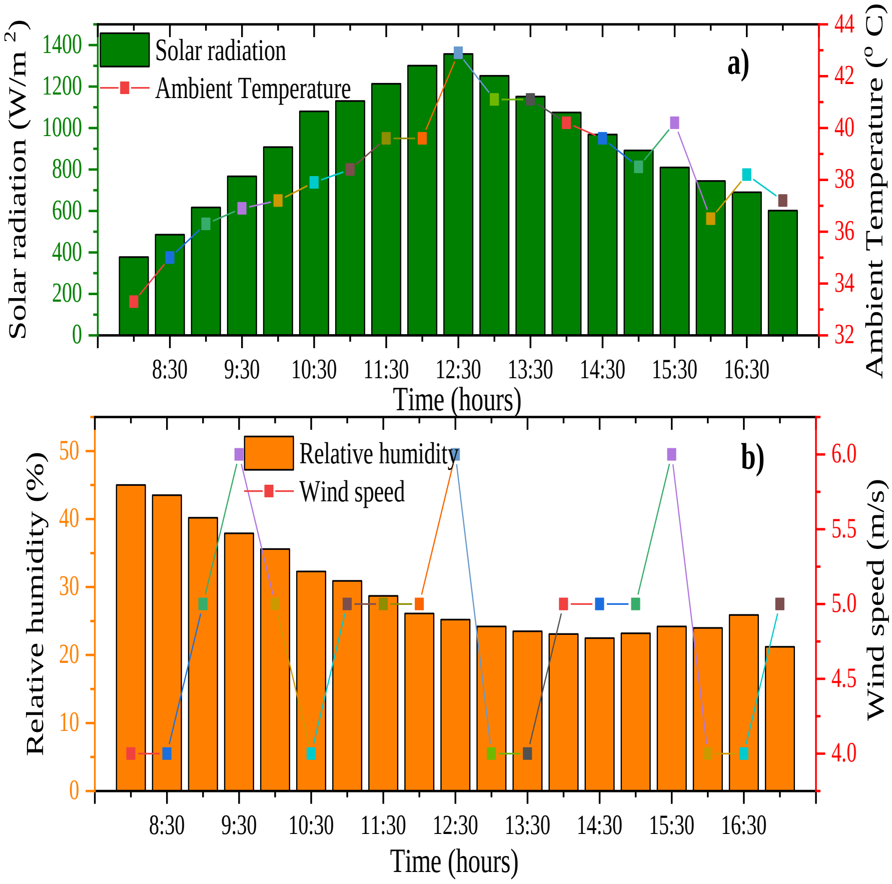

Figure 73 Time dependence: a) solar radiation & wind speed, and b) relative humidity & ambient temperature

4.3.5 Temperature distribution of PV panel

In the present study, we employed five K-type thermocouples at different location on each PV configuration to record the temperature distribution of PV panel. The recorded PV three PV configurations during the experimental day is depicted in **Fig.74a.** From the findings it was observed that the temperature curve of the three PV configurations progressively increased due to the increase in solar radiation during the first half day of the experiment and hits maximum at 12:30. On the other hand, the temperature profiles of three PV configurations starts decreasing during the second half-day of the experiment as shown in **Fig.74a**. The recorded peak temperatures of the reference PV panel, PVT, and PVT/TEG/nanofluid over the experimental day is 56.1 °C, 44.8 °C, and 39.7 °C, respectively. The findings reveal the proposed cooling solar PV panel with TEG, and nanofluid recorded the least temperature. The average reduction temperatures of PVT and PVT/TEG/nanofluid configurations are 11.2 °C, and 16.5 °C, leading to average drop of 25.1%, and 41.2%, respectively as shown in **Fig.74b**.

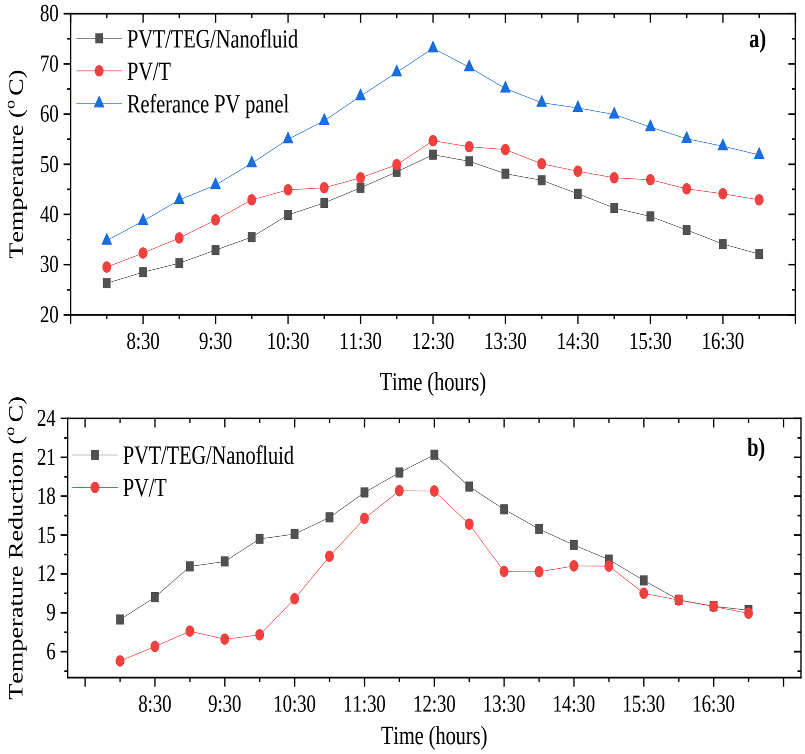

Figure 74 Time dependence a) Temperature profile b) reduction in temperature with respect to the referenced PV panel

4.3.6 Electrical efficiency

The electrical efficiency and improvement in the electrical efficiency for the present study is presented. The recorded electrical efficiency of the present study is presented in **Fig.75a**, for the three PV configurations i.e., referenced PV panel, PVT, and PV/TEG/nanofluid, which are 11.64%, 12.3%, and 12.62%, respectively. Moreover, the average electrical efficiency improvement for PVT, and PVT/TEG/nanofluid are 5.8%, and 8.5%, respectively, that is depicted **Fig.75b**.

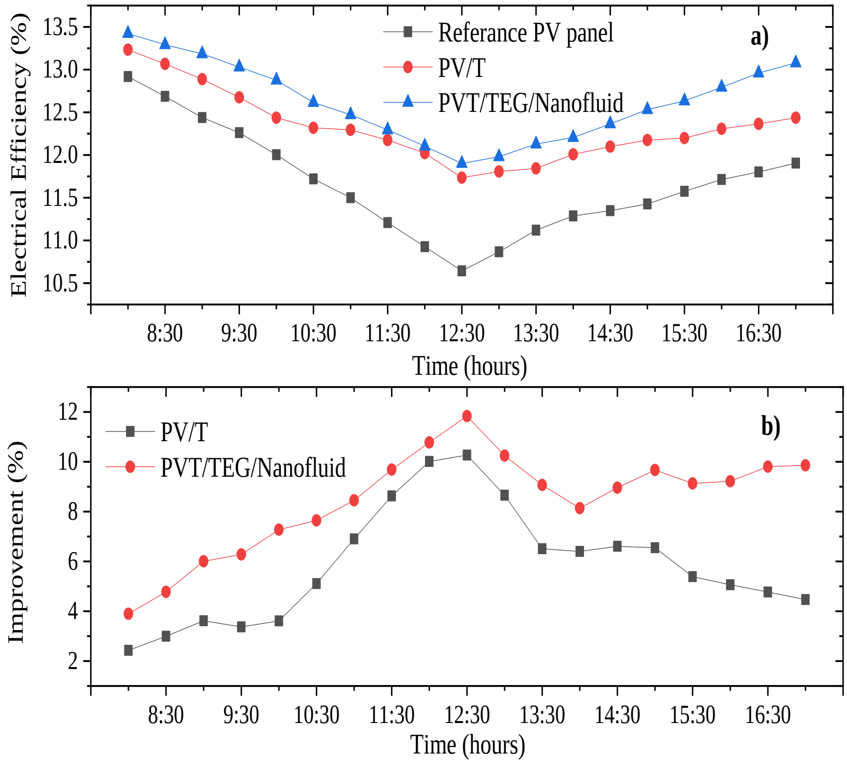

Figure 75 Time dependence a) electrical efficiency, and b) improvement in electrical efficiency with respect to the referenced PV panel

4.3.7 Electrical performance of the PV panels

The electrical performance of the three PV configurations i.e., referenced PV panel, PVT, and PVT/TEG/nanofluid are depicted in **Fig.76,** and **Fig.77.** From the **Fig.76,** it is evident that the voltage and current profile of the PV module follows similar trend as the solar radiation in the first half-day of the experiment, and it starts decreasing solar radiation after mid-day. Since the attribute to the negative impact of increase in temperature of the PV module. It is seen from the results that, although the voltages of the three different PV configurations increased with increasing solar radiation, that of the PVT and the PVT/TEG/nanofluid increased more compared to the referenced PV module as a result of the high temperature of the referenced module. Similarly, due to the positive impact of the nanofluid in reducing the temperature of the PVT/TEG system, it also performed better than the PVT- only system. As such, the average recorded voltage for the three modules is 20.07 V, 21.53 V, and 21.82 for reference PV panel, PVT, PVT/TEG/nanofluid systems, respectively. The average recorded current for the three PV configurations is 1.71 A, 1.74 A, 1.86 A for the referenced PV panel, PVT, PVT/TEG/nanofluid systems, respectively

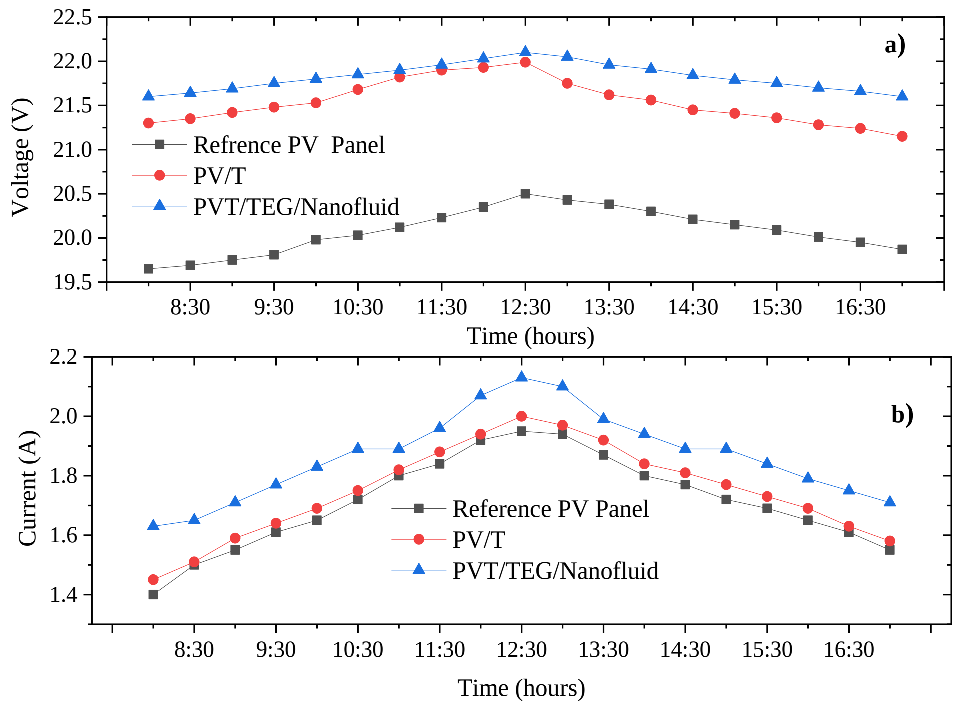

Figure 76 Time dependence a) voltage, and b) current

The electrical performance of the three PV configurations is depicted in **Fig.77.** The findings show the influence of temperature of the temperature profiles are negatively affected the performance of the electrical power output. In the present study, a total of 0.35W IMM-Water-Pump is installed for the up-ward and down-ward stream flow of the fluid for both the modified PV panels, which is PVT, and PVT/TEG/nanofluid. Hence, the electrical performance of the modified PV/TEG/nanofluid and PVT was found to be higher compared to the referenced PV panel. The significant achievement is due to the addition of the nanoparticles, and TEGs. Therefore, the average power generation from the three studied reference PV panel, PVT, and PVT/TEG/nanofluid are 34.39 W, 37.67 W, and 40.7 W, respectively, which leads to an improvement of 9.5%, and 18.5%, against the referenced PV panel as shown in **Fig.77a.** However, in the present study, we employed 0.35 W IMM-Water-Pump used an external source of power for the experiment, it is important to assess its impact on the output power of the modified PV panels. Therefore, the findings if the power pump is deducted then the average recorded referenced PV panel, PVT, and PVT/TEG/nanofluid are 36.97 W, and 40.0 W, respectively, that leads an improvement of 7.50%, and 16.42%, while the power of the referenced PV panel remains unchanged is depicted in **Fig.77b.** Finally, the power deducted by the water pump the output performance of the PVT, and PVT/TEG/nanofluid still put above that of the referenced system. Thus, the results justify that the proposed cooling system upon the addition of TEG/nanoparticles are more effective.

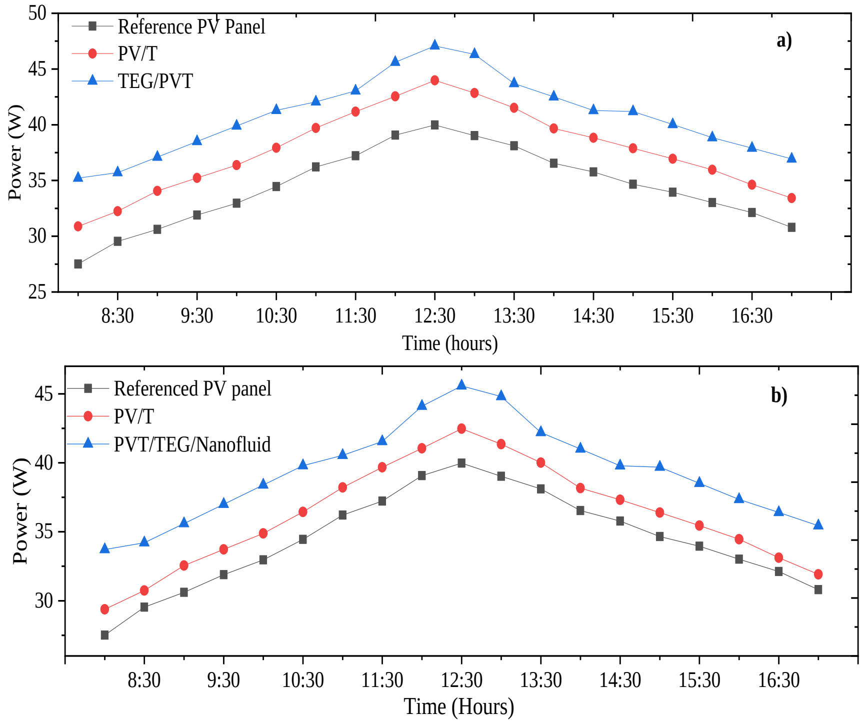

Figure 77 Time dependence a) with water pump, and b) without water pump

4.3.8 The effect of temperature gradient on TEGs

The temperature gradient of the TEGs we employed a four more K-type thermocouples are place at the cold side of TEC-12706, and the hot side of TEGs are taken from the temperature of a PV panel, the results are depicted in the **Fig.78.** It can be observed, that the TEGs follow the same trend as the temperature profile of the PVT/TEG panel. The highest temperature difference between the hot side and cold side TEGs are found to be 13.4 °C at 12:30 pm, and lowest is at 4.6 ˚C at 08:00 am. The average temperature gradient across the TEGs over the day of the experiment is 8.7 °C.

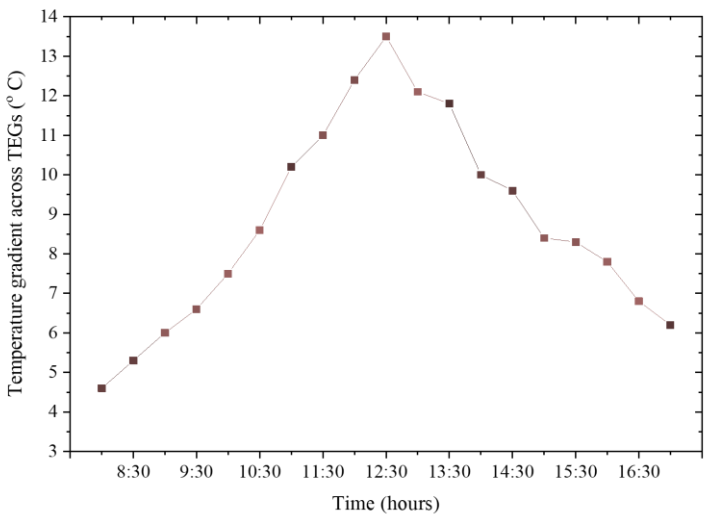

Figure 78 Time dependence temperature gradient of TEGs

4.3.9 The effect of efficiency on TEGs

The effect of efficiency of TEG's performance is significantly dependent on the temperature of hot and cold sides. Thus, the TEG's efficiency was calculated using in the given **Eq. (50),** and a figure of merit value of 0.008/K was used for the estimation. The recorded average temperatures of the hot and cold sides of TEG are 39.73 °C, and 30.9 °C, respectively. The mean average temperature of hot and cold side of TEG's are 35.5 °C. The efficiency of TEGs at 30 minutes interval time are depicted in **Fig.79.** The efficiency followed the same trend as the temperature profile of TEGs. The lowest efficiency is occurred 0.83% occurred at 08:00 am, and the highest TEGs efficiency occurred around 2.27% at 12:30. Hence, the average efficiency of TEGs over the experimental day is 1.52%. **Table 33** depicts the present study compared with other literatures.

$$\eta_{TEG} = \left(1 - \frac{T_c}{T_H}\right) \times \frac{\sqrt{1 + Z\bar{T}} - 1}{\sqrt{1 + Z\bar{T}} + \frac{T_c}{T_H}} \tag{50}$$

Here, Z, T_H, T_C, and $\bar{T}$ are signifies the figure of merit, hot side, cold side, and mean temperature of thermoelectric generators i.e., $\frac{T_h+T_c}{2}$. The value of figure of merit is 0.008/K[175].

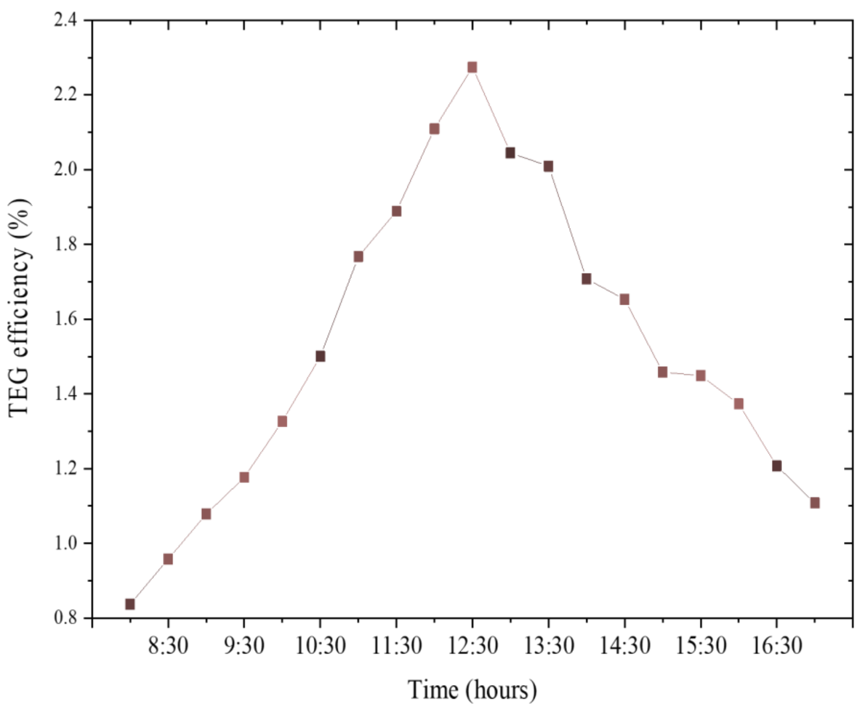

Figure 79 Time dependence TEG efficiency

Table 33 Comparison with other studies

Ref. No	Proposed Cooling	Location /Country	Key Findings
[176]	Silica/Water nanofluid	Mashhad, Iran	1.Overall electrical efficiency improved 7.1 %. 2.Exergy efficiency increased to 24.31 %
[177]	Graphene nanoplatelets-water nanofluid	Karabuk /Turkey	1.Temperature reduction about 16 ˚C. 2.Electrical efficiency improved 8.5%
[178]	PVT/PCM/nano fluids	Tehran/Iran	1.Temperature reduction about 12 ˚C 2. Electrical efficiency is improved about 3-4.2 %
[179]	Low concentrated photovoltaic/TEG	Beijing/China	1.Temperature of a PV reduced to 9.2 ˚C 2. Highest TEG is achieved 1.4 W 3. PV efficiency improved in summer 8.17%
[180]	Spectral splitting of PV/thermal hybrid system	China	1.Temperature reduction by 3% 2. Power generation improved by 10% 3.Efficiency of PV panel is improved 0.64%
[181]	PV/TEG/PCM	Shiraz/Iran	1.Temperature reduction about 4-15 ˚C 2. The improvement efficiency of PV panels are 0.29-1.67 %.
[182]	Numerical analysis on hybrid PV/TEG	Iran	1.Average exergy improvement is 16.73% 2. Electrical efficiency improved by 14.88 %.
Present study	Hybrid grid evaporator/TEG/nanofluids	Yekaterinburg/ Russian Federation	1.Average temperature reduction PVT and PVT/TEG is 11.2 ˚C and 16.5 ˚C 2. Electrical efficiency improved PVT and PVT/TEG 5.8 % and 8.5 %. 3. Power output improved PVT and PVT/TEG 7.50 % and 16.42 %.

4.3.10 Economic analysis

The cost of energy in the present experimental study is calculated LCOE approach. In the present experimental investigation, we used three PV panels i.e., referenced PV panel, PVT, and PVT/TEG/nanofluid used. The investment cost for cooled PV panel is little higher due to the addition of materials such as aluminium sheet, thermo electric generator, 0.35 W water pump, thermocouples, pipes and a storage tank. **Table 34** present the items used for the experimental investigation and LCOE calculations.

Table 34 Parameters used for LCOE calculations

Items	Reference PV panel	PVT panel	PVT/TEG/ nanofluid panel
PV panels	45	45	45
K-Type thermo couples	3.5	3.5	3.5
HY-510 thermal paste	0.5	0.5	0.5
Silicone gel	1.5	1.5	1.5
Water Pump	6	6	-
Thermoelectric coolers (TEC1-12706)	20	-	-
Aluminium plate	3	-	-
Al_2O_3 nanoparticle	3	-	-
Total investment	82.5	56.5	50.5

The estimated cost of the present study at the time of purchase of Russian federation. However, the estimated cost may be differed from country-to-country.

The economic analysis is assessing the financial implications of the project. Thus, the **Table 35** shows the calculations of LCOE is one of the best approaches for the calculations of economic analysis. In the present study, the LCOE calculations were calculated in two prospects i.e., for one-year period (365 days), where there is continuous availability of solar radiation. On the other hand, the second scenario assumed for the Russian Federation climatic conditions. This is due to the present study, is conducted in Yekaterinburg city, Russia. The number of days of the availability of solar radiation is to be 105-120 days in the period of May, June, July, and August. Moreover, the availability of solar radiation in a day is assumed to be 12h for both the scenarios. The total power achieved is also assumed be to same achieved from the electrical performance of three PV configurations i.e., referenced PV panel, PVT, and PVT/TEG/nanofluid. Hence, the calculations the expected annual electricity for the first scenario (365 days) i.e., referenced PV panel, PVT, and PVT/TEG/nanofluid are 150.62 kWh, 161.92 kWh, and 175.2 kWh, respectively. From the calculations the LCOEs in the first scenario for the referenced PV panel, PVT, and PVT/TEG/nanofluid PV panels are 0.044 $/kWh, 0.044 $/kWh, and 0.051 $/kWh, respectively. Similarly, the second scenario the expected annual electricity generation for the referenced PV panel, PVT, and

PVT/TEG/nanofluid PV panel are 43.3 kWh, 46.58 kWh, and 50.4 kWh, respectively. Therefore, the LCOEs achieved for the second scenario for 105 days i.e., for referenced PV panel, PVT, and PVT/TEG/nanofluids are 0.156 $/kWh, 0.159 $/kWh, and 0.178 $/kWh, respectively. From the calculations the LCOE achieved for PV/TEG/nanofluid is little higher than the PVT, and referenced PV panel in both the scenarios. The significant achievement is due to the additional capital cost of the materials used for the construction PVT/TEG/nanofluid systems. It is also revealed from the findings that the influence of pumping power on the economics of the module is relatively insignificant.

Table 35 LCOE calculations

Parameters	PV/TEG cooled panel ($)	PVT/ Panel ($)	Un-cooled PV panel ($)	Reference
Effective discount rate (i_{eff}), %	5	5	5	[183]
Nominal escalation rate (r_n), %	1	1	1	[183]
Available of solar radiation (hours)	12	12	12	Assumed
Lifetime of solar PV plant, (n)	25	25	25	Manufacturer recommendations
$K_{O\&M}$	0.96	0.96	0.96	Calculated
Capital recovery factor (CRF)	0.07	0.07	0.07	
Constant escalation levelized factor O&M, (CELF), %	1.08	1.08	1.08	
Annual operation and maintenance cost ($C_{O\,\&M}$), $	3	3	3	
$LC_{O\,\&M}$, $	3.24	3.24	3.24	
C_{inv}, $	82.5	56.5	50.5	
LC_{inv}, $	5.77	3.95	3.53	

Levelized cost of fuel (LC fuel), $/kWh	0	0	0
E_{out} (W)	40	36.97	34.39
E_{annual} (kWh) for 365 days	175.2	161.92	150.62
LCOE for 365 days ($/kWh)	0.051	0.044	0.0.044
E_{annual} (kWh) for 105 days	50.4	46.58	43.33
LCOE for 105 days ($/kWh)	0.178	0.154	0.156

4.4 Conclusions of chapter 4

The present section evaluated three active cooling methods of PV module by using fanless heat pipe, thermoelectric cooling, and PVT/TEG/nanofluids. The following conclusions can be made:

1) The **first active cooling** experimental investigation using the fanless heat pipe sink the temperature of a cooled PV module over the period of the experiment is 40.76 °C, against un-cooled PV panel is 47.49 °C.
2) The average reduction in the temperature by fanless heat pipe sink active cooling approach is 6.73 °C. Furthermore, the average voltage for the cooled and un-cooled PV panel are 18.36 V, and 17.01 V, respectively. Similarly, the average recorded current for the cooled and un-cooled PV modules are 0.619 A, and 0.57 A, respectively.
3) On the other hand, the recorded average for the fanless heat pipe for the cooled and un-cooled PV panels are 11.39 W, and 9.73 W, respectively. The improvement in the cooled power is 1.66 W. Moreover, the exergy efficiency for the cooled and un-cooled for the PV panels are 7.88 %, and 4.54 %, respectively.
4) The economic analysis for the cooled PV panel integrated fanless heat pipe is 0.61 $/kWh-0.206 $/kWh, and for the un-cooled PV panel 0.61 $/kWh-0.277 $/kWh, depend upon the number of days of the operation.
5) The **second active cooling** experimental investigation by using thermo electric coolers (TEC) and TEGs are incorporated at the back side of a PV panel. The temperature of the cooled PV incorporated with TEC and TEGs are 33.37 °C, against referenced PV panel

are 45.60 °C. The reduction in the temperature PV module integrated with TEC/TEGS are 12.23 °C.

6) The electrical performance of the cooled PV panel by integrating TEC/TEGs are 6.31 W, and for the un-cooled PV panel is 5.22 W. The increase in the electrical performance of a PV panel by integrating TEC/TEGs are 1.09 W, leading to the improvement 20.88 %.
7) The electrical efficiency of the cooled PV module integrating with TEC/TEGs is 14.5 %, and for the un-cooled PV module is 13.8 %. The improvement in the electrical efficiency is 0.7%, which leads in the efficiency of a PV module is by 5.07 %.
8) The economic analysis for the cooled PV module and un-cooled PV module integrated by using TEC/TEGs are 0.410 $/kWh, and 0.414 $/kWh, respectively.
9) The **third active cooling** experimental approach using u-shaped copper grid pipe integrated with TEGs and Al_2O_3 nanofluids. The average temperature reduction over the experimental day for the referenced PV panel, PV panel with simple u-shaped grid copper **(PVT)**, and PV panel integrated with TEGs/u-shaped grid copper pipe/Al_2O_3 nanofluids **(PVT/TEG/nanofluids)** are 56.1 °C, 44.8 °C, and 39.7 °C, respectively. The reduction in the PV configurations for PVT, and PV/TEG/nanofluids are 11.2 °C, and 16.5 °C, leading to an improvement of 25.1 %, and 41.2 %, respectively.
10) The average electrical efficiency for the referenced PV panel, PVT, and PVT/TEG/nanofluids are 11.64 %, 12.3 %, and 12.62 %, respectively. The improvement in the average electrical efficiency is 5.8 %, and 8.5 %, respectively.
11) The electrical performance of the active cooling approach using referenced PV panel, PVT, and PVT/TEG/nanofluids are 34.39 W, 36.97 W, and 40.0 W, respectively without any external power source, leading an improvement of 7.50 %, and 16.42 %.
12) The average temperature gradient across the TEGs i.e., TEC1-12706 for the experimental day is 8.7 °C.
13) The average electrical efficiency temperature gradient across the TEGs is 1.52 %, over the experimental day.
14) Finally, the LCOE for the referenced PV panel, PVT, and PVT/TEGs are 0.044 $/kwh to 0.178 $/kWh, depends on the number of days of operation of the PV plant.

5 EXPERIMENTAL INVESTIGATION FOR THE IMPROVEMENT EFFICIENCY OF SOLAR PV PANELS USING PASSIVE COOLING MECHANSIMS

5.1 The influence of discontinuous aluminium heat sinks for a thermal management solar PV to enhance output performance

The present work signifies achieving maximum electricity output and cooling the PV panel. Therefore, two 30 W PV panels were selected that have similar characteristics. However, we developed a "brush-like" discontinuous aluminum heat sink that integrated on the rare side of one of the selected PV panels and the second PV panel without any modifications for the enhancement.

5.1.1 Material and Methods

The study objective is to cool down the solar PV panel employing free air convention (i.e., passive cooling). Therefore, we used aluminum for the quick heat dissipation of air at the edges. Thus, heat is removed easily and quickly from the solar PV panels. The motivation behind selecting aluminum over other metals is explained further in section 2.4.2.

5.1.2 Aluminium Characteristics

Aluminum is lightweight and rigid, with thermal conductivity and malleability. Aluminum is used in aircraft carriers, foils, home appliances to strengthen the material, and many more [184] . The thermal conductivity behavior of aluminum is almost as of copper, up to 60%. The highest thermal conductivity of aluminum is 62%; International Annealed Copper Standard (IACS) certified that the usage of aluminum is suitable for use [185]. Besides the above discussions, aluminum can be available in energy markets and relatively cheaper than other metallic materials. That made it convenient to use in the current study.

5.1.3 Mathematical Modelling for Solar Cell

Due to the fall of solar radiation on the solar cell of a PV panel, electricity is created. Nevertheless, of the energy produced by solar radiation, only 47% is converted into electricity, and the rest will be the heat loss that negatively affects the solar PV panels, which decreases the lifetime of a plant. The V_{OC} is the open-circuit voltage when the current is zero, and I_{sc} is the short circuit current when the voltage is zero, which defines the maximum power theoretically [186]. The I-V equation of solar cell is expressed in the **Eq. (51).** [187].

$$I_{total} = I_0 \left(e^{\frac{av}{nkt}} - 1\right) - I_l \tag{51}$$

Here, $I_l = qAG\ (L_n + L_p + W)$ represent the light generated current that shows that the carriers produced inside the volume of cross-sectional area A as well as the length $(L_n + L_p + W)$.

Parameters such as fill factor (FF), V_{OC}, I_{SC} and efficiency (η) are used to compare solar cells. The V_{OC} depends on the PV panel's temperature, this can be seen from **Eq. (52)**.

$$V_{OC} = V_{OC}(T_0) - \left[\frac{E_{g0}}{e} - V_{OC}(T_0)\right]\left[\frac{T}{T_o} - 1\right] - \frac{3kT}{e} In \frac{T}{T_o} \tag{52}$$

When the temperature increases by 40 K and T_o = 300 K, then T = 340 K becomes the PV panel's temperature. The Boltzmann constant is k, E_{g0} is the band-gap energy. These can be ignored: $\frac{T}{T_o}$ = 0.125 and $\frac{3kT}{e} In \frac{T}{T_o}$ = 10 mV. V_{OC} varies with temperature as presented in **Eq. (53).** Where E_{g0} = 1.21 eV and T = 300 K and V_{OC} = 0.55 V, which is a characteristic of a silicon solar cell, it reduces in V_{OC} with a rise in T of $\frac{dV_{OC}}{dT}$ = -2.45 mVK^{-1} at 25 °C [188]

$$\frac{dV_{OC}}{dT} = -\frac{\left[\frac{E_{g0}}{e} - V_{OC}(T_0)\right]}{T_O} - \frac{3kT}{e} \tag{53}$$

5.1.4 Experimental Test Rig

The passive mechanism used for the cooling process of a PV panel has relative advantages, such as being easy to construct and no requirement of any additional water. We used a heat sink naturally cooled by air in the present experimental study. Moreover, we used an aluminum sheet sliced into several pieces, and small holes were created with the driller enabling the driller to pass natural convection of air from the atmosphere to the heat sink and remove heat dissipation from the PV panel. Moreover, the present work is a modified work of Grubišić-Čabo et.al [189], i.e., we changed the surface area of the sheets and perforated holes drilled in the current study. The modified pieces are represented in **Fig.80 (a)** vertical direction of heat sink, and **Fig. 80 (b)** horizontal direction of heat sink directions for the reference.

The modified hear sink sheets were integrated at the rear end of the PV panel (i.e., cooled panel), as shown in **Fig. 81 (a)**. The modified heat sinks are integrated with the help of universal silicone gel. To achieve the contact and conduction of heat from the cooled panel to the modified heat sinks, a thermal grease (HY170) was employed between the PV panel and the heat sink. On the other hand, the second panel remains unchanged for the enhancement, as shown in **Fig. 81 (b)**. Moreover, the strings were placed strategically with the proper measurement string to string.

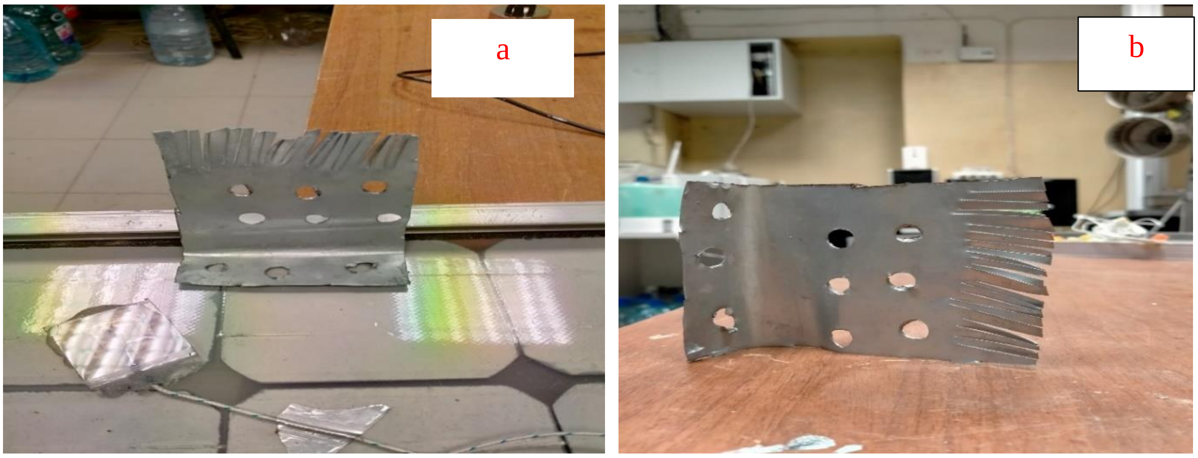

Figure 80 (a) vertical, and (b Horizontal direction of heat sink

The PV panel configuration has 950mm×450mm with an efficiency of 15%. We employed seven K-type thermocouples for the cooled and un-cooled panels to record the temperature of a PV panel. The resolution of solar PV panels is 0.1 °C. A solar pyranometer was employed to record the solar radiation from the sun. Moreover, Voltage (V) and Ampere (A) were recorded using a clamp meter. The thermometer is employed to record the relative humidity and ambient temperature. An Infrared thermal imager is also used to record the temperature distribution of the two panels.

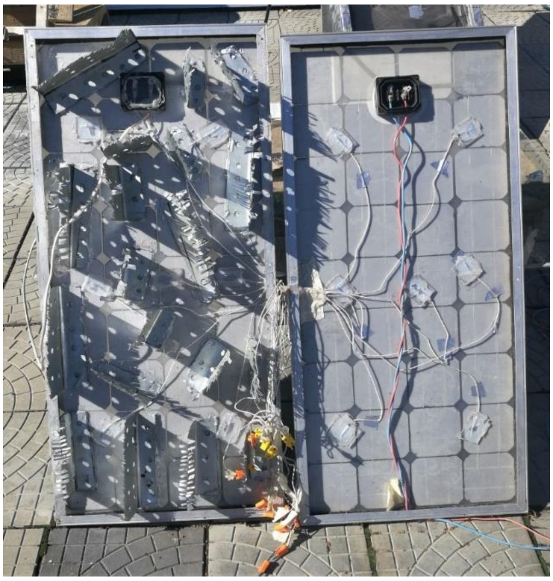

Figure 81 Images for the PV panels (a) modified heat sink, (b) Reference

The experimental test rig is shown in **Fig.82 (a)** modified PV panel and **Fig.82 (b)** reference PV panel. The experiment was done on a clear day with continuous availability of solar radiation on 7th July 2021, at Ural Federal University, Yekaterinburg, Russian Federation (Latitude 56.84 °N, and Longitude 60.64 °E). Meanwhile, the present experiment is between from 09:00 to 5:00 PM. Thus, the thermal performance of cooled and referenced PV panels is recorded every 30 minutes.

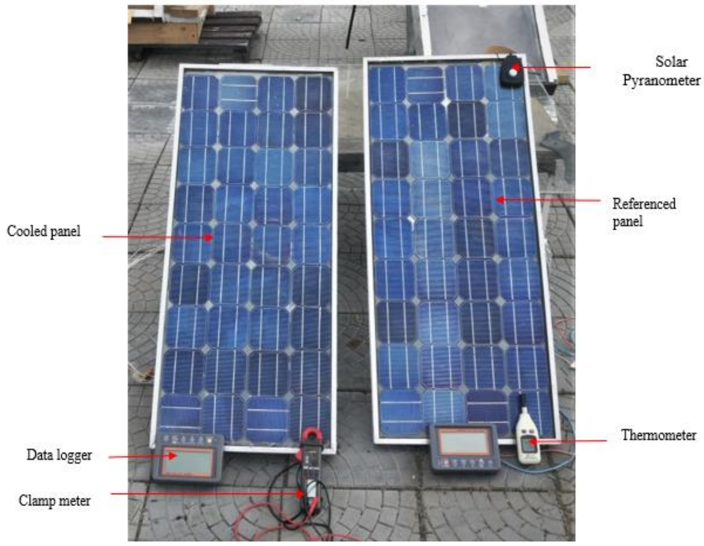

Figure 82 (a) Modified PV panel (b) Reference PV panel

5.1.5 Performance Weather Characteristics

The experiment was carried out in the peak month of July, which is the peak summer period in Yekaterinburg city. The weather characteristics of the investigation are shown in **Fig. 83**. The highest solar radiation on the day of the experiment was 1349 W/m^2 at the peak time around 12:30 pm. Moreover, the average solar radiation, ambient temperature, humidity, and wind speed on the day of the experiment are 976.35 W/m^2, 33.78 °C, 43.75%, and 5.29 m/s, respectively. Furthermore, in **Fig. 83 (b),** the relative humidity in summer gradually decreases with the day hours because of an increase in the ambient temperature of the day. Thus, the present work justifies as the humidity decreases with an increase in the temperature.

5.1.6 Thermal management

In the present work, seven K-type thermocouples were employed at different locations for each panel to record the temperature every 30 minutes. The data were recorded using a logger from 9:00 am to 5:00 pm. The recorded temperature of the cooled and un-cooled PV panels is presented in **Fig. 84**. The cooled and un-cooled PV panels' temperatures peaked around 2:30 pm, and recorded temperatures are 52.53 ˚C and 63.60 ˚C, respectively. Meanwhile, the average temperature during the entire period for the cooled and un-cooled are 41.09 ˚C, and 52.53 ˚C, respectively. The reduction in the temperature of a cooled PV panel is 9.93 ˚C, which was influential in the present study. Moreover, we compared the present with other studies already in the literature; for instance, Arifin et al. [190], Mojumder et al.[191] , and Hasan et al [192]. proposed a cooling mechanism using aluminum heat sinks. Their study results show that the temperature reduction between cooled and un-cooled PV panels are 12.8 ˚C, 3-8 ˚C, and 5.7 ˚C, respectively. The thermal images also access the temperature distribution of the cooled and un-cooled panels on the experimental day. The cooled PV panel recorded an average temperature of 37.2 ˚C and a maximum temperature of 40.5 ˚C, whereas the un-cooled PV panel recorded an average temperature of 40.8 ˚C and a maximum temperature of 54.6 ˚C. The thermal images are presented in **Fig.85**. (a, b, c) for cooled and un-cooled PV panels. There was a slight difference in average temperatures between thermocouples and recorded thermal images. Thus, the difference may be because the thermocouples have close contact with the PV panels and, as a result, has the potential to give relatively accurate results, hence the variations.

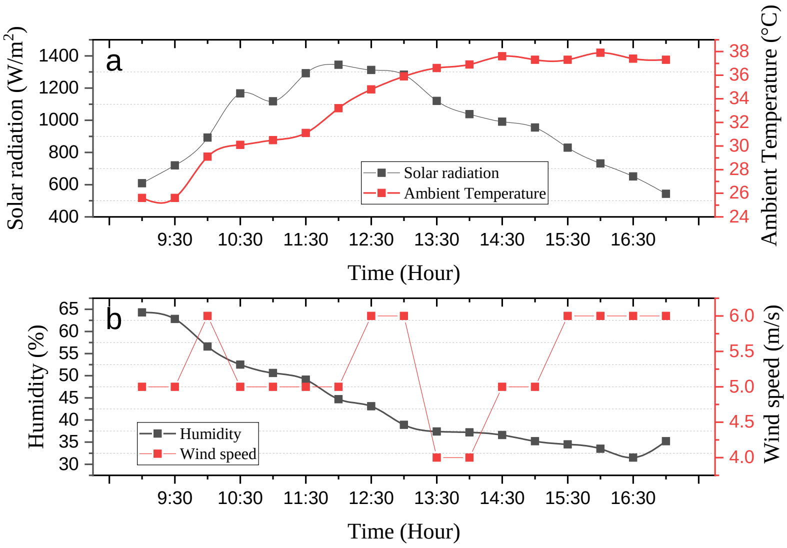

Figure 83 Weather Characteristics (a) solar radiation & Ambient temperature, and (b) Humidity & wind speed day of experiment

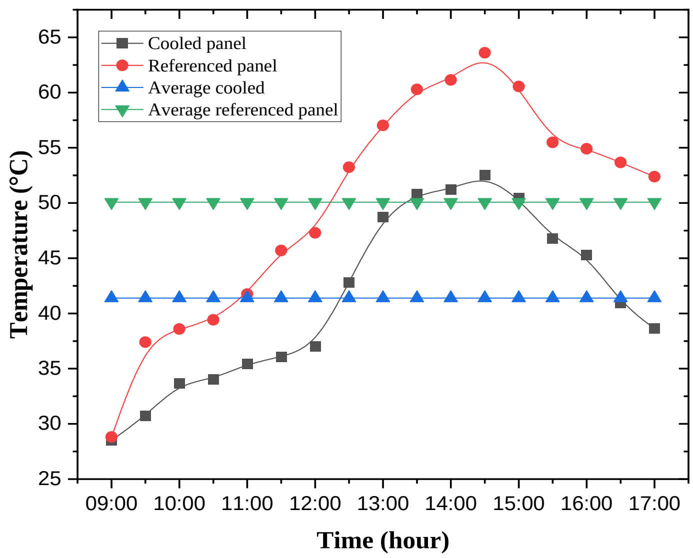

Figure 84 Temperature characteristics of both PV panels

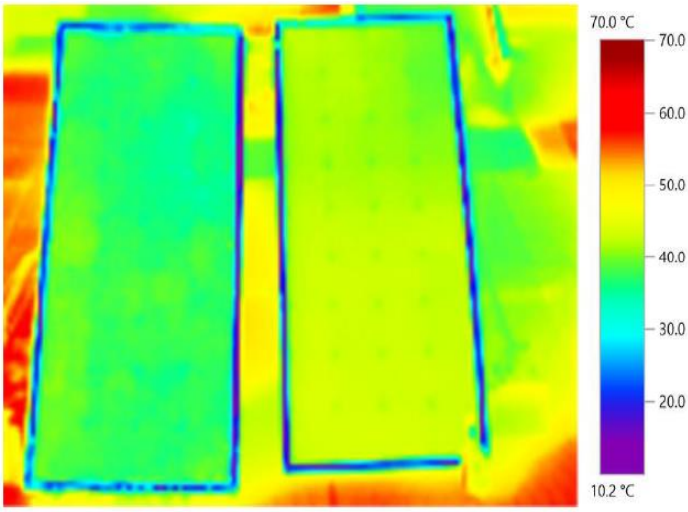

(a)

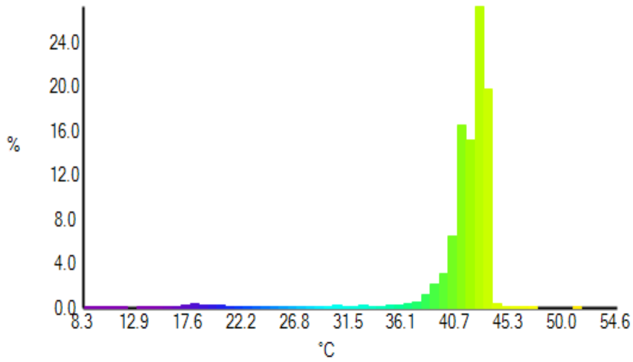

(b)

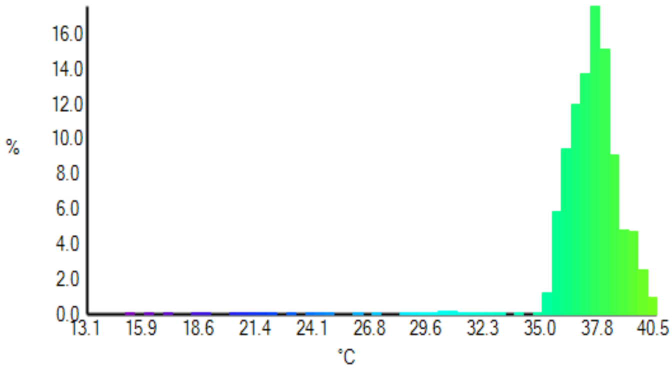

(c)

Figure 85 Temperature distribution: a) Thermal images, b) cooled PV panel, c) referenced PV Panel

5.1.7 Power Characteristics of PV Panels

The effect of voltage and ampere for modified and reference PV panels is illustrated in the present section. The two PV modules almost recorded the same current; a modified PV's average current is about 0.646 A, and the referenced PV panel's average current is 0.641 A.

The average difference between these two PV panel currents is about 0.0005 A, as shown in **Fig. 86 (a)**. Moreover, the recorded voltage of both PV panels is recorded, and it demonstrates that temperature showed a significant effect on both the PV panels. In this case, the average voltage of a modified PV panel is 18.85 V, while for the un-cooled PV panel is 17.39 V. The average increase in the voltage of a modified PV panel is 1.46 V against the referenced PV panel. The difference in the voltage of PV modules started from the experiment time when humidity was high and temperature relatively cool but as much. However, **Fig. 86 (b)** concludes that as the temperature rose and the humidity fell, the modified cooled PV panel's voltage was constantly maintained, while the referenced PV panel voltage dropped significantly. Meanwhile, **Fig. 86 (b)** also signifies the voltage reduction started when the highest temperature in the entire period of the experiment.

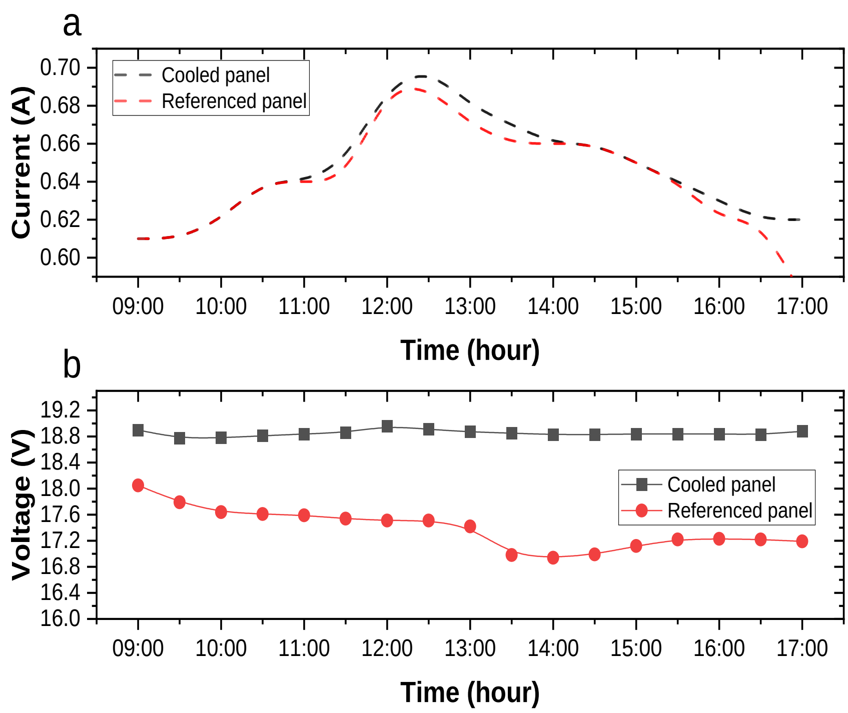

Figure 86 Current and Voltage for the PV panels

The power output achieved from modified and referenced PV panels is shown in **Fig. 87**. The highest power for a cooled PV against referenced PV panels is 13.24 W and 12.08 W, respectively, and the power recording time was 12:30 pm. The effect of power on the proposed cooling mechanism was observed throughout the day of the experiment. Thus, the power output for the cooling module at any time during the investigation was higher than the referenced module. The average power output of cooled PV panels is 12.19 W, against referenced PV panel is 11.14 W. This translates to the improvement in the output power for a modified PV panel is 9.43%. This progress level is expected since we employed only aluminum fins at the rear side of a PV panel, which saved the cost of water and other resources.

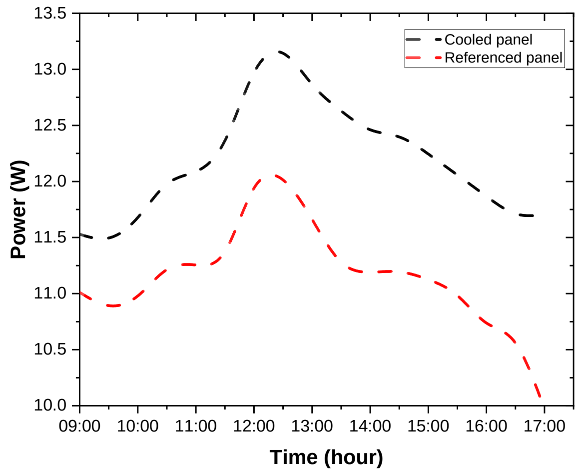

Figure 87 Variation of power on both the panels

5.1.8 Efficiencies of a PV panel

The efficiency of a cooled and uncooled PV panel is shown in **Fig. 88a**. The results obtained from the average cooled PV panel efficiency over un-cooled PV panel are 14% and 13%, respectively. The improvement in the efficiency shown in **Fig.88b**, obtained by **Eq. (30),** and the overall improvement in the modified PV panel is 4.%. The obtained power output and efficiency that compared already adopted a similar approach to cool the PV modules. For example, AlAmiri et al. [193] analytically designed and optimized the heat sink of a solar PV panel for the summer and winter seasons. Their study reveals that solar panel power raised and achieved around 8.7% and 6.5% during summer and winter. El Mays et al. [194] employed an aluminum finned plate to the rear side of a PV panel. The results showed that the electrical efficiency of a PV panel improved to 1.75%. Similarly, Kim et al.[195] proposed aluminum fins and metal mesh to improve electrical efficiency. Their study showed that a cooled PV module's efficiency increased to 1.44%. Sedaghat et al. [196] also theoretically proposed using aluminum pin fins. They obtained an improvement in the electrical efficiency of 1.24-4.16%. Furthermore, Hasan et al. [197] also presented copper cell foam fins. The outcome of progress in the efficiency of a PV panel is 4.9%. Hernandez-Perez [198] investigated the discontinuous heat sink numerically. They obtained an improvement in the efficiency by about 4%, similar to the present investigation experiment. To that effect, the comparison results covered supra; the current experiment showed improvement in efficiency and power output of the PV panel. Fig. 34 depicts the exergy efficiency of the tested for both the modified and referenced PV panel. The exergy efficiency of a solar PV panel reveals that solar radiation plays a significant role in the exergy analysis—the findings from **Fig. 89** show that the higher the solar radiation, the lower the exergy efficiency. The exergy of both PV modules was calculated using **Eq. (31-35)**. Thus, it is accounted for the continuous reduction in the exergy and thermal efficiencies for both panels until the intensity of the solar radiation starts reducing. The average exergy efficiency for a modified PV panel over a reference panel is 7.55% and 5.56%, respectively. The relatively low exergy efficiency recorded by the referenced module is due to the high cell temperatures recorded during the day—the highest exergy from the current investigation was achieved at 5:00 pm, i.e., 13.6% for the modified PV panel. In contrast, the highest exergy for the reference PV panel at 9:00 am morning, i.e., 11.6%.

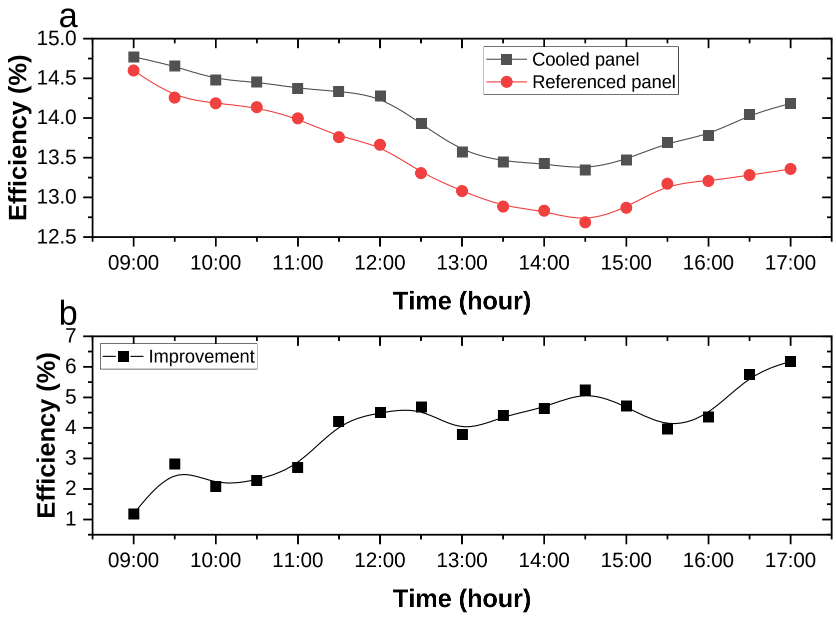

Figure 88 Efficiency variation and improvement in the PV panel

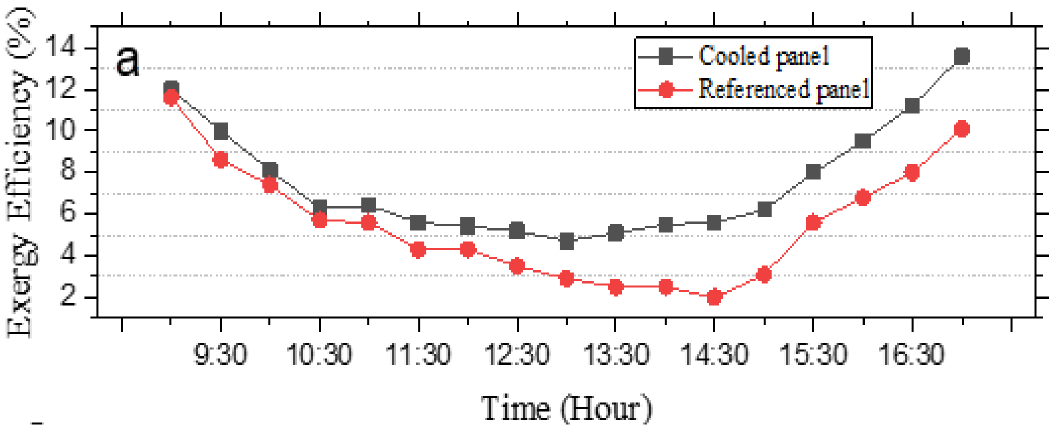

Figure 89 Exergy efficiency assessment on the PV panel

5.1.9 Entropy Analysis

Fig.90, depicts the entropy generation findings for both modified and unmodified PV panels. It has been recognized that the average entropy efficiency for a cooled PV panel is 9.73%, while the average entropy for the un-cooled PV panel is 6.73%. Furthermore, it is clear that as the relationship between exergy generation and entropy generation are reciprocal to each other. The peak entropies are hits for the cooled and un-cooled PV panels at noon, i.e., 15.60% and 12.30%, respectively.

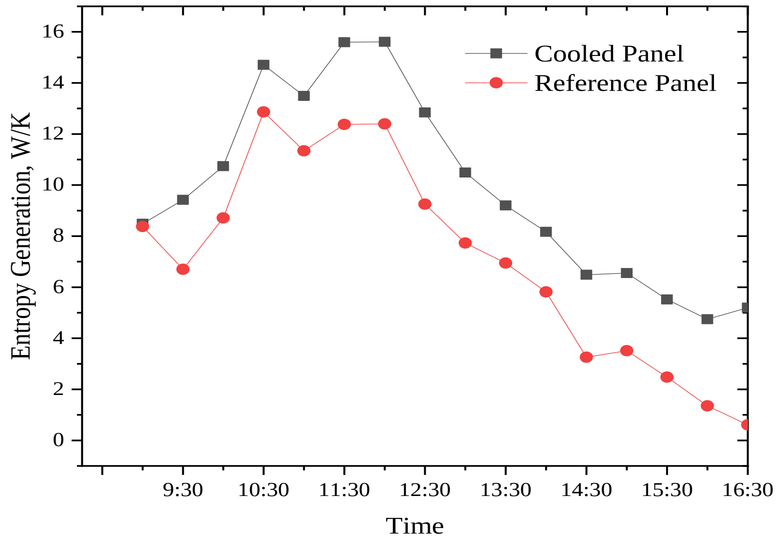

Figure 90 Entropy generation for cooled and un-cooled PV panel

The proposed study integrates brush-like fins at the rear end of a PV pane for heat dissipation along the edges is studies. The results from the present study compared with other form mechanisms that already available in the literature is presented in the **Table 36**.

Table 36 Comparison study with other literatures

Ref	Proposed study	Electrical Efficiency (%)		Avg. Temperature Panel (˚C)	
		Cooled PV panel	Referenced Panel	Cooled PV panel	Referenced Panel
[199]	Fins and planar reflector	11.2	9.81	39.73	64.3
[195]	Fins and metal mesh	14.39	13.24	47.65	62.78
[200]	Rectangular Fins	14.5	-	58	64
[194]	Al Fins	17.7	15.9	49.9	56

[201]	PCM heat sinks	9.82	9.33	51.8	57.9
[202]	Mounting Al fins	13.43	11.09	63.5	71
[203]	Spraying cooling mechanism	13.27	11.8	49	61
[204]	Water spray	15.92	13.92	24.1	56
[205]	Cotton Wick	10.4	9	45	65
[206]	Capillary action with burlap	9	14.75	49.3	66.4
Present Study		9.43% improvement		51.09	41.09

5.1.10 Cost analysis

Table 37 illustrates the achieved economic analysis using the Levelized cost of energy (LCE) approach using **Eq (16-21).** However, the present work is done in Russia. Hence, the LCEs are calculated in two stages. With the poor solar insulation in Russia, particularly from September to April, we assumed the solar PV panels actively work from May to August for a year, i.e., 120 days. On the other hand, we took the entire year, for hot climatic conditions are 365 days. Moreover, we also assumed that solar radiation is available for 12hrs in a day at both stages. The energy generated for 120 days per year for the modified PV panel is 17.556 kWh, and for the reference panel is 16.042 kWh. Furthermore, the total power generated for 365 days per year for the cooled PV panel is 53.31 kWh, and the un-cooled PV panel is 48.793 kWh—the data provided in Table 3. LCOE for both PV panels. The cost of an aluminum sheet is 640 Rubles, but we used one-third of the total aluminum sheet, which translates to $ 2.88; this adds to the total investment cost. A $ 60 was assumed for the purchase and installation cost of a 30W PV panel. In the present study, the cost of fuel is taken to zero. The results show that the modified PV panel that is incurred an additional investment cost due to the incorporation of thermal heat sinks still recorded lower LCOE for both the stages, i.e., 0.13-0.42 $/kWh for the modified cooled PV panel, while for the un-cooled PV panel us 0.14-0.45$/kWh.

Table 37 Economic parameters used to calculate LCOE

Parameter	Cooled PV	Referenced PV	Reference
Nominal escalation rate (r_n), %	1.00	1.00	[207]
Effective discount rate (i_{eff}), %	5.00	5.00	[207]
$K_{O\&M}$, %	0.96	0.96	Calculated
Capital recover factor (CRF),	0.065	0.065	Calculated
Constant-escalation levelization factor O&M, (CELF)	1.10	1.10	Calculated
Annual operation and maintenance cost ($\boldsymbol{C_{O\&M}}$), $	3.00	3.00	Calculated
Investment cost ($\boldsymbol{C_{inv}}$), $	62.88	60.00	Calculated
Life time of plant	30 yr	30 yr	Calculated

5.2 Solar PV modules coupled with low-cost aluminum reflectors and integrated with PCM using natural air convection: An experimental investigation

The present study signifies to enhance the performance of a Pv modules by coupling a aluminium reflectorы to one of the modified PV panels with an integration of PCM/ZnO nano particle at the rear end of the PV panels. In the present experimental investigation, a three identical PV panels each of 50 W were used namely, a conventional PV panel (un-cooled or referenced PV panel), a PV panel by integration with PCM/ZnO nanoparticle (PV/PCM), and PV panel coupling with two aluminium reflectors to one of the modified PV panel by integrating suspended PCM/ZnO (reflector/PCM/nanoparticles) on the rear end of the PV panel.

5.2.1 Construction of experimental setup

The experimental work setup is constructed in the department of REs laboratory at Ural Federal University, Russia. The setup is constructed in several stages in the first stage we constructed eight PCM containers and eight Aluminium zig-zag shaped heat sinks were constructed in the laboratory. The PCM containers with each size of 35 mm×30 mm×30 mm, and the sizes of zig zag shape heat sinks are 50 mm × 30 mm×30 mm. A 4 kg of solid paraffin wax was melted under room temperatures on the electrical stove, on that 1% ZnO nanoparticles has been suspended as shown in **Fig.91a**. The mixed ZnO nanoparticle with paraffin is poured in the eight aluminium containers and dried for four hours in a room temperature as shown in **Fig.91b**. For the purpose of experimental investigation, a three identical PV panels each of 50W were chosen for the study viz., PV modules without any modifications named as un-cooled PV panel, PV integrated with PCM/ZnO nanoparticles, named as (PV/PCM) and PV coupled aluminium reflector with suspended with PCM/ZnO nanoparticles (reflected/PCM/nanoparticles). One of the modified PV panels is selected and aluminium reflectors are coupled to one of the modified PV modules at an angle of 120° as shown in **Fig.91C**. The aluminum reflector is having similar dimensions of the PV panel of (670 mm×550 mm×25 mm). Moreover, the three PV panels are well cleaned, on the rear side of a PV panel five K-type of thermocouples were fixed at several calculations to record the temperature distribution of the PV panel. The thermocouples fixed at the each of PV module is fixed using silicone gel, as shown in **Fig.91d**. Further, to achieve higher dissipation rates, four zig-zag aluminium heat sinks were attached at the back surface of the PV module using universal silicone gel, as shown in **Fig.91e**. Finally, aluminium PCM/ZnO containers were fixed at the back surface of the PV panel as shown in **Fig.91F**. **Table 38** depicts the characteristics of the PV panels used for the present experimental investigation.

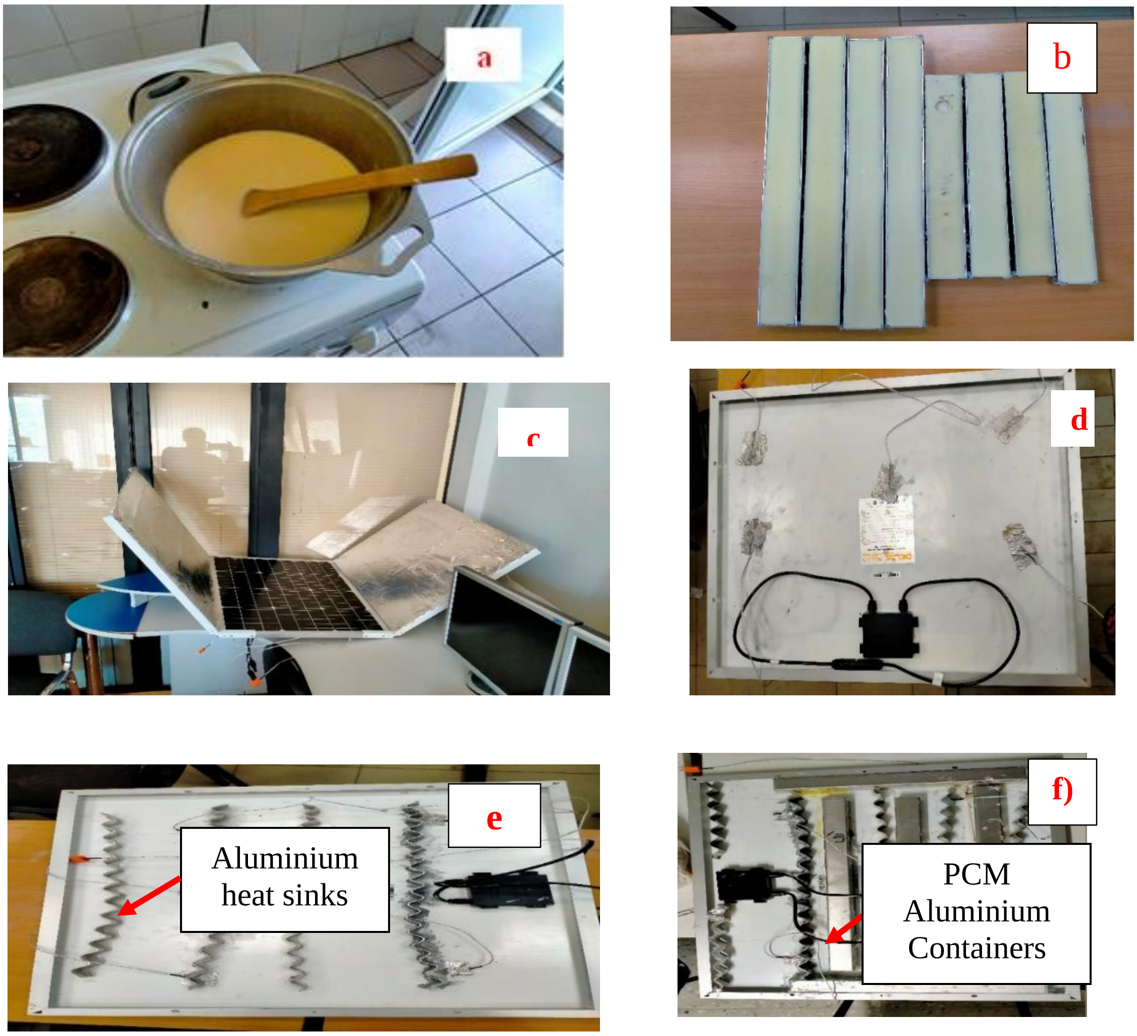

Figure 91 Construction of experimental test rig: a) preparation of PCM/ZnO mixture, b) PCM filled in aluminium container, c) aluminium reflectors coupled to PV panels, d) K-type thermocouples attached to PV modules, e) aluminium heat sinks fixed to back surface of PV module, and f) aluminium container with PCM fixed to back side of PV aluminium

Table 38. Characteristics of the PV panel

S. No		Parameter	Value	Units
1	Mechanical characteristics	Module dimensions	670×550×25	mm
2		Weight	4.4	kg
3		Cable length	600	mm
4		Number of diodes	2	-
5	Electric Parameters	Electric power	50	W
6		Tolerance	+3	%
7		Nominal voltage	12	V
8		Voltage at maximum power point	18.05	V
9		Current at maximum power point	2.77	A
10		Fill Factor	0.71	%
11		Short-circuit current	3.1	A
12		Open-circuit voltage	22.5	V
13		Cell efficiency	19	%
14		Module efficiency	13.5	%

5.2.2 Experimental setup

The setup has three PV configuration i.e., PV panel without any modifications (front), PV incorporated with PCM/ZnO nanoparticles (PV/PCM, back right), and PV coupled with aluminium reflectors/PCM/ZnO nanoparticles (reflectors/PCM/nanoparticles, back left). The experimental test rig is shown in **Fig.92** and also schematic of the front and rear surfaces of the modified PV configuration is shown in **Fig.93**. The three PV configuration were mounted on a wooden stand on true south. Finally, in order to measure the performance of three PV configurations various sensors were used in the study.

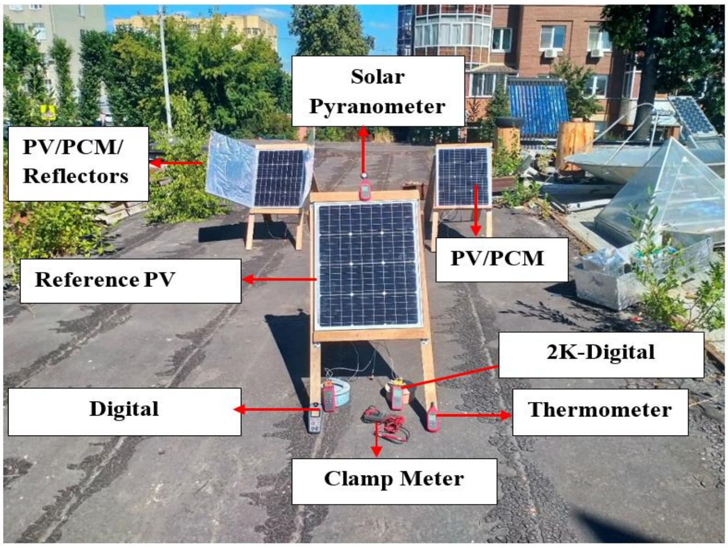

Figure 92 Experimental test rig

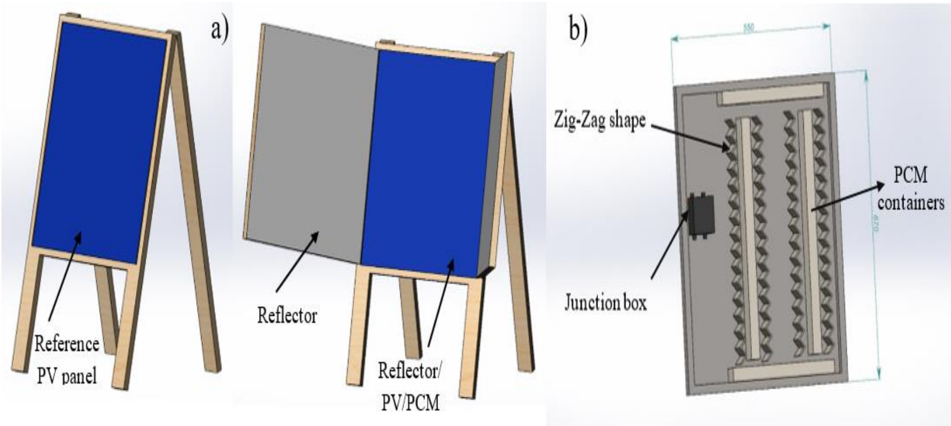

Figure 93 Schematic diagram a) Front surfaces reference and modified PV panels, b) back surface of modified PV panel

5.2.3 Weather characteristics

The performance of weather characteristics recorded during the period of the experiment day is depicted in **Fig.94**. It is evident from the **Fig.94a**. that the solar insulation values starts increasing from 404 W/m^2 at 8:00 am and reaches a maximum values of 1292 W/m^2 at 12:30 pm on the first day half day of the experimental day. It is then gradually starts decreases and reaches minimum solar radiation value of 560 W/m^2. The findings also revealed in that the average solar radiation value during the experimental day is about 866 W/m^2. The recorder relative humidity values progressively decreased from morning to the end day of the experimental day, an average relative humidity is recorded on the day of the experiment day is 31.91%.

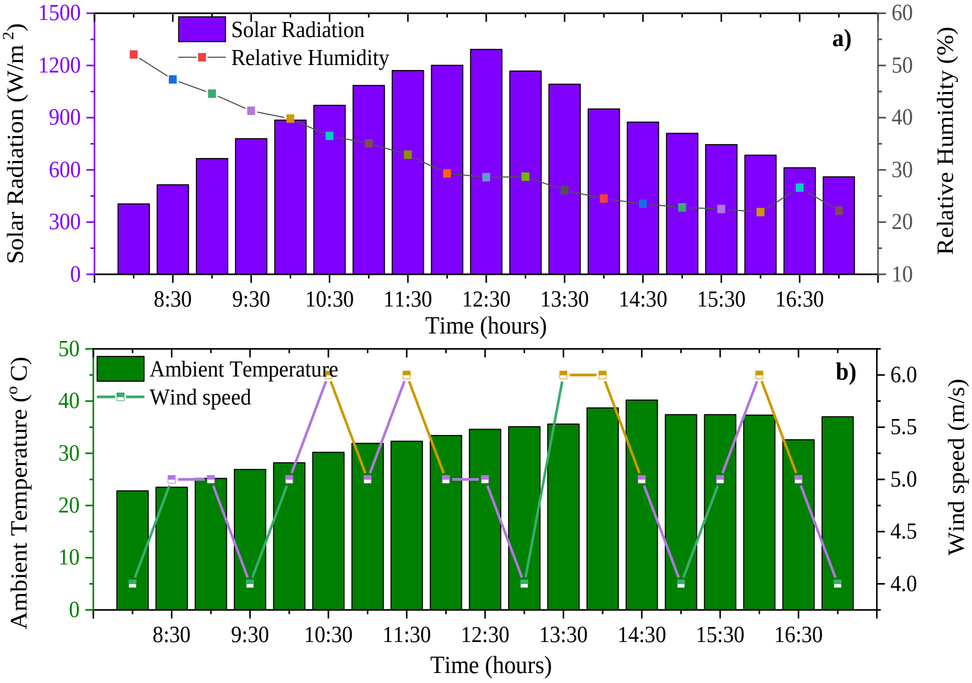

Figure 94 Time dependence: a) Solar heat flux and relative humidity; b) Ambient temperature & wind speed

Furthermore, the recorded values of the ambient temperature and wind speed is on the experimental is depicted in **Fig.94b**. The findings revealed that the ambient temperature started increasing gradually and hits a maximum 14:30 afternoon, with an average value of 32.46 °C during the experimental day. Finally, the average wind speed during the day of the experiment is achieved around 5 m/s.

5.2.4 Temperature variations

The temperature of the experimental study for the three PV configurations is depicted in **Fig.95**. For recording the temperature distribution on the surface of a PV panel, since a total of five k-type thermocouples are installed at different locations are attached, and a data logger is used to record the temperature of three PV modules for every 30 minutes. From the findings, **Fig.95a** the temperature variation among three PV configurations, and it can be observed that PV/PCM and reflector/PCM/nanoparticles experienced the lowest temperature relatively the whole day when compared with the referenced PV panels, which means that an effective cooling has been achieved for PV/PCM, and reflector/PCM/nanoparticles configurations. From the recorded the average temperature for the referenced PV panel, PV/PCM, and reflector/PCM/nanoparticles during the experimental day is 50.29 °C, 41.95 °C, and 36.04 °C, respectively.

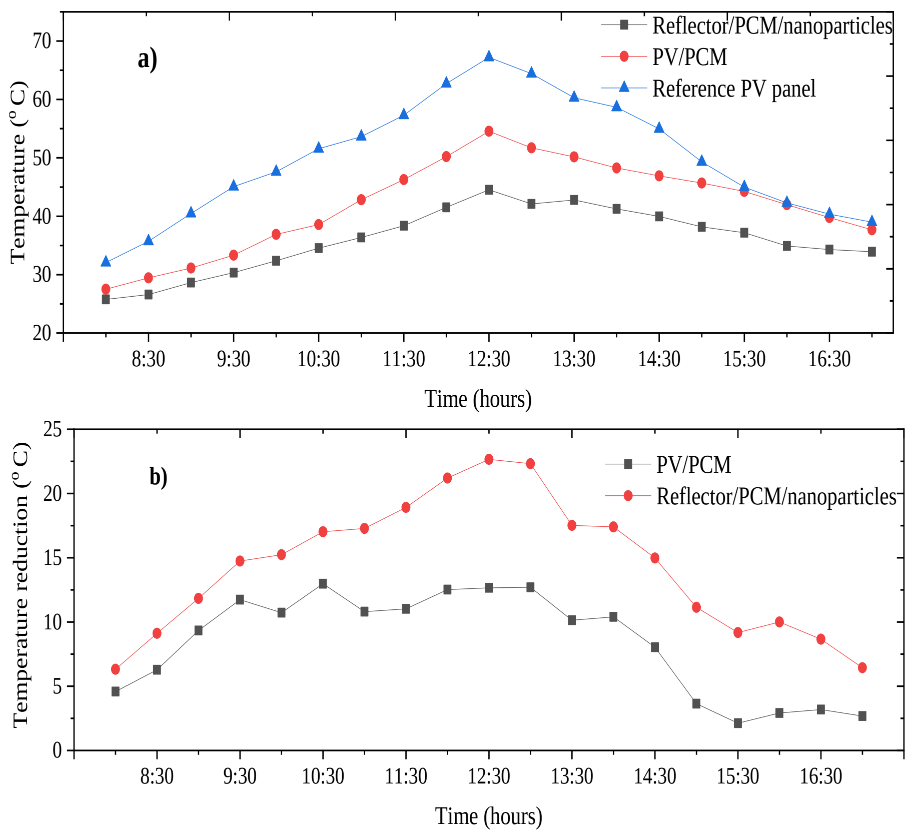

Figure 95 Time dependence: a) Temperature profile, b) Temperature reduction

The results of the reduction as shown in the temperature profile of the PV/PCM and reflector/PCM/nanoparticles is also depicted in **Fig. 95b**, has been achieved due to the positive impact of the addition of the reflector and the nanoparticles against that of the other two configurations. The findings also revealed, that the average temperature reduction for the PV/PCM and reflector/PCM/nanoparticles are 8.34 °C and 14.25 °C, which means leading to reduction of 16.5% and 28.3%, respectively, compared to that of referenced PV panel.

5.2.5 Electrical efficiency and improvement

The electrical performance of three PV configurations is depicted in **Fig.96**. It can be observed, the temperature profile of three PV panels negatively affected the electrical performance of three PV configurations. The findings from **Fig.96a** revealed, that the electrical efficiency of reflector/PCM/nanoparticles and PV/PCM improved more than of the referenced PV panels. The findings of the average electricity of three configuration i.e., referenced PV panel, PV/PCM, and reflector/PCM/nanoparticles over the day of the experiment was recorded to be 11.09 %, 12.49 %, and 12.84 %, respectively. The improvement of PV/PCM and reflector/PCM/nanoparticles are as depicted in **Fig.96b**. Each PV panel's average improvement in electrical efficiency is about 4.17 % and 7.18 %, respectively, while compared to uncooled PV panel.

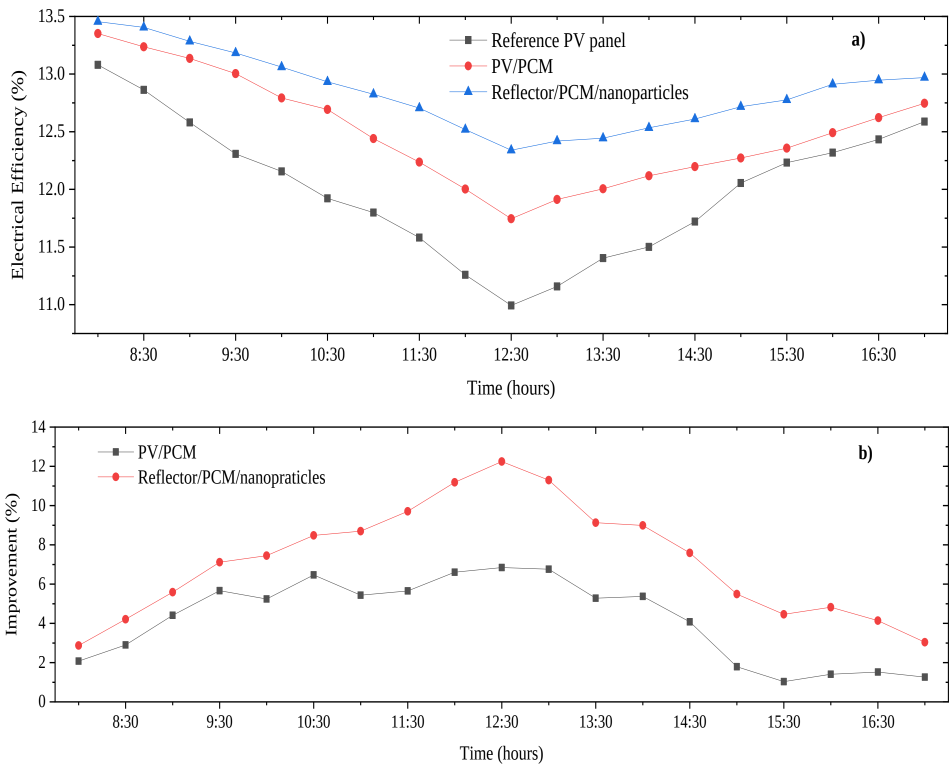

Figure 96 Time dependence: a) Electrical efficiency b) Improvement in electrical efficiency

5.2.6 Electrical Performance of PV configurations

The electrical performance of three PV configuration is recorded using clamp meter, and the results are presented in the. It has been clearly noted that the electrical performance of three PV configurations has been increased from the start day of the experiment hits maximum at 12:30, significantly start decreasing on the second day of the experiment. The findings also, observed that the recorded temperature of the reference PV panel strongly influenced it electrical output compared to that of the PV/PCM and reflectors/PCM/nanoparticles. **Fig.97** depicts the electrical performance of three PV configurations viz., referenced PV panel, PV/PCM, reflector/PV/PCM nanoparticles. The recorded data found the average electrical power out of a three PV configuration are 32.8 W, 36.91 W, and 39.03 W, respectively. Hence, the recorded average power improved for PV/PCM and reflector/PCM/nanoparticles are improved by 12.18 % and 18.61 %, respectively, against the referenced PV panel. Finally, the electrical performance output for the proposed cooling PV system (reflector/PCM/nanoparticles) showed better performance compared to the PV/PCM and referenced PV panel. **Table 39** depicts the comparison with other published literature works.

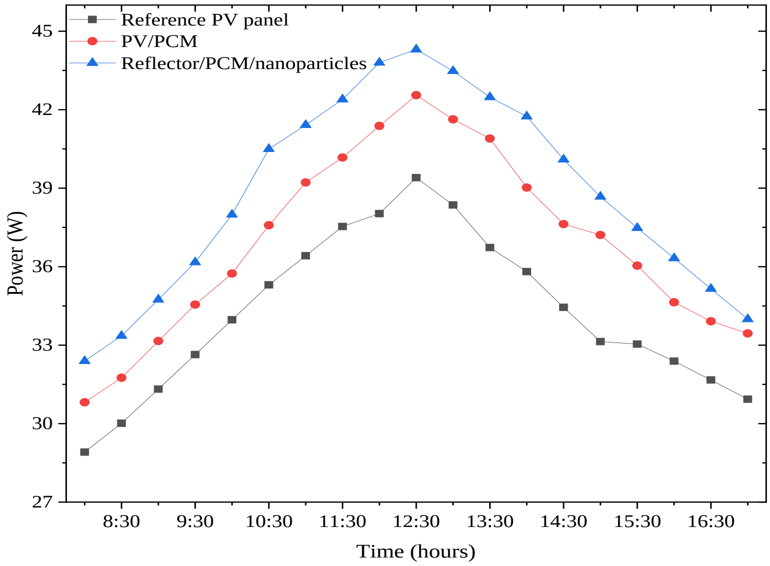

Figure 97 Time dependence electrical performance

Table 39 Comparison with other literature works

Ref. No	Type of cooling	Location	Key findings
[208]	Passive cooling	Sochi, Voronezh and Arkhangelsk/ Russia	1. The average heat flow rate of PV panel in January is achieved 36.3 W/m^2. 2. The EPBT is achieved in 9.5 years. 3.Experimental and numerical investigation showed good agreements.

[209]	Active and Passive cooling	Tehran/Iran	1. Temperature reduction around 3.6-4.3 °C. 2. Average increase in power output 5.9-7.2 W. 3. Electrical efficiency improved 11-11.5%.
[148]	Active and Passive cooling	Lhasa, China	1. Electrical efficiency improved 6.98%. 2. Thermal efficiencies improved about 58.35-69.84%. 3. Temperature reduction is 15.84 °C.
[210]	Active and Passive cooling	Malaysia	1.Experimental and numerical investigation for the study 2.Temperature reduction about 8.1-12.8 °C Electrical efficiency improved by 4.8-7.6 %.
[211]	Hybrid active cooling	Hull/United Kingdom	1.Reduction in temperature about 6 °C 2. Power improved by 3.92 W.
[212]	Hybrid active cooling	Kermanshah, Iran	1.Temperature reduction in 3.9 °C. 2. Productivity, energy and exergy efficiencies are about 81%, 80.6% and 112.5%, respectively.
[213]	Passive cooling and active	Iran	1.Temperature reduction in 1.2 -5.1 °C. 2.Power consumption for cooling about 16.8 W.
[214]	Passive cooling	Harbin/China	1.Temperature drop about 14 °C. 2. Average total cooling capacity from May to August 8792W. 3.Coefficient of performance is achieved 27.2 %.
[215]	Passive cooling	Pakistan	1. Copper foam with porosity 0.95 and 0.97 is investigated. 2.Temperature reduced by 9.81 %.
[216]	Passive cooling	Bristol/United Kingdom	1.Temperature reduced by 10 °C. 2.Efficiency increased to 7 %.
Present Study	Passive cooling	Yekaterinburg/Russian Federation	1.Reduction in temperature 14.25 °C. 2. Electrical efficiency is improved by 7.18%. 3. Power output of reflector/PCM panel is improved to 18 %.

5.2.7 Exergy efficiency

The results of exergy efficiency of the PV/PCM and reflector/PCM/nanoparticles is much higher than the exergy efficiency achieved from the referenced PV panel. The results are due to low temperature that effected the performance of PV panel. The results observed, that the exergy efficiency decreases from the morning and reaches minimum at 12:30, and starts gradually increases from the mid-day the behaviour of exergy is efficiency follows the opposite trend of the solar radiation. The values of recorded exergy efficiency for PV/PCM and reflector/PCM/nanoparticles are 13.30 %, and 14.60 %, respectively, against the un-cooled PV panel recorded for 12.35 % and leading an improvement of 7.6 % (PV/PCM), and 12.9 % (reflector/PCM/nanoparticles).

5.2.8 Entropy generation

The entropy generation of three PV configuration i.e., referenced PV panel, PV/PCM, and reflector/PCM/nanoparticles. The entropy generation of from the calculations of average entropy generation for the uncooled PV panel was 8.19 W/K, compared to 8.12 W/K for the PV/PCM configuration and 8.08 W/K for the reflector/PCM/nanoparticles configuration. Hence, the results signify that the entropy generation for three PV configuration is almost same on the experimental day.

5.2.9 Economic analysis

The materials used for the present experimental investigation is purchased in Russian Rubbles (RUR) from local energy markets and translated immediately into the American Dollars (USD). The estimated cost associated with each material in the construction is presented in **Table 40**. In the present study, for the calculation of economic analysis two scenarios were considered in the economic analysis, i.e., 365 days where is there is availability of solar radiation, and 105 days for Russian climatic which experience solar radiation only in May, June, July and mid of August. In the present study, a 4 kg of PCM is employed, solar radiation in both scenarios is assumed to be 12 hours, life time of a PV panels is 25 years

Table 40 Cost estimation of PV panels

Items	Reference PV panel	PV/PCM ($)	Reflector/PCM/nanoparticles ($)
PV panels	45	45	45
K-Type thermocouples	3.5	3.5	3.5
Silicone gel	1.5	1.5	1.5
PCM	-	3.5	3.5
Aluminium sink	-	4.5	4.5
Aluminium reflectors	-	-	1.5
ZnO nano particles (1%)		1.5	1.5
Total investment	50	60	61

Table 41 highlights the economic performance of three PV configurations. It can be seen that in the first scenario i.e.,365 days the economic analysis for the referenced PV panel, PV/PCM, and reflector/PCM/nanoparticles are 0.4 $/kWh, 0.38 $/kWh, and 0.393 $/kWh, respectively. Similarly, the economic analysis for 105 days for the for the referenced PV panel, PV/PCM, and reflector/PCM/nanoparticles are 0.149 $/kWh, 0.146 $/kWh, and 0.139 $/kWh, respectively. The findings revealed that the economic analysis of reflector/PCM/nanoparticles is achieved almost less LCOE for the present study. Therefore, the present study signifies that the economically also viable for the construction of PV panels.

Table 41 Economic analysis calculations

Parameters		Reference PV panel	PV/PCM ($)	Reflector/PCM/nanoparticles ($)	Reference
Effective discount rate (i_{eff}), %		5	5	5	[217]
Nominal escalation rate (r_n), %		1	1	1	[156]
$K_{O\&M}$		0.96	0.96	0.96	Calculated
Life time of solar PV plant, (n)		25	25	25	Manufacturer recommendations
Capital recovery factor (CRF)		0.07	0.07	0.07	Calculated
Constant escalation levelized factor O&M, (CELF), %		1.08	1.08	1.08	
Annual operation and maintenance cost ($C_{O\&M}$), $		2.5	2.5	2.5	Assumed
$LC_{O\&M}$, $		2.7	2.7	2.7	Calculated
C_{inv}, $		50	60	61	
LC_{inv}, $		3.5	4.2	4.27	
Levelized cost of fuel (LC fuel), $/kWh		0	0	0	-
Available of solar radiation (hours)		12	12	12	Assumed
P_{out} (W)		32.89	36.89	39.03	Calculated
For 365 Days	P_{annual} (kWh) for 365 days	144.05	161.57	170.95	
	LCE for 365 days ($/kWh)	0.043	0.042	0.039	
For 105 Days	P_{annual} (kWh) for 105 days	41.49	46.48	49.17	
	LCE for 105 days ($/kWh)	0.149	0.146	0.139	

5.3 Conclusions from the experimental study

The present section evaluates the cooling approach by using passive cooling (natural air convection) methods such as aluminium "brush-shaped" heats sinks, and low-cost aluminium reflectors/PCM/ZnO nanoparticles. The following conclusions can be drawn as:

1) The **first passive cooling** approach using dis-continuous aluminium heat sinks with brush-shapes. The reduction in the temperature for the cooled PV panel 41.09 °C, against for the un-cooled PV panels are 51.09 °C. The reduction in the temperature for the proposed cooling approach is 10 °C.
2) The average electrical efficiency for the cooled PV module is 14 %, while for the uno-cooled PV module is 13 %, leading to an improvement in the average electrical efficiency is 4 %.
3) The average electrical performance of the cooled PV module for the proposed cooling approach is 12.19 W, and for the un-cooled PV module is 11.14 W, leading an improvement for the electrical performance is 9.43 %.
4) The average exergy efficiency for the cooled PV module is 7.55 %, against for the un-cooled PV module is 5.56 %. The difference in the average exergy efficiency for the proposed passive cooling approach is 1.99 %, leading an improvement in the average exergy efficiency is 35.9 %.
5) The economic analysis for the cooled PV module is 0.42 $/kWh, while for the un-cooled PV module is 0.45 $/kWh.
6) The **second passive cooling** approach using low-cost aluminium reflectors with integration of PCM and suspended with 1 % ZnO nanoparticles. In the present study, three PV configurations such as referenced PV panel, PV panel integrated with PCM/ZnO nanoparticle, and PV integrated with aluminum reflectors/PCM/ZnO nanoparticles.
7) The recorded average temperatures for the referenced PV panel, PV panel with PCM, and reflectors/PCM/ZnO nanoparticles are 50.29 °C, 41.95 v, and 36.04 °C, respectively. The recorded average temperature for the proposed cooling system is 8.34 °C, and 14.25 °C, respectively, leading to reduction about 16.5 %, and 28.3 %, respectively against the uno-cooled PV panel
8) The average electrical efficiency for the three PV configurations i.e., referenced PV panel, PV/PCM, and PV/PCM/ZnO nanoparticles during the experimental period is 11.99 %, 12.49 %, and 12.64 %, respectively. The electrical efficiency improvement for

the cooled PV/PCM, and PV/PCM/ZnO nano particles are 4.17 %, and 7.18 %, respectively.

9) The electrical performance for the passive cooling method for the referenced PV panel, PV/PCM, and PV/PCM/ZnO nanoparticles are 32.8 W, 36.91 W, and 39.03 W, respectively, leading an improvement for the PV/PCM, and PV/PCM/ZnO nanoparticles are 12.18 %, and 18.61 %, respectively.

10) The average exergy efficiency for the reference PV panel, PV/PCM, and PV/PCM/ZnO nanoparticles are 12.35 %, 13.30 %, 14.06 %, respectively, leading an improvement in the exergy efficiency of PV/PCM, and for the PV/PCM/ZnO nanoparticles are 7.6 %, and 12.9 %, respectively.

11) Similarly, the entropy generation for the referenced PV panel, PV/PCM, and PV/PCM/ZnO nanoparticles are 8.19 W/K, 8.12 W/K, 8.08 W/K, respectively

12) The cost analysis for the proposed cooling system for the referenced PV panel. PV/PCM, and PV/PCM/ZnO nanoparticles are 0.039 $/kWh to 0.149 $/kWh depends upon the number of days of the operation of the PV plant.

General Conclusion

The present works offers the strengthening the position of the Republic of India in the field of renewable energy sector.

The results obtained from the theoretical and experimental investigations; the following conclusions can be drawn:

1) The results of the techno-economic assessment for the potential of solar energy are as follows:

- The results of the solar PV power plant with the capacity of 20 MW using fixed tracking (FT), single axis tracking (SAT), and double axis tracking (DAT) for the south Indian sates of India are 33 GWh, 40 GWh, and 44 GWh, respectively. The DAT mechanism generated maximum energy, and the LCOE (real) minimized for the DAT mechanism is about 3 cents/kWh to 3.5 cents/kWh.
- The thermodynamic cycle of solar tower power plant (STPP) using wet-cooled model and dry-cooled model for the six potential sites of Republic of India. The techno-economic results showed that the wet-cooled STPP model is feasible for the six potentials. Although, the Bhopal site is more potential site. The LCOE (real) of the STPP for the wet-cooled model is minimized from 11.88 cents/kWh to 14.09 cents/kWh.
- The techno-economic assessment for the production of solar PV/hydrogen hybrid system for the five potential locations is feasible for the generation of electrical charging mobile and the production. Moreover, the LCOE (real) is also reduced, and the production of hydrogen is also improved.

2) The active cooling method using fanless heat pipe of PV modules in the hot weather climatic conditions can be reduced about 6.07 °C. The decrease in the temperature of the solar led to an overall in the electrical efficiency is about 11.9 %.

3) The active cooling modified PV panel with combination of TEC/TEGs are incorporated at the back side of the PV panel, resulted reduction in temperature 12.23 °C. The resulted decrease in the temperature of the PV module leads to increase in the efficiency is about 6.05 %.

4) Modified PV panel with active cooling approach incorporated with u-shaped grid copper pipe/TEGs/Al_2O_3 nanoparticles reduction in the temperature about 16.5 °C, leading an improvement in the efficiency is about 8.5 %.

5) The passive cooling method using discontinuous aluminium heats sinks for the cooled PV module is reduction in temperature about 10 °C, leading an improvement in the electrical efficiency is about 4%.

6) The second passive cooling approach reflectors/PV-PCM/ZnO nanoparticles is leading to reduction in the temperature of 14.25 °C, leading to the reductio of the efficiency of 28.3%. The average electrical efficiency for the cooled efficiency is improved by 7.18 %.

Recommendation for the use of research materials:

According to the state of research India's is setting to install a 100 % of REs by the 2070, the following recommendations mix by electricity is given below:

- The identified territorial sites in the present study for the production of solar PV plant and thermodynamic cycles should be promoted for the country's potential energy by the local and foreign investors.
- The methods implemented for the production of hydrogen solar PV plants is strictly implemented in the country premises and also union territory of the country.
- Developing countries like India, has major potential barriers such as political barriers, social barriers, financial barriers, infrastructural barriers, technological barriers, and policy barriers should be minimized by implementing policies such as "Niti-Aayog" policy, and "Atmanirbhar Bharat" policy must be implemented [216].
- Finally, the Central government of India need to provide "Special status" to the states of India. Thus, this "special status" can lead to attract the investors, policy makers for the future development of India.

References

1. Agyekum E.B. et al. A bird's eye view of Ghana's renewable energy sector environment: A Multi-Criteria Decision-Making approach // Utilities Policy. 2021. Vol. 70. P. 101219.
2. Al-Amri F. et al. Innovative technique for achieving uniform temperatures across solar panels using heat pipes and liquid immersion cooling in the harsh climate in the Kingdom of Saudi Arabia // Alexandria Engineering Journal. 2022. Vol. 61, № 2. P. 1413–1424.
3. • Renewable energy capacity worldwide by country 2021 | Statista [Electronic resource]. URL: https://www.statista.com/statistics/267233/renewable-energy-capacity-worldwide-by-country/ (accessed: 29.05.2022).
4. The Fastest Growing Economies in the World (2019-2023) [Electronic resource]. URL: https://www.focus-economics.com/blog/fastest-growing-economies-in-the-world (accessed: 29.05.2022).
5. Energy in India today – India Energy Outlook 2021 – Analysis - IEA [Electronic resource]. URL: https://www.iea.org/reports/india-energy-outlook-2021/energy-in-india-today (accessed: 29.05.2022).
6. Profiling the five largest solar power plants in India - NS Energy [Electronic resource]. URL: https://www.nsenergybusiness.com/features/largest-solar-power-plants-india/ (accessed: 29.05.2022).
7. Profiling the top five wind power farms operating in India [Electronic resource]. URL: https://www.nsenergybusiness.com/features/top-wind-power-farms-india/ (accessed: 29.05.2022).
8. The five biggest hydroelectric power plants in India [Electronic resource]. URL: https://www.nsenergybusiness.com/features/hydroelectric-power-plants-india/ (accessed: 29.05.2022).
9. Sharmila N. et al. Wave powered desalination system // Energy. 2004. Vol. 29, № 11. P. 1659–1672.
10. Kumar A. et al. Renewable energy in India: Current status and future potentials // Renewable and Sustainable Energy Reviews. 2010. Vol. 14, № 8. P. 2434–2442.
11. Tariff Policy 2006 – Policies [Electronic resource] // IEA. URL: https://www.iea.org/policies/4731-tariff-policy-2006 (accessed: 13.06.2022).
12. Podcast | Does hybrid energy policy make sense for India? Find out. [Electronic resource]. URL: https://www.moneycontrol.com/news/business/economy/podcast-does-hybrid-energy-policy-make-sense-for-india-find-out-2573439.html (accessed: 14.06.2022).

13. Offshore Wind | Ministry of New and Renewable Energy, Government of India [Electronic resource]. URL: https://mnre.gov.in/wind/offshore-wind/ (accessed: 14.06.2022).

14. Govt plans push for hydro power | Business Standard News [Electronic resource]. URL: https://www.business-standard.com/article/economy-policy/govt-plans-push-for-hydro-power-116041100037_1.html (accessed: 14.06.2022).

15. India’s tidal power potential hampered by high costs and environmental risks [Electronic resource] // Mongabay-India. 2021. URL: https://india.mongabay.com/2021/08/indias-tidal-power-potential-hampered-by-high-costs-and-environmental-risks/ (accessed: 15.06.2022).

16. Ghosh U. et al. Biomass Energy Potential in India: A Review // International Journal of Engineering Research & Technology. IJERT-International Journal of Engineering Research & Technology, 2021. Vol. 9, № 11.

17. Kumar A. et al. A review on biomass energy resources, potential, conversion and policy in India // Renewable and Sustainable Energy Reviews. 2015. Vol. 45. P. 530–539.

18. Preet S., Bhushan B., Mahajan T. Experimental investigation of water based photovoltaic/thermal (PV/T) system with and without phase change material (PCM) // Solar Energy. 2017. Vol. 155. P. 1104–1120.

19. Abdallah A. et al. Experimental investigation of thermal management techniques for improving the efficiencies and levelized cost of energy of solar PV modules // Case Studies in Thermal Engineering. 2022. Vol. 35. P. 102133.

20. Nisar H. et al. Thermal and electrical performance of solar floating PV system compared to on-ground PV system-an experimental investigation // Solar Energy. 2022. Vol. 241. P. 231–247.

21. B R., Ck S., Sudhakar K. Sustainable passive cooling strategy for PV module: A comparative analysis // Case Studies in Thermal Engineering. 2021. Vol. 27. P. 101317.

22. Raina G. et al. Assessment of photovoltaic power generation using fin augmented passive cooling technique for different climates // Sustainable Energy Technologies and Assessments. 2022. Vol. 52. P. 102095.

23. Kabeel A.E. et al. Improvement of thermal performance of the finned plate solar air heater by using latent heat thermal storage // Applied Thermal Engineering. 2017. Vol. 123. P. 546–553.

24. Browne M.C. et al. Indoor Characterisation of a Photovoltaic/ Thermal Phase Change Material System // Energy Procedia. 2015. Vol. 70. P. 163–171.

25. Agyekum E.B. et al. Effect of dual surface cooling of solar photovoltaic panel on the efficiency of the module: experimental investigation // Heliyon. 2021. Vol. 7, № 9. P. e07920.
26. Agyekum E.B. et al. Experimental Study on Performance Enhancement of a Photovoltaic Module Using a Combination of Phase Change Material and Aluminum Fins—Exergy, Energy and Economic (3E) Analysis: 4 // Inventions. Multidisciplinary Digital Publishing Institute, 2021. Vol. 6, № 4. P. 69.
27. Agyekum E.B. et al. Experimental Investigation of the Effect of a Combination of Active and Passive Cooling Mechanism on the Thermal Characteristics and Efficiency of Solar PV Module: 4 // Inventions. Multidisciplinary Digital Publishing Institute, 2021. Vol. 6, № 4. P. 63.
28. Al-Waeli A.H.A. et al. Comparison of prediction methods of PV/T nanofluid and nano-PCM system using a measured dataset and artificial neural network // Solar Energy. 2018. Vol. 162. P. 378–396.
29. Zubeer S.A., Ali O.M. Performance analysis and electrical production of photovoltaic modules using active cooling system and reflectors // Ain Shams Engineering Journal. 2021. Vol. 12, № 2. P. 2009–2016.
30. Lebbi M. et al. Energy performance improvement of a new hybrid PV/T Bi-fluid system using active cooling and self-cleaning: Experimental study // Applied Thermal Engineering. 2021. Vol. 182. P. 116033.
31. Murali S. et al. Performance evaluation of PV powered solar tunnel dryer integrated with a mobile alert system for shrimp drying // Solar Energy. 2022. Vol. 240. P. 246–257.
32. Navakrishnan S. et al. An experimental study on simultaneous electricity and heat production from solar PV with thermal energy storage // Energy Conversion and Management. 2021. Vol. 245. P. 114614.
33. Gad R. et al. Energy, exergy, and economic assessment of thermal regulation of PV panel using hybrid heat pipe-phase change material cooling system // Journal of Cleaner Production. 2022. P. 132489.
34. Bevilacqua P. et al. A novel thermal model for PV panels with back surface spray cooling // Energy. 2022. P. 124401.
35. Elminshawy N.A.S. et al. The performance of a buried heat exchanger system for PV panel cooling under elevated air temperatures // Geothermics. 2019. Vol. 82. P. 7–15.

36. Dubey S., Sarvaiya J.N., Seshadri B. Temperature Dependent Photovoltaic (PV) Efficiency and Its Effect on PV Production in the World – A Review // Energy Procedia. 2013. Vol. 33. P. 311–321.
37. Skoplaki E., Palyvos J.A. On the temperature dependence of photovoltaic module electrical performance: A review of efficiency/power correlations // Solar Energy. 2009. Vol. 83, № 5. P. 614–624.
38. Arun K.R. et al. Influence of the location of discrete macro-encapsulated thermal energy storage on the performance of a double pass solar plate collector system // Renewable Energy. 2020. Vol. 146. P. 675–686.
39. Jeter S.M. Maximum conversion efficiency for the utilization of direct solar radiation // Solar Energy. 1981. Vol. 26, № 3. P. 231–236.
40. Zondag H.A. Flat-plate PV-Thermal collectors and systems: A review // Renewable and Sustainable Energy Reviews. 2008. Vol. 12, № 4. P. 891–959.
41. Ramkumar R. et al. Enhancing the performance of photovoltaic module using clay pot evaporative cooling water // 2016 International Conference on Energy Efficient Technologies for Sustainability (ICEETS). 2016. P. 217–222.
42. Notton G. et al. Modelling of a double-glass photovoltaic module using finite differences // Applied Thermal Engineering. 2005. Vol. 25, № 17. P. 2854–2877.
43. Evans D.L., Florschuetz L.W. Cost studies on terrestrial photovoltaic power systems with sunlight concentration // Solar Energy. 1977. Vol. 19, № 3. P. 255–262.
44. Madhankumar S., Viswanathan K., Wu W. Energy, exergy and environmental impact analysis on the novel indirect solar dryer with fins inserted phase change material // Renewable Energy. 2021. Vol. 176. P. 280–294.
45. Praveenkumar S. et al. Thermo-enviro-economic analysis of solar photovoltaic/thermal system incorporated with u-shaped grid copper pipe, thermal electric generators and nanofluids: An experimental investigation // Journal of Energy Storage. 2023. Vol. 60. P. 106611.
46. Mugi V.R., Chandramohan V.P. Energy, exergy, economic and environmental (4E) analysis of passive and active-modes indirect type solar dryers while drying guava slices // Sustainable Energy Technologies and Assessments. 2022. Vol. 52. P. 102250.
47. Bayrak F., Oztop H.F., Selimefendigil F. Experimental study for the application of different cooling techniques in photovoltaic (PV) panels // Energy Conversion and Management. 2020. Vol. 212. P. 112789.

48. Hepbasli A. A key review on exergetic analysis and assessment of renewable energy resources for a sustainable future // Renewable and Sustainable Energy Reviews. 2008. Vol. 12, № 3. P. 593–661.
49. Akyuz E. et al. A novel approach for estimation of photovoltaic exergy efficiency // Energy. 2012. Vol. 44, № 1. P. 1059–1066.
50. Bayrak F., Oztop H.F. Effects of static and dynamic shading on thermodynamic and electrical performance for photovoltaic panels // Applied Thermal Engineering. 2020. Vol. 169. P. 114900.
51. Chow T.T. et al. Energy and exergy analysis of photovoltaic–thermal collector with and without glass cover // Applied Energy. 2009. Vol. 86, № 3. P. 310–316.
52. Rezvanpour M. et al. Using CaCl2·6H2O as a phase change material for thermo-regulation and enhancing photovoltaic panels' conversion efficiency: Experimental study and TRNSYS validation // Renewable Energy. 2020. Vol. 146. P. 1907–1921.
53. Saffarian M.R., Moravej M., Doranehgard M.H. Heat transfer enhancement in a flat plate solar collector with different flow path shapes using nanofluid // Renewable Energy. 2020. Vol. 146. P. 2316–2329.
54. Sardarabadi M. et al. Experimental investigation of the effects of using metal-oxides/water nanofluids on a photovoltaic thermal system (PVT) from energy and exergy viewpoints // Energy. 2017. Vol. 138. P. 682–695.
55. Joshi A.S., Dincer I., Reddy B.V. Thermodynamic assessment of photovoltaic systems // Solar Energy. 2009. Vol. 83, № 8. P. 1139–1149.
56. Firoozzadeh M., Shiravi A.H., Chandel S.S. An experimental analysis of enhancing efficiency of photovoltaic modules using straight and zigzag fins // J Therm Anal Calorim. 2022.
57. Mahian O. et al. Entropy generation during Al2O3/water nanofluid flow in a solar collector: Effects of tube roughness, nanoparticle size, and different thermophysical models // International Journal of Heat and Mass Transfer. 2014. Vol. 78. P. 64–75.
58. Petela R. An approach to the exergy analysis of photosynthesis // Solar Energy. 2008. Vol. 82, № 4. P. 311–328.
59. Agyekum E.B. et al. Effect of Two Different Heat Transfer Fluids on the Performance of Solar Tower CSP by Comparing Recompression Supercritical CO2 and Rankine Power Cycles, China: 12 // Energies. Multidisciplinary Digital Publishing Institute, 2021. Vol. 14, № 12. P. 3426.

60. Montes M.J. et al. Performance analysis of an Integrated Solar Combined Cycle using Direct Steam Generation in parabolic trough collectors // Applied Energy. 2011. Vol. 88, № 9. P. 3228–3238.
61. Baloch A.A.B. et al. Experimental and numerical performance analysis of a converging channel heat exchanger for PV cooling // Energy Conversion and Management. 2015. Vol. 103. P. 14–27.
62. Chandrika V.S. et al. Experimental analysis of solar concrete collector for residential buildings // null. Taylor & Francis, 2021. Vol. 18, № 6. P. 615–623.
63. K S. et al. Performance and emission characteristics of diesel engine fueled with ternary blends of linseed and rubber seed oil biodiesel // Fuel. 2021. Vol. 285. P. 119255.
64. Karthick A., Murugavel K.K., Ramanan P. Performance enhancement of a building-integrated photovoltaic module using phase change material // Energy. 2018. Vol. 142. P. 803–812.
65. Agyekum E.B. et al. Experimental Investigation of the Effect of a Combination of Active and Passive Cooling Mechanism on the Thermal Characteristics and Efficiency of Solar PV Module // Inventions. 2021. Vol. 6, № 4. P. 63.
66. Alwan N.T. et al. Experimental Study of a Tilt Single Slope Solar Still Integrated with Aluminum Condensate Plate: 4 // Inventions. Multidisciplinary Digital Publishing Institute, 2021. Vol. 6, № 4. P. 77.
67. Hafez A.Z., Yousef A.M., Harag N.M. Solar tracking systems: Technologies and trackers drive types – A review // Renewable and Sustainable Energy Reviews. 2018. Vol. 91. P. 754–782.
68. Zhang J., Yin Z., Jin P. Error analysis and auto correction of hybrid solar tracking system using photo sensors and orientation algorithm // Energy. 2019. Vol. 182. P. 585–593.
69. Abdelghani-Idrissi M.A. et al. Solar tracker for enhancement of the thermal efficiency of solar water heating system // Renewable Energy. 2018. Vol. 119. P. 79–94.
70. Gerra D.D., Iakovleva E.V. Sun tracking system for photovoltaic batteries in climatic conditions of the Republic of Cuba // IOP Conf. Ser.: Mater. Sci. Eng. IOP Publishing, 2019. Vol. 643, № 1. P. 012155.
71. Hoffmann F.M. et al. Monthly profile analysis based on a two-axis solar tracker proposal for photovoltaic panels // Renewable Energy. 2018. Vol. 115. P. 750–759.
72. Batayneh W. et al. Investigation of a single-axis discrete solar tracking system for reduced actuations and maximum energy collection // Automation in Construction. 2019. Vol. 98. P. 102–109.

73. Agyekum E.B. Techno-economic comparative analysis of solar photovoltaic power systems with and without storage systems in three different climatic regions, Ghana // Sustainable Energy Technologies and Assessments. 2021. Vol. 43, № November 2020.
74. Our Team | EnergySage [Electronic resource]. URL: https://www.energysage.com/about-us/team/ (accessed: 14.03.2022).
75. Pillai G., Naser H.A.Y. Techno-economic potential of largescale photovoltaics in Bahrain // Sustainable Energy Technologies and Assessments. Elsevier, 2018. Vol. 27, № March. P. 40–45.
76. Jordan D.C., Kurtz S.R. Photovoltaic degradation rates - An Analytical Review // Progress in Photovoltaics: Research and Applications. 2013. Vol. 21, № 1. P. 12–29.
77. Hernández-Moro J., Martínez-Duart J.M. Analytical model for solar PV and CSP electricity costs: Present LCOE values and their future evolution // Renewable and Sustainable Energy Reviews. 2013. Vol. 20. P. 119–132.
78. Wang Q., Pei G., Yang H. Techno-economic assessment of performance-enhanced parabolic trough receiver in concentrated solar power plants // Renewable Energy. Elsevier Ltd, 2021. Vol. 167. P. 629–643.
79. Budget Inflation: India’s growth budget sparks concerns on inflation, tighter rates - The Economic Times [Electronic resource]. URL: https://economictimes.indiatimes.com/news/economy/policy/indias-growth-budget-sparks-concerns-on-inflation-tighter-rates/articleshow/89294664.cms?from=mdr (accessed: 07.03.2022).
80. India Inflation Rate 1960-2022 | MacroTrends [Electronic resource]. URL: https://www.macrotrends.net/countries/IND/india/inflation-rate-cpi (accessed: 07.03.2022).
81. OECD-IEA. Scenarios & Strategies To 2050 // Strategies. 2008.
82. Embargo U. - : Hstcqe = Uyvywy : // Strategies. 2008. № June.
83. Power C.S. Technology Roadmap Concentrating Solar Power // Current. 2010. Vol. 5. P. 1–52.
84. Income Tax Slab for FY 2022-23, FY 2021-22 | Revised Income Tax Slabs, New & Old Tax Rates in India [Electronic resource]. URL: https://cleartax.in/s/income-tax-slabs (accessed: 07.03.2022).
85. : Welcome to Commercial Taxes Department : . [Electronic resource]. URL: https://apct.gov.in/apportal/AllActs/APVAT/APVATSchedules.aspx (accessed: 07.03.2022).

86. Sales Tax Systems In India: A P rofile. 1956. P. 1–15.
87. Hafeez H. et al. Techno-economic perspective of a floating solar PV deployment over urban lakes: A case study of NUST lake Islamabad // Solar Energy. 2022. Vol. 231. P. 355–364.
88. Ahmed N. et al. Techno-economic potential assessment of mega scale grid-connected PV power plant in five climate zones of Pakistan // Energy Conversion and Management. 2021. Vol. 237. P. 114097.
89. Ud-Din Khan S. et al. Techno-economic analysis of solar photovoltaic powered electrical energy storage (EES) system // Alexandria Engineering Journal. 2022. Vol. 61, № 9. P. 6739–6753.
90. Uddin M.N., Biswas M.M., Nuruddin S. Techno-economic impacts of floating PV power generation for remote coastal regions // Sustainable Energy Technologies and Assessments. 2022. Vol. 51. P. 101930.
91. Zhang Y. et al. Battery sizing and rule-based operation of grid-connected photovoltaic-battery system: A case study in Sweden // Energy Conversion and Management. 2017. Vol. 133. P. 249–263.
92. Martín-Pomares L. et al. Analysis of the long-term solar potential for electricity generation in Qatar // Renewable and Sustainable Energy Reviews. 2017. Vol. 73. P. 1231–1246.
93. Shabani M. et al. Techno-economic impacts of battery performance models and control strategies on optimal design of a grid-connected PV system // Energy Conversion and Management. 2021. Vol. 245. P. 114617.
94. Said Z. et al. Central versus off-grid photovoltaic system, the optimum option for the domestic sector based on techno-economic-environmental assessment for United Arab Emirates // Sustainable Energy Technologies and Assessments. 2021. Vol. 43. P. 100944.
95. Li C. Economic and performance evaluation of grid-connected residential solar photovoltaic systems in Northwest China // Energy Sources, Part A: Recovery, Utilization, and Environmental Effects. Taylor & Francis, 2022. Vol. 44, № 2. P. 5473–5489.
96. Trabelsi S.E. et al. Techno-economic performance of concentrating solar power plants under the climatic conditions of the southern region of Tunisia // Energy Conversion and Management. 2016. Vol. 119. P. 203–214.

97. Kamel S. et al. Comparative Analysis of Rankine Cycle Linear Fresnel Reflector and Solar Tower Plant Technologies: Techno-Economic Analysis for Ethiopia: 3 // Sustainability. Multidisciplinary Digital Publishing Institute, 2022. Vol. 14, № 3. P. 1677.
98. Tahir S. et al. Techno-economic assessment of concentrated solar thermal power generation and potential barriers in its deployment in Pakistan. // Journal of Cleaner Production. 2021. Vol. 293. P. 126125.
99. Agyekum E.B., Velkin V.I. Optimization and techno-economic assessment of concentrated solar power (CSP) in South-Western Africa: A case study on Ghana // Sustainable Energy Technologies and Assessments. 2020. Vol. 40. P. 100763.
100. Lashari A.A. et al. The performance prediction and techno-economic analyses of a stand-alone parabolic solar dish/stirling system, for Jamshoro, Pakistan // Cleaner Engineering and Technology. 2021. Vol. 2. P. 100064.
101. Aly A. et al. Is Concentrated Solar Power (CSP) a feasible option for Sub-Saharan Africa?: Investigating the techno-economic feasibility of CSP in Tanzania // Renewable Energy. 2019. Vol. 135. P. 1224–1240.
102. Abbas M. et al. Dish Stirling technology: A 100 MW solar power plant using hydrogen for Algeria // International Journal of Hydrogen Energy. 2011. Vol. 36, № 7. P. 4305–4314.
103. Bataineh K., Taamneh Y. Performance analysis of stand-alone solar dish Stirling system for electricity generation // IJHT. 2017. Vol. 35, № 3. P. 498–508.
104. Zayed M.E. et al. Performance prediction and techno-economic analysis of solar dish/stirling system for electricity generation // Applied Thermal Engineering. 2020. Vol. 164. P. 114427.
105. EL BOUJDAINI L. et al. Techno-economic investigation of parabolic trough solar power plant with indirect molten salt storage // 2019 International Conference of Computer Science and Renewable Energies (ICCSRE). 2019. P. 1–7.
106. Salisu L., Enaburekhan J.S., Adamu A.A. Techno-Economic and Life Cycle Analysis of Energy Generation Using Concentrated Solar Power (CSP) Technology in Sokoto State. Nigeria: 5 // Journal of Applied Sciences and Environmental Management. 2019. Vol. 23, № 5. P. 775–782.
107. Sundaray S., Kandpal T.C. Preliminary feasibility evaluation of solar thermal power generation in India // International Journal of Sustainable Energy. Taylor & Francis, 2014. Vol. 33, № 2. P. 461–469.

108. Xu Y. et al. Concentrated solar power: technology, economy analysis, and policy implications in China // Environ Sci Pollut Res. 2022. Vol. 29, № 1. P. 1324–1337.
109. Lipu M.S.H., Jamal T. Techno-economic Analysis of Solar Concentrating Power (CSP) in Bangladesh: 5 // International Journal of Advanced Renewable Energy Research. 2013. Vol. 2, № 5.
110. Bhuiyan N. et al. Performance optimisation of parabolic trough solar thermal power plants – a case study in Bangladesh // International Journal of Sustainable Energy. Taylor & Francis, 2020. Vol. 39, № 2. P. 113–131.
111. Kalogirou S.A. Solar thermoelectric power generation in Cyprus: Selection of the best system // Renewable Energy. 2013. Vol. 49. P. 278–281.
112. Luo Y. et al. Impacts of solar multiple on the performance of direct steam generation solar power tower plant with integrated thermal storage // Front. Energy. 2017. Vol. 11, № 4. P. 461–471.
113. Boretti A., Castelletto S. Concentrated Solar Power Solar Tower with Oversized Solar Field and Molten Salt Thermal Energy Storage Working at an Annual Average Capacity Factor of 95% in NEOM City // Energy Technology. 2021. Vol. 9, № 4. P. 2001097.
114. Agyekum E.B. et al. A 3E, hydrogen production, irrigation, and employment potential assessment of a hybrid energy system for tropical weather conditions – Combination of HOMER software, shannon entropy, and TOPSIS // International Journal of Hydrogen Energy. 2022.
115. Song Y. et al. Techno-economic analysis of a hybrid energy system for CCHP and hydrogen production based on solar energy // International Journal of Hydrogen Energy. 2022. Vol. 47, № 58. P. 24533–24547.
116. Rad M.A.V. et al. Techno-economic analysis of a hybrid power system based on the cost-effective hydrogen production method for rural electrification, a case study in Iran // Energy. 2020. Vol. 190. P. 116421.
117. Gu Y. et al. Techno-economic analysis of green methanol plant with optimal design of renewable hydrogen production: A case study in China // International Journal of Hydrogen Energy. 2022. Vol. 47, № 8. P. 5085–5100.
118. Wang B. et al. Techno-economic analysis and optimization of a novel hybrid solar-wind-bioethanol hydrogen production system via membrane reactor // Energy Conversion and Management. 2022. Vol. 252. P. 115088.

119. Nasser M. et al. Techno-economic assessment of clean hydrogen production and storage using hybrid renewable energy system of PV/Wind under different climatic conditions // Sustainable Energy Technologies and Assessments. 2022. Vol. 52. P. 102195.
120. Paladugula A.L. et al. A multi-model assessment of energy and emissions for India's transportation sector through 2050 // Energy Policy. 2018. Vol. 116. P. 10–18.
121. Al-Sharafi A. et al. Techno-economic analysis and optimization of solar and wind energy systems for power generation and hydrogen production in Saudi Arabia // Renewable and Sustainable Energy Reviews. 2017. Vol. 69. P. 33–49.
122. Cano A., Arévalo P., Jurado F. Energy analysis and techno-economic assessment of a hybrid PV/HKT/BAT system using biomass gasifier: Cuenca-Ecuador case study // Energy. 2020. Vol. 202. P. 117727.
123. Xia T. et al. Techno-Economic Assessment of a Grid-Independent Hybrid Power Plant for Co-Supplying a Remote Micro-Community with Electricity and Hydrogen // Processes. 2021. Vol. 9, № 8.
124. Singh S. et al. Cost Optimization of a Stand-Alone Hybrid Energy System with Fuel Cell and PV: 5 // Energies. Multidisciplinary Digital Publishing Institute, 2020. Vol. 13, № 5. P. 1295.
125. Ghenai C., Salameh T., Merabet A. Technico-economic analysis of off grid solar PV/Fuel cell energy system for residential community in desert region // International Journal of Hydrogen Energy. 2020. Vol. 45, № 20. P. 11460–11470.
126. Brka A., Al-Abdeli Y.M., Kothapalli G. Predictive power management strategies for stand-alone hydrogen systems: Operational impact // International Journal of Hydrogen Energy. 2016. Vol. 41, № 16. P. 6685–6698.
127. Demiroren A., Yilmaz U. Analysis of change in electric energy cost with using renewable energy sources in Gökceada, Turkey: An island example // Renewable and Sustainable Energy Reviews. 2010. Vol. 14, № 1. P. 323–333.
128. Ur Rashid M. et al. Techno-Economic Analysis of Grid-Connected Hybrid Renewable Energy System for Remote Areas Electrification Using Homer Pro // J. Electr. Eng. Technol. 2022. Vol. 17, № 2. P. 981–997.
129. Feasibility study and economic analysis of stand-alone hybrid energy system for southern Ghana // Sustainable Energy Technologies and Assessments. Elsevier, 2020. Vol. 39. P. 100695.

130. Thirunavukkarasu M., Sawle Y. An Examination of the Techno-Economic Viability of Hybrid Grid-Integrated and Stand-Alone Generation Systems for an Indian Tea Plant // Frontiers in Energy Research. 2022. Vol. 10.
131. Al-Buraiki A.S., Al-Sharafi A. Hydrogen production via using excess electric energy of an off-grid hybrid solar/wind system based on a novel performance indicator // Energy Conversion and Management. 2022. Vol. 254. P. 115270.
132. Jahangiri M. et al. Using fuzzy MCDM technique to find the best location in Qatar for exploiting wind and solar energy to generate hydrogen and electricity // International Journal of Hydrogen Energy. 2020. Vol. 45, № 27. P. 13862–13875.
133. Jahangiri M. et al. Feasibility study on the provision of electricity and hydrogen for domestic purposes in the south of Iran using grid-connected renewable energy plants // Energy Strategy Reviews. 2019. Vol. 23. P. 23–32.
134. Khare V., Nema S., Baredar P. Optimization of hydrogen based hybrid renewable energy system using HOMER, BB-BC and GAMBIT // International Journal of Hydrogen Energy. 2016. Vol. 41, № 38. P. 16743–16751.
135. Silva S.B., Severino M.M., de Oliveira M.A.G. A stand-alone hybrid photovoltaic, fuel cell and battery system: A case study of Tocantins, Brazil // Renewable Energy. 2013. Vol. 57. P. 384–389.
136. Pal P., Mukherjee V. Off-grid solar photovoltaic/hydrogen fuel cell system for renewable energy generation: An investigation based on techno-economic feasibility assessment for the application of end-user load demand in North-East India // Renewable and Sustainable Energy Reviews. 2021. Vol. 149. P. 111421.
137. Gökçek M., Kale C. Techno-economical evaluation of a hydrogen refuelling station powered by Wind-PV hybrid power system: A case study for İzmir-Çeşme // International Journal of Hydrogen Energy. 2018. Vol. 43, № 23. P. 10615–10625.
138. Won W. et al. Design and operation of renewable energy sources based hydrogen supply system: Technology integration and optimization // Renewable Energy. 2017. Vol. 103. P. 226–238.
139. Almutairi K. et al. Use of a Hybrid Wind—Solar—Diesel—Battery Energy System to Power Buildings in Remote Areas: A Case Study: 16 // Sustainability. Multidisciplinary Digital Publishing Institute, 2021. Vol. 13, № 16. P. 8764.
140. Abdin Z., Mérida W. Hybrid energy systems for off-grid power supply and hydrogen production based on renewable energy: A techno-economic analysis // Energy Conversion and Management. 2019. Vol. 196. P. 1068–1079.

141. Almutairi K. et al. Technical, economic, carbon footprint assessment, and prioritizing stations for hydrogen production using wind energy: A case study // Energy Strategy Reviews. 2021. Vol. 36. P. 100684.
142. Ayodele T.R. et al. Optimal design of wind-powered hydrogen refuelling station for some selected cities of South Africa // International Journal of Hydrogen Energy. 2021. Vol. 46, № 49. P. 24919–24930.
143. Okonkwo P.C. et al. Utilization of renewable hybrid energy for refueling station in Al-Kharj, Saudi Arabia // International Journal of Hydrogen Energy. 2022.
144. Das H.S. et al. Feasibility analysis of hybrid photovoltaic/battery/fuel cell energy system for an indigenous residence in East Malaysia // Renewable and Sustainable Energy Reviews. 2017. Vol. 76. P. 1332–1347.
145. Li C. et al. Exploration on the feasibility of hybrid renewable energy generation in resource-based areas of China: Case study of a regeneration city // Energy Strategy Reviews. 2022. Vol. 42. P. 100869.
146. Webb R.L. Next Generation Devices for Electronic Cooling With Heat Rejection to Air // Journal of Heat Transfer. 2005. Vol. 127, № 1. P. 2–10.
147. Chang Y.-W. et al. Heat pipe for cooling of electronic equipment // Energy Conversion and Management. 2008. Vol. 49, № 11. P. 3398–3404.
148. Mohamed H.A. Elnaggar. Heat Pipes for Computer Cooling Applications // Electronics Cooling / ed. Ezzaldeen Edwan ED1 - S M Sohel Murshed. Rijeka: IntechOpen, 2016. P. Ch. 4.
149. Nemec P., Čaja A., Malcho M. Mathematical model for heat transfer limitations of heat pipe // Mathematical and Computer Modelling. 2013. Vol. 57, № 1. P. 126–136.
150. Yang X. et al. Experimental investigation on performance comparison of PV/T-PCM system and PV/T system // Renewable Energy. 2018. Vol. 119. P. 152–159.
151. Harahap H.A., Dewi T., Rusdianasari. Automatic Cooling System for Efficiency and Output Enhancement of a PV System Application in Palembang, Indonesia // J. Phys.: Conf. Ser. IOP Publishing, 2019. Vol. 1167. P. 012027.
152. Moharram K.A. et al. Enhancing the performance of photovoltaic panels by water cooling // Ain Shams Engineering Journal. 2013. Vol. 4, № 4. P. 869–877.
153. Sredenšek K. et al. Experimental Validation of a Thermo-Electric Model of the Photovoltaic Module under Outdoor Conditions: 11 // Applied Sciences. Multidisciplinary Digital Publishing Institute, 2021. Vol. 11, № 11. P. 5287.

154. Colţ G. Performance evaluation of a PV panel by rear surface water active cooling // 2016 International Conference on Applied and Theoretical Electricity (ICATE). 2016. P. 1–5.
155. Experimental Performance Evaluation of a Photovoltaic Thermal (PV/T) Air Collector and Its Optimization [Electronic resource] // Journal of Mechanical Engineering. URL: https://www.sv-jme.eu/article/experimental-performance-evaluation-of-a-photovoltaic-thermal-pvt-air-collector-and-its-optimization/ (accessed: 08.06.2022).
156. PraveenKumar S. et al. Experimental assessment of thermoelectric cooling on the efficiency of PV module: 3 // International Journal of Renewable Energy Research (IJRER). 2022. Vol. 12, № 3. P. 1670–1681.
157. Fatoni E.K.A., Taqwa A., Kusumanto R. Solar Panel Performance Improvement using Heatsink Fan as the Cooling Effect // J. Phys.: Conf. Ser. IOP Publishing, 2019. Vol. 1167. P. 012031.
158. Teffah K., Zhang Y., Mou X. Modeling and Experimentation of New Thermoelectric Cooler–Thermoelectric Generator Module: 3 // Energies. Multidisciplinary Digital Publishing Institute, 2018. Vol. 11, № 3. P. 576.
159. Irwan Y.M. et al. Comparison of solar panel cooling system by using dc brushless fan and dc water // Journal of Physics: Conference Series. 2015. Vol. 622, № 1.
160. Erol H., Uçman M., Kesilmiş Z. The Effect of Fan Cooling on Photovoltaic Efficiency of PV Panels in Osmaniye Environment. 2017. Vol. 6, № 3. P. 29–33.
161. Yusoff M.I. et al. Analysis Air Cooling Mechanism for Photovoltaic Panel by Solar Simulator: 4 // International Journal of Electrical and Computer Engineering (IJECE). 2015. Vol. 5, № 4. P. 636–643.
162. Irwan Y.M. et al. Analysis air cooling mechanism for photovoltaic panel by solar simulator // International Journal of Electrical and Computer Engineering. 2015. Vol. 5, № 4. P. 636–643.
163. Soliman A.M.A., Hassan H., Ookawara S. An experimental study of the performance of the solar cell with heat sink cooling system // Energy Procedia. Elsevier B.V., 2019. Vol. 162. P. 127–135.
164. Hallal J., Hammoud M., Moussa T. Experimental optimization of the Si photovoltaic panels cooling system on maximum allowable temperature criteria // Renewable Energy Focus. Elsevier Ltd, 2020. Vol. 35, № December. P. 178–181.
165. Sultan T.N., Farhan M.S., Salim Alrikabi H.T.H. Using Cooling System for Increasing the Efficiency of Solar Cell // Journal of Physics: Conference Series. 2021. Vol. 1973, № 1.

166. Mahone, Mark E., Denckla, Martha B. untitled _ Enhanced Reader.pdf // Clinical Infectious Diseases. 2017.
167. Indartono Y.S., Suwono A., Pratama F.Y. Improving photovoltaics performance by using yellow petroleum jelly as phase change material // International Journal of Low-Carbon Technologies. 2016. Vol. 11, № 3. P. 333–337.
168. Mahamudul H. et al. Development of a temperature regulated photovoltaic module using phase change material for Malaysian weather condition // Optoelectronics and Advanced Materials, Rapid Communications. 2014. Vol. 8, № 11–12. P. 1243–1245.
169. Chandrasekar M., Senthilkumar T. Passive thermal regulation of flat PV modules by coupling the mechanisms of evaporative and fin cooling // Heat and Mass Transfer/Waerme- und Stoffuebertragung. 2016. Vol. 52, № 7. P. 1381–1391.
170. Ho C.J., Chou W.L., Lai C.M. Thermal and electrical performance of a water-surface floating PV integrated with a water-saturated MEPCM layer // Energy Conversion and Management. 2015. Vol. 89. P. 862–872.
171. Habeeb L. et al. Cooling Photovoltaic Thermal Solar Panel by Using Heat Pipe at Baghdad Climate // International Journal of Mechanical & Mechatronics Engineering IJMME-IJENS. 2017. Vol. 17, № February. P. 6.
172. Arifin Z. et al. Numerical and experimental investigation of air cooling for photovoltaic panels using aluminum heat sinks // International Journal of Photoenergy. 2020. Vol. 2020.
173. Firoozzadeh M., Shiravi A.H., Shafiee M. An Experimental Study on Cooling the Photovoltaic Modules by Fins to Improve Power Generation: Economic Assessment // Iranian Journal of Energy and Environment. 2019. Vol. 10, № 2. P. 80–84.
174. Haidar Z.A., Orfi J., Kaneesamkandi Z. Photovoltaic panels temperature regulation using evaporative cooling principle: Detailed theoretical and real operating conditions experimental approaches // Energies. 2021. Vol. 14, № 1.
175. Garud K.S., Lee M.-Y. Thermodynamic, environmental and economic analyses of photovoltaic/thermal-thermoelectric generator system using single and hybrid particle nanofluids // Energy. 2022. Vol. 255. P. 124515.
176. Sardarabadi M., Passandideh-Fard M., Zeinali Heris S. Experimental investigation of the effects of silica/water nanofluid on PV/T (photovoltaic thermal units) // Energy. 2014. Vol. 66. P. 264–272.

177. Alous S., Kayfeci M., Uysal A. Experimental investigations of using MWCNTs and graphene nanoplatelets water-based nanofluids as coolants in PVT systems // Applied Thermal Engineering. 2019. Vol. 162. P. 114265.
178. Naghdbishi A., Yazdi M.E., Akbari G. Experimental investigation of the effect of multi-wall carbon nanotube – Water/glycol based nanofluids on a PVT system integrated with PCM-covered collector // Applied Thermal Engineering. 2020. Vol. 178. P. 115556.
179. Zhang H. et al. Experimental studies on a low concentrating photovoltaic/thermal (LCPV/T) collector with a thermoelectric generator (TEG) module // Renewable Energy. 2021. Vol. 171. P. 1026–1040.
180. Liang H. et al. Experimental investigation on spectral splitting of photovoltaic/thermal hybrid system with two-axis sun tracking based on SiO2/TiO2 interference thin film // Energy Conversion and Management. 2019. Vol. 188. P. 230–240.
181. Motiei P., Yaghoubi M., GoshtasbiRad E. Transient simulation of a hybrid photovoltaic-thermoelectric system using a phase change material // Sustainable Energy Technologies and Assessments. 2019. Vol. 34. P. 200–213.
182. Alian Fini M., Gharapetian D., Asgari M. Efficiency improvement of hybrid PV-TEG system based on an energy, exergy, energy-economic and environmental analysis; experimental, mathematical and numerical approaches // Energy Conversion and Management. 2022. Vol. 265. P. 115767.
183. PraveenKumar S. et al. Performance evaluation with low-cost aluminum reflectors and phase change material integrated to solar PV modules using natural air convection: An experimental investigation // Energy. 2023. Vol. 266. P. 126415.
184. Aluminium - Element information, properties and uses | Periodic Table [Electronic resource]. URL: https://www.rsc.org/periodic-table/element/13/aluminium (accessed: 19.06.2022).
185. staff W. Aluminium: Properties and Advantages [Electronic resource]. URL: https://www.weerg.com/en/global/blog/aluminum-properties-and-advantages-of-aluminum (accessed: 19.06.2022).
186. Shastry D.M.C., Arunachala U.C. Thermal management of photovoltaic module with metal matrix embedded PCM // Journal of Energy Storage. 2020. Vol. 28. P. 101312.
187. M. R. et al. Experimental investigation on the abasement of operating temperature in solar photovoltaic panel using PCM and aluminium // Solar Energy. 2019. Vol. 188. P. 327–338.

188. Bhargava A.K., Garg H.P., Agarwal R.K. Study of a hybrid solar system—solar air heater combined with solar cells // Energy Conversion and Management. 1991. Vol. 31, № 5. P. 471–479.
189. Grubišić-Čabo F. et al. Experimental investigation of the passive cooled free-standing photovoltaic panel with fixed aluminum fins on the backside surface // Journal of Cleaner Production. 2018. Vol. 176. P. 119–129.
190. Arifin Z. et al. Numerical and Experimental Investigation of Air Cooling for Photovoltaic Panels Using Aluminum Heat Sinks // International Journal of Photoenergy / ed. Álvarez-Gallegos A. Hindawi, 2020. Vol. 2020. P. 1574274.
191. Mojumder J.C. et al. An experimental investigation on performance analysis of air type photovoltaic thermal collector system integrated with cooling fins design // Energy and Buildings. 2016. Vol. 130. P. 272–285.
192. Enhancement the Performance of PV Panel by Using Fins as Heat Sink // ETJ. 2018. Vol. 36, № 7A.
193. AlAmri F. et al. Analytical Modeling and Optimization of a Heat Sink Design for Passive Cooling of Solar PV Panel: 6 // Sustainability. Multidisciplinary Digital Publishing Institute, 2021. Vol. 13, № 6. P. 3490.
194. El Mays A. et al. Improving Photovoltaic Panel Using Finned Plate of Aluminum // Energy Procedia. 2017. Vol. 119. P. 812–817.
195. Kim J. et al. Experimental and Numerical Study on the Cooling Performance of Fins and Metal Mesh Attached on a Photovoltaic Module: 1 // Energies. Multidisciplinary Digital Publishing Institute, 2020. Vol. 13, № 1. P. 85.
196. Sedaghat A., Karami M.R., Eslami M. Improving Performance of a Photovoltaic Panel by Pin Fins: A Theoretical Analysis // Iran J Sci Technol Trans Mech Eng. 2020. Vol. 44, № 4. P. 997–1004.
197. Farhan A.A., Hasan D.J. Enhancing the efficiency of Photovoltaic panel using open-cell copper metal foam fins: 4 // International Journal of Renewable Energy Research (IJRER). 2019. Vol. 9, № 4. P. 1849–1855.
198. Hernandez-Perez J.G. et al. Thermal performance of a discontinuous finned heatsink profile for PV passive cooling // Applied Thermal Engineering. 2021. Vol. 184. P. 116238.
199. Elbreki A.M. et al. An innovative technique of passive cooling PV module using lapping fins and planner reflector // Case Studies in Thermal Engineering. 2020. Vol. 19. P. 100607.

200. Amber K.P. et al. Experimental performance analysis of two different passive cooling techniques for solar photovoltaic installations // J Therm Anal Calorim. 2021. Vol. 143, № 3. P. 2355–2366.
201. Wongwuttanasatian T., Sarikarin T., Suksri A. Performance enhancement of a photovoltaic module by passive cooling using phase change material in a finned container heat sink // Solar Energy. 2020. Vol. 195. P. 47–53.
202. Shiravi A.H., Firoozzadeh M. Thermodynamic and Environmental Assessment of Mounting Fin at the Back Surface of Photovoltaic Panels // Journal of Applied and Computational Mechanics. Shahid Chamran University of Ahvaz, 2021. Vol. 7, № 4. P. 1956–1963.
203. Benato A. et al. Spraying Cooling System for PV Modules: Experimental Measurements for Temperature Trends Assessment and System Design Feasibility: 2 // Designs. Multidisciplinary Digital Publishing Institute, 2021. Vol. 5, № 2. P. 25.
204. Nižetić S. et al. Water spray cooling technique applied on a photovoltaic panel: The performance response // Energy Conversion and Management. 2016. Vol. 108. P. 287–296.
205. Chandrasekar M. et al. Passive cooling of standalone flat PV module with cotton wick structures // Energy Conversion and Management. 2013. Vol. 71. P. 43–50.
206. Dida M. et al. Experimental investigation of a passive cooling system for photovoltaic modules efficiency improvement in hot and arid regions // Energy Conversion and Management. 2021. Vol. 243. P. 114328.
207. PraveenKumar S. et al. Thermal Management of Solar Photovoltaic Module to Enhance Output Performance: An Experimental Passive Cooling Approach Using Discontinuous Aluminium Heat Sink. 2021. P. 13.
208. Sheps R. et al. New passive solar panels for Russian cold winter conditions // Energy and Buildings. 2021. Vol. 248. P. 111187.
209. Choubineh N., Jannesari H., Kasaeian A. Experimental study of the effect of using phase change materials on the performance of an air-cooled photovoltaic system // Renewable and Sustainable Energy Reviews. 2019. Vol. 101. P. 103–111.
210. Fayaz H. et al. Numerical and outdoor real time experimental investigation of performance of PCM based PVT system // Solar Energy. 2019. Vol. 179. P. 135–150.
211. Shittu S. et al. Experimental study and exergy analysis of photovoltaic-thermoelectric with flat plate micro-channel heat pipe // Energy Conversion and Management. 2020. Vol. 207. P. 112515.

212. Nazari S., Safarzadeh H., Bahiraei M. Performance improvement of a single slope solar still by employing thermoelectric cooling channel and copper oxide nanofluid: An experimental study // Journal of Cleaner Production. 2019. Vol. 208. P. 1041–1052.
213. Hekmat S., Molaeimanesh G.R. Hybrid thermal management of a Li-ion battery module with phase change material and cooling water pipes: An experimental investigation // Applied Thermal Engineering. 2020. Vol. 166. P. 114759.
214. Li H. et al. Experimental investigation on the cooling performance of an Earth to Air Heat Exchanger (EAHE) equipped with an irrigation system to adjust soil moisture // Energy and Buildings. 2019. Vol. 196. P. 280–292.
215. Rehman T.-, Ali H.M. Experimental investigation on paraffin wax integrated with copper foam based heat sinks for electronic components thermal cooling // International Communications in Heat and Mass Transfer. 2018. Vol. 98. P. 155–162.
216. Abdo S. et al. Hydrogels beads for cooling solar panels: Experimental study // Renewable Energy. 2020. Vol. 153. P. 777–786.
217. PraveenKumar S. et al. Thermal management of solar photovoltaic module to enhance output performance: an experimental passive cooling approach using discontinuous aluminum heat sink: 4 // International Journal of Renewable Energy Research (IJRER). 2021. Vol. 11, № 4. P. 1700–1712.
218. Praveenkumar S. et al. Techno-Economics and the Identification of Environmental Barriers to the Development of Concentrated Solar Thermal Power Plants in India: 20 // Applied Sciences. Multidisciplinary Digital Publishing Institute, 2022. Vol. 12, № 20. P. 10400.